komunikácie

COMMUNICATIONS

SCIENTIFIC LETTERS OF THE UNIVERSITY OF ŽILINA

Volume 27

JOURNAL FOR SCIENCES IN TRANSPORT

UNIVERSITY
OF ŽILINA

ISSN 1335-4205

2/2025

UNIVERSITY OF ŽILINA
EDIS-Publishing House
UNIZA

EDIS-Publishing House of the University of Žilina (UZ) is one of the University of Žilina's consituents. The beginning of its existence dates back to 1990. In the course of its work, the publishing house has published more than 5 000 titles of book publications, especially university textbooks, scientific monographs, scripts, prose, but also enriched the book market with titles of regional, children's and popular literature.
Students and professional public have the opportunity to purchase published titles in the „Selling Study Literature" directly on the premises of the University of Žilina, in the EDIS shop or upon order on a „cash on delivery" basis. All published titles are available at: www.edis.uniza.sk.

EDIS-Publishing House of the University of Žilina offers book titles in English

Lenka Černá, Jozef Daniš
APPLICATION OF COST ALCULATIONS IN THE TARIFF POLICY FORMATION IN RAILWAY TRANSPORT
ISBN 978-80-554-1391-4 Price 7.61 €

Eva Nedeliaková, Jana Sekulová
EVALUATION OF QUALITY IN RAILWAY TRANSPORT
ISBN 978-554-1272-6 Price 8.00 €

Martin Bugaj
AEROMECHANICS 1
ISBN 978-80-554-1675-5 Price 14.50 €

Anna Tomová
ECONOMICS OF AIR NAVIGATION SERVICES
ISBN 978-80-554-0905-4 Price 14.30 €

Marica Mazurek
MODELS OF BRANDING AND THEIR APPLICATION
ISBN 978-80-554-1705-9 Price 9.00 €

Jozef Melcer
DYNAMICS OF STRUCTURES
ISBN 978-80-554-1698-4 Price 19.00 €

Jozef Gašparík et al.
RAILWAY TRAFFIC OPERATION
ISBN 978-80-554-1281-8 Price 15.80 €

Tetiana Hovorushchenko et.al.
CD - INTELLIGENT INFORMATION-ANALYTICAL TECHNOLOGIES...
ISBN 978-80-554-1729-5 Price 3.50 €

Karol Matiaško, Michal Kvet, Marek Kvet
CD - PRACTICES FOR DATABASE SYSTEMS
ISBN 978-80-554-1397-6 Price 2.20 €

Michal Kvet, Karol Matiaško, Štefan Toth
USB - PRACTICAL SQL FOR ORACLE CLOUD
ISBN 978-80-554-1880-3 Price: 11,30 €

Veronika Valašková, Daniela Kucharová
USB - STATICS OF STRUCTURES 3
ISBN 978-80-554-1826-1 Price: 8,90 €

Michal Kvet, Karol Matiaško, Marek Kvet
USB - BECOME EXPERT IN MYSQL PRACTICES FOR DATABASE SYSTEMS IN MYSQL
ISBN 978-80-554-1786-8 Price 13.50 €

Michal Kvet, Alenka Baggia, Monika Borkovcová, Diana Mudrinić, Frane Urem
E-book - Environmental Data Analysis
ISBN 978-80-554-2145-2 Price 0,00 €

Michal Kvet
E-book – Become master in SQL
ISBN 978-80-554-2132-2 Price 0,00 €

EDIS-Publishing House UNIZA
Univerzitná 8215/1,
010 26 Žilina,
Slovakia

e-mail: edis_objednavky@uniza.sk, edis@uniza.sk
www.edis.uniza.sk

KOMUNIKÁCIE
COMMUNICATIONS

A - OPERATION AND ECONOMICS IN TRANSPORT

B - MECHANICAL ENGINEERING IN TRANSPORT

C - ELECTRICAL ENGINEERING IN TRANSPORT

D - CIVIL ENGINEERING IN TRANSPORT

E - MANAGEMENT SCIENCE AND INFORMATICS IN TRANSPORT

F - SAFETY AND SECURITY ENGINEERING IN TRANSPORT

INTEGRATING PESTLE AND SWOT FOR ADVANCING SUSTAINABLE INLAND WATERWAY TRANSPORTATION: INSIGHTS FROM WEST JAVA, INDONESIA

Ade Ratih Ispandiari[1,*], Ibnu Fauzi[2], Nanda Yustina[1], Zulfa Qonita[3]

[1]Research Center for Transportation Technology, National Research and Innovation Agency, Serpong, South Tangerang, Indonesia
[2]Research Center for Hydrodynamics Technology, National Research and Innovation Agency, Surabaya, East Java, Indonesia
[3]Research Center for Geological Disaster, National Research and Innovation Agency, Bandung, West Java, Indonesia

*E-mail of corresponding author: ader006@brin.go.id

Ade Ratih Ispandiari 0000-0002-8274-5828,
Ibnu Fauzi 0000-0002-0396-8928,
Nanda Yustina 0009-0007-1287-4484,
Zulfa Qonita 0000-0002-3224-1138

Resume

The potential and challenges of Inland Waterway Transportation (IWT) in West Java, Indonesia were examined in this research, with a focus on sustainability using the SWOT and PESTLE analyses. Key findings show that IWT provides significant environmental benefits, such as reduced carbon emissions, and supports social equity through affordable and accessible transport. However, challenges include sedimentation, water hyacinth proliferation, poor waste management, infrastructure deficiencies and high investment costs. Overcoming these obstacles requires strategic planning that emphasises centralisation of governance, modernisation of infrastructure, environmental management and integration of technology. The findings provide applicable insights for policymakers and stakeholders to foster sustainable and inclusive transport in West Java.

Article info

Received 15 October 2024
Accepted 31 January 2025
Online 19 February 2025

Keywords:

inland waterways transportation
PESTLE
SWOT
West Java rivers
sustainable transportation

Available online: https://doi.org/10.26552/com.C.2025.022

ISSN 1335-4205 (print version)
ISSN 2585-7878 (online version)

1 Introduction

Transportation is a basic human need and a critical element for the economic development of a country [1]. Inland Waterway Transport (IWT) is a key component of sustainable transportation systems, contributing to environmental and economic sustainability, while creating employment opportunities, as well [2]. The IWT offers several benefits, such as enhanced safety and cost savings [3]. Furthermore, its development plays a crucial role in reducing emissions and mitigating the external costs associated with pollution and congestion [4]. Despite its advantages, IWT faces numerous barriers, including challenges related to logistics, infrastructure, and political, economic, environmental, and technological landscape [3].

Indonesia, as an archipelago with over 5,950 watersheds and more than 500 major rivers, has significant potential to expand its IWT network. However, out of the many rivers, only 214 are currently utilized for transport purposes [5]. In West Java, despite the presence of a promising river network, the development and use of IWT remains limited. This study aim was to identify and address the challenges and opportunities associated with the development of IWT in the region.

The IWT is a form of local transport traditionally use by communities, often reflecting local culture and conditions [6]. It was highlighted in a UN report on informal transport [7]. The IWT is recognized for its resource efficiency, affordability, and adaptability to technological advancements. In Indonesia, these systems are often designed by local communities to meet specific needs, functioning independently and in traditional environments [8-9]. Although the IWT is classified as public transport [6, 10], its underdevelopment remains

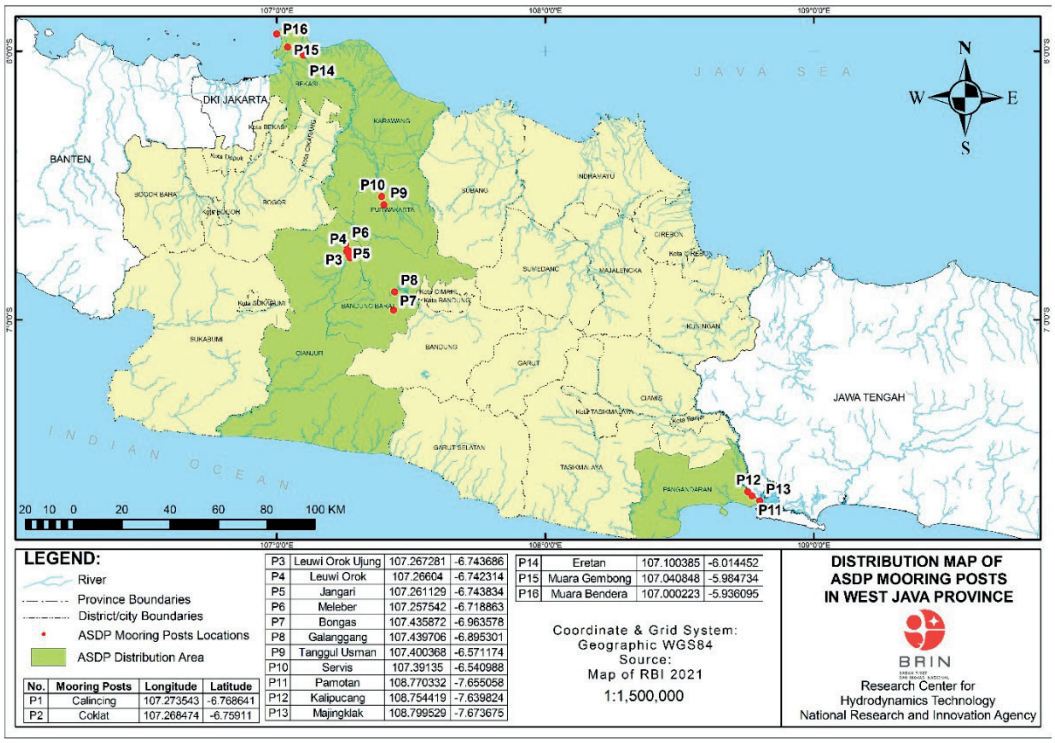

Figure 1 *Distribution Map of River, Lake and Ferry Transport Mooring Posts for West Java Province*

especially evident in West Java, where the potential of IWT is yet to be fully realized.

The primary objective of this study was to assess the current challenges and opportunities for the development of IWT in West Java. This research has utilized a SWOT analysis (Strengths, Weaknesses, Opportunities, Threats) analysis combined with the PESTLE (Political, Economic, Technological, Social, Legal, Environmental) framework to provide a comprehensive evaluation of the factors influencing the IWT development in this region. By addressing these challenges, the study has aimed to offer actionable recommendations for policymakers, transport operators, and local communities, contributing to the sustainable development of IWT.

2 Data and methods

2.1 Research location

The research on Inland Waterway Transport (IWT) was conducted in West Java, focusing on 6 (six) service area as shown in Figure 1. These areas include the Cirata service area for Cirata reservoir transportation in Cianjur Regency, the Saguling service area for Saguling for reservoir transportation in West Bandung Regency, the Jatiluhur service area for reservoir transportation in Purwakarta Regency, the Kalipucang and Majingklak service areas for river transportation in Pangandaran Regency, and the Muara Gembong service area for river transportation in Bekasi Regency [11-12].

2.2 Theoretical and operational framework

This study employs an integrated approach combining the PESTLE and SWOT frameworks to evaluate and to identify external and contextual parameters, while SWOT categorizes those parameters into strengths, weaknesses, opportunities, and threats.

2.2.1 Theoretical basis for PESTLE and SWOT

Both PESTLE and SWOT are established tools in strategic planning and decision-making processes. **PESTLE**: focuses on macro-level external factors influencing sectoral performance, including political, economic, social, technological, legal and environmental dimensions [13]. **SWOT**: provides a structured method to evaluate internal and external factors by categorizing them into strengths, weaknesses, opportunities, and threats [14]. The Integration Process begins with PESTLE Analysis, which identifies and examines relevant factors to provide a foundational understanding of the contextual environment. Subsequently, SWOT Analysis evaluates the factors identified through PESTLE to classify them into actionable insights, ultimately guiding the formulation of strategic recommendations. This two-step process ensures a comprehensive evaluation of both macro environmental and sector-specific factors influencing IWT development.

2.2.2 Operationalization of PESTLE for IWT analysis

In this study is combined a review of existing literature and secondary data from the Central Bureau of Statistics and the West Java Transportation Agency to identify key PESTLE indicators. To enhance the reliability and depth of the analysis, primary data was collected through the semi-structured interviews with the key stakeholders, including government officials, transportation operators, and local communities. The Political Aspect Examined government policies, regulatory frameworks, and IWT development plans to identify enabling and constraining factors. The Economic Aspect includes a Location Quotient (LQ) analysis to assess the economic potential of the region. The LQ values above 1 indicate areas with promising development potential [15-16]. The Social and Technological Aspects Evaluated IWT's authenticity and adaptability to modern technology by analyzing its social acceptance, cultural alignment, and technological readiness [6]. Table 1 shows the characteristics of IWT indigeneity. The legal aspect reviews spatial and regulatory policies affecting IWT at both provincial and district levels. Lastly, the environmental aspect assesses the use of watersheds and reservoirs, water quality and navigability, focusing on their implications for sustainable IWT operations.

Primary Data Collection:

Semi-structured interviews provided valuable insights into the challenges and opportunities directly perceived by local stakeholders. These interviews were conducted with representatives from government agencies, transportation operators, and community members who rely on IWT. Primary data complemented the secondary data analysis, enabling a more nuanced understanding of the current state and future potential of IWT in the region.

2.2.3 SWOT analysis and integration with PESTLE

The SWOT framework was employed to systematically evaluate the parameters identified through PESTLE. Strengths and weaknesses represent internal factors such as infrastructure capacity, operational efficiency, and resource availability, while opportunities and threats capture external factors, including governmental support, environmental risks, and socio-economic

Table 1 *Indigeneity Characteristics of IWT, source: [6-9]*

Indigeneity	Attributes	Characteristics
Locally Grown	Appropriate use of local resources	Being resource-efficient by using existing resources appropriately
	Domestically produced	Modes of transport are localized in response to the local community's needs.
Operated Locally	Serving the area without transportation infrastructure worthy	Transport facilities and infrastructure for the area served are not available or appropriate. Such as not having roads or bridges. So, the transport system is almost inadequate.
	Serve as transit passengers	Serves as transit transport or is used to complement other modes of transport in response to the surrounding community's needs.
Accepted Socially	Reachable	Affordable transport for the surrounding community.
	Source of livelihood for the lower middle class	As a privately operated livelihood and operating in a traditional environment
	Benefit vulnerable groups	Benefit vulnerable groups such as children, women, and the elderly
According to local culture	Support local culture	As a cultural part of the local community that grows and operates in a traditional environment
Adjust with technology	Adapt to the latest technology	Transport modes adapt to the latest technology to support greater capacity and shorten journey times.

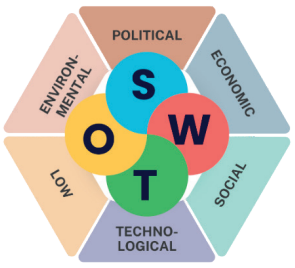

Figure 2 *Integration of PESTLE - SWOT Method*

dynamics. The integration of PESTLE and SWOT, as illustrated in Figure 2, provides a structured approach to understanding the challenges and opportunities for the IWT development in West Java. By categorizing and analyzing the key parameters, the combined framework provides actionable insights to support evidence-based policymaking and stakeholder engagement.

3 Results

3.1 Political aspects

The management of the Cirata Reservoir involves multiple institutional stakeholders, including the Cirata Reservoir Management Agency (BPWC – Badan Pengelola Waduk Cirata), PT Pembangkit Jawa Bali Cirata (PT PJB – Perseroan Terbatas Pembangkit Jawa Bali Cirata), the West Java Provincial Government, and the local governments of Cianjur, Purwakarta, and West Bandung districts. This multi-stakeholder management structure gives rise to various governance issues. Although the reservoir spans three districts, its management authority has been delegated to the West Java Provincial Government. Consequently, local policies, such as Regent Decrees and district-level regulations, do not apply to the reservoir.

Despite holding full authority, the West Java Provincial Government's programs often fail to address stakeholder needs due to limited human resources and conflicts arising from regional autonomy. Approximately 30% of local regulations are misaligned with provincial directives, further exacerbating inefficiencies. The BPWC, appointed by PT PJB with the Governor's approval, plays a crucial role in maintaining the reservoir but is limited to tasks like cleaning, greening, and monitoring water quality and quantity. However, stakeholders perceive the BPWC as the "owner" of the reservoir, overshadowing the provincial government. Overlapping policies and interests among stakeholders exacerbate tensions, complicating the integrated utilization of rivers and lakes in West Java.

Given the diverse functions of these water bodies - including navigation, water balance, and fisheries - formulating a shared sustainability vision is essential to resolving conflicts. Drawing lessons from the Netherlands, where a centralized water authority harmonizes policies across jurisdictions, [17] West Java could adopt a similar integrated governance framework to reduce policy fragmentation and improve stakeholder collaboration. Such an approach is particularly crucial for balancing the multifunctional roles of water bodies in navigation, fisheries, and water resource management.

Programs like Citarum Harum, based on Presidential Regulation No. 15/2018 on Controlling Pollution and Damage in the Citarum River Watershed, exemplify government efforts to improve water management. These initiatives have achieved significant progress, including a 25% improvement in water quality over five years, reducing pollution in the Citarum to a lightly polluted level. However, governance conflicts and limited resources hinder its broader impact. Additionally, the development of IWT is a key agenda in the 2024 West Java Regional Government Work Plan and in district-level plans, such as Pangandaran District Regulation No. 48/2022 on the 2023 Work Plan.

An integrated governance framework, inspired by successful models like the Netherlands, could help to align local and provincial polices, optimize resource allocation, and strengthen stakeholder collaboration. Such a framework is crucial for ensuring the sustainability and multifunctional utility of the Cirata Reservoir and other water bodies in West Java.

3.2 Economic aspects

Economic sector analysis, using the Location Quotient (LQ) metric, highlights strong development potential in various regions of West Java. For instance, Cianjur demonstrates a significant advantage in agriculture, forestry, and fisheries (LQ ≥1.5), while Bekasi showcase strengths in manufacturing and electricity supply (LQ ≥1.2). Purwakarta, West Bandung, and Pangandaran also display similar patterns, where agriculture, forestry, and fisheries dominate their respective regional economies. The findings suggest that Inland Waterway Transport (IWT) can play an important role in reducing logistics costs and facilitating market access, especially for export goods [18]. Figure 3 illustrates these economic benefits, emphasising the potential for sectoral growth through improved transport infrastructure.

The IWT implementation also supports local economic development by addressing logistical bottlenecks. Strengthening transport networks, especially waterways, not only improves the distribution of goods but also reduces road congestion. Figure 3 further underlines the potential for leading sectors to benefit from this infrastructure, facilitating inter-regional trade and export opportunities.

Passenger data (Figure 4) reveals seasonal fluctuations caused by sedimentation and water hyacinth growth, which reduce the channel depth by an average of 30%. The irregular positioning of the floating nets further exacerbates operational inefficiency, hampering the ship movements and passenger comfort. These factors have contributed to the decline in the number of passengers served in recent years [19-25].

Despite these challenges, the IWT fares remain highly affordable, ranging from IDR 5,000 to 7,000 (EUR 0.30–0.41), depending on the route and service area. For example, fares in Saguling range from IDR 5,000 to 7,000 (EUR 0.30–0.41), while boat rentals in Jatiluhur costs IDR 25,000 (EUR 1.47) for both long and short routes. In Kalipucang, fares start at IDR 15,000 (EUR

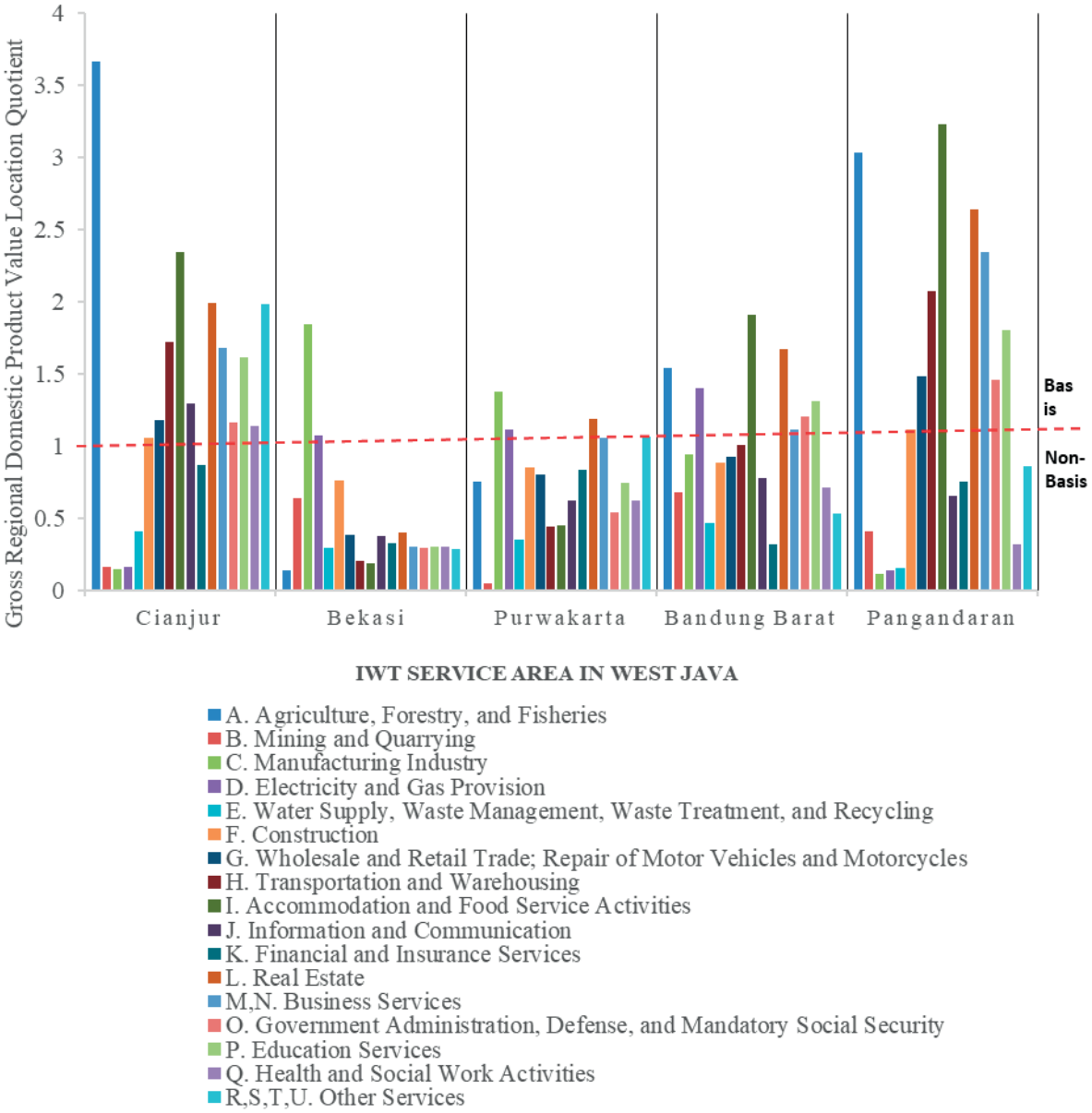

Figure 3 *Location Quotient Gross Regional Domestic Product Value*

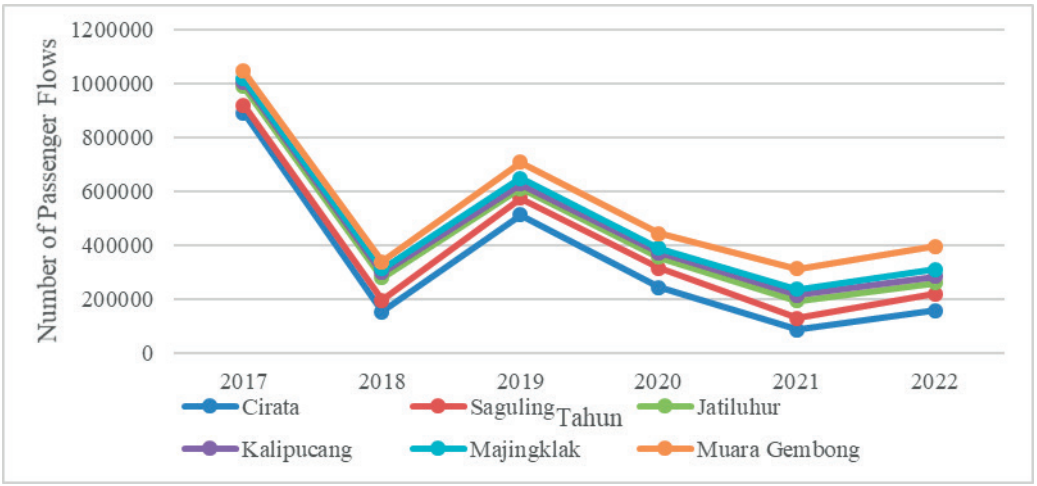

Figure 4 *Number of Passenger Flows in Cirata, Saguling, Jatiluhur, Kalipucang, Majingklak, Muara Gembong Service Areas, [28-29]*

0.88), with an additional charge for motorbike transport. These affordable rates ensure equitable access for lower - income populations, fostering economic inclusivity [21, 25].

Global experiences highlight the transformative potential of IWT integration. For example, the Rhine River in Europe has successfully connected trade hubs through multimodal transport systems, combining waterways with road and rail networks. This approach has significantly enhanced regional economic competitiveness and seamless trade connectivity [26-27]. West Java could adopt a similar framework to harmonize its transport infrastructure and maximize IWT's economic impact.

The environmental benefits of IWT are equally noteworthy. By offering a low-carbon alternative to road transport, IWT contributes to the reduction of greenhouse gas emissions, aligning with West Java's environmental goals. The integration of IWT has already resulted in a 15% reduction in road congestion, further enhancing transport efficiency across the region. These initiatives underscore the importance of sustainable transportation systems in supporting economic growth and environmental sustainability.

In conclusion, while challenges such as sedimentation and fluctuating passenger demand persist, the development of IWT presents significant opportunities for West Java. By leveraging affordable fares, enhancing transport infrastructure, and drawing lessons from global best practices, the region can foster economic equity, improve trade connectivity, and achieve its environmental objectives.

3.3 Socio-cultural aspects

The Inland Waterway Transportation (IWT) in West Java reflects significant socio-cultural characteristics, including community acceptance, local operation, and cultural compatibility. Previous studies have demonstrated IWT's vital role in supporting community mobility, particularly between Saguling and Batujajar, facilitating market access and educational activities, and stimulating local economic movements [18, 30]. Beyond providing access, IWT fosters economic integration between regions and strengthens social ties.

Affordability is another key aspect, ensuring accessibility for various socio-economic groups, particularly the middle and lower classes. For instance, fares in Saguling range from IDR 5,000 to 7,000 (EUR 0.30–0.41), while boat rental rates in Jatiluhur are IDR 25,000 (EUR 1.47) for both long and short routes. In Kalipucang, fares start at IDR 15,000 (EUR 0.88), and increase if transporting motorbikes. These affordable rates highlight IWT's role in promoting social equity and inclusivity.

The IWT complements other modes, particularly in areas with limited land infrastructure. It connects regions unreachable by road, facilitates goods distribution, and encourages social mobility. For instance, in Saguling, 60% of users rely on IWT for accessing markets and educational facilities.

The IWT is also deeply integrated with local cultural life. In the Cirata Reservoir, various recreational activities and traditional ceremonies, such as annual boat races organized by the Indonesian Rowing Sports Association at Jangari, underline the cultural significance of waterways [31]. Traditional boats like the Compreng in Majingklak and Kalipucang, and the Eretan in Muara Gembong, not only serve functional purposes but also preserve cultural heritage, reflecting traditions from the Javanese culture of Cirebon and the Tarumanegara Kingdom [32-33].

Despite these benefits, the IWT faces socio-environmental challenges. Waste mismanagement, particularly in the Citarum River Basin, causes severe pollution, disrupting ecosystems and affecting water quality. Of the 445,000 tons of waste generated annually, only 27% is processed, leading to health and environmental issues [34]. Learning from initiatives like India's Namami Gange program [35-37], West Java could adopt community engagement and technological interventions to mitigate pollution while preserving its socio-cultural identity.

3.4 Technology aspects

West Java's IWT systems reflect a blend of traditional craftsmanship and modern technology. Traditional watercraft, such as boat taxis in Cirata, Saguling, and Jatiluhur, Compreng boats in Kalipucang and Majingklak, and bamboo rafts in Muara Gembong, showcase local ingenuity. These vessels are often crafted by artisans in Cipeundeuy and Baleendah, emphasizing the region's skill in boat-making [38-39]. Motorized boats and fiberglass vessels have enhanced operational efficiency, but traditional crafts remain prevalent, particularly in areas like Muara Gembong. However, maintenance costs and inadequate infrastructure hinder their utilization, with 40% of vessels in Saguling underutilized due to inadequate infrastructure, as illustrated in Figure 5 [40].

Technological advancements in countries like Bangladesh - including digital navigation systems and maintenance subsidies - offer insights for revitalizing the IWT systems [41-42]. Implementing such innovations in West Java, along with operator training programs, could enhance efficiency and sustainability. Challenges such as irregular mooring facilities, insufficient docks, and inadequate equipment (e.g., fenders, jetties, and traffic signs) [43] persist in service areas like Cirata, Saguling, and Jatiluhur [30]. Addressing these infrastructure deficiencies is essential for improving operational reliability.

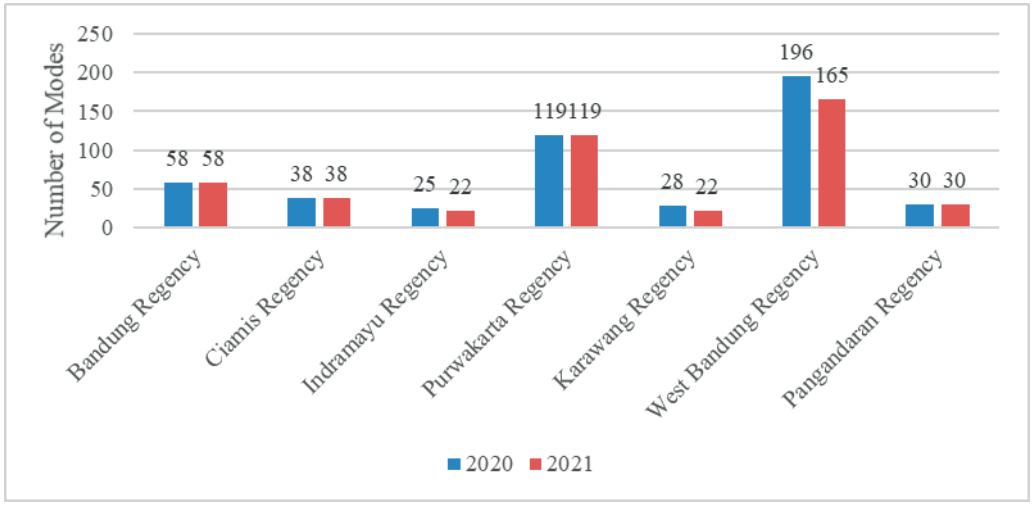

Figure 5 *Number of Modes of IWT, [12]*

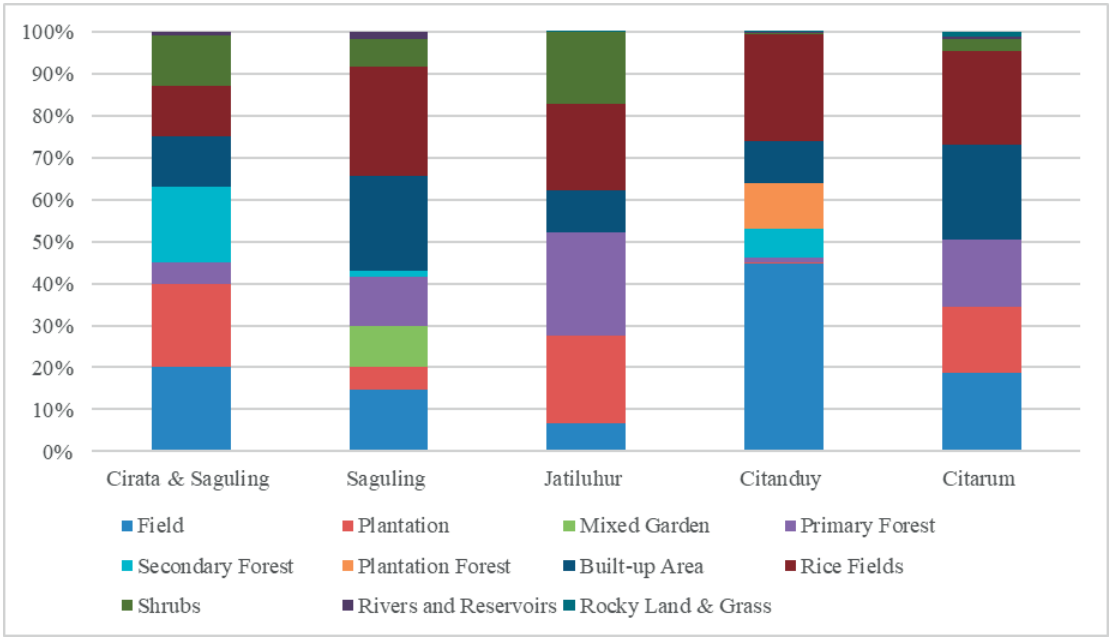

Figure 6 *Land Use of the West Java IWT River Basin / Reservoir, [55-59]*

3.5 Legal aspects

Provincial and district spatial plans in West Java incorporate zoning regulations to support the IWT development by safeguarding waterway corridors and restricting disruptive activities. Those plans outline critical infrastructure programs, such as river and lake crossing piers and transport routes, while enforcing restrictions to protect water bodies and shipping lanes [44-49].

However, enforcement remains inconsistent, with 35% of zoning violations attributed to inadequate regulatory oversight. The Mississippi River in the United States demonstrates the effectiveness of real-time monitoring and strict enforcement in maintaining waterway safety and efficiency [50]. By adopting similar practices, such as real-time tracking and robust regulatory frameworks, West Java could strengthen compliance and protect critical transport infrastructure

3.6 Environmental aspects

Environmental challenges significantly impact the IWT systems in West Java. Sedimentation, accumulating at 1.2 million cubic meters annually, and invasive water hyacinths reduce navigable capacity by up to 40% during peak seasons. These issues increase operational costs and disrupt services. For example, reservoirs like Cirata, Saguling, and Jatiluhur face declining waterway accessibility due to sediment build-up and water hyacinth growth [19, 51-52].

Land use surrounding watersheds, including agriculture, forestry, and urbanized areas, exacerbates these challenges by contributing to sedimentation and pollution. Figure 6 illustrates the impact of land use on transport demand, emphasizing the need for sustainable practices. Furthermore, overuse of driftnets in reservoirs exacerbates water pollution, complicating IWT operations [53-54].

Strategies from the Danube River, such as dredging and riverbank restoration, provide a model for addressing sedimentation and maintaining navigability. Adopting these measures in West Java, alongside regulating fishing activities and controlling water hyacinth growth, could enhance waterway resilience and operational sustainability [60-64].

4 Discussion

The PESTLE analysis presented in Section 3 was integrated into a SWOT matrix for IWTs in West Java, Indonesia (Table 2). The results highlighted key strengths, such as central government support for watershed management, affordable tariffs, and cultural integration of IWTs. Challenges faced, including overlapping policies and environmental issues, such as water hyacinth and sedimentation, were identified as weaknesses. Opportunities for the IWT development include promoting social equity and strengthening regulations. However, threats such as management inefficiencies and environmental degradation must be addressed to ensure sustainable growth of IWT services.

5 Conclusion

In this study is underscored both the significant potential and challenges in developing Inland Waterway Transportation (IWT) in West Java. Key opportunities

Table 2 *Matrix PESTLE_SWOT IWT West Java Indonesia*

	Strengths
Political	P1: Support from the central government on watershed management
Economic	Ec1: Have affordable fares for local people
Socio-Cultural	S1: Transport that is socially acceptable and integrated with local culture
Technological	T1: Transport modes have the characteristic of adjusting to technology
Legal	L1: Direction of controlling the spatial utilization of the shipping channel area in provincial and district spatial planning
Environmental	E1: Reduce carbon emissions
	Weaknesses
Political	P2: Overlapping policies and interests of various stakeholders
Economic	Ec2: Passenger flows tend to fluctuate (unstable)
Socio-Cultural	S2: Lack of public awareness of the importance of water resources (The habit of throwing garbage in the watershed or reservoir and the industrial community does not yet have a waste disposal permit)
Technological	T2: Inadequate mooring facilities
Legal	L2: The complexity of licensing and approval procedures may slow down IWT development.
Environmental	E2: Water hyacinth and garbage growth and sedimentation
	Opportunities
Political	P3: The West Java IWT development program is one of the important agendas of the West Java local government work plan
Economic	Ec3: Encourage regional base sector commodity distribution
Socio-Cultural	S3: Promoting social equality
Technological	T3: The mode or boat is a local innovation
Legal	L3: Opportunities to strengthen regulations favoring IWT transportation development through advocacy and collaboration with relevant stakeholders.
Environmental	E3: Diversity of land uses that have activities indicating potential transport demand
	Threats
Political	P4: Implementation of management policies that are considered ineffective
Economic	Ec4: The investment cost of maintaining shipping lanes by widening and dredging rivers and lakes, which is costly
Socio-Cultural	S4: Social conflicts or protests from local communities who feel aggrieved by the IWT arrangement
Technological	T4: The number of modes owned tends to remain fixed and decrease and there are still areas with modes that are not adaptive to technology.
Legal	L4: Risk of lawsuits from parties who feel aggrieved by the IWT arrangement
Environmental	E4: Distribution of driftnet cages

include strong governmental support, affordable fares promoting social equity, and alignment with local cultural and technological contexts. The IWT's potential to reduce carbon emissions and facilitate economic growth through improved commodity distribution further enhances its strategic value. However, environmental issues, such as sedimentation, water hyacinth proliferation, and waste mismanagement, pose significant barriers, compounded by infrastructure inadequacies, policy fragmentation, and economic challenges, including high investment costs and fluctuating passenger demand. These factors collectively impede the development of a sustainable and efficient IWT system in the region.

To address these challenges, a multi-faceted strategy is essential. This includes centralizing governance to align policies, modernizing infrastructure, and implementing sediment and waste management programs to enhance the environmental sustainability. Environmental protection is a crucial and inseparable part of any economic activity that significantly impacts the environment; therefore, economic development must be conducted in an environmentally safe manner [65]. Technological advancements, such as motorized boats and digital navigation systems, should be promoted, alongside preserving cultural heritage through traditional boat integration. Strengthening multimodal connectivity and exploring new trade routes can further boost economic viability. With a coordinated and evidence-based approach, the IWT in West Java can become a cornerstone of sustainable transportation, fostering economic equity, reducing environmental impacts, and preserving the local cultural identity.

Acknowledgements

The authors received no financial support for the research, authorship and/or publication of this article.

Conflicts of interest

The authors declare that they have no known competing financial interests or personal relationships that could have appeared to influence the work reported in this paper.

References

[1] ISPANDIARI, A. R., FAUZI, I., KARTIKASARI, D., SADIAH, S., SHABRINA, N., GUTAMI, N. I. Initial identification of seaplane accident risk at a marine airport. *G-Tech: Journal of Applied Technology* [online]. 2022, **6**(2), p. 201-210. ISSN 2580-8737, eISSN 2623-064X. Available from: https://doi.org/10.33379/gtech.v6i2.1682

[2] TRIVEDI, A., JAKHAR, S. K., SINHA, D. Analyzing barriers to inland waterways as a sustainable transportation mode in India: a dematel-ISM based approach. *Journal of Cleaner Production* [online]. 2021, **295**, 126301. ISSN 0959-6526, eISSN 1879-1786. Available from: https://doi.org/10.1016/j.jclepro.2021.126301

[3] MIRCETIC, D., NIKOLICIC, S., BOJIC, S., MASLARIC, M. Identifying the barriers for development of inland waterway transport: a case study. *MATEC Web of Conferences* [online]. 2017, **134**, 00039. eISSN 2261-236X. Available from: https://doi.org/10.1051/matecconf/201713400039

[4] PLOTNIKOVA, E., VIENAZINDIENE, M., SLAVINSKAS, S. Development of inland waterway transport as a key to ensure sustainability: a case study of Lithuania. *Sustainability* [online]. 2022,**14**(17), 10532. eISSN 2071-1050. Available from: https://doi.org/10.3390/su141710532

[5] CAHYADI, D., SUTANHAJI, A. T. Morpho-hydrology operators on DEM (Digital Elevation Model) and digital maps for initial mapping of hydroelectric power plant and microhydro power plant potential (case study of Mamberamo watershed). *Journal of Natural Resources and Environment*. 2013, **1**(1), p. 1-6. eISSN 2710-8724.

[6] UTOMO, D. M., MATEO-BABIANO, I. Exploring indigeneity of Inland Waterway Transport (IWT) in Asia: case studies of Thailand, Vietnam, the Philippines, and Indonesia. *East Asian Transport Studies* [online]. 2015, **11**, 2316. eISSN 1881-1124. Available from: https://doi.org/10.11175/easts.11.2316

[7] CERVERO, R. *Informal transport in the developing world*. Nairobi: United Nations Centre for Human Settlements (Habitat), 2000. ISBN 92-1-131453-4.

[8] AMES, A., MATEO-BABIANO, I. B., SUSILO, Y. O. Transport workers' perspective on indigenous transport and climate change adaptation. *Transportation Research Record: Journal of the Transportation Research Board* [online]. 2014, **2451**(1), p. 1-9. ISSN 0361-1981, eISSN 2169-4052. Available from: https://doi.org/10.3141/2451-01

[9] MATEO-BABIANO, I. B., SUSILO, Y. O., ENG, D., DANIELLE, M., GUILLEN, V., JOEWONO, T. B. Indigenous transport futures: a strategy for Asian cities toward climate change adaptation. In: Eastern Asia Society for Transportation Studies (EASTS) Conference: proceedings. 2011.

[10] Archaeological remains of Jukung in South Kalimantan: evidence of the prototype of modern Banjar Jukung, and floating markets as archaeological-based tourism objects [online] [accessed 2023-03-08]. 2012. Available from: https://iaaipusat.wordpress.com/category/pia-2011/

[11] West Java transport GIS 2017 - West Java Transportation Agency [online] [accessed 2023-03-06]. Available from: http://dishub.jabarprov.go.id/gis.html

[12] Number of river, lake and ferry transport modes by regency/city in West Java - West Java Transportation Agency [online]. Available from: https://OpendataJabarprovGo.Id/2022
[13] AGUILAR, F. J. *Scanning the business environment*. Macmillan, 1967.
[14] LEARNED, E., CHRISTENSEN, C., ANDREWS, K., GUTH, W. Business policy: text and cases. In: *Strategy and the strategy formation process*. HAX, A. C., MAJLUF, N. S. (Eds.). Homewood, IL: Richard D Irwin, 1986.
[15] VAJARI, S. M., ASL, I. M., HAJINABI, K., RIAHI, L. An ANP and MULTIMOORA-based SWOT analysis for strategy formulation management SWOT MULTIMOORA ANP medical equipment management medical equipment replacement. *Iranian Journal of Optimization*. 2019, **11**(2), p. 161-176. ISSN 2588-5723, eISSN 2008-5427.
[16] SEVKLI, M., OZTEKIN, A., UYSAL, O., TORLAK, G., TURKYILMAZ, A., DELEN, D. Development of a fuzzy ANP based SWOT analysis for the airline industry in Turkey. *Expert Systems with Applications* [online]. 2012, **39**(1), p. 14-24. ISSN 0957-4174, eISSN 1873-6793. Available from: https://doi.org/10.1016/j.eswa.2011.06.047
[17] DUIJN, M., VAN BUUREN, A., EDELENBOS, J., VAN POPERING-VERKERK, J., VAN MEERKERK, I. Community-based initiatives in the Dutch water domain: the challenge of double helix alignment. *International Journal of Water Resources Development* [online]. 2019, **35**(3), p. 383-403. ISSN 0790-0627, eISSN 1360-0648. Available from: https://doi.org/10.1080/07900627.2019.1575189
[18] LITA, I. Saguling boat taxi. Indonesia Morning Show NET, 2016.
[19] ARIFIANTO, B. Water hyacinth returns to Cirata reservoir in West Bandung Regency. People's Mind, 2023.
[20] BUDIANTO, A. Snagged by water hyacinth, boat carrying 23 passengers stuck in Jatiluhur reservoir - Megapolitan Okezone Com [online] [accessed 2023-03-09]. 2021. Available from: https://megapolitan.okezone.com/read/2021/10/17/338/2487707/tersangkut-eceng-gondok-perahu-bawa-23-penumpang-terjebak-di-waduk-jatiluhur
[21] CHAZAR, I. Rejuvenating the Jatiluhur reservoir - Mediaindonesia Com [online] [accessed 2023-03-09]. 2018. Available from: https://mediaindonesia.com/weekend/195303/menyehatkan-kembali-waduk-jatiluhur
[22] Sector 12 and Bpwc move quickly to handle water hyacinth in Cirata - citarumharum [online] [accessed 2023-03-09]. 2021. Available from: http://citarumharum.jabarprov.go.id/
[23] Citarum Recedes, Sector 7 dredges sediment - citarumharum [online] [accessed 2023-03-09]. 2022. Available from: https://citarumharum.jabarprov.go.id/citarum-surut-sektor-7-lakukan-pengerukan-sedimen/
[24] Sector 9 patrols water hyacinth and garbage removal in Saguling - citarumharum [online] [accessed 2023-03-09]. 2022. Available from: https://citarumharum.jabarprov.go.id/sektor-9-patroli-pengangkatan-eceng-gondok-dan-sampah-di-saguling/
[25] Newswire. Cirata reservoir water quality polluted by floating nets. BisnisCom [online] [accessed 2023-03-09]. 2018. Available from: https://foto.bisnis.com/view/20181203/865706/javascript
[26] Barge containers, volumes and outlook - Rhine Transport 2022 [online] [accessed 2025-01-27]. 2024. Available from: https://www.identecsolutions.com/news/rhine-transport-2022-barge-containers-volumes-and-outlook
[27] WOJCIECHOWSKI, P. Rhine Alpine. Fourth Work Plan of the European Coordinator. Brussels, Belgium: 2020.
[28] Surveillance activities at Each Jetty during Eid Mubarak Holidays. 2022.
[29] Monitoring passenger boarding and unloading and loading and unloading of cargo. 2022.
[30] HUMAEDI, A. O. Evaluation of the Jetty at the Jatiluhur Serpis Jetty in the Ir. H. Djuanda reservoir, West Java Province. Traffic Study Programme for River, Lake, and Crossing Transportation Polytechnic of Indonesian Land Transportation, 2021.
[31] HIDAYATULAH, S. Cirata Jangari reservoir becomes the location for rowing boat competition - Online Expert [online] [accessed 2023-03-17]. 2022. Available from: https://pakuanraya.com/waduk-cirata-jangari-jadi-lokasi-lomba-perahu-dayung/
[32] JASTRO, E. Study of traditional Indonesian boats at the maritime museum. North Jakarta: University of Indonesia, 2010.
[33] MULYADI, A. Citarum expedition 2011 Eretan Iringi breathes life into the Citarum - KompasCom [online] [accessed 2023-03-21]. 2011. Available from: https://tekno.kompas.com/ead/2011/05/15/06380623/~Regional~Jawa?page=all#page3
[34] Waste management performance of the Citarum river basin - National Waste Management Information System Ministry of Environment and Forestry [online] [accessed 2024-03-28]. 2023. Available from: https://sipsn.menlhk.go.id/sipsn/public/home/das/1
[35] Restoring and rejuvenating the Ganga river - Revolve 2024. Shreya [online] [accessed 2025-01-27]. Available from: https://revolve.media/interviews/restoring-the-ganga-river
[36] CHAURASIA, D. K., RANA, N. K., SHARMA, V. N. From pollution to preservation: impacts of the Namami Gange project on the Ganga river ecosystem in the Varanasi urban area. *Journal of Research in Environmental and Earth Sciences* [online]. 2024, **10**(10), p. 1-8. eISSN 2348-2532. Available from: https://doi.org/10.35629/2532-10100108

[37] DUTTA, V., DUBEY, D., KUMAR, S. Cleaning the river Ganga: impact of lockdown on water quality and future implications on river rejuvenation strategies. *Science of The Total Environment* [online]. 2020, **743**, 140756. eISSN 1879-1026. Available from: https://doi.org/10.1016/j.scitotenv.2020.140756
[38] ANGGARA, D. In picture: Pagirikan village, Boat village in Indramayu regency - RepublikaCoId [online] [accessed 2023-03-09]. 2022. Available from: https://sindikasi.republika.co.id/berita/rfqawr314/desa-pagirikan-kampung-perahu-di-kabupaten-indramayu-1
[39] ARIFIANTO, B. In a remote Village, Cirata reservoir boat artisans survive - People's Mind [online] [accessed 2023-03-09]. 2020. Available from: https://www.pikiran-rakyat.com/bandung-raya/pr-01369218/di-perkampungan-terpencil-perajin-perahu-tepi-waduk-cirata-bertahan?page=3
[40] West Java Transportation Agency. Profile of the technical implementation unit of the river, lake and crossing transport office. 2018.
[41] GUILLOSSOU, J. People's Republic of Bangladesh revival of inland water transport: options and strategies. The World Bank [online]. 2007. Available from: http://documents.worldbank.org/curated/en/329261468003908999
[42] HASSAN, M. M., XUEFENG, W. The challenges and prospects of inland waterway transportation system of Bangladesh. *International Journal of Engineering and Management Research* [online]. 2022, **12**(1), p. 132-143. ISSN 2394-6962, eISSN 2250-0758. Available from: https://doi.org/10.31033/ijemr.12.1.17
[43] NAUFAL, H. Analysis of ship docking facility needs in Cirata reservoir, Cianjur regency, West Java province in 2021. 2021.
[44] Bekasi District Government. Regional regulation of Bekasi regency on the spatial plan of Bekasi regency year 2011-2031. Indonesia, 2011.
[45] Cianjur District Government. Regional regulation on the spatial plan of Cianjur regency year 2011-2031. Indonesia: LD 2012/45, 2012.
[46] Pangandaran Regency Government. Regional regulation on the spatial plan of Pangandaran regency year 2018-2038. Indonesia, 2018.
[47] Government of Purwakarta Regency. Regional regulation on the spatial plan of Purwakarta regency year 2011-2031. Indonesia, LD.2012/11; 2012.
[48] West Bandung District Government. Regional regulation on the spatial plan of West Bandung regency year 2009-2029. Indonesia: LD 2012/No.2 Seri E, 2012.
[49] West Java Provincial Government. Regional regulation West Java provincial spatial plan 2009-2029. Indonesia: LD 2010/22 seri E, 2010.
[50] SNOW, S. Sensors and systems keep Mississippi river traffic flowing - Esri [online] [accessed 2025-01-27]. 2018. Available from: https://www.esri.com/about/newsroom/blog/keeping-inland-waterways-traffic-flowing/
[51] DEWANTARA, E. F., PURWANTO, Y. J., SETIAWAN, Y. management strategy of water hyacinth (eichorniacrassipes) Injatiluhur Reservoir, West Java. *Journal of Forestry Social and Economic Research* [online]. 2021, **18**(1), p. 63-74. ISSN 1979-6013, eISSN 2502-4221. Available from: https://doi.org/10.20886/jpsek.2021.18.1.63-74
[52] SUSANTI, R. 35,000 floating net cages threaten saguling hydroelectric power plant operations - KompasCom [online] [accessed 2023-03-10]. 2021. Available from: https://money.kompas.com/read/2021/11/12/131120826/35000-keramba-jaring-apung-ancam-operasional-plta-saguling
[53] BUDI, I. S. Influence of land use towards movement demand along Gadjah Mada street, Batam City. 2007.
[54] PAQUETTE, A. J. *Transportation planning*. New York: John Willey and Sons Inc.; 1908.
[55] ARKAN PRATAMA, F., CHAMID, C. The effect of land use on water quality of Jatiluhur reservoir West Java. *Journal of Urban and Regional Planning*. 2021, **16**, p. 1-8. ISSN 01412-0690.
[56] FADHIL, M. Y., HIDAYAT, Y., BASKORO, D. P. T. Identification of land use change and hydrological characteristics of the upper Citarum watershed. *Indonesian Journal of Agricultural Sciences* [online]. 2021, **26**(2), p. 213-220. ISSN 0853-4217, eISSN 2443-3462. Available from: https://doi.org/10.18343/jipi.26.2.213
[57] FERDIANSYAH, A., YUNINGSIH, S. M., GINANJAR, M. R., AKROM, I. F. Potential local flow discharge of Saguling reservoir using Rainfall Runoff modelling. *Journal of Water Resources* [online]. 2020, **16**(1), p. 35-50. ISSN 1907-0276, eISSN 2548-494. Available from: https://doi.org/10.32679/jsda.v16i1.606
[58] HIDAYAT, A. K., IRAWAN, P., HENDRA, IKHSAN, J., ATMADJA, S., SARI, N., KOMALA. Surface runoff Analysis and mapping in upper Citanduy das using SCSN method. *Journal Rona Agricultural Engineering*. 2021, **14**(1), p. 73-86. ISSN 2085-2614, eISSN 2528-2654. Available from: https://doi.org/10.17969/rtp.v14i1.17699
[59] NAGARANA, O. Y. Analysis of water balance changes in several land use scenarios with the GenRiver model and characterisation of population and stakeholders in the catchment area between Saguling and Cirata reservoirs. Bandung: Universitas Padjadjaran, 2016.
[60] AMIRUDDIN, F. The thick sediment deposits at the mouth of the Citanduy river are complained about by fishermen in the area. Detiknews, 2020.

[61] HAKIKI, I. A., SEMBIRING, L. E., NUGROHO, C. N. R. Sedimentation analysis of Segara Anakan lagoon by numerical modelling of cohesive sediment transport. *Journal of Hydraulic Engineering*. *Journal of Hydraulic Engineering* [online]. 2021, **12**(1), p. 1-14. ISSN 2087-3611, eISSN 2580-8087. Available from: https://doi.org/10.32679/jth.v12i1.642

[62] IRWAN, A., WICAKSONO, A., KHAIRIN, F. A. Identification of sedimentation load distribution in intake DAM and reservoir of hydropower plant (case study: Cirata hydropower plant, Purwakarta-West Java). 2020, 2.

[63] NOVIARINI, R. K., YUSUF, R., MARDIANI. Analysis of sedimentation rate and estimation of service life of Saguling reservoir, West Bandung regency. Indonesia: University of Education, 2019.

[64] SARACH SHEFTIANA, U., PURWANTO, M. Y. J., TARIGAN, S. D. Estimated sedimentation in 2018 in Jatiluhur reservoir, Purwakarta regency. *Journal of Soil and Environmental Sciences* [online]. 2021, **23**, p. 18-21. Available from: https://doi.org/10.29244/jitl.23.1.18-21

[65] FAUZI, I., ISPANDIARI, A. R. Green LNG Supply Chain: Optimizing Distribution in Eastern Indonesia. Evergreen [online]. 2024, 11(3), pp. 2624–2637. ISSN 2189-0420, 2432-5953. Available from: https://doi.org/10.5109/7236902.

SHOPPING TRIP MODELLING CONSIDERING THE IMPACT OF MARTIAL LAW

Mykola Zhuk[1], Halyna Pivtorak[1,2]*, Yevhen Pruskyi[1], Mykola Skyba[1]

[1]Department of Transport Technologies, Institute of Mechanical Engineering and Transport, Lviv National Polytechnic University, Lviv, Ukraine
[2]Department of Transport Management, Marketing and Logistics, Faculty of Transport Engineering, University of Pardubice, Pardubice, Czech Republic

*E-mail of corresponding author: halyna.v.pivtorak@lpnu.ua

Mykola Zhuk 0000-0003-1989-1053,
Yevhen Pruskyi 0009-0005-2364-3441,
Halyna Pivtorak 0000-0003-3645-1586,
Mykola Skyba 0009-0004-9057-2770

Resume
The purchasing behavior of the population affects both passenger and freight traffic in cities. On the contrary, indicators of purchasing behavior are influenced by the characteristics of an individual, as well as external factors. The purpose of the conducted research was to analyze the population's purchasing behavior under martial law conditions. Data was collected by surveying residents of Ukraine's rear regions. Multinomial models of the frequency of purchases and transportation choice during shopping were formed. Martial law conditions and changes in the population size in the rear regions, change the general trends in purchasing behavior. The most visible trends are: a significant share of purchases made online, the popularity of shopping close to home, and the tangible impact of owning a car on the frequency and mode of shopping trips. The results obtained may be helpful in predicting consumer behavior in crisis scenarios.

Article info
Received 14 October 2024
Accepted 29 January 2025
Online 25 February 2025

Keywords:
shopping trip
socio-demographic characteristics
multinomial logit model
martial law

Available online: https://doi.org/10.26552/com.C.2025.023

ISSN 1335-4205 (print version)
ISSN 2585-7878 (online version)

1 Introduction

Changes in logistical concepts associated with the development of production and changes in consumer expectations imply an increase in the frequency of deliveries, which, in contrast, reduces the required level of stocks and sizes of deliveries and ensures the speed of delivery desired by customers. Conversely, it raises the volume of freight traffic, increasing congestion, pollution and accidents [1]. Transport also consumes many energy resources [2].

Urban freight flows related to shopping consist of three main components [3]:

- movement patterns of the population for shopping in stores (markets, etc.) - shopping mobility,
- trips of commercial transport that delivers goods to stores (to markets, etc.) - shop restocking mobility,
- trips of commercial transport that delivers goods to online buyers - E-purchase delivering mobility.

The global COVID-19 pandemic had a significant impact on the purchasing behavior of the population in many countries, which is confirmed by numerous studies [4-6]. The volume of online purchases, which has already been actively growing since 2010, increased rapidly in 2020. According to the data from Statista, in 2020, the volume of global online sales totaled $4.29 trillion, which is $0.83 trillion higher than in 2019; in 2010, the volume of online trade totaled $572 billion. In 2023, the volume reached $6.52 trillion.

However, possible assumptions that the growth of online trade will significantly reduce the volume of purchases in physical stores are not conclusive at this time. According to previously conducted research, summarized in the work of Le et al. [7], four types of influence of online shopping on the behavior of the population during movements are distinguished:

- online purchases can *substitute* shopping trips (and, therefore, reduce their number),
- online purchases can *complement* shopping trips (and, therefore, increase their number),
- online shopping can *modify* the nature of shopping trips (change of routes, modes of transportation,

destinations, duration of trips, etc.),
- online purchases may not affect shopping trips.

There are still no definitive conclusions about whether substitution or complementation has more influence [8]. Some studies observe the effect of substituting physical shopping with online shopping [9-11], other studies confirm that online shopping complements shopping in stores [12-14]. According to Rai [15], the likelihood that active online shoppers will make fewer shopping trips is potentially limited.

The pandemic and related economic changes have impacted supply chains in general and last-mile logistics in particular [16]. It was the pandemic that highlighted the potential fragility of supply chains in the face of unpredictable risks [17]. However, unfortunately, the COVID-19 pandemic is not the only risk that logistics has faced in recent years. A full-scale Russian invasion of Ukraine in 2022 posed new challenges to supply chains [18-19]. The conditions of martial law impact not only logistical processes but the purchasing behavior of the population, as well.

Traditionally, work-related mobility is considered as the primary movement type in cities. Secondly, depending on the type of settlement, there is mobility related to education, leisure, or shopping. Nonetheless, shopping trips are most interconnected with urban freight traffic. The increase in demand for shopping leads to an increase in demand for delivery of goods to places of purchase, last-mile delivery and, in part, an increase in the volume of garbage removal.

In this paper were examined the peculiarities of the formation of demand for mobility to shop in the rear regions under the conditions of martial law, considering the following features:
- significant population growth in the rear regions due to internally displaced persons (IDPs),

Table 1 *Study of purchasing behavior parameters of the population that affect the frequency of purchases*

Reference	Research purpose	Survey place, sample size	Applied methods	Demographic characteristics	Other characteristics
Ding and Lu, 2017 [13]	correlation between online purchases and in-store purchases	Beijing (China), 537	Structural Equation Modelling	age, gender, occupation type, income level, household size, car availability	presence of a physical store, experience using the Internet
Lee et al., 2017 [12]	correlation between online purchases and in-store purchases	Davis, California, 2000	Pairwise Copula Models	education, occupation type, income level, car availability	shopping attitude factors, level of the physical store accessibility
Maat, K., Konings, R. (2018) [21]	online and in-store purchase frequency modelling	Leiden urban region (the Netherlands), 534	Binary Logit Model, Fractional Logit Model	age, gender, education, occupation type, income level, household size, car availability	goods type (books, clothes, groceries), physical store accessibility
Kalia, P. (2019) [22]	online purchase frequency modelling	India, 308	Chi-square Statistic	age, gender, education, occupation type, income level, marital status	-
Shi et al., 2019 [10]	correlation between online purchases and in-store purchases	Chengdu (China), 710	Regression Analysis	age, gender, education, income level, car availability, cost of living	goods type (clothes and shoes, electronics, food and drink, cosmetics)
Truong and Truong, 2022 [4]	influence of the pandemic	USA, U.S. Census Bureau data	Logistic Regression	age, gender, race, income level, marriage status	fears for health and financial conditions
Arranz-Lopez et al., 2023 [29]	correlation between online and in-store purchases	Germany, Mobilitat in Deutschland (MiD) survey data	Fractional Regressions	age, gender, education, income level	city size and the weekday: working day, weekend

Table 2 *Study of purchasing behavior parameters of the population*

Reference	Research purpose	Survey place, sample size	Applied methods	Demographic characteristics	Other characteristics
Comi and Nuzzolo, 2016 [3]	shopping model sub-system, which combines demand estimation for in-store and online purchases	Rome (Italy), 800	Multinomial Logit Model (MNL), Scenario Forecasting	age, gender, occupation type, household size	goods type (clothing, electronics, hygiene and household products, other goods)
Suel and Polak, 2017b [20]	general model that includes the choice of store, purchase method (offline or online) and shopping trip mode	London (UK), 121	Discrete Choice Modelling, Monte Carlo Method	age	distance to the physical store, cost of delivery when buying online
Russo and Comi, 2020 [24]	modelling the demand for urban shopping trips	Rome (Italy), 200	MNL	age, gender, occupation type, income level, household size	trip characteristic (trip time, accessibility), goods type and weight
Spurlock et al., 2020 [8]	modelling of the choice of receiving the purchase method (delivery or trip)	California (USA), 1012	MNL	age, income level, presence of children in the household	goods type (groceries, clothing, household items, meals), population density
Tao et al., 2022 [28]	changes in purchase behavior under the influence of the pandemic	China, 1742	Regression Analysis	age, gender, education, income level	purchase object, place, timeframe, and method
Vrba et al., 2024 [30]	demand for online shopping (the difference in the buying behavior of local residents and foreign city users)	Czech Republic, 307	MNL	age, gender, foreign city user status	-

- curfew and related restrictions in the work of shopping establishments, public transport (PT) and movement in general,
- suspending trading establishments during the working hours due to air raid alarms or lack of electricity.

In general, in the context of military operations, rear regions are considered to be areas located away from the front line and active combat, providing relative safety for the placement of critical infrastructure, industrial enterprises, and humanitarian aid. The Government of Ukraine, as of 2024, classified seven Ukrainian regions as rear areas (for more details, see section 3.1).

Given the secrecy of most statistical data under martial law, the study's information was collected by conducting questionnaire surveys. The paper is organized as follows. Section 2 presents the results of the analysis of literary sources on the study of the purchasing behavior of the population and modeling of the parameters of demand for purchases. Section 3 describes the results of surveys conducted to study the purchasing behavior of the population of differently sized settlements in the rear regions of Ukraine during the period of martial law. Section 4 presents the results of the formation of logit models of the frequency of purchase and the choice of the mode of transportation when making a purchase, which are the components of the general model of the demand for purchases. A discussion of the obtained results and conclusions is given in Section 5.

2 Literature review

Within the literature review, the focus was on sources related to the study of the population's purchasing behavior and modelling the parameters of demand for purchases (Tables 1-3).

Table 1 presents research focused on modelling the frequency of purchases.

Table 3 presents research aimed at the choice of the mode of transport for the shopping trip.

According to the scientists, the main indicators, characterizing the purchasing behavior, are: the time of purchase, the place of purchase, the method of purchase and the method of movement after the purchase. Purchasing behavior is influenced by the socio-demographic characteristics of an individual, as

Table 3 *Study of purchasing behavior parameters of the population that affect the mode of shopping trips*

Reference	Research purpose	Survey place, sample size	Applied methods	Demographic characteristics	Other characteristics
Meena et al., 2019 [23]	mode choice for shopping mall trip modeling (for economically developing region)	Mumbai, 650	MNL, Nested Logit	age gender occupation type income level car availability	-
Anwari et al., 2021 [25]	purchase frequency and mode choice in shopping trip modelling (impact of the COVID-19 pandemic for economically developing region)	Bangladesh, 572	Ordinal Logistic Regression, Sankey Diagrams	age gender occupation type income level region of living	-
Ramezani et al.,_2021 [26]	mode choice modelling in shopping trips (focused on older adults -aged 55-75)	Helsinki (Finland), 607	Factor Analysis, Integrated Choice and Latent Variable Model	gender income level having a pet living in an apartment	travel time cost and frequency
Zhang et al., 2021 [27]	mode choice modelling in shopping trips (focused on millennials)	Beijing (China), 1555	MNL, latent class model	income level household size car availability presence of children in the household	distance to the store, land use type, attitude to active movement types

well as external factors (characteristics of land use, transport system parameters, etc.).

The work of Suel and Polak [9] includes a review of earlier studies related to the research of buyer behavior in choosing a place of purchase, frequency of purchase and mode of transportation for shopping. In addition, we did not conduct a more detailed review of the literature on the impact of online shopping on travel demand, as this is thoroughly covered in Le et al. [7].

Summarizing the literature review, it is mentioned to note the interest in modelling the behavior of transport systems users considering regional conditions and characteristics. Many studies use an integrated modelling approach, combining several methods for a more comprehensive analysis. The results obtained contribute to understanding the features of urban transport systems' functioning in different conditions and allow for the proposal of measures to increase the sustainability of transport systems.

The analysis also highlights several gaps in existing research. Firstly, only one study was found [30], which concerns Eastern European countries (however, it is worth noting that the search was conducted only among English-language sources). Although the impact on purchasing behavior of differences related to national culture is confirmed, for example, in the studies of Pena-Garcia_et al. [31], which focused on e-commerce and Liobikiene_et al. [32], which investigated "green" shopping. Secondly, apart from studies examining the impact of the COVID-19 pandemic, there are almost no studies conducted in cities (or countries) that examine the long-term effects of a particular risk factor (such as martial law).

3 Data collection and describing

The purpose of the conducted research was to determine the purchasing behavior of the population under long-term conditions of increased risk. To achieve our objectives, we use a step-by-step research approach, as illustrated in Figure 1: conducting a literature review about the study of purchasing behavior parameters of the population (Section 2), data collection using a survey and analyzing research conditions and data results (Section 3), formation of shopping trips model in martial law conditions (Section 4).

3.1 Peculiarities of the functioning of the rear regions of Ukraine under martial law

Russia's full-scale invasion of Ukraine caused, among other things, significant changes in the structure of the population and the displacement of Ukrainians. Millions of people were forced to leave their homes: as of June 2024, there are 3.3 million IDPs [33]. About a quarter of IDPs were received by the rear (according to the classification of the Cabinet of Ministers of Ukraine) western regions of Ukraine (Table 4) - 770 thousand

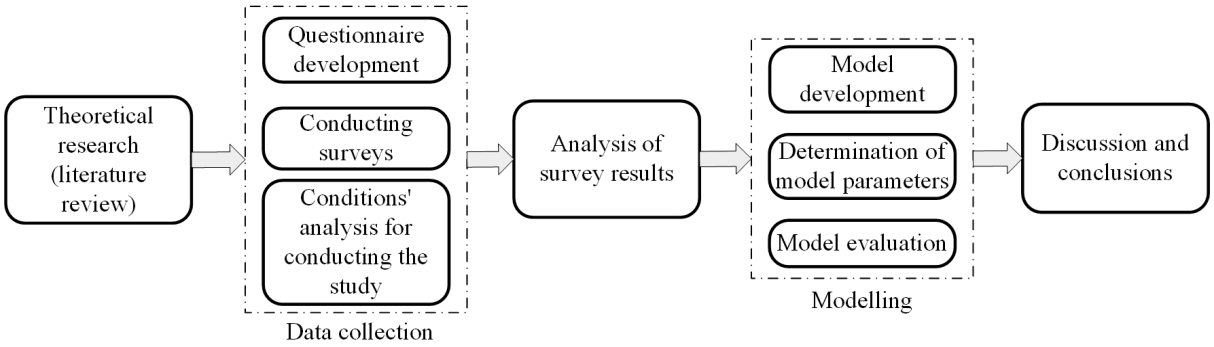

Figure 1 *Stages used in the study*

Table 4 *Some characteristics of the functioning of the rear regions of Ukraine*

Region	Number of officially registered IDPs as of June 2024: thousands of people	Change in population as of June 2024 compared to January 2022	Curfew	The period of PT operation in the regional center
Lviv region	213	+ 8%	00:00 - 05:00	06:00 - 22:00
Ivano-Frankivsk region	116	+9%	00:00 - 05:00	06:00 - 22:00
Ternopil region	66	+7%	00:00 - 05:00	06:00 - 21:00
Zakarpattia region	126	+10%	-	06:00 - 22:00
Volyn region	45	+5%	00:00 - 05:00	06:00 - 22:00
Rivne region	46	+4%	00:00 - 05:00	06:00 - 22:00
Chernivtsi region	88	+12%	00:00 - 04:00	06:00 - 22:00
Khmelnytskyi region	70	+7%	00:00 - 05:00	06:00 - 22:00

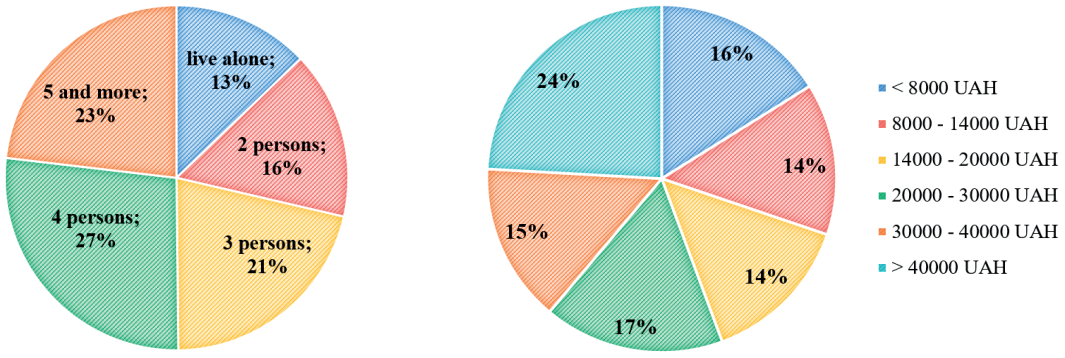

a) *b)*

Figure 2 *Structure of the sample of respondents: a) by household size, b) by the average monthly income of the household (during the survey period, 1 euro ≈ 43 UAH)*

people. The actual increase in the population in the rear regions is even higher since some of the people who moved from other regions are not registered as IDPs. The share of women among IDPs ranges from 60% (Rivne region) to 65% (Zakarpattia region), the share of the population aged 18 to 59 years - from 50% (Chernivtsi and Zakarpattia regions) to 60% (Lviv region) [33].

Changes in the parameters of population movements are affected not only by changes in its structure but also by other characteristics typical for martial law, in particular, the curfew and related restrictions on the work of both points of interest and transport.

Among the cities of the western part of Ukraine, Lviv belongs to a category of big cities with a population of more than 500 thousand people. Another seven cities have a population of 100 thousand to 500 thousand people, and 55 cities - from 10 to 100 thousand people. The total share of the urban population is 47% and varies from 37% in the Zakarpattia region to 61% in the Lviv region.

3.2 The structure of the interviewed sample

To collect data on the purchasing behavior of the population, an online questionnaire was created, which consists of three parts: purchasing behavior (frequency and places of purchases of groceries and non-food

products), data on the last purchase and socio-economic characteristics of the respondent. The resulting sample includes 323 responses: 37% from men and 63% from women. Among all the respondents, 54% are residents of Lviv (a large city with a population of more than 500 thousand people), 5% - residents of towns with a population of 100 thousand to 500 thousand people, 22% - residents of cities with a population of less than 100 thousand people and 19% - residents of rural settlements. The average age of respondents is 28 years, and 71% of respondents are under 30 years old. The total of 60% have a personal car in the household. The share of the working population in the sample is 41%, students - 52%. Data on the distribution of the sample of respondents by household size and average monthly household income is presented in Figure 2.

Since the share of residents of medium-sized cities in the sample structure is small, for further analysis, medium-sized and small cities are combined into one group.

3.3 General survey results

Among the residents of Lviv, half of the respondents chose several options for mode of transportation for the purpose of shopping, which they use with approximately the same frequency (Figure 3). In general, among this share of the population, there is an even distribution of movements by public transport and on foot (16% of respondents chose it as the main mode of movement and 16.5% use it regularly), slightly fewer respondents chose private transport (17% - as the main mode of movement and 11% use it regularly). Among residents of medium-sized and small cities, the majority of trips for shopping are made by private transport (33% of respondents consider it the main way to travel for shopping, and another 7% use it regularly). Among the residents of the villages, trips by personal transport also prevail: 38% chose it as the main type of movement when making purchases, and another 15% use it regularly).

When asked about the mode of transportation during the last purchase, 33% of respondents chose the option “personal car”, 19% chose “public transport”, 41% chose “walking”, and 7% chose the “Other” option.

General trends in frequency of purchases vary by product type. The settlement size has a more noticeable effect on the frequency of purchases of non-food products (Figure 4).

Most respondents shop for groceries several times a week: this is characteristic of 67% of rural residents and 73% of urban residents. Among residents of villages, the percentage of answers “once a week” and “several times a month” is slightly higher compared to residents of cities. This may be due to less available stores (smaller selection, greater distance to the store, etc.). The frequency of purchases of non-food products is expectedly lower: most respondents make such purchases several times a month. However, for residents of medium-sized and small cities, the difference in the frequency of such purchases is the smallest.

Analysis of the data on the popularity of making a purchase in various ways (Table 5) confirms some assumptions made during analyzing the distribution of purchases by frequency. In particular, rural residents are less likely to shop for groceries in stores within walking distance (61% of respondents against 68.5% of

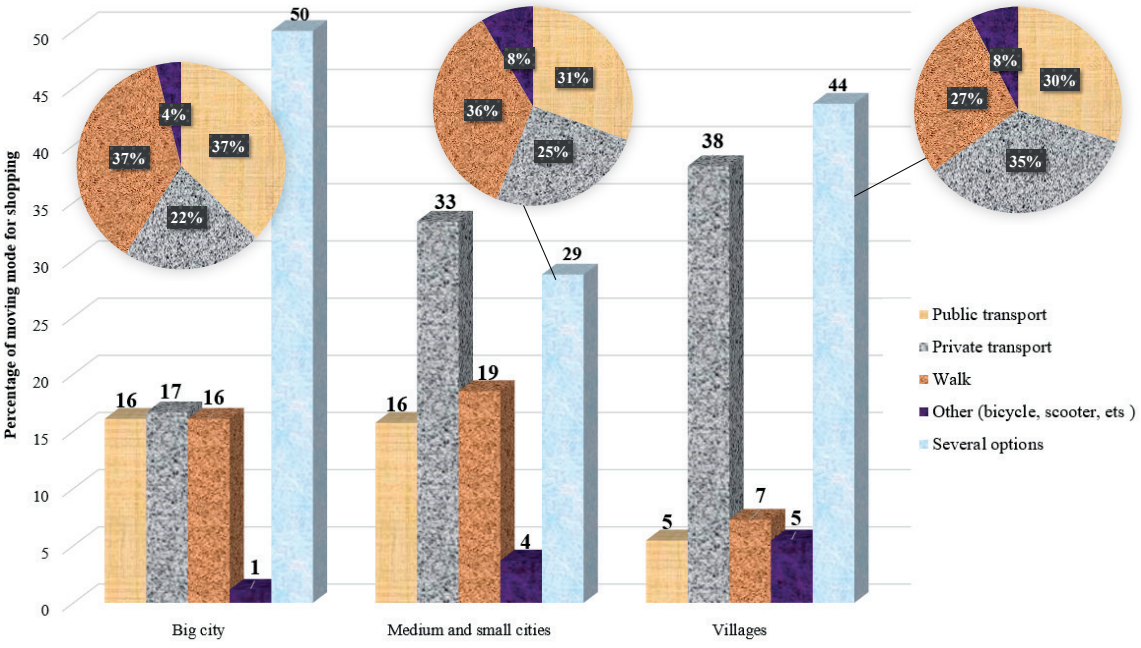

Big cities - cities with population >500 000 people (Lviv), medium and small cities - cities with population < 500 000 people

Figure 3 *Distribution of respondents’ answers regarding the mode of transportation for shopping*

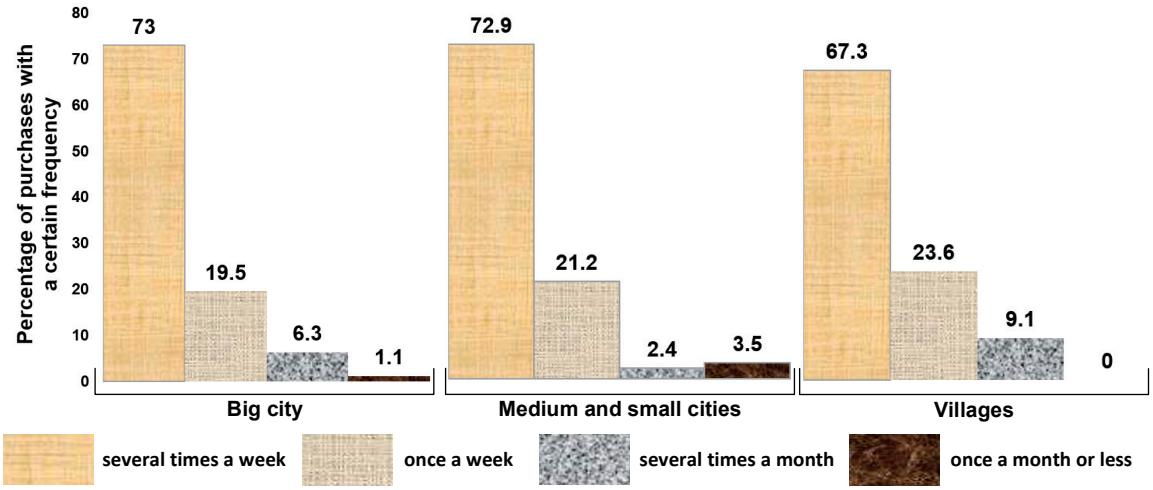

a)

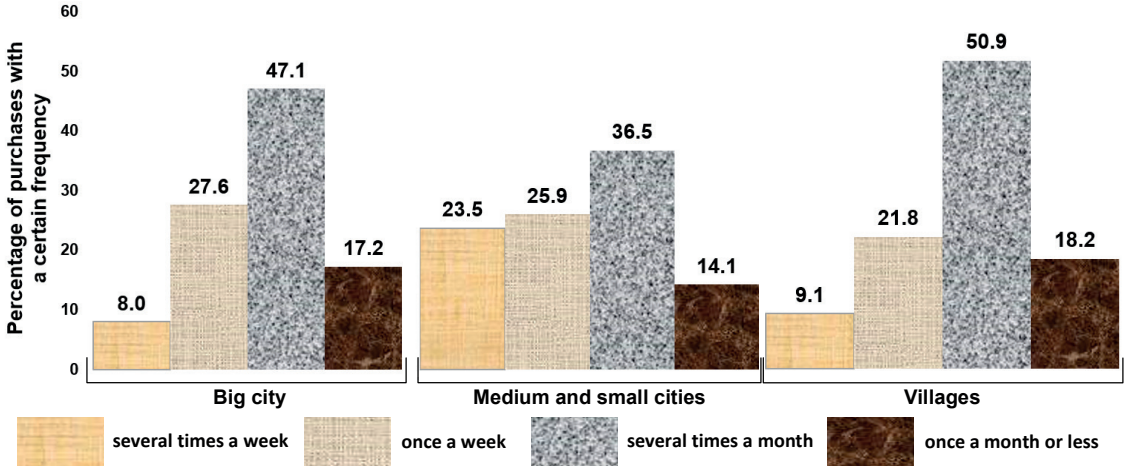

b)

Figure 4 *Frequency of purchases: a) groceries, b) non-food products*

Table 5 *Places where people usually shop (percentage of responses)*

Shopping place	Big cities		Medium and small cities		Villages	
	Groceries	Non-food products	Groceries	Non-food products	Groceries	Non-food products
Shops near the house	71.7	42.4	68.5	38.1	61.0	42.5
Trip to the shopping center	12.5	26.7	14.8	23.8	18.1	21.3
Online-shopping	15.8	30.9	16.7	38.1	21.0	36.3

residents of small and medium-sized cities and 72% of residents of large cities).

Among the respondents, 25% have never made online purchases of groceries and only 8% of non-food products. With a breakdown by the size of the settlement among the residents of Lviv, these values are 33% and 10%, respectively, among residents of medium and small cities - 19% and 6%, respectively, and among the inhabitants of villages - 17% and 9%.

The average purchase size does not differ significantly for residents of different settlements. Most respondents said that a purchase weighing up to 2 kg is "very typical" for them (55% of responses). At the same time, a purchase weighing more than 10 kg was called "very typical" by only 5% of respondents.

4 Results

4.1 Attributes of the travel mode choice model

A multinomial logit model (MNL), based on the utility theory, is used to estimate the parameters of shopping trips [34].

The formed MNL includes four options for mode of movement when making purchases:

- public transport (PuT),
- private transport (PrT),
  walking (w),
  bicycle, scooter, etc. (b).

The formula determines the probability of choosing a certain type of movement:

$$p_{\text{mod}}^{shopping} = \exp(V_{\text{mod}\_i}) / \sum_{i=1}^{4} \exp(V_{\text{mod}\_i}). \quad (1)$$

The benefits of using each of these modes of movement is a function of nine attributes:

$$V_{\text{mod}} = \sum_{i=1}^{9} (\beta_i \cdot attr_i) + asa, \quad (2)$$

where: *asa* - alternative specific attribute,
attr1 - settlement size: 1 - big cities, 2 - medium and small cities, 3 - villages,
*attr*2 - purchase size: 1 - up to 2 kg, 2 - from 2 to 5 kg, 3 - from 5 to 10 kg, 4 - more than 10 kg,
*attr*3 - car ownership: 1 - yes, 0 - no,
*attr*4 - age of respondent,
*attr*5 - gender of the respondent: 1 - male, 2 - female,
*attr*6 - household size: numbers from 1 to 4 correspond to the number of people in a household, number 5 - household size of 5 or more,
*attr*7 - average monthly household income: 1 - less than 8 thousand UAH (≈185 euro), 2 - from 8 thousand to 14 thousand UAH (≈185-325 euro), 3 - from 14 thousand to 20 thousand UAH (≈325-465 euro), 4 - from 20 thousand to 30 thousand UAH (≈465-700 euro), 5 - from 30 thousand to 40 thousand UAH (≈700-930 euro), 6 - more than 40 thousand UAH (≈930 euro),
*attr*8 - professional status: 1 if the consumer is a student, 0 otherwise,
*attr*9 - professional status: 1 if the consumer is employed, 0 otherwise.

The selected attributes characterize the proposed movement alternatives and the individuals (respondents) who make these trips. The relative convenience of each type of movement option depends on the purchase size. The settlement size affects the accessibility of the specific trip options.

4.2 Selection of the model parameters

The model parameters were calculated in the software product XLSTAT 2024.2.2.1422. Statistical quality indicators of the model are provided in Table 6 (Nagelkerke's $R^2 = 0.57$, Count $R^2 = 0.72$).

Low values of Pr > Chi² (<0.0001) in the log-likelihood test, the Score test and the Wald test indicate that the used variables contribute a significant amount of information to the model [35].

Values of model parameters allow for an analysis of the impact of individual attributes on the probability of choosing a certain mode of transportation for shopping. At the value of p > 0.10, a parameter is not considered significant for the model. According to the initial simulation results, the customer's gender is an insignificant parameter, so we decided to exclude it from the model. The final parameters of the model are provided in Table 7. The value of Tolerance > 0.1 indicates the absence of multicollinearity between attributes. When the mode of private transport is a reference modality, then:

Table 6 *Goodness of fit statistics*

Statistic	Chi-square	Pr > Chi²
-2 Log(Likelihood)	152.358	<0.0001
Score	126.941	<0.0001
Wald	78.575	<0.0001

Table 7 *Model parameters (reference modality - private transport)*

Coefficient of attribute	Tolerance	Public transport		Walking		Bicycle, Scooter	
		Value	p (Pr > Chi²)	Value	p (Pr > Chi²)	Value	p (Pr > Chi²)
ß1	0.786	0.005	0.987	-0.511	0.129	1.335	0.004‡
ß2	0.737	-0.721	0.041‡	-0.652	0.041‡	0.403	0.220
ß3	0.843	-3.279	< 0.0001‡	-2.884	0.000‡	-4.686	< 0.0001‡
ß4	0.390	-0.008	0.795	0.019	0.518	-0.094	0.032‡
ß6	0.762	0.022	0.915	0.018	0.927	-0.905	0.001‡
ß7	0.708	-0.307	0.081‡	-0.043	0.804	0.350	0.102
ß8	0.134	-1.141	0.461	-1.433	0.293	-5.105	0.001‡
ß9	0.198	-0.890	0.506	-1.639	0.160	-5.071	0.000‡
asa		6.024	0.010	5.308	0.013	8.077	0.003

‡ - the value of p < 0.10; the most significant parameters

$$\exp(V_{\mathrm{Pr}T}) = 1 + \exp(V_{PuT}) + \exp(V_w) + \\ + \exp(V_b). \quad (3)$$

Owning a car reduces the likelihood of using the public transport, walking, cycling or riding a scooter for shopping. Moreover, owning a car has the most significant negative impact on the likelihood of using bicycles or scooters. In addition, the probability of using own car increases compared to the probability of using public transport or walking with the increase in purchase size (for the bicycle/scooter mode, this attribute does not have a statistically significant impact). The probability of using public transport decreases with the growth of the household's average monthly income. However, income does not affect the change in probability of using active types of movement (walking and cycling or riding a scooter).

Assessing the impact of the remaining buyer's socio-economic characteristics on the change in probability of using other modes of transportation, in relation to the use of private transport, is practical to be carried out only for the bicycle/scooter mode (for the "public transport" and "walking" modes, the value of p > 0.10). Residents of smaller settlements are more likely to use a bicycle/scooter. However, the probability of using this mode of transportation will decrease compared to the probability of using private transport with the increase in the age of buyers and the increase in the number of people in the household.

4.3 Shopping frequency model attributes and parameters

A binomial logit model with two choice parameters has been used to estimate the frequency of food purchases:

- several times per week (1),
- once a week or less (2).

To estimate the frequency of purchases of non-food products, a multinomial logit model with four choice parameters has been used:

- several times per week (1),
- once a week (2),
- several times per month (3),
- once a month or less (4).

Based on the initial modelling results, the attributes that have a statistically significant impact on the frequency of purchases were determined.

The systematic utility of frequency of grocery purchases is expressed as a linear combination of such attributes:

$$V_{fr}^{food} = \beta_{gen} \cdot attr_{gen} + \beta_{in} \cdot attr_{in} + asa\,, \quad (4)$$

where: $attr_{gen}$ - gender: 1 - male, 2 - female,
$attr_{in}$ - average monthly income level of a household: from 1 to 6.

The probability of grocery purchase frequency of once a week or less:

$$p_{fr2}^{food} = 1/\left(1 + \exp(-V_2^{food})\right). \quad (5)$$

The systematic utility of frequency of non-food purchases is expressed as a linear combination of such attributes:

$$V_{fr}^{non-food} = \beta_{age} \cdot attr_{age} + \beta_{gen} \cdot attr_{gen} + \\ + \beta_{car} \cdot attr_{car} + \beta_{city} \cdot attr_{city} + asa, \quad (6)$$

where: $attr_{age}$ - age of customer,
$attr_{car}$ - owning a car: 1 - yes, 0 - no,
$attr_{city}$ - settlement size: 1 - big city, 2 - medium and small cities, 3 - villages.

The parameters of the binomial model for the frequency of purchasing groceries are presented in Table 8 (Nagelkerke's $R^2 = 0.16$, Count $R^2 = 0.65$).

Values of grocery shopping frequency model parameters are presented in Table 9.

The probability of grocery shopping several times a week increases as the average monthly income level of the household goes up. Women are also more likely to shop for groceries more often than men.

The parameters of the multinomial model of the purchasing frequency of non-food products are presented in Table 10 (Nagelkerke's $R^2 = 0.11$, Count $R^2 = 0.53$)

Table 8 *Goodness of fit statistics*

Statistic	Chi-square	Pr > Chi²
-2 Log(Likelihood)	15.807	0.000
Score	15.493	0.000
Wald	14.876	0.001
Hosmer-Lemeshow Statistic	65.062	<0.0001

Table 9 *Model parameters (reference modality - purchase`s frequency several times per week)*

Coefficient of attribute	Tolerance	Value	p (Pr > Chi²)
βgen	0.995	-0.605	0.010
βincome	0.995	-0.201	0.002
asa		1.701	0.000

Table 10 *Goodness of fit statistics*

Statistic	Chi-square	Pr > Chi²
-2 Log(Likelihood)	33.667	0.001
Score	33.003	0.001
Wald	30.457	0.002

Table 11 *Model parameters (reference modality - purchase`s frequency several times per week)*

Coefficient of attribute	Tolerance	Once a week		Several times per month		Once a month or less	
		Value	p (Pr > Chi²)	Value	p (Pr > Chi²)	Value	p (Pr > Chi²)
βage	0.962	0.020	0.215	0.024‡	0.143	0.044	0.004‡
βgen	0.970	0.114	0.729	0.649	0.057‡	0.210	0.535
βcar	0.974	-0.761	0.037‡	-0.984	0.007‡	-1.173	0.001‡
βcity	0.987	-0.291	0.056‡	-0.318	0.043‡	-0.240	0.004‡
asa		0.438	0.552	-0.345	0.651	-0.225	0.762

‡ - the value of p < 0.10; the most significant parameters

The values of the parameters of the non-food shopping frequency model are provided in Table 11.

As the age of the respondent increases, the frequency of non-food purchases decreases (the probability of making purchases of non-food products with a frequency of "once a month or less" increases compared to the probability of making such purchases with a frequency of "several times a week"). Women are more likely than men to make such purchases with a frequency of "several times per month" rather than "several times per week". Owning a car and living in a smaller settlement increases the frequency of non-food purchases.

4.4 Demand model of purchase

Based on Russo and Comi [36], the number of shopping trips generated by the transport area O can be determined by the equation:

$$N^{O}_{shopping} = N^{O}_{res} \cdot p_{shopping}\,, \tag{7}$$

where: N^{O}_{res} - the number of residents in the transport area of departure O,
$p_{shopping}$ - the probability of making a purchase.

The number of trips in the transport system caused by the need to make a purchase will be:

$$N^{O}_{\mathrm{Pr}T} = N^{O}_{shopping} \cdot p^{shopping}_{\mathrm{Pr}T}\,, \tag{8}$$

$$N^{O}_{PuT} = N^{O}_{shopping} \cdot p^{shopping}_{PuT} \tag{9}$$

where: $N^{O}_{\mathrm{Pr}T}$ - the number of movements with the purpose of purchasing within the transport area of departure *O*, made by private transport,
N^{O}_{PuT} - the number of movements with the purpose of purchasing within the transport area of departure *O*, made by public transport,
$p^{shopping}_{\mathrm{Pr}T}$ - the probability of choosing private transport as a mode of transportation to make a purchase,
$p^{shopping}_{\mathrm{Pr}T}$ - the probability of choosing public transport as a mode of transportation to make a purchase.

The overall probability of purchasing depends on the frequency of purchases of a certain product type.

For groceries:

$$p_{shopping} = p_{fr(1)} \cdot \overline{p_{fr(2)}} + \overline{p_{fr(1)}} \cdot p_{fr(2)}\,. \tag{10}$$

For non-food goods:

$$\begin{aligned} p_{shopping} = {} & p_{fr(1)} \cdot \overline{p_{fr(2)}} \cdot \overline{p_{fr(3)}} \cdot \overline{p_{fr(4)}} + \overline{p_{fr(1)}} \cdot \\ & \cdot p_{fr(2)} \cdot \overline{p_{fr(3)}} \cdot \overline{p_{fr(4)}} + \overline{p_{fr(1)}} \cdot \overline{p_{fr(2)}} \cdot p_{fr(3)} \cdot \\ & \cdot \overline{p_{fr(4)}} + \overline{p_{fr(1)}} \cdot \overline{p_{fr(2)}} \cdot \overline{p_{fr(3)}} \cdot p_{fr(4)}, \end{aligned} \tag{11}$$

where: $p_{fr(1)}, p_{fr(2)}, p_{fr(3)}, p_{fr(4)}$ - the probability of making a purchase with a certain frequency (see section 4.3),
$\overline{p_{fr(i)}} = 1 - p_{fr(i)}$ - the probability that an individual will not make a purchase with a certain frequency.

5 Discussion and conclusions

The purpose of the conducted research is to determine the purchasing behavior of the population under the long-term conditions of increased risk. Data collection for the study was carried out by surveying the residents of the rear regions of Ukraine under martial law.

According to survey results, 92% of respondents purchase at least once a week. This frequency of making purchases is slightly higher than the data for other countries and regions: according to Statista, these figures range from 75% to 87%. However, the obtained results are consistent with the research of Larson and Shin [37] on the purchasing behavior of the population

during natural disasters. People may purchase more often out of fear of shortages or anxiety about rising prices (and the desire to stock up) and for a hedonistic purpose.

According to the studies conducted, in general, the frequency of making purchases is influenced by socio-economic characteristics such as age, gender, income level, and ownership of a car. The frequency of grocery purchases is affected by fewer factors, which is expected since these are products of daily consumption and are needed by all population categories.

The frequency of purchasing groceries is more significant for women than for men, which is consistent with many other studies [10, 13, 29]. However, men are more likely to purchase non-food items.

Having a higher income also increases the frequency of purchasing groceries, although the effect of gender is more pronounced. The results for the impact of income differ from some of the other studies where the dependency is reversed [10, 27, 29]. Shi et al. [10] explained the decrease in shopping frequency of people with higher income levels by the fact that they can drive to the mall and buy more goods in one trip. However, according to our research, most grocery purchases are made at stores within walking distance of one's home, and driving to the mall is less likely than even online shopping. A possible explanation could be the reluctance to go shopping relatively far from home due to the risk of an air raid alarm (and therefore closing of the store), which would obviously increase the time spent shopping (among other inconveniences and dangers). Therefore, the population prefers to make more frequent purchases of smaller quantities of goods closer to home.

The frequency of purchasing non-food products also depends on the settlement size and having a personal car. All the other conditions being equal, the frequency of purchases of non-food goods increases with a decrease in the settlement size. At the same time, the actual probability of such a purchase several times a week is higher for individuals who have a personal car (compared to those who do not own a car), and this difference is more significant for villages. The possible explanation would be a smaller selection of non-food goods in village stores, thus the need to travel to another settlement for them, so people who own a car make such purchases more often, as they are more mobile.

An increase in age has little effect on the probability of making purchases of non-food products with the frequency of "Once a week" and "Several times per month". Instead, it decreases the probability of purchases with the frequency of "several times per week" and increases the probability of purchases with the frequency of "Once a month or less".

Owning a car has the greatest impact on the choice of the mode of transportation for shopping, and, quite expectedly, this parameter significantly increases the probability of choosing the private transport mode. It is interesting to note that the absence of a personal car does not significantly affect the probability of shopping on foot but significantly increases the probability of using the bicycle/scooter transportation mode. The second most impactful parameter is professional status. Moreover, this parameter has very little influence on the probability of using a personal car and bicycle/scooter transportation mode. However, students are more likely to travel on foot, while the working population is more likely to use the public transport.

As the settlement size decreases, the probability of using the bicycle/scooter transportation mode increases, but the probability of moving on foot decreases (perhaps, due to the increase of distance to the store).

The likelihood of using a personal car for shopping trips increases as the income level goes up. In general, this trend is also observed in other studies [26-27]. The probability of using a non-motorized type of movement also increases with the income level but is inverted for the probability of using public transport.

An increase in purchase size has a negative impact on the probability of walking and increases the probability of using private transportation.

It is worth highlighting the high level of online buyers - in general, 92% of respondents made an online purchase at least once during the last year. According to Eurostat data for 2023 [38], among European countries only the Netherlands (92%) and Norway (91%) had such a high share of online buyers (data for Ukraine is not available in the report). Conditions of war and martial law, such as:

- a significant proportion of IDPs do not know the surroundings well enough and prefer to shop online,
- restrictions and unpredictability in the working hours of stores due to air raid alarms,
- lack of electricity and curfews,
- lack of desired brands in physical stores due to issues in the supply chain,
- the possibility of a lower price of purchase, which can be an important factor under the conditions of deterioration of the population's financial situation,

as well as other conditions, can have an impact on the high value of this parameter, although additional research is required to confirm this hypothesis and determine the degree of influence of each of the listed factors. It is also interesting to note that the residents of villages make online purchases of groceries more often compared to the residents of cities (it may be related to a much wider range of products in online stores in combination with the efficient work of delivery services in Ukraine - both the national postal operator "Ukrposhta" and private services).

The obtained results can be helpful in developing measures to adjust logistic processes in long-term crisis situations, considering changes in population behavior.

It is worth noting that the study has limitations due to the complexity of data collection and the absence or confidentiality of statistical information during the martial law.

Acknowledgement

Halyna Pivtorak conducted this study during her participation in the MSCA4 Ukraine program (AvH ID 1233185). This project has received funding through the MSCA4 Ukraine project, which is funded by the European Union. Views and opinions expressed are however those of the author(s) only and do not necessarily reflect those of the European Union. Neither the European Union nor the MSCA4 Ukraine Consortium as a whole nor any individual member institutions of the MSCA4 Ukraine Consortium can be held responsible for them.

Conflicts of interest

The authors declare that they have no known competing financial interests or personal relationships that could have appeared to influence the work reported in this paper.

References

[1] CROCCO, F., DE MARCO, S., IAQUINTA, P., MONGELLI, D. W. Freight transport in urban areas: an integrated system of models to simulate freight demand and passengers demand for purchase trips. *International Journal of Mathematical Models and Methods in Applied Sciences*. 2010, **4**(4), p. 295-273. eISSN 1998-0140.

[2] MACIOSZEK, E., GRANA, A., FERNANDES, P., COELHO, M. C. New Perspectives and challenges in traffic and transportation engineering supporting energy saving in smart cities - a multidisciplinary approach to a global problem. *Energies* [online]. 2022. **15**(12), 4191. eISSN 1996-1073. Available from: https://doi.org/10.3390/en15124191

[3] COMI, A., NUZZOLO, A. Exploring the Relationships Between e-shopping Attitudes and Urban Freight Transport. *Transportation Research Procedia* [online]. 2016, **12**, p. 399-412. ISSN 2352-1457, eISSN 2352-1465. Available from: https://doi.org/10.1016/j.trpro.2016.02.075

[4] TRUONG, D., TRUONG, M. D. How do customers change their purchasing behaviors during the COVID-19 pandemic? *Journal of Retailing and Consumer Services* [online]. 2022, **67**, 102963. ISSN 0969-6989, eISSN 1873-1384. Available from: https://doi.org/10.1016/j.jretconser.2022.102963

[5] TYRVAINEN, O., KARJALUOTO, H. Online grocery shopping before and during the COVID-19 pandemic: A meta-analytical review. *Telematics and Informatics* [online]. 2022, **71**, 101839. ISSN 0736-5853, eISSN 1879-324X. Available from: https://doi.org/10.1016/j.tele.2022.101839

[6] ARYANI, D. N., NAIR, R. K., HOO, D. X. Y., HUNG, D. K. M., LIM, D. H. R., CHEW, W. P., DESAI, A. A study on consumer behaviour: Transition from traditional shopping to online shopping during the Covid-19 pandemic. *International Journal of Applied Business and International Management (IJABIM)* [online]. 2021, **6**(2), p. 81-95. AISSN 2614-7432, eISSN 2621-2862. Available from: https://doi.org/10.32535/ijabim.v6i2.1170

[7] LE, H. T. K., CARREL, A. L., SHAH, H. Impacts of online shopping on travel demand: a systematic review. *Transport Reviews* [online]. 2021, **42**(3), p. 273-295. ISSN 0144-1647, eISSN 1464-5327. Available from: https://doi.org/10.1080/01441647.2021.1961917

[8] SPURLOCK, C. A., TODD-BLICK, A., WONG-PARODI, G., WALKER, V. Children, income, and the impact of home delivery on household shopping trips. *Transportation Research Record: Journal of the Transportation Research Board* [online]. 2020, **2674**(10), p. 335-350. ISSN 0361-1981, eISSN 2169-4052. Available from: https://doi.org/10.1177/0361198120935113

[9] SUEL, E., POLAK, J. W. Incorporating online shopping into travel demand modelling: challenges, progress, and opportunities. *Transport Reviews* [online]. 2017, **38**(5), p. 576-601. ISSN 0144-1647, eISSN 1464-5327. Available from: https://doi.org/10.1080/01441647.2017.1381864

[10] SHI, K., DE VOS, J., YANG, Y., WITLOX, F. Does e-shopping replace shopping trips? Empirical evidence from Chengdu, China. *Transportation Research Part A: Policy and Practice* [online]. 2019, **122**, p. 21-33. ISSN 0965-8564, eISSN 1879-2375. Available from: https://doi.org/10.1016/j.tra.2019.01.027

[11] BJERKAN, K. Y., BJORGEN, A., HJELKREM, O. A. E-Commerce and prevalence of Last mile practices. *Transportation Research Procedia* [online]. 2020, **46**, p. 293-300. ISSN 2352-1457, eISSN 2352-1465. Available from: https://doi.org/10.1016/j.trpro.2020.03.193

[12] LEE, R. J., SENER, I. N., MOKHTARIAN, P. L., HANDY, S. L. Relationships between the online and in-store shopping frequency of Davis, California residents. *Transportation Research Part A: Policy and Practice* [online]. 2017, **100**, p. 40-52. ISSN 0965-8564, eISSN 1879-2375. Available from: https://doi.org/10.1016/j.tra.2017.03.001

[13] DING, Y., LU, H. The interactions between online shopping and personal activity travel behavior: an analysis with a GPS-based activity travel diary. *Transportation* [online]. 2017, **44**, p. 311-324. ISSN 0049-4488, eISSN 1572-9435. Available from: https://doi.org/10.1007/s11116-015-9639-5

[14] XI, G., ZHEN, F., CAO, X., XU, F. The Interaction between e-shopping and store shopping: empirical evidence from Nanjing, China. *Transportation Letters* [online]. 2020, **12**(3), p. 157-165. ISSN 1942-7867, eISSN 1942-7875. Available from: https://doi.org/10.1080/19427867.2018.1546797

[15] RAI, H. B. The net environmental impact of online shopping, beyond the substitution bias. *Journal of Transport Geography* [online]. 2021, **93**, 103058. ISSN 0966-6923, eISSN 1873-1236. Available from: https://doi.org/10.1016/j.jtrangeo.2021.103058

[16] SRINIVAS, S., MARATHE, R. Moving towards "mobile warehouse": last-mile logistics during COVID-19 and beyond. *Transportation Research Interdisciplinary Perspectives* [online]. 2021, **10**, 100339. eISSN 2590-1982. Available from: https://doi.org/10.1016/j.trip.2021.100339

[17] YOUNIS, H., ALSHARAIRI, M., YOUNES, H., SUNDARAKANI, B. The impact of COVID-19 on supply chains: systematic review and future research directions. *Operational Research* [online]. 2023, **23**, 48. ISSN 1109-2858, eISSN 1866-1505. Available from: https://doi.org/10.1007/s12351-023-00790-w

[18] KRYKAVSKYY, Y., CHORNOPYSKA, N., DOVHUN, O., HAYVANOVYCH, N., LEONOVA, S. Defining supply chain resilience during wartime. *Eastern-European Journal of Enterprise Technologies* [online]. 2023, **1/13**(121), p. 32-46. ISSN 1729-3774, eISSN 1729-4061. Available from: https://doi.org/10.15587/1729-4061.2023.272877

[19] ALLAM, Z., BIBRI, S. E., SHARPE, S. A. The rising impacts of the COVID-19 pandemic and the Russia-Ukraine war: energy transition, climate justice, global inequality, and supply chain disruption. *Resources* [online]. 2022, **11**, 99. eISSN 2079-9276. Available from: https://doi.org/10.3390/resources11110099

[20] SUEL, E., POLAK, J. W. Development of joint models for channel, store, and travel mode choice: grocery shopping in London. *Transportation Research Part A: Policy and Practice* [online]. 2017, **99**, p. 147-162. ISSN 0965-8564, eISSN 1879-2375. Available from: https://doi.org/10.1016/j.tra.2017.03.009

[21] MAAT, K., KONINGS, R. Accessibility or innovation? Store shopping trips versus online shopping. *Transportation Research Record: Journal of the Transportation Research Board* [online]. 2018, **2672**(50), p. 1-10. ISSN 0361-1981, eISSN 2169-4052. Available from: https://doi.org/10.1177/0361198118794044

[22] KALIA, P. Does demographics affect purchase frequency in online retail? In: *Gender Economics: Breakthroughs in Research and Practice* [online]. IGI Global, 2019. ISBN 9781522575108, eISBN 9781522575115, p. 636-652. Available from: https://doi.org/10.4018/978-1-5225-7510-8.ch031

[23] MEENA, S., PATIL, G. R., MONDAL, A. Understanding mode choice decisions for shopping mall trips in metro cities of developing countries. *Transportation Research Part F: Traffic Psychology and Behaviour* [online]. 2019, **64**, p. 133-146. ISSN 1369-8478, eISSN 1873-5517. Available from: https://doi.org/10.1016/j.trf.2019.05.002

[24] RUSSO, F., COMI, A. Behavioural simulation of urban goods transport and logistics: the integrated choices of end consumers. *Transportation Research Procedia* [online]. 2020, **46**, p. 165-172. ISSN 2352-1457, eISSN 2352-1465. Available from: https://doi.org/10.1016/j.trpro.2020.03.177

[25] ANWARI, N., AHMED, M. T., ISLAM, M. R., HADIUZZAMAN, M., AMIN, S. Exploring the travel behavior changes caused by the COVID-19 crisis: a case study for a developing country. *Transportation Research Interdisciplinary Perspectives* [online]. 2021, **9**, 100334. eISSN 2590-1982. Available from: https://doi.org/10.1016/j.trip.2021.100334

[26] RAMEZANI, S., LAATIKAINEN, T., HASANZADEH, K., KYTTA, M. Shopping trip mode choice of older adults: an application of activity space and hybrid choice models in understanding the effects of built environment and personal goals. *Transportation* [online]. 2021, **48**, p. 505-536. ISSN 0049-4488, eISSN 1572-9435. Available from: https://doi.org/10.1007/s11116-019-10065-z

[27] ZHANG, Y., ZHAO, P., LIN, J.-J. Exploring shopping travel behavior of millennials in Beijing: Impacts of built environment, life stages, and subjective preferences. *Transportation Research Part A: Policy and Practice* [online]. 2021, **147**, p. 49-60. ISSN 0965-8564, eISSN 1879-2375. Available from: https://doi.org/10.1016/j.tra.2021.03.012

[28] TAO, H., SUN, X., LIU, X., TIAN, J., ZHANG, D. The Impact of consumer purchase behavior changes on the business model design of consumer services companies over the course of COVID-19. *Frontiers in Psychology* [online]. 2022, **13**, 818845. eISSN 1664-1078. Available from: https://doi.org/10.3389/fpsyg.2022.818845

[29] ARRANZ-LOPEZ, A., BLITZ, A., LANZENDORF, M. Exploring the associations between E-shopping and the share of shopping trip frequency and travelled time over total daily travel demand. *Travel Behaviour and Society* [online]. 2023, **31**, p. 202-208. ISSN 2214-367X, eISSN 2214-3688. Available from: https://doi.org/10.1016/j.tbs.2022.11.007

[30] VRBA, R., GALKIN, A., SVADLENKA, L., COMI, A. Research on purchasing behavior of foreign city users: The Czech Republic experience. *Transportation Research Procedia* [online]. 2024, **78**, p. 467-474. ISSN 2352-1457, eISSN 2352-1465. Available from: https://doi.org/10.1016/j.trpro.2024.02.059

[31] PENA-GARCIA, N., GIL-SAURA, I., RODRIGUEZ-OREJUELA, A., SIQUEIRA-JUNIOR, J. R. Purchase intention and purchase behavior online: a cross-cultural approach. *Heliyon* [online]. 2020, **6**(6), e04284. eISSN 2405-8440. Available from: https://doi.org/10.1016/j.heliyon.2020.e04284

[32] LIOBIKIENE, G., MANDRAVICKAITE, J., BERNATONIENE, J. Theory of planned behavior approach to understand the green purchasing behavior in the EU: a cross-cultural study. *Ecological Economics* [online]. 2016, **125**, p. 38-46. ISSN 0921-8009, eISSN 1873-6106. Available from: https://doi.org/10.1016/j.ecolecon.2016.02.008

[33] Registered IDP area baseline assessment dashboard - International Organization for Migration [online] [accessed 2024-08-27]. Available from: https://dtm.iom.int/online-interactive-resources/registered-idp-area-baseline-assessment-dashboard-aba

[34] TRAIN, K. E. *Discrete choice methods with simulation*. Cambridge University Press, 2003. ISBN 0-521-81696-3.

[35] KUTNER, M. H., NACHTSHEIM, C. J., NETER, J., WILLIAM, L. *Applied linear statistical models*. 5th ed. New York: McGraw-Hill/Irwin, 2005. ISBN 0-07-238688-6.

[36] RUSSO, F., COMI, A. A modelling system to simulate goods movements at an urban scale. *Transportation* [online]. 2010, **37**, p. 987-1009. ISSN 0049-4488, eISSN 1572-9435. Available from: https://doi.org/10.1007/s11116-010-9276-y

[37] LARSON, L. R., SHIN, H. Fear during natural disaster: its impact on perceptions of shopping convenience and shopping behavior. *Services Marketing Quarterly* [online]. 2018, **39**(4), p. 293-309. ISSN 1533-2969, eISSN 1533-2977. Available from: https://doi.org/10.1080/15332969.2018.1514795

[38] Individuals who ordered goods or services over the internet for private use - Eurostat data [online] [accessed 2024-09-07]. Available from: https://ec.europa.eu/eurostat/databrowser/view/isoc_r_blt12_i/default/table?lang=EN

INDONESIAN AVIATION ACT 1/2009: AN EXAMINATION AND THE QUEST FOR REFORM IN CERTAIN ISSUES

Adhy Riadhy Arafah[1,*], Rosa Ristawati[1], Kautsar Ismail[1,2], Gerlyana Shafa Putri Hardriani[1]

[1]Faculty of Law, Airlangga University, Surabaya, East Java, Indonesia
[2]Faculty of Law, University of Palangka Raya, Palangka Raya, Central Kalimantan, Indonesia

*E-mail of corresponding author: adhy@fh.unair.ac.id

Adhy Riadhy Arafah 0000-0001-7955-1726, Rosa Ristawati 0000-0002-4020-8928

Resume

Indonesian Aviation Act 1/2009, which has been adopted for more than 14 years ago, was made to accommodate the ICAO's Universal Safety Oversight Audit Programme (USOAP) findings in 2007, which highlighted the need for legislative changes to reduce air transport accidents in Indonesia. The Act regulates two aspects of aviation activity, covering the public and private. The public sector regulates aircraft activities in Indonesia's airspace, certain issues are missed owing to (the) controversy over its legal terminology. In the private sector, the jurisdiction issue and applicability of the Act have consequently regarding the applicability of the Montreal Convention 1999 was ratified by Indonesia in 2016. In this paper were examined some provisions in the Act by normative juridical and comparative approaches, emphasizing the urgent need for legal reform. It is ultimately recommended to amending the Act to align it with current conditions.

Article info

Received 11 September 2024
Accepted 12 February 2025
Online 25 March 2025

Keywords:

amendment
Indonesian aviation act
jurisdiction
legal terms
transportation

Available online: https://doi.org/10.26552/com.C.2025.030

ISSN 1335-4205 (print version)
ISSN 2585-7878 (online version)

1 Introduction

The Indonesian Aviation Act Number 1/2009 has played a significant role in the success of the aviation industry in Indonesia. Since it came into force in 2009, the Act has contributed to a significant improvement in the global safety ranking achieved by Indonesia in 2017, in the average global safety standard by the USOAP [1]. In its establishment, the Indonesian Aviation Act 1/2009 replaced the previous Indonesian Aviation Act Number 15/1992, which was deemed unable to meet the significant needs of the national aviation industry [2].

In 2007, Indonesia was the subject of international concern because of several serious accidents in air transport [3]. Both the number and scale of the accidents were alarming [2]. To call a halt to these accidents, the Indonesian government instituted several safety categories throughout the Indonesian airline companies. These safety levels had three categories: the first level was the highest practicable for all the safety instruments, however the second and the third were not satisfactory enough to fulfill all safety instruments. As a result, not a single national airline was in accordance with the first-level safety category, even the airlines where the majority of shares were owned by the Indonesian government, such as Garuda Indonesia and Merpati [4].

At that time, several Indonesian airlines flew across many countries globally, including countries in Europe like the Netherlands. The report ranks the Indonesian government's response to the European Union's (EU) ban of all Indonesian airlines from flying across European skies [5]. In addition, the Federal Aviation Administration of the USA (FAA) also took action by sending officers to evaluate [6] and explain the aviation situation in Indonesia [7]. Meanwhile, the International Civil Aviation Organization (ICAO) evaluated Indonesia using the USOAP programme [8]. The USOAP audit report revealed unsatisfactory results in numerous areas of the audit, including legislation, organization, licensing, operations, airworthiness, accident investigation, air navigation services, and airports. As a result, it concluded that Indonesia's national legislation regarding aviation, the Indonesian Aviation Act Number 15/1992, was not satisfactory enough to fulfill the Indonesian aviation industry and international standardization. Therefore, to achieve

a minimum global standard, improvements were required by the government in these sectors, starting with the creation of a new Act in 2009.

The evaluation of the USOAP result for Indonesia generated political awareness at the executive and legislative levels [9]. Both parties then agreed to draft a new Act to put a stop to the many accidents that had taken many passengers' lives. The new Act is also wished to be a solution for safety issues and other issues relating to significant points in aviation, such as security and liability issues.

Two years later, in 2009, the new Act was passed. The Act regulates many aspects of the aviation industry and ends the deregulation era for the domestic industry by tightening the requirements for establishing new airlines. As a result, according to Article 11 (2) of the Act, anyone planning to establish an airline company was required to operate with a minimum of ten aircraft, five of which were legally owned or not leased. The operating minimum of the aircraft and the classification that were asked of every company required a huge capital investment [10]. The drafter of the Act realized that aviation safety investment must be prioritized, not only in the operational aspect of business.

Meanwhile, the Indonesian aviation industry ecosystem is gradually finding the right model. Airline companies are slowly adapting to standardization for safety, including all the airlines based on a Low-Cost Carrier (LCC) business model. As a result, some companies that were the majority LCC collapsed due to difficulties financing their operations [11].

This situation has also had consequences for ticket prices, which are not as low as before. The Indonesian government awards safety costs to issue minimum and maximum standards for ticket prices for passengers. Therefore, this policy has also been criticized by the Indonesia Commission for the Supervision of Business Competition (KPPU). The intervention of the Ministry of Transportation on ticket prices gave rise to the Commission's disagreement with fixing a minimum and maximum price for passengers for safety.

The passage of the new Act in 2009 has significantly changed the Indonesia aviation industry in various sectors and wish to increase the safety score for the next audit result of the USOAP in 2014. Owing to the various controversies regarding the new Act, in 2014 the USOAP results for Indonesia were even lower compared to 2007, with only 45% compliance compared to 54% in 2007 [12]. Specifically, in the legislative aspect, the result still needed improvement for the global average. The ICAO required Indonesia to take more legal actions to adopt international aviation regulation standardization in its implementations, including in its Aviation Act [13]. Surprisingly, in 2017, Indonesia successfully achieved a minimum global average for international safety standards in the USOAP audit result, although in the legislative part, it is still less than the international average standard (see Figure 1). However, this has been achieved with no amendment to the Act since 2009.

According to a report by the Indonesian National Accident Investigation Committee, the accident rate in Indonesia exceeded 40 in 2018, as illustrated in the table below (see Figure 2). While there was a decline in this rate after 2018, it began to rise again from 2022 to 2023. This paper does not explore the reasons behind the fluctuations in aircraft accident rates in Indonesia. However, findings from the USOAP reports in 2014 and 2017 indicate that legislative improvements are necessary, as the rates remain below the global average. Nonetheless, the Aviation Act 1/2009 was enacted as a response to the findings of the USOAP audit conducted in 2007.

Figure 1 *USOAP results for Indonesia in 2017, ICAO [14]*

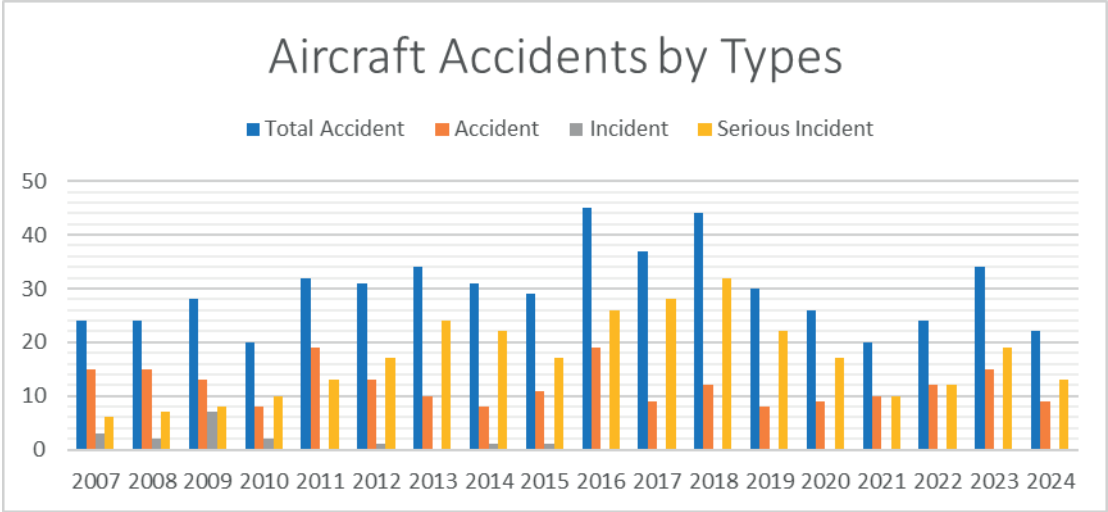

Figure 2 *Aircraft accidents in Indonesia from 2007 - 2024, Indonesian National Accident Investigation Committee [15]*

The Aviation Act 1/2009 was designed to fulfill the safety audit reports in target [16]. However, as a primary law in civil aviation, the Act plays an important role in some issues that are related to aviation activities, not only safety. Some provision issues, like security issues in airspace, the nationality of the aircraft and jurisdiction which are stipulated in legal terms and regulations, are missed by unclear definitions and legal words that affect legal enforcement. Furthermore, some legal issues related to harmonizing other international provisions that the Indonesian government will ratify also have an issue with contradictory definitions, implementation, and legal consequences [17].

While the Act was established mainly because of safety issues that affect the public sector, the Indonesian Aviation Act 1/2009 is designed to regulate all aviation activities, that has a structure to regulate not only public but private provisions, as well. However, in both cases, either in the public or private sector, the issue of jurisdiction is the fundamental question that arises. In circumstances such as jurisdiction on unruly passengers, liability on damage caused by accidents, and mortgaging aircraft, the Act cannot be applied by contradicting other Articles in the Act, other Indonesian laws [18] and other international provisions [19] that apply to most other countries [20].

Therefore, fourteen years after its implementation, the Act has faced more challenges over its provisions. The ratification of international conventions in aviation by Indonesia, such as the Montreal Convention 1999 in 2016, has a significant recommendation to review and adopt international principles. In addition, establishing the Protocol of Montreal 2014 to amend the Tokyo Convention 1963 also has consequences for adjusting the Indonesian Aviation Act if the Indonesian government decides to ratify the Protocol. Lastly, establishing the Law on Job Creation in 2020 has replaced the Act's provision on minimum ownership of an aircraft for the airline company with only one, which indicates the Act also needs adjustment for a safety issue that requires an airline company to invest, not only focusing on the operational aspect of the aircraft number, but also on safety matters [21].

Hence, some issues – like jurisdiction, authorized institution, aviation liberalization industry and delegation of air navigation over Indonesia's territory in the Indonesian Aviation Act 1/2009 – need legal reform, due to changes in the industry and adjustments to domestic and international legal instruments. In addition, it is necessary to examine the Act in order to analyze certain provisions and make necessary adjustments to international legal instruments that have been ratified or will be ratified.

2 Methodology

In this study, a rigorous two-fold methodological approach was employed to thoroughly examine selected provisions of the Indonesian Aviation Act. The first aspect involves normative juridical analysis, which entails a comprehensive examination of legal principles and interpretations within the Act. This analysis has focused on addressing controversies surrounding the definition of key legal terms and the jurisdictional complexities inherent in its application. Additionally, a comparative framework was utilized to evaluate the Act's coherence with international legal standards. This aspect is particularly relevant given Indonesia's ratification of the Montreal Convention 1999 in 2016, agreement on the Realignment of the Boundary between the Jakarta Flight Information Region and the Singapore Flight Information Region in 2022 and its willingness to ratify the Montreal Protocol in 2014.

In addition, in this paper is highlighted the crucial importance of legal reform in both the public and the private aviation industries. The urgency of addressing the challenges that hinder the effective utilization and

enforcement of the Act is emphasized. Consequently, in this study the recommendations were put forward that call for timely amendments to the Act, to align it with modern legal requirements and ensure its effectiveness in addressing present-day aviation safety and regulatory issues.

3 Analysis and discussion

3.1 Jurisdiction issue through the Act

The territory of a state plays a central role in the fundamental legal concepts of sovereignty and jurisdiction. Exclusivity on the jurisdiction concerning aviation can be defined in implementation with many actions in airline activity. This situation means that sovereignty over airspace is the point of common problems in regulation, such as the entry and departure of an aircraft, crews, passengers, and cargo and jurisdiction over them, and the applicability of criminal law, private law and special rules for the protection of international civil aviation [22]. Hence, for jurisdiction issues, the Indonesian Aviation Act covers various areas of regulation, including criminal acts related to public security in the context of a public issue [23] and also a place of jurisdiction court for lawsuits of damages caused by an accident of the aircraft [24].

While Indonesia's legal jurisdiction applies, the rules concerning public safety in Indonesian aviation, including offenses such as hijacking, unruly passenger behavior, and sabotage, are very specific. The Act also governs the legal authority for enforcing laws in cases of unruly passenger behavior, which is only granted to specially trained civil aviation investigators under the authority of the relevant civil aviation agency. This authority is comprised of civil servants from the Directorate General of Civil Aviation (PPNS) [18]. The authority's establishment was prompted by the criminalization of a pilot following the Garuda Indonesia accident at Adi Sucipto airport in Yogyakarta in 2007 [25]. This incident also served as the catalyst for regulating the authority's powers in investigating aviation accidents, which are now the responsibility of the National Transport Investigation Committee (KNKT). As a result, the determination of suspect status in the air transport accidents should not be solely based on the perspective of the police, as was the case in the 2007 accident prior to the enactment of the Indonesian Aviation Act 2009 [26].

Furthermore, according to the specific characteristics of the jurisdiction in Indonesian aviation, the Act is taking differential authority of work with other justice authorities like police institutions for investigation in crime and the Indonesian special authority (PPNS) for unruly passengers. However, specific criminal acts, such as hijacking and sabotage are still under the police authority in view of the impact and advanced technology involved.

As previously mentioned, the Indonesian special authority (PPNS) on criminal air transport for unruly passengers has been established to address incidents involving unruly passengers on both domestic and international flights. In terms of national regulations, Indonesia is looking to adopt the 2014 Montreal Protocol to enhance its legal framework and jurisdiction. However, there are challenges that Indonesia needs to address through legislative measures. For instance, implementing jurisdictional principles, particularly with regard to defining 'Indonesian Aircraft' as outlined in Article 4 Alphabet (C), poses significant difficulties that need to be addressed in harmony with the provisions stated in Article 1, Paragraph 6 of the Act and the Indonesian Criminal Code.

Article 4 of the Act states the validity of the Act for:

a. all utilization activities of air/space territory, flight navigation, aircraft, airports, airbases, air transportation, aviation safety and security, and other related supporting and general facilities, including preservation of the environment within the territory of the Republic of Indonesia;
b. all foreign aircraft conducting activities from and/or to the territory of the Republic of Indonesia; and
c. all Indonesian aircraft present outside the territory of the Republic of Indonesia.

In addition, Article 1, Paragraph 6 states:

An Indonesian aircraft is an aircraft that has Indonesian registration marks and markings of Indonesian nationality.

The Act's applicability, as outlined in Article 4, requires greater consistency compared to other Articles. A prime example of a problematic legal term can be found in Article 1, Paragraph 6, particularly in ensuring safety within the Indonesia's airspace. The definition of an Indonesian aircraft in Article 1, Paragraph 6 stipulates that it must be "an aircraft registered in Indonesia and bearing the national identity of Indonesia." This means that the Indonesian national identity, such as the airline's flag, must be displayed on the aircraft, and the registration code of Indonesia, PK, must also be borne on the aircraft body. The usage of the word "and" in Article 1, Paragraph 6 indicates that both requirements are essential, and if one of the criteria is not met, the classification is not fulfilled.

Therefore, the use of leasing a foreign aircraft by private entity, for example as was done by the owner of MS Glow company, Mr. Gilang, without any changes in the registration code to "PK", has the consequence that an aircraft cannot be classified as an Indonesian aircraft [27]. The Act at this point still maintains a "traditional" way of identifying the nationality of the aircraft, so that all the foreign aircraft need deregistration and then re-registration before using the aircraft in another territory [28] that can be classified as Indonesian aircraft. To return the aircraft to the lessor or other lessee, the lessee or lessor must undertake deregistration and re-registration, i.e. the same procedure as previously.

In contrast, Article 83 (bis) of the 1944 Chicago Convention outlines more feasible regulations "when an aircraft registered in a contracting State is operated pursuant to an agreement for the lease, charter or interchange of the aircraft or any similar arrangement by an operator who has his principal place of business or, if he has no such place of business, his permanent residence in another contracting State, the State of registry may, by agreement with such other State, transfer to it all or part of its functions and duties as State of registry in respect of that aircraft under Articles 12, 30, 31 and 32(a)." This Article stipulates that no-changing the registration mark can also be alternated by transferring the function and duty by only agreement in order to ensure aircraft safety is standardized under a jurisdiction where the aircraft is operated, while this provision will be more flexible in time and procedure [29].

In line with the previous argument, the definition is also outlined in the Indonesian Criminal Code, specifically Article 95a, which states that Indonesian aircraft include not only those registered in Indonesia, but foreign aircraft that are chartered without a crew and operated by Indonesian airlines, as well. This provision in the Criminal Code enables an aircraft to be classified as Indonesian even without a "PK" registration, provided that it is operated by an Indonesian airline company. Hence, the phrase 'the state of the operator' related to jurisdiction in Article 3 of the Montreal Protocol 2014 does not align with Article 1, Paragraph 6 of the Indonesian Aviation Act. However, it does correlate with the definition of national aircraft as per the Indonesian Criminal Code. As a result, there is ambiguity surrounding Indonesian jurisdiction, which may not extend to all the Indonesian aircraft not registered in Indonesia, even when these aircraft are operated by an Indonesian company or individual.

The difference in definition between the two Indonesian laws will be implicated in the law that will apply. While the Criminal Code defines the terms consistency through the international law rather than the Aviation Act, however, a principle of *Lex Specialis Derogate Legi Generalis* indicates that the Act as a specific law in aviation will be more applicable than the Criminal Code as a general law. Consistency on legal principles is also challenged; the use of another registration code for civil aircraft, like a "P" code registration [30], for civil purposes but used for state institutions like the Indonesian Police then gives more complexity to the consistency of the national regulation on state registration. As a civil institution, rules and regulations on aircraft operations shall be under civilian rules as stated in the Indonesian Aviation Act, even then the functional or the aircraft for non-civilian.

In addition, the issue of Article 4 pertaining to the implementation of jurisdiction in private matters under the Montreal Convention of 1999, which Indonesia ratified in 2016 through a Presidential Decree, is also significant, not only in public matters as mentioned earlier. The hierarchy of Indonesian law has implications for the applicability of the Montreal Convention of 1999 under the Indonesian Aviation Act. This raises concerns, as the ratification may not align with the principle of *Lex Superiori Derogate Legi Inferiori*, given that the Indonesian Aviation Act holds a higher position than the Presidential Decree [24]. In light of the Indonesian AirAsia QZ 8501 accident in 2014, it was observed that Indonesian passengers received compensation based on the Indonesian Ministerial Regulation of Transportation 77/2011 [31]. There remains substantial potential for Indonesian passengers to obtain compensation in accordance with the Indonesian Ministerial Regulation of Transportation, which serves as an implementing rule of the Indonesian Aviation Act rather than being based on the Montreal Convention of 1999.

The jurisdictional issue in the Indonesian Aviation Act is crucial, considering the significant role of the air transport industry in Indonesia's national economy as an archipelagic state [32]. National aviation regulations, including the Act, must accommodate the intricate requirements of the aviation sector at both domestic and international levels.

3.2 Challenges to the act in the development of use of the national airspace

The challenges of implementing the Indonesian Aviation Act have become increasingly apparent in recent years, particularly in regard to security and safety measures. In certain areas of Indonesian airspace, there has been a noticeable rise in the use of foreign civil aircraft for non-procedural purposes. As a result, the actions taken by law enforcement entities, such as civil servant investigators and public prosecutors, to address illegal civil aircraft have not been deemed sufficient by the military institution responsible for bringing down the illegal aircraft that enter Indonesia's airspace [33]. At the same time, the development of technology in the aviation industry, such as drones, has led to questions over security and privacy issues.

In regard to the security of the national airspace, the civil authority, as stipulated by the Indonesian Aviation Act, holds jurisdiction over civilian aircraft activities. This extends to addressing violations of laws within a state by aircraft, particularly foreign aircraft. However, it is important to note that only the military institution possesses the necessary tools and capabilities to enforce the landing of a civil aircraft using military jets. The Indonesian Air Force currently lacks authority over civil aircraft, leading to the conclusion that there needs to be a sharing of authority for the legal process between the civil and military sectors in relation to the law enforcement for civil aircraft [34]. As a result, there is a need to draft new provisions in the Law of National Air Space Management to address this issue

effectively. In 2019, an Ethiopian Airways cargo aircraft was compelled to land by the Indonesian Air Force for unauthorized passage through Indonesia's airspace [35]. The fact that the military authorities were not involved in the investigation process led to widespread dissatisfaction. Subsequently, the aircraft was released after being subjected to a minimal fine [36].

In response to legal issues regarding violations of Indonesia's airspace laws, the Indonesian Air Force is proposing a new law to address concerns with the current Indonesian Aviation Act [37]. The draft of this law aims to enhance the authority of the Indonesian Air Force in enforcing the law pertaining to civil aircraft, particularly focusing on the investigation process conducted by the Military Police of the Indonesian Air Force, as stipulated in Article 46. The proposed law also highlights the need for better coordination among government institutions in Indonesia with respect to the Indonesian Aviation Act. Therefore, the drafting of a new law is deemed necessary to address these shortcomings in the existing Act. The future law may improve several aspects of aviation, including safety and security and the adoption of new aviation technologies, all of which may improve the fulfillment of passengers' rights.

Upon reviewing most cases of the violation of Indonesia's airspace, it has been observed that the law enforcement investigator on the ground typically handles the violation by releasing the illegal aircraft and crews after they pay a small fee as an administration sanction. Therefore, it has been noted that the operational costs of law enforcement incurred by the Indonesian Air Force in intercepting these illegal civil aircraft and imposing sanctions is disproportionate from the side of the Indonesian Air Force. This has led the Ministry of Defense to initiate the drafting of a new law. This proposed law aims to involve the Air Force personnel in the legal process for intercepting illegal civil aircraft. Although the presence of military police is seen as a beneficial development in law enforcement, the potential involvement of military personnel in civil aviation raises concerns as it may contradict the Indonesian Aviation Act 1/2009. After all, this Act is also designed to handle law enforcement issues in civil aviation through the civil legal enforcement authority [38].

The security and law enforcement considerations for civil aviation within national airspace should also encompass the governance of drone development alongside the traditional aircraft, as mandated by relevant legislation. As technology continues to progress rapidly, it becomes increasingly imperative to establish regulations that account for all the airspace activities. While the Act currently governs all such activities, drones were not as prevalent when it was initially established in 2009. Drones, classified as aircraft, possess distinct characteristics that necessitate specialized rules and regulations [39]. Unlike conventional aircraft, which adhere to specific requirements for function, size, passenger and cargo capacity, drones must meet separate operational standards [40]. Hence, drones require specific operational knowledge, such as registration and personal licensing for the pilot of the drones.

The fact that small drones are traded on the open market suggests that they are accessible to the public. However, concerns regarding privacy arose when the small drones were first developed, as they were often used for taking pictures or filming as a hobby, which impacted people's sense of security [41]. Today, with advancements in drone technology, they are not just seen as a hobby but also as a primary mode of transportation for expeditions [42] and humans [43], as well. They are becoming bigger in size, especially for use in remote areas not covered by commercial flights, as in Australia. Australia's Civil Aviation Safety Authority (CASA) describes drones for transportation as RPA (Remotely Piloted Aircraft) [44].

Safety procedures and liability issues on drone activities are examples of how the Act needs to be updated. While a drone is categorized as an aircraft, the difference in character and technology of a drone compared to a conventional aircraft needs more specific rules and regulations than in an Act which does not specifically regulate and only regulates at the level of the Ministry of Transportation Decree [45]. Therefore, the amendment is absolutely necessary to meet the changing paradigm in aviation activities in the future.

3.3 Indonesian law number 11/2020 and liberation in aviation industry

Historically, Indonesia has implemented strict rules on operating aircraft. Ministry Decree 127/1990 limited the number of aircraft that may be operated to Garuda Indonesia, Merpati, Mandala, Sempati, Bouraq and Dirgantara Air Service [46, p. 30]. However, the policy changed after the reformation era in 1998, caused by economic crises in all sectors, including air transport. Therefore, competition was lacking in the air transport industry of Indonesia during the pre-reform era.

The Indonesian air transport economy collapsed during 1998 – 2001, which prompted the Indonesian government to take action to improve the aviation industry by introducing a deregulation policy [47]. The policy was replaced by Ministry Transportation Decree Number 11/2001, with a rule to limit the operational airlines by allowing new scheduled airlines to operate with only a minimum of two aircraft. As a result, many new airlines were born. However, most were Low-Cost Carrier airlines and these dominated the market [48].

While airline business increased dramatically with the number of new scheduled airlines and passengers, at the same time, the number of accidents also increased. As a result, international authorities such as the ICAO, EASA and FAA imposed an audit of Indonesian safety quality. Hence, the Indonesian government issued

Ministry Decree Number 25/2008, which terminated the deregulation policy era by applying strict rules for the establishment of new airlines. The government hoped that in the future the airlines would be high capital, and invest not only in the commercial side, but on the safety side as their first priority, as well.

Therefore, the government adopted a policy of requiring a minimum fleet of ten aircraft, with five aircraft being owned and the other five leased. The policy was then put into the provisions of the Act, in Article 118 Paragraph 2 Alphabet (a). As a result, only airline companies that owned high capital could fulfill the requirements. However, a decade after its implementation, the Act has succeeded in minimizing the number of air transport accidents. At the same time, many airlines collapsed "by natural selection", unable to fulfill strict requirements in their operations [49]. Regulation also had economic implications. It was shown that fewer airlines operated fewer routes, whereas demand remained high. As a consequence, the aviation consumer has had to pay higher prices for tickets. While airline companies have had to struggle with their operational costs, the service provided to consumers has been minimal. This situation might also lead to minimizing the fulfillment of passengers' rights. The restrictive policy might also have an effect on tourism and business revenues.

At the beginning of 2020, the Covid-19 pandemic spread sporadically. As a result, the economy slumped dramatically and the transportation business suffered. Air transport was the most vulnerable compared to other transportation models [50]. Consequently, many existing airline companies returned their aircraft to the lessor and failed to pay their debts. Other airlines, like Indonesia AirAsia, stopped operations during the pandemic [51].

Due to the reduction in operational aircraft of various airline companies during the pandemic, the government issued a new Law on Job Creation Number 11/2020 in order to address this trend. Additionally, the new law included provisions for development of the aviation business sector and ownership regulations. Unlike the Aviation Act 1/2009, which required airline companies to own a certain number of aircraft, the new law instead offers greater flexibility by not mandating ownership of more than one aircraft. This approach reflects a shift away from the previous restrictive policy towards a more liberal one, similar to what was observed in the early 2000s. The requirement is further elaborated in Article 65 (2) of Government Regulation Number 32/2021, which mandates that commercial airlines with scheduled flights must possess at least one aircraft and have operational control over a minimum of two aircraft. Similarly, commercial airlines without scheduled flights must own at least one aircraft and maintain control over an additional aircraft.

Hence, the new law regarding the minimum aircraft ownership requirements for airlines, as specified in legislation other than the Aviation Act, needs to be adapted to meet safety standards and address any related safety concerns. Furthermore, there is a need to regulate the provisions in the Indonesian Aviation Act that pertain to safety restrictions based on aircraft ownership, to prevent the unfair competition that happened before the birth of the Indonesian Aviation Act.

In 2015, the Aviation Law, particularly the rules concerning minimum ownership of aircraft, was reviewed in the Indonesian Constitutional Court. However, the Court rejected it. The review concerned Article 118 (1), (2). It was argued by the applicant that the regulation on minimum ownership of aircraft discriminated against small capital entrepreneurs. In Court Decision No. 29/PUU-XIII/2015, the Court said that the aviation business is not merely about commercialization, but it is about the safety and security aspects. The Court affirmed that the aviation business had different characteristics and specifications. Therefore, the Court affirmed that the policy of minimum ownership of aircraft was not about discrimination, but due to the safety of the consumer, as well as the safety and security of the aviation industry.

3.4 Delegation of Indonesian air navigation

At the beginning of 2022, the government of the Republic of Indonesia and the Republic of Singapore signed a cooperation agreement on delegating air navigation services from Indonesia to Singapore. The agreement allowed both parties to renew the previous agreement signed in 1995. While the agreement in 1995 delegated the rights to air navigation services from sea level up to 37,000 feet for sector A, and from sea level to unlimited height level for sector B, the latest agreement of 2022 stipulates that Indonesia delegates its navigation services to Singapore in sectors A and B from the surface only up to 37,000 feet, and the rest is still under the control of Indonesia [52].

While the first agreement had never regulated any technical agreement, the replacement agreement implements two agreements at the same time. The first agreement, as an umbrella agreement, regulates the main focus of the agreement to delegate the services from Indonesia to Singapore. The second agreement is a technical agreement, known as a Letter of Operational Coordination Agreement (LOCA).

According to Article 458 of the Act, for fifteen years after the application of the Act, Indonesia is required to evaluate and serve the airspace of the Republic of Indonesia, which provides navigation services; its flights are delegated to other countries based on the agreement by the Indonesian aviation navigation service provider agency. The timeline of fifteen years runs from 2009 to 2024, though in fact, in 2022, the government of the Republic of Indonesia then continued the delegation rather than stopped the delegation.

The issue of jurisdiction within this agreement will directly impact its enforceability in the event of an accident occurring within Indonesia's airspace, which is under the control of Singapore. Additionally, this issue will heavily influence the LOCA, which will require the Air Traffic Controller (ATC) of Indonesia to operate within the Singapore Air Traffic Control Centre (SATCC). Learning from the case of the Uberlingen crash [53], as the Indonesian ATC assumes control within the SATCC, located in Singapore, it is highly likely that Singapore's jurisdiction will be applied more prevalently than Indonesia's jurisdiction based on the ATC position during the control.

The lack of clear jurisdictional guidelines regarding the Indonesian Aviation Act has heightened concerns about safeguarding the Indonesian air traffic control in accordance with the bilateral agreement between Indonesia and Singapore on delegation of navigation control [54]. Although Article 4 of the Act specifies that Indonesia's jurisdiction applies to all the activities within its airspace, including foreign aircraft operating within its airspace and Indonesian aircraft outside its territory, the issue of protecting the Indonesian ATC under Indonesia's jurisdiction falls outside the purview of the Act. It is important for the Act to regulate Indonesia's jurisdiction, particularly in relation to international obligations. This regulation should align with Article 28 of the International Civil Aviation's Chicago Convention 1944, which specifies how such obligations may be applied [55, p. 113].

In numerous state practices, air traffic controllers are protected in their operations by national law. This protection, referred to as immunity [56], is granted based on the air traffic controller's citizenship under national law, rather than being subject to the laws of other states. In Indonesia, the concept of 'immunity' as a privilege for air traffic controllers is not explicitly defined in the national regulations. The Indonesian Aviation Act, in Article 271 Paragraph 1, simply states, "The Government shall be responsible for the operation of flight navigation services for aircraft operating within the airspace being served."

There are several key issues in the Act that the Indonesian government must address to effectively manage the delegation of air navigation with Singapore in 2022. Specifically, the statutory mandate outlined in Article 458, coupled with the terms of the bilateral agreement, may lead to legal repercussions if not properly addressed. Therefore, it is imperative that the Indonesian government conducts a thorough review of the Act to ensure compliance and mitigate any potential legal risks [57].

3.5 Legal remedies

There are several aspects which need to be considered as subject for the future Aviation Legislation, such as aspects concerning the safety and security of aviation in improving the fulfilment of the rights of the passengers. With regard to other aspects, the rules adapting new technologies, including eco-friendly aviation rules, need to be proposed in the future Indonesian Aviation Act. If the rules are addressed, they will not only add several new obligations to the aviation business provider, but make it support a sustainable aviation system, as well. On the other hand, the need to refine rules regarding the airline network and operation nationally, regionally, as well as globally, including the coordination among the aviation authorities, will be an urgent agenda to improve the aviation system in Indonesia. In this context, an urgent agenda to modify the Indonesian Aviation Act needs to be prioritized in the *Prolegnas* (a priority agenda in the National Legislation Program by the House of Representatives). In doing so, the aviation authorities, the stakeholders and academia need to convince parliament to upgrade the modification of the Aviation Act, which has already been going on for 15 years alongside the dynamic of development and technologies in the aviation industry.

A significant learning opportunity arose from the Republic of Korea (ROK) which can also be implemented in Indonesia. In 2002, Korea was placed in Category 2 by the United States Federal Aviation Administration (FAA), indicating non-compliance with ICAO standards [58, p. 58]. To address this, ROK established the International Aviation Safety Task Force Team (IASTFT), consisting of representatives from various institutions involved in the preparation for the ICAO Universal Safety Oversight Audit Programme (USOAP). The task force was tasked with comparing international provisions against national legislation. The Constitution of the ROK delineates three branches of government: the National Assembly (legislative), the President (executive), and the Supreme Court along with its subordinate courts (judicial). Consequently, close cooperation with the Ministry of Government Legislation (MOLEG) was essential. It took two years to identify discrepancies and align national legislation with the Annexes to the Convention on International Civil Aviation, as well as to translate the relevant texts into English using appropriate aviation terminology [58, pp. 60–61].

Given to the problems analyzed, an urgent agenda of making a new regulation to adjust to the current problems in aviation is of the utmost concern in Indonesia. Indeed, the implementation of the Aviation Act in Indonesia is facing challenges in several crucial aspects, as a result not only of the USOAP, the Montreal Convention of 1999 and the requirements of the Montreal Protocol of 2014, but also of aviation development. The most crucial challenges are about concerns for the safety and security of passengers. The Indonesian government should provide legal guarantees for a range of factors, including regulatory, financial, institutional, and operational issues. Efforts to provide a legal framework

to adjust to the development of aviation will mainly involve addressing legislative and regulatory gaps.

In this context, there is a legal vacuum, which urgently requires a legal instrument for anticipating the worst consequences and boosting public confidence, as well as addressing the global issue of aviation safety and security. On the other hand, while the revision of the Aviation Act may be an urgent agenda, other aspects, such as political and institutional challenges may throw up barriers to fulfilling the international standards and global expectations. This is due to the fact that in Indonesia, legislative priority agendas are somewhat in the pocket of political interests. The legislator is not really concerned with the development of safety and security prior to the chaos and accidents in aviation. Another barrier to filling the legislation gap is the complicated interagency coordination, which influences the implementation of technical regulations relating to aviation.

Indonesia may need to consider regulating its aviation safety and security by executive laws or Government Regulation in Lieu of Law (*Perpu*) to prioritize efficiency and protection. In this context, the mechanism for making it an emergency may be the solution, as it is provided for in the Indonesian Constitution for several reasons. First, the safety and security of the aviation business are both fundamental to fulfilling the rights of passengers, particularly the right to life and the right to safety, as guaranteed in Article 28G of the Indonesian Constitution. The emergency law or other executive laws may have the content of immediate and urgent concerns regarding at least several aspects, such as anticipating catastrophic accidents, anticipating the sudden outbreak of a crisis, including a pandemic, disasters like volcanic eruptions which potentially happen in Indonesia, and earthquakes impacting the air travel, which happen everywhere in Indonesia. These are the reasons why Indonesia needs to have an emergency law to fill the gaps in its aviation regulations. Another rational justification for an emergency law is the fact that technological advancement and unforeseen crises threaten the aviation industry and passengers' rights.

The constitutional requirements of regulating the safety and security of aviation in this context are met with the qualification of 'urgent need' as is required in Article 22 of the Indonesian Constitution [59]. The urgent need requirement in this context includes the need to fulfill the constitutional rights in Article 28G of the Indonesian Constitution, providing for the safety and security of passengers as the constitutional obligation of the government of Indonesia. The mechanism of emergency law that is used *Perpu* by the executive will be a bridging law to gain legislative approval and may be converted into a revision of the Aviation Act.

The rationale for issuing an emergency law in this context will be in line with the Constitutional Court Decision No. 138/PUU-VII/2009 on the judicial review against the Emergency Law No. 4/2009. The emergency law on aviation is necessary because the existing law is out of date and does not meet with current aviation developments. It meets with the criteria of there being an urgent need to solve problems with aviation safety and security in Indonesia, bridging the regulation gaps as to the implementation of the results of the USOAP audit, Montreal Convention 1999 and interest on the implementation of Montreal Protocol 2014, as well as there being a legal gap in dealing with the current threats, including technological advances and the unforeseen crises of cyber-attacks and natural disasters.

4 Conclusion

The Indonesian Aviation Act 1/2009 has undeniably improved aviation safety and regulatory frameworks in response to the ICAO's USOAP findings. However, it still presents challenges in both the public and private sectors due to ambiguities in legal definitions, jurisdictional conflicts, and the implementation of international agreements like the Montreal Convention 1999. Therefore, there remains a pressing need for comprehensive legal reform to bring the Act in line with contemporary conditions and international standards. An amendment to the Act is highly recommended to address these issues and enhance its overall effectiveness. Hence, the stakeholders, government, and academia need to work together to convince parliament to expedite modification of the Aviation Act, which is not suitable for the present state of aviation development.

Acknowledgements

This research has been funded by the Airlangga Research Fund 2024 Program.

Conflicts of interest

The authors declare that they have no known competing financial interests or personal relationships that could have appeared to influence the work reported in this paper.

References

[1] Safety audit results: USOAP interactive viewer - ICAO [online] [accessed 2023-04-13]. Available from: https://www.icao.int/safety/pages/usoap-results.aspx

[2] DENNIS, W. Indonesia faces scrutiny over transport disasters. *Engineering and Technology* [online]. 2007, **2**(4), p. 24-25 [accessed 2024-05-15]. ISSN 1750-9637. Available from: https://doi.org/10.1049/et:20070402
[3] PRAMONO, A., MIDDLETON, J. H., CAPONECCHIA, C. Civil aviation occurrences in Indonesia. *Journal of Advanced Transportation* [online]. 2020, p. 1-17 [accessed 2024-05-15]. eISSN 2042-3195. Available from: https://doi.org/10.1049/et:20070402
[4] Ranking airlines as an evaluation / Peringkat airlines sebagai evaluasi - Indonesian Ministry of Transportation [online] [accessed 2023-08-04]. Available from: https://dephub.go.id/post/read/PERINGKAT-AIRLINES-SEBAGAI-EVALUASI-783
[5] REITZFELD, A. D., CHERYL, S. EU regulation on banning of airlines for safety concerns. *Air and Space Law* [online]. 2008, **33**(2), p. 132-154 [accessed 2024-03-03]. ISSN 0927-3379, eISSN 1875-8339. Available from: https://doi.org/10.54648/aila2008011
[6] FAA announces aviation safety rating for Indonesia - Federal Aviation Administration [online] [accessed 2023-08-04]. Available from: https://www.faa.gov/newsroom/faa-announces-aviation-safety-rating-indonesia
[7] LATIPULHAYAT, A., ARIANANTO, A. Legality of the European Union flight ban towards Indonesian airlines. *International Journal of Public Law and Policy* [online]. 2012, **2**(2), p. 149-161 [accessed 2024-05-15]. ISSN 2044-7663, eISSN 2044-7671. Available from: http://dx.doi.org/10.1504/IJPLAP.2012.046071
[8] KANIA, D. D., ULFA, A., SARI, M. Indonesia's diplomacy on flight safety issues. *Jurnal Manajemen Transportasi and Logistik* [online]. 2020, **7**(2), p. 22-31 [accessed 2024-05-15]. ISSN 2442-3149, eISSN 2355-472X. Available from: http://dx.doi.org/10.25292/j.mtl.v7i2.421
[9] PASSARELLA, R., NURMAINI, S. Data analysis investigation: Papua is the most unsafe province in Indonesia for aviation: an exploratory data analysis study from KNKT-database accidents and incidents (1988-2021). *Journal of Engineering Science and Technology Review* [online]. 2022, **15**(3), p. 158-164 [accessed 2024-05-15]. ISSN 1791-2377. Available from: https://doi.org/10.25103/jestr.153.17
[10] Aircraft ownership requirements to ensure aviation safety / Syarat kepemilikan pesawat jamin keselamatan penerbangan - Hukumonline [online] [accessed 2023-10-08]. Available from: https://www.hukumonline.com/berita/a/syarat-kepemilikan-pesawat-jamin-keselamatan-penerbangan-lt552d09eff1acb/
[11] MAJID, S. A., SUCHERLY, KALTUM, U. Analysis on the factors causing airlines bankruptcy: cases in Indonesia. *International Journal of Management Sciences and Business Research* [online]. 2016, **5**(2), p. 25-40 [accessed 2024-05-22]. ISSN 2226-8235. Available from: https://papers.ssrn.com/sol3/papers.cfm?abstract_id=2848106
[12] NUGROHO, E. Good news! Audit result of Indonesian aviation is above the average of other countries' implementation effectiveness - Indo Cargo Times [online] [accessed 2023-10-07]. Available from: https://indocargotimes.com/2017/good-news-audit-result-of-indonesian-aviation-is-above-the-average-of-other-countries-implementation-effectiveness
[13] SILITONGA, T., SUMADINATA, R. W. S., SUDIRMAN, A., HIDAYAT, T. Implementation of ICAO standards for civil aviation security in Indonesia. *Journal of Positive School Psychology* [online]. 2022, **6**(5), p. 8193-8203 [accessed 2024-05-20]. ISSN 2717-7564. Available from: https://journalppw.com/index.php/jpsp/article/view/9341
[14] Safety audit results: USOAP interactive viewer - ICAO [online] [accessed 2023-10-07]. Available from: https://www.icao.int/safety/pages/usoap-results.aspx
[15] Accident rates by type of event / Angka kecelakaan penebangan berdasarkan jenis peristiwa - Komite Nasional Kecelakaan Transportasi (KNKT) [online] [accessed 2024-11-18]. Available from: https://knkt.go.id/statistik
[16] Thirteenth air navigation conference committee: Indonesia progress of implementing the state safety programme (SSP) - ICAO [online] [accessed 2023-10-07]. Available from: https://www.icao.int/Meetings/anconf13/Documents/WP/wp_278_en.pdf
[17] SUDIARTO. Indonesian aviation law reform. *International Journal of Multidisciplinary Research and Analysis* [online]. 2023, **6**(4), p. 1563-1569 [accessed 2024-05-20]. ISSN 2643-9840, eISSN 2643-9875. Available from: https://doi.org/10.47191/ijmra/v6-i4-27
[18] MAULANI, N., SURYAATMADJA, S. The concept of jurisdiction in the air: to what extent can it be upheld against unruly passengers in international air transport? *Padjadjaran Journal of International Law* [online]. 2021, **5**(1), p. 21-36 [accessed 2024-05-20]. ISSN 2549-2152, eISSN 2549-1296. Available from: https://doi.org/10.23920/pjil.v5i1.416
[19] SIREGAR, N. Air rage arrangement between the United Kingdom and Indonesia based on the Tokyo convention 1963. *Fiat Justisia* [online]. 2019, **13**(1), p. 19-30 [accessed 2024-05-20]. ISSN 1978-5186, eISSN 2477-6238. Available from: https://doi.org/10.25041/fiatjustisia.v13no1.1472
[20] WIRSAMULIA, F. The legal problem of aircraft mortgage in Indonesia. *Indonesia Law Review* [online]. 2022, **12**(1), p. 17-31 [accessed 2024-09-03]. ISSN 2088-8430, eISSN 2356-2129. Available: from: https://scholarhub.ui.ac.id/ilrev/vol12/iss1/2

[21] Aviation safety Indonesia: New law means death small Indonesian airlines? - Indonesia Investments [online] [accessed 2023-10-10]. Available from: https://www.indonesia-investments.com/id/news/todays-headlines/aviation-safety-indonesia-new-law-means-death-small-indonesian-airlines/item5471?

[22] CHENG, B., BERNHARDT, R. Air law. In: *Encyclopedia of public international law. Vol. 1*. North-Holland Publications, 1992. ISBN 9780444862440, p.66-72.

[23] SUDIRO, A., MARTONO, D. K. The development of civil aviation laws and regulations applicable in Indonesia. *International Journal of Business and Management Invention* [online]. 2016, **5**(12), p. 45-53 [accessed 2024-09-03]. ISSN 2319-801X, eISSN 2319 - 8028. Available: from: https://www.ijbmi.org/papers/Vol(5)12/version-2/I5120204553.pdf

[24] ARAFAH, A. R., PUTRO, Y. M., BAIS, A. N., SOLITA, S., PRAKASA, S. U. W. Voyage rights in review: Indonesian tourism and aviation legislation. *Cogent Social Sciences* [online]. 2024, **10**(1), p. 1-13 [accessed 2024-07-02]. eISSN 2331-1886. Available from: https://doi.org/10.1080/23311886.2024.2333980

[25] Garuda pilot jailed over fatal crash - ABC News [online] [accessed 2024-03-02]. Available from: https://www.abc.net.au/news/2009-04-06/garuda-pilot-jailed-over-fatal-crash/1643068

[26] DANU, R. F., NOVIANTO, W. T., HARTIWININGSIH. Non-punitive action against pilots due to accidents and serious civil aircraft incidents in Indonesia / Non punitive action terhadap pilot akibat kecelakaan dan insiden serius pesawat udara sipil di Indonesia. *Jurnal Hukum dan Pembangunan Ekonomi* [online]. 2017, **5**(2), p. 87-100 [accessed 2024-04-11]. ISSN 2338-1051, eISSN 2777-0818. Available from: https://doi.org/10.20961/hpe.v5i2.18294

[27] WIANANTO, A., KURNIAWAN, D. Who's Gilang Juragan 99, crazy rich of Malang, the owner of MS glow, who apparently doesn't have a private jet - Voi [online] [accessed 2023-10-16]. Available from: https://voi.id/en/economy/148569

[28] GERBER, D. N., WALTON, D. R. De-registration and export remedies under the Cape Town convention. *Cape Town Convention Journal* [online]. 2014, **3**(1), p. 49-68 [accessed 2024-05-16]. ISSN 2049-761X, eISSN 2049-7628. Available from: https://doi.org/10.5235/204976114814222485

[29] REULEAUX, M., JAKOBSEN, M. L. H., SAND, P. Aircraft repossession under leasing arrangements pursuant to article 83bis Chicago convention. *Air and Space Law* [online]. 2019, **44**(6), p. 545-564 [accessed 2024-07-12]. ISSN 0927-3379, eISSN 1875-8339. Available from: https://doi.org/10.54648/aila2019034

[30] Boeing 737 aircraft for national police operations / Pesawat Boeing 737 untuk operasional polri - Antara [online] [accessed 2023-10-13]. Available from: https://www.antaranews.com/infografik/3642192/pesawat-boeing-737-untuk-operasional-polri

[31] PRIMADHYTA, S. Paying IDR 31 billion, AirAsia fully pays compensation for QZ8501 victims / Kucurkan Rp31 M, AirAsia bayar penuh kompensasi korban QZ8501 - CNN Indonesia [online] [accessed 2024-04-03]. Available from: https://www.cnnindonesia.com/ekonomi/20150730202327-92-69197/kucurkan-rp31-m-airasia-bayar-penuh-kompensasi-korban-qz8501#:~:text=Jakarta%2C CNN Indonesia -- PT,Kamis(30/7)

[32] NASUTION, A. A., AZMI, Z., SIREGAR, I. Impact of air transport on the Indonesian economy. *MATEC Web of Conferences* [online]. 2018, **236**, 02010. eISSN: 2261-236X. Available from: https://doi.org/10.1051/matecconf/201823602010

[33] RISDIARTO, D. Legal obstacles to enforcement against unlicensed foreign civil aircraft entering Indonesia's airspace / Kendala hukum penindakan terhadap pesawat udara sipil asing tidak berizin yang memasuki wilayah udara Indonesia. *Jurnal Legislasi Indonesia* [online]. 2019, **16**(3), p. 353-368 [accessed 2024-03-03]. ISSN 0216-1338. Available from: https://e-jurnal.peraturan.go.id/index.php/jli/article/view/492/pdf

[34] SINAGA, N. Authority of military police of the Indonesian air force in handling national airspace boundaries. *Central European Journal of International and Security Studies* [online]. 2018, **12**(4), p. 111-126 [accessed 2024-03-03]. ISSN 1802-548X, eISSN 1805-482X. Available from: https://cejiss.org/authority-of-military-police-of-the-indonesian-air-force-in-handling-national-airspace-boundaries

[35] Indonesian jets force Ethiopian cargo plane to land over airspace breach - Reuters [online] [accessed 2024-09-03]. Available from: https://www.reuters.com/article/world/indonesian-jets-force-ethiopian-cargo-plane-to-land-over-airspace-breach-idUSKCN1P815R/

[36] Ethiopian airlines cargo plane permitted to take off from Indonesia - Antara [online] [accessed 2024-09-03]. Available from: https://en.antaranews.com/news/121883/ethiopian-airlines-cargo-plane-permitted-to-take-off-from-indonesia

[37] Discussion meeting on the draft law on air space management / Rapat pembahasan rancangan undang-undang tentang pengelolaan ruang udara - Indonesian Defence Ministry [online] [accessed 2023-10-13]. Available from: https://www.kemhan.go.id/strahan/2022/08/30/rapat-pembahasan-rancangan-undang-undang-tentang-pengelolaan-ruang-udara.html

[38] FIORINO, F. Garuda pilot arrest stirs criminalization concerns - Aviationweek [online] [accessed 2024-04-23]. Available from: https://aviationweek.com/garuda-pilot-arrest-stirs-criminalization-concerns

[39] HASSANALIAN, M., ABDELKEFI, A. Classifications, applications, and design challenges of drones: a review. *Progress in Aerospace Sciences* [online]. 2017, **91**, p. 99-131 [accessed 2024-04-17]. ISSN 0376-0421. Available from: http://dx.doi.org/10.1016/j.paerosci.2017.04.003

[40] TRAN, T. H., NGUYEN, D. D. Management and regulation of drone operation in urban environment: a case study. *Social Sciences* [online]. 2022, **11**(10), p. 1-19 [accessed 2024-07-03]. ISSN 2076-0760. Available from: https://doi.org/10.3390/socsci11100474

[41] GALLARDO-CAMACHO, J., BREIJO, V. R. Relationships between law enforcement authorities and drone journalists in Spain. *Media and Communication* [online]. 2020, **8**(3), p. 112-122 [accessed 2024-09-03]. ISSN 2183-2439. Available from: https://doi.org/10.17645/mac.v8i3.3097

[42] NURGALIEV, I., ESKANDER, Y., LIS, K. The use of drones and autonomous vehicles in logistics and delivery. *Logistics and Transport* [online]. 2023, **57**(1-2), p. 77-92 [accessed 2024-09-03]. ISSN 1734-2015. Available from: https://system.logistics-and-transport.eu/index.php/main/article/view/777/691

[43] KELLERMANN, R., FISCHER, L. Drones for parcel and passenger transport: a qualitative exploration of public acceptance. *Sociology and Technoscience* [online]. 2020, **2**(2), p. 106-138 [accessed 2024-09-03]. eISSN 1989-8487. Available from: http://uvadoc.uva.es/handle/10324/44871

[44] Drone transport: info, projects and resources - iMOVE Australia [online] [accessed 2025-01-26]. Available from: https://imoveaustralia.com/topics/drone-transport/

[45] PRIANTO, Y., SASMITA, P. Y., MOURIN, A. A. The urgency of government regulations in substitute of law about the drone usage regulation. In: 2nd Tarumanagara International Conference on the Applications of Social Sciences and Humanities TICASH 2020: proceedings. Vol. 478. 2020. ISSN 2352-5398, p. 15-18. Available from: https://doi.org/10.2991/assehr.k.201209.003

[46] KPPU five-year report: period of institutional development and initial implementation / Laporan lima tahun KPPU: periode pengembangan kelembagaan dan implementasi awal - KPPU [online] [accessed 2024-03-04]. Available from: https://www.yumpu.com/id/document/view/33870854/periode-pengembangan-kelembagaan-dan-implementasi-awal-kppu

[47] ISTIFADAH, N. The concentration pattern and implication of 2001 flight deregulation policy on domestic commercial flight industry in Indonesia. *Journal of Indonesian Economy and Business* [online]. 2009, **24**(1), p. 69-80 [accessed 2024-09-03]. ISSN 2085-8272, eISSN 2338-5847. Available from: https://journal.ugm.ac.id/jieb/article/view/6333/17952

[48] HIRSH, M. Emerging infrastructures of low-cost aviation in Southeast Asia. *Mobilities* [online]. 2017, **12**(2), p. 259-276 [accessed 2024-09-03]. ISSN 1745-0101, eISSN 1745-011X. Available from: https://doi.org/10.1080/17450101.2017.1292781

[49] HIJRIYA, S. The bankruptcy of airlines as lessee in finance leasing based on Cape Town convention 2001 and harmonization with the bankruptcy and suspension of payment act number 37 years 2004. *Jurnal Hukum and Pembangunan* [online]. 2018, **47**(3), p. 377-391 [accessed 2024-07-03]. ISSN 0125-9687, eISSN 2503-1465. Available from: https://scholarhub.ui.ac.id/jhp/vol47/iss3/6

[50] ADJIE, H. K., BAHARI, D. M. Examining Indonesian government strategies in the aviation sector post Covid-19 pandemic. *Journal Contemporary Governance and Public Policy* [online]. 2021, **2**(2), p. 79-91 [accessed 2023-09-08]. ISSN 2722-3981, eISSN 2722-3973. Available from: https://doi.org/10.46507/jcgpp.v2i2.45

[51] AFIFA, L., RANGGASARI, R. Pandemic: AirAsia plans to stop flying 3 months - Tempo [online] [accessed 2024-03-04]. Available from: https://en.tempo.co/read/1349307/pandemic-airasia-plans-to-stop-flying-3-months

[52] SUNDA, U. FIR agreement with Singapore affirms Indonesia's sovereignty / Perjanjian FIR dengan Singapura tegaskan kedaulatan Indonesia - Rakyat Merdeka [online] [accessed 2022-11-22]. Available from: https://rm.id/baca-berita/internasional/111112/perjanjian-fir-dengan-singapura-tegaskan-kedaulatan-indonesia

[53] EHLERS, P. N., Case note: lake constance mid-air collision: Bashkirian Airlines v. Federal Republic of Germany. *Air and Space Law* [online]. 2007, **32**(1), p. 75-79 [accessed 2024-05-03]. ISSN 0927-3379, eISSN 1875-8339. Available from: https://doi.org/10.54648/aila2007007

[54] KOREMENOS, B. When, what, and why do States choose to delegate? *Law and Contemporary Problems* [online]. 2008, **71**(1), p. 150-180 [accessed 2024-08-03]. ISSN 0023-9186, eISSN 1945-2322. Available from: https://www.jstor.org/stable/27592225

[55] VAN ANTWERPEN, N. *Cross-border provision of air navigation services with specific reference to Europe: safeguarding transparent lines of responsibility and liability*. Wolters Kluwer Law and Business, 2008. ISBN 9789041126887.

[56] LEVY, S. J. The Expanding responsibility of the government air traffic controller. *Fordham Law Review* [online]. 1968, **36**(3), p. 401-424 [accessed 2024-06-03]. ISSN 0015-704X. Available from: https://ir.lawnet.fordham.edu/flr/vol36/iss3/2

[57] ARAFAH, A. R, BAIS, A. N., TJITRAWATY, A. T., NURKHALISHA, F. H. FIR Agreement Indonesia-Singapore: what are the legal implications? *Heliyon* [online]. 2024, **10**(8), e29708 [accessed 2024-04-03]. ISSN 2405-8440. Available from: https://doi.org/10.1016/j.heliyon.2024.e29708

[58] SEO, D. M, A Comparative study on the effective implementation of the mandatory IMO member state audit scheme: a case study of the Republic of Korea - World Maritime University Dissertation [online] [accessed 2024-12-03]. 2010 Available from: https://commons.wmu.se/cgi/viewcontent.cgi?article=1429&context=all_dissertations

[59] HUDA, N. PERPU legal examining by the constitutional court / Pengujian PERPU oleh mahkamah konstitusi. *Jurnal Konstitusi* [online]. 2010, **7**(5), p. 73-91 [accessed 2024-04-03]. ISSN 1829-7706, eISSN 2548-1657. Available from: https://doi.org/10.31078/jk754

Dear colleagues,

Journal for sciences in transport Communications - Scientific Letters of the University of Zilina are a well-established open-access scientific transport journal aimed primarily at the topics connected with the field of transport. The main transport-related areas covered include Civil engineering, Electrical engineering, Management and informatics, Mechanical engineering, Operation and economics, Safety and security, Travel and tourism studies. Research in the field of education also falls under these categories. The full list of main topics and subtopics is available at: *https://komunikacie.uniza.sk/artkey/inf-990000-0500_Topical-areas.php*

Journal for sciences in transport Communications - Scientific Letters of the University of Zilina is currently indexed and accepted by CEEOL, Crossref (DOI), DOAJ, EBSCO Host, Electronic Journals Library (EZB), ERIH Plus, Google Scholar, Index Copernicus International Journals Master list, iThenticate, JournalGuide, Jouroscope, Norwegian Register for Scientific Journals Series and Publishers, ROAD, ScienceGate, SCImago Journal & Country Rank, SciRev, SCOPUS, Web of Science database, WorldCat (OCLC).

Journal for sciences in transport Communications - Scientific Letters of the University of Zilina is preserved in CLOCKSS and Portico to guarantee long-term digital preservation and is archived in the national deposit digitalne pramene.

Authors can share their experiences with publishing in our journal on SciRev.

Journal for sciences in transport Communications - Scientific Letters of the University of Zilina has been selected for inclusion in the Web of Science™. Articles published after 2022, beginning with 24(1), will be included in the product Emerging Sources Citation Index (ESCI).

I would like to invite authors to submit their papers for consideration. We have an **open access policy under Creative Commons (CC BY) license** and Article Processing Charge (APC) is **400 Euro** (price excluding VAT). The price of one additional page of the submitted article beyond the prescribed scope (15 pages) is **50 Euro** (price excluding VAT). Print edition fee is **100 Euro** per one piece (price excluding VAT) including shipping costs. Our journal operates a standard single-anonymous peer-review process, the successful completion of which is a prerequisite for publication of articles.

Our journal is issued four times a year (in January, in April, in July and in October).

I would also like to offer you the opportunity of using already published articles from past issues as source of information for your research and publication activities. All papers are available at our webpage: http://komunikacie.uniza.sk, where you can browse through the individual volumes. Our journal offers access to its contents in the open access system on the principles of the license Creative Commons (CC BY 4.0).

For any questions regarding the journal Communications - Scientific Letters of the University of Zilina please contact us at: *komunikacie@uniza.sk.*

We look forward to future cooperation.

Sincerely

Branislav Hadzima
editor-in-chief

A SYSTEMIC APPROACH TO FORMALIZED DESCRIPTION OF FACTORS AFFECTING THE BRAKE SYSTEM ELEMENTS OF WAGON BOGIES

Sergii Panchenko[1], Juraj Gerlici[2], Alyona Lovska[2,*], Vasyl Ravlyuk[1]

[1]Ukrainian State University of Railway Transport, Kharkiv, Ukraine
[2]University of Zilina, Zilina, Slovak Republic

*E-mail of corresponding author: Alyona.Lovska@fstroj.uniza.sk

Sergii Panchenko 0000-0002-7626-9933,
Alyona Lovska 0000-0002-8604-1764,
Juraj Gerlici 0000-0003-3928-0567,
Vasyl Ravlyuk 0000-0003-4818-9482

Resume

The article highlights the results of the traffic safety analysis conducted in the wagon industry of Ukrainian Railways. Based on this study, it was found that the largest number of transport accidents are caused by the braking equipment of wagons. The study is based on the statistical data on malfunctions of the mechanical part of the brake equipment of bogies, in particular, those caused by the wear of wagon brake pads. The results obtained were arranged and processed in the data analysis and visualization program STATISTIKA.

Using a systemic approach, the structural, technological and operational factors that affect the reliability and efficiency of the brake system of bogies and the wagon safety were classified.

The research could contribute to increase the efficiency of the railway transport operation and maintenance of its position in the spectrum of the transportation process.

Available online: https://doi.org/10.26552/com.C.2025.016

Article info

Received 7 October 2024
Accepted 17 December 2024
Online 27 January 2025

Keywords:

railway transport
traffic safety
brake system
systemic approach
formalized description

ISSN 1335-4205 (print version)
ISSN 2585-7878 (online version)

1 Introduction

The development of Ukraine's transport system requires a comprehensive solution for increasing the operational efficiency of railway rolling stock and ensuring the safety of trains [1-2]. Whereas an increased volume of the freight transported by Ukrainian Railways (UZ) requires greater weight and higher speeds of freight trains [3-5]. All of these can be achieved by reliable operation of the automatic wagon brakes. However, the analysis of the rail transport accidents has proved that the technical condition of the brake equipment has significantly deteriorated in recent years. The largest number of damages has occurred to the mechanical part of brakes, which is the key element of the train traffic safety. The inspections of the brake systems of bogies, belonging to the UZ's inventory wagon fleet and industrial enterprises, have shown that most of the devices for the parallel retraction of brake shoes are in an unsatisfactory condition. One of the reasons is the imperfect design of the brake lever transmission (BLT) of bogies.

A typical break beam used in bogies has a balanced suspension. However, this condition is violated after the BLT elements are attached. Under the influence of forces, generated by the weight of the attached elements, the brake beams incline and come closer to the wheels while the upper ends of the pads press the wheels. When the wagon moves without braking, the upper ends of the pads rub against the wheels. As a result, the upper parts of the brake pad area are subjected to intense abrasion, which causes abnormal wear. During the braking, a harmful abrasion of the pads adds unwanted contact friction, which reduces the braking performance of trains and increases the risk of train derailments. It also creates conditions for the high-temperature surface damage to the wheels. Therefore, most wagons are running with loud tapping wheels, which increases the resistance to movement and leads to unnecessary energy consumption for train traction. In addition,

this circumstance may contribute to the occurrence of rail transport accidents. In this regard, the issue of identifying the factors affecting the reliability of the wagon brake system is urgent.

Given the acute urgency of the problem of ensuring the train safety, experts and scientists from different countries have carried out numerous studies, based on which various devices and brake lever transmission mechanisms have been developed to eliminate or slow down the intensive wear of pads, for example, such as the dual wedge-shaped wear. Thus, in [6] the authors proposed a brake pad retraction device for wagon bogies with automatic correction of the relative position of the brake pads with respect to the rolling surfaces of wheels. However, such a device complicates the BLT and requires periodic labour-intensive adjustments in operation, thus making it impractical.

The issue of improving the efficiency of the pneumatic brake on the hopper wagon is covered in [7], where the authors proposed the modernisation of the BLT design and substantiate it using Solid Edge Siemens PLM Software. However, it is not quite clear how the maintenance and repair of the functionally configurated levers can be carried out. In addition, it should be noted that the calculations did not take into account the final forces acting on the pads for which such a BLT was designed.

Over the past decade, experts from many countries have been studying the specifics of the braking process in rail vehicles so that to improve the efficiency and reliable operation of BLT. For example, in study [8] is described the calculations of the braking force of a vehicle equipped with a UIC pneumatic brake designed for passenger trains, while in study [9] is presented an attempt to integrate this idea into the wagon fleet, which would improve the braking efficiency and, consequently, traffic safety.

The peculiarities of ensuring the stable friction properties of brakes used for railway rolling stock are given in [10]. A new approach to achieve a stable friction coefficient during different train brake modes is proposed. Various designs were used to modernise the elements of the brake pad/wheel tribotechnical pair and their mechanical characteristics; the results were experimentally confirmed. However, these studies were made for the disc brake.

In study [11] the analysis is highlighted of some typical block brakes rationally used on Chinese subway vehicles. Among their advantages are flexible operation, quick response and compact structure. In some countries block brakes are used on wagon bogies for more efficient braking and uniform wear of brake pads. However, their use in wagon bogies will increase the weight, air consumption for braking, repair time and complexity of wagon maintenance.

A scientific approach to assessing the efficiency of the wagon brake system is presented in study [12]. An information model for describing the wagon braking is proposed. The study also presents mathematical models with the main characteristics of the braking system, which allows estimating the braking efficiency of the train. However, the calculations of braking processes do not include the coefficient of abnormal wear of brake pads, which can significantly affect the wagon braking distance.

An analysis of the quality performance of cast-iron and composite pads used on different vehicles is highlighted in [13]. Some negative factors of the brake pad operation are given, their impact on the environment and processes that cause damage to the rolling surface of wheels of the rolling stock are described.

An analysis of braking devices in the shoe/wheel tribotechnical pair is given in [14]. The negative consequences of using shoe brakes are also given. The recommendations for the use of disc brakes with conventional tribotechnical pairs are provided [15].

Authors of [16] have dealt with the effect of brake pad material (composite rubber compound) on the rolling surfaces of wheels under operating conditions. The study also gives a review of literature sources covering similar research. It is established that the causes of wheel malfunctions are affected by the thermal conditions mainly during braking. The authors prove that the temperature on the rolling surfaces of wheels during braking with composite-rubber-compound pads can reach values of more than 900 °C. The main reason for this is the relatively low thermal conductivity of composite-rubber-compound pads in comparison with the thermal conductivity of cast-iron pads. However, the studies described do not take into account the fact that in most wagons, more than 90% of composite brake pads have dual wedge-shaped wear. Therefore, such pads have a smaller brake area if compared to new pads, which negatively affects both the braking efficiency and the appearance of surface high-temperature defects on the wheels in operation.

Authors of studies [17-19] emphasize that the overheating of tribotechnical pairs can cause malfunctions of the brake system and adversely affect the traffic safety. Thus, theoretical studies were carried out regarding the possibility of increasing the heating temperature of tribotechnical pairs during braking for different speeds and brake disk designs.

The results presented in [20-22] confirm the predominant influence of thermal loads over the mechanical ones, as well as the residual stresses caused by the high thermal loads in the all-metal wheel with a block brake.

The analysis of literature sources has made it possible to conclude that the issues of better rail traffic safety by improving the operating conditions of brake systems are quite relevant. At the same time, these issues require further research.

The purpose of the study is to formally describe the factors affecting the functioning of the BLT elements using a systemic approach. To achieve this purpose, the

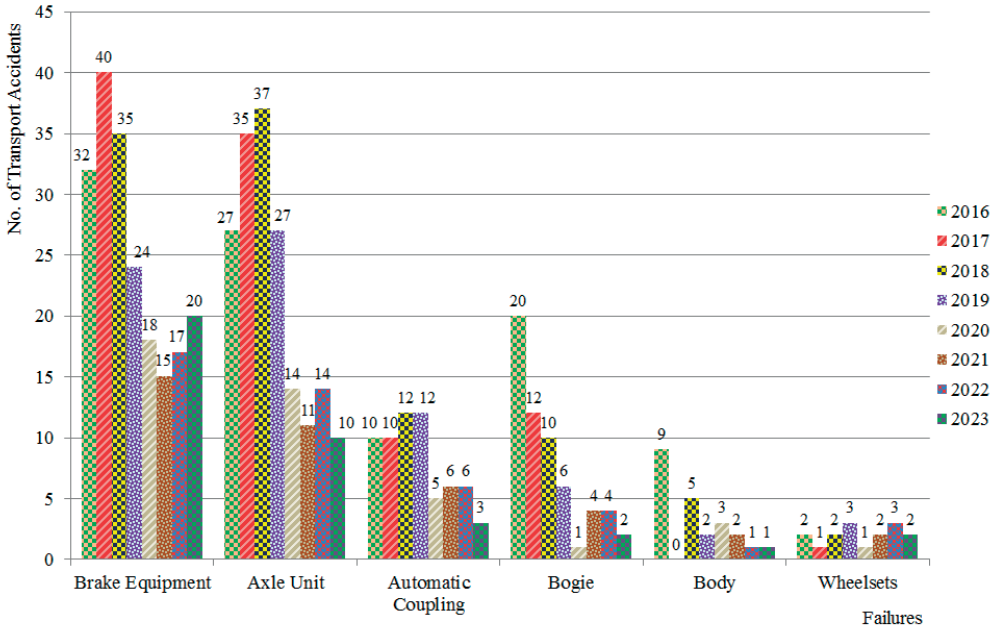

Figure 1 *The comparative bar chart of transport accidents in the wagon industry by type of wagon component failures*

following tasks were defined:

- to analyse the state of the problem of train safety; and
- to classify the factors affecting the reliability and efficiency of the wagon brake system using a systemic approach.

2 Materials and methods

The main causes of railway accidents, due to wagon malfunctions caused by the fault of wagon repair enterprises, are:

- faulty wagon components due to low-quality repairs;
- poor organisation of train maintenance;
- lack of equipment, instruments, tools, means of diagnosis and flaw detection, spare parts for quality repair and maintenance in accordance with the requirements given in regulatory and technical documentation;
- poor-quality repair and testing of brake equipment units;
- violation of the regulatory and technical requirements during scheduled repairs and maintenance; and
- unsatisfactory technical training provided for maintenance and operating personnel.

The quality of work of the wagon industry can be assessed by the number of transport accidents, failures and malfunctions of technical means over a certain time period. For UZ the main condition of traffic safety is ensuring the reliability of the brake equipment of wagons, which is the backbone of traffic safety. For modern rolling stock it can be improved by means of proper identification of causes of malfunctions of the brake equipment [23].

The analysis of traffic safety for the UZ wagon fleet over a period from 2016 to 2023 was based on the number of failures in wagon units, as shown in the comparative bar chart (Figure 1).

Figure 1 shows that in recent years, the wagon brake equipment has become one of the most vulnerable elements under modern operating conditions and for most wagons it is in a poor state. It can also be seen that the number of transport accidents with wagons has been steadily declining over the past few years. The main cause is the reduction in the UZ inventory wagons fleet. It can also be seen that the number of wagons repaired at depots or repair enterprises has been steadily declining recently. Therefore, the reduction dynamics regarding the number of transport accidents in relation to the number of wagons repaired in recent years has amounted to 0.23%. This indicates that the reduction in transport accidents in the wagon industry invariably depends on the number of repaired wagons, however the traffic safety is not improving [24].

Based on the analysis (Figure 1), it was found that the largest number of transport accidents in the wagon industry between 2016 and 2023, caused by unsatisfactory operation of brake equipment, occurred in 2017 and amounted to 40 accidents. Therefore, it was decided to pay more careful attention to the quantitative assessment of failures in braking equipment that had led to transport accidents on the Ukrainian railways.

Such a qualitative analysis of brake equipment failures between 2002 and 2023 was based on the regulatory and technical documentation. Based on the results, a bar chart was constructed (Figure 2), which shows that the largest number of transport accidents due to brake equipment failures, 113 accidents in 2003, occurred due to poor quality repairs provided by UZ

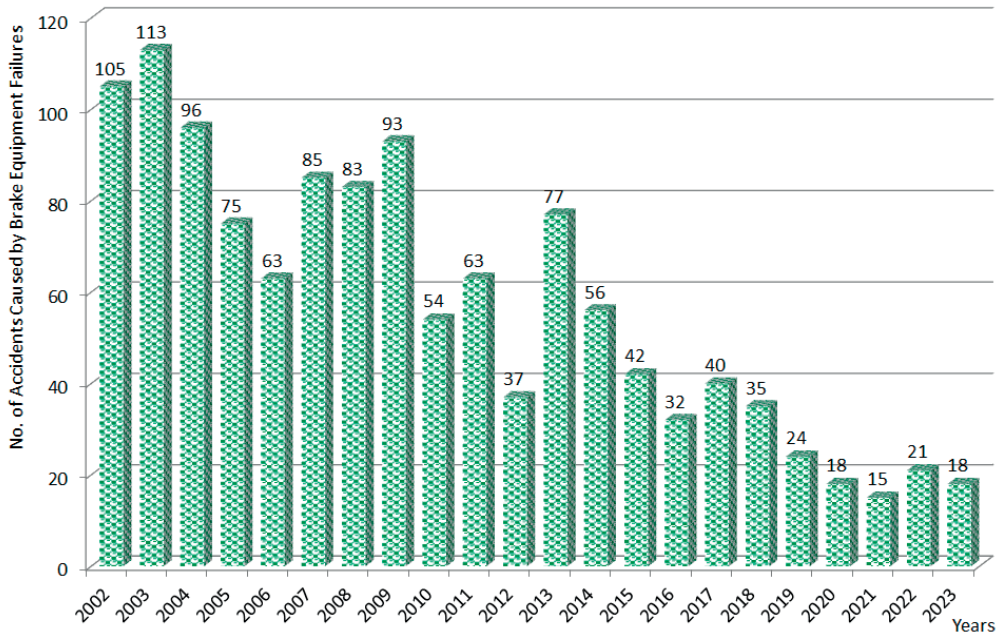

Figure 2 *The bar chart of the distribution of failures in the wagon brake equipment that led to transport accidents*

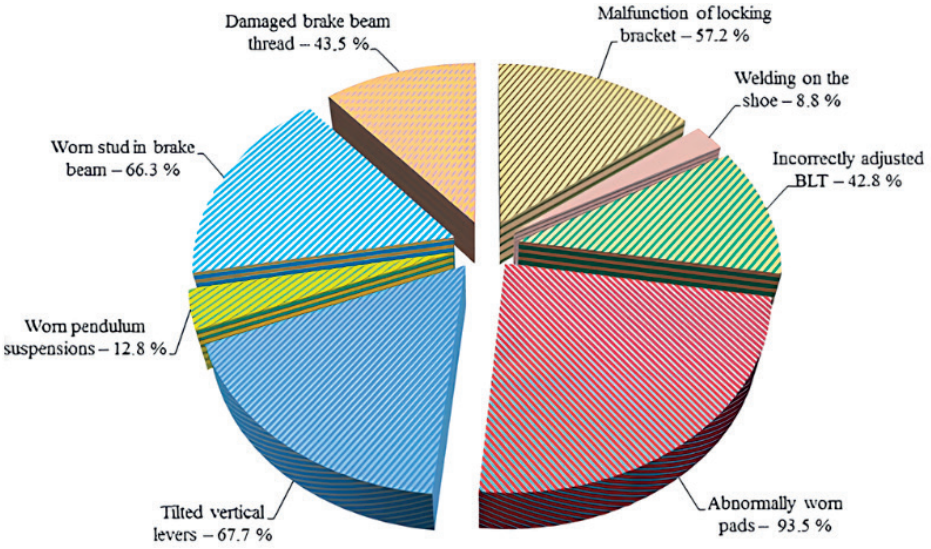

Figure 3 *The distribution diagram of malfunctions in the mechanical part of the brake equipment of wagon bogies*

wagon repair enterprises. It can also be seen that the number of transport accidents due to brake equipment failures had been constantly changing by year. This has proved once again that Ukrainian wagon repair enterprises provide poor quality repairs of wagon brake components due to the use of outdated equipment. Despite the fact that the number of failures has been decreasing rapidly in recent years, the safe operation of wagons it not guaranteed.

Based on the results of the analysis of transport accidents in the wagon industry, it was found that the wagon braking equipment ranked first in terms of failures and malfunctions occurred in operation. Therefore, the technical condition of the mechanical part of wagon brake elements was studied at wagon repair enterprises through 2023. The BLT of wagons was inspected at wagon repair enterprises specializing in brake beams. During those inspections, all the dimensions of the BLT components were checked using measuring tools and templates; then the components were divided into the following groups:

- components that can be used without repair;
- components that need repairing according to the technological process;
- components that cannot be repaired but can be used for other purposes at the wagon repair enterprise; and
- components that cannot be repaired and should be sent for scrap.

While dividing the BLT components into these

groups, their defects were thoroughly recorded and further used in the research. A total of 5,702 BLT components were inspected, and the following diagram was drawn based on the results of the statistical data obtained (Figure 3).

Based on the observation results, the following main types of malfunctions were identified:

- abnormal brake pad wear formed due to failures of the device for the parallel retraction of the brake shoes - 93.5% (Figure 4, a);
- malfunctions of brackets and locks (devices for parallel retraction of the brake shoes), i.e., incomplete retraction of brake pads from the rolling surface of wheels in operation due to the inoperability of standard devices - 57.2% (Figure 4, b);
- wear of the brake beam stud due to its interaction with the bracket - 66.3% (Figure 4, c);
- increased tilt angles of vertical two-arm levers, especially the internal levers of the BLT of bogies in the braked state with full-size and maximally worn composite brake pads due to a relatively large thickness of pads reinforced to 65 mm, which negatively affects the braking efficiency of wagons - 67.7% (Figure 4, d);
- damage to the threaded part of the brake beam head for connecting the crown nut, which forces the shoe with a pad to slip behind the outer edge of the wheel thread and causes the ridge wear of the pad in operation - 43.5% (Figure 4, e);
- misalignment of the BLT due to the incorrectly

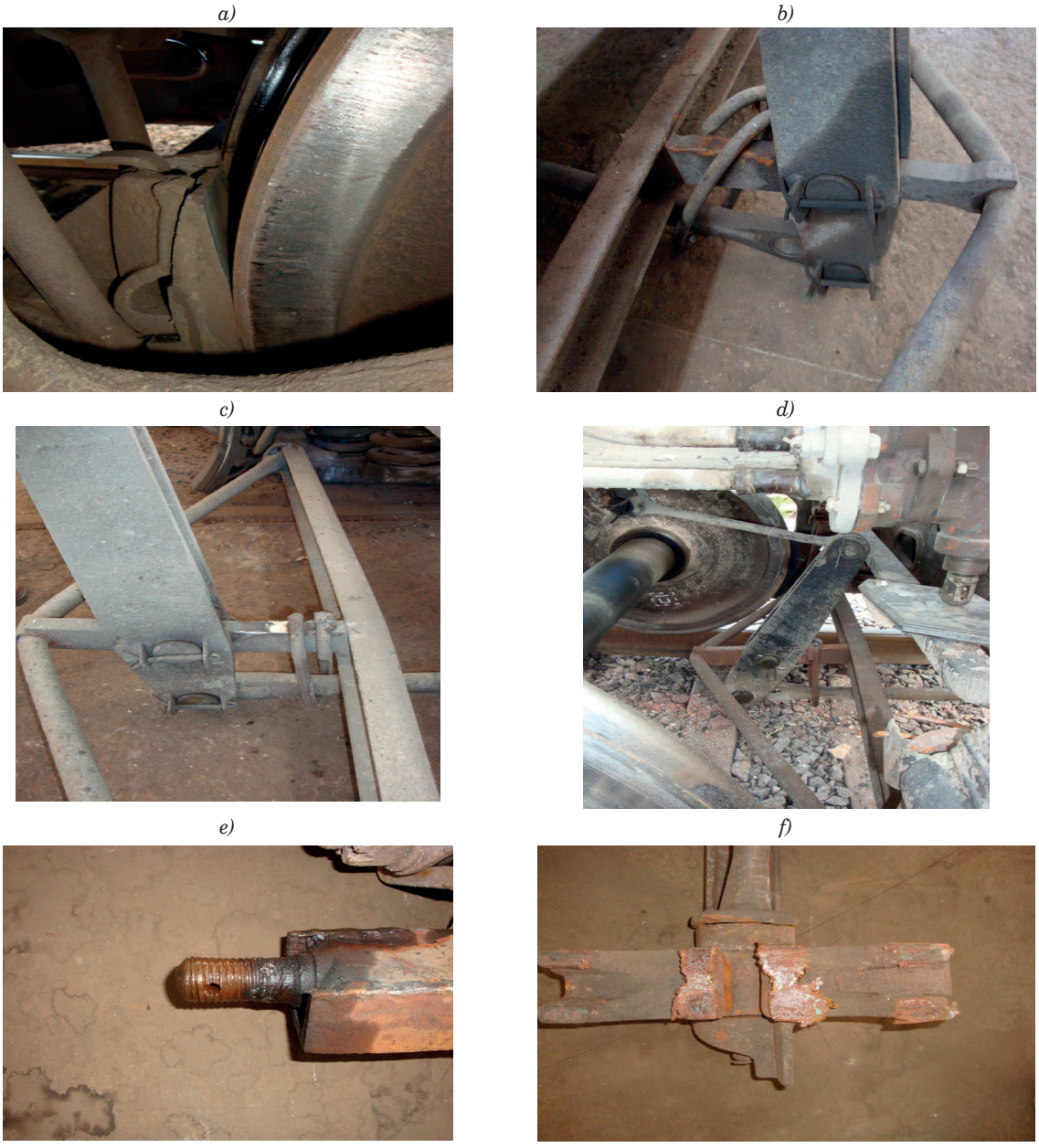

Figure 4 *Malfunctions of the mechanical part of the braking equipment in wagon bogies*
a) abnormal pad wear; b) deformation of bracket and absence of lock; c) worn brake beam stud; d) tilt of the vertical lever; e) damage to the threaded part on the brake beam head; f) welding on the shoe

selected locations for the pivot pins in rods and links - 42.8%;
- worn pendulum suspensions resulting from the local contact of their cylindrical part with the shoe - 12.8%;
- welding on the shoe due to a maximally worn pad with its subsequent destruction - 8.8% (Figure 4, f)).

In practice, the malfunction of the pad can occur in operation due to the adverse effect of forces that reduce the braking efficiency; in terms of the traffic safety, it is unacceptable. Thus, the investigation of the brake pad wear in wagons cannot be carried out without taking into account the cause - wear - effect relationship.

3 Results

The statistical data obtained by inspecting the brake pads for different wagon types made it possible to analyse the formation of dual wedge-shaped wear and assess the braking efficiency for the rolling stock.

The statistical data on the wear of wagon brake pads were arranged and processed in STATISTIKA. The results of the calculations are shown in Figure 5. The results of statistical data processing in the "STATISTIKA" software package made it possible to establish that the distribution of the wedge-dual wear of brake pads during their use in a typical brake lever transmission is not described by a normal law (red curve in Figures 5-6). At the initial stage of wagon operation, new pads wear out mostly due to the free-running and traction modes rather than the braking mode. Thus, the upper parts of the working surfaces of pads wipe (the edge vibration wear) due to the wagon dynamics; it becomes the centre of the dual wedge-shaped wear with the simultaneous tilting of the pad [25-26].

When the wagon mileage increases from 23,000 to 26,400 km (Figure 6, Position 1), the pad wears intensively forming the dual wedge-shaped wear. However, when the wagon mileage increases from 35,000 to 44,700 km, the wear in the upper part of the pad slows down (Figure 6, b, Position 2) [27].

The analysis of field surveys and analytical studies of the dual wedge-shaped wear of brake pads have made it possible for the first time to identify the negative factors associated with significant damage to the railway infrastructure and the environment.

The current development of the wagon-building and wagon-repair industry involves the search for the new scientific methods on how to design and modernize wagon assemblies. Therefore, the systemic approach is the basis for developing a classification of factors affecting the reliability and efficiency of the mechanical BLT of wagons [28]. This approach can help to consider the BLT as an integrated system of components, connections, and properties that specify the whole brake system in operation. An important step of this systemic approach is determining the BLT structure, i.e., the identification of elements, their connections and interactions. The structure of the mechanical BLT of the wagon under study can be considered for both analyzing its properties and describing it as a set of individual interconnected elements.

The systemic approach can also be used for the classification of factors contributing to the abnormal wear of the brake pads of bogies in operation; these factors can be divided into the following groups:
- structural, including the shape, size, materials of brake system components, types of their interconnections, etc.;
- technological, including specific requirements for the BLT components in production and repairs; and
- operational, ensuring the proper use of the BLT of wagons over the guaranteed inter-repair period.

Figure 7 presents a classification of structural, technological and operational factors affecting the reliability and efficiency of the braking system of wagon bogies, and train safety, based on the systemic approach.

The structural factors include:
- offset hole in the brake beam due to the BLT design features of wagon bogies. This can lead to the brake beam disbalance and cause the dual wedge-shaped wear of pads;
- a guide mechanism for the brake lever gears is not provided in the design, therefore the pads incline to the wheels when the brakes are released in the

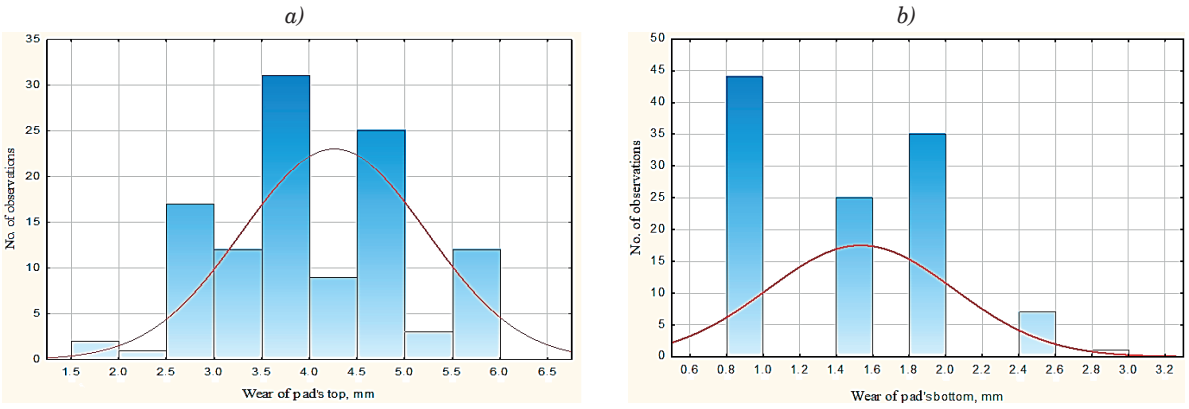

Figure 5 *The brake pad wear for the wagon mileage from 7,200 to 10,000 km a) pad's top; b) pad's bottom*

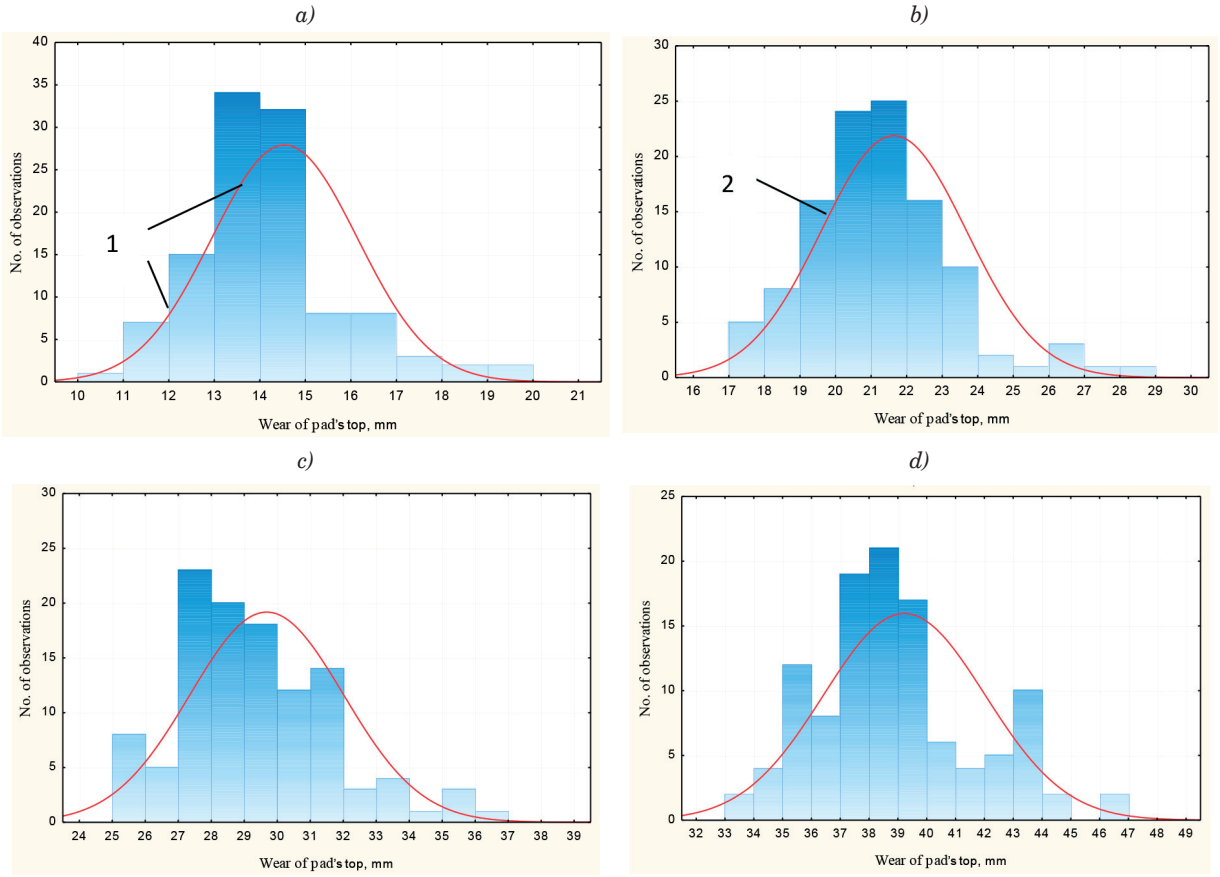

Figure 6 *The wear of the pad's top for the wagon mileages a) 23,000 - 26,340 km; b) 35,000 - 42,300 km; c) 44,700 - 48,000 km; d) 59,300 - 62,400 km*

traction and free-running modes, which causes abnormal wear of the pads; and

- geometrical features of pads affect the contact area of the brake pad/wheel tribotechnical pair. Pads must have the geometric friction surfaces, which are similar to the rolling surfaces of wagon wheels. If geometric parameters of the pads change, that will negatively affect the braking efficiency of a vehicle.

The technological factors include:

- violation of the production technology of the BLT of wagon bogies, which results in changes in the mechanical properties of the BLT components, increased wear and violation of nominal dimensions accompanied by operational defects;
- violation of the repair technology of the BLT of wagon bogies, which results in changes in the geometric dimensions of the components. During the welding and surfacing, the metal structure can be distorted, which changes the properties of components, creates microcracks and other defects, thus reducing the BLT reliability;
- violation of the assembly technology for the brake beam, which results in changes in the geometric dimensions of its parts. In braking, it can lead to the BLT malfunctions and displacements of pads relative to the rolling surfaces of wheels;
- violation of the BLT adjustment technology, which results in an increase or a decrease of clearances between the shoe and the wheel, provided that the M 1180.000 device is in a good working condition. If the clearances were reduced and the BLT was not adjusted properly, the pads may rub against the wheels when the brakes are released; it results in defects on the rolling surfaces of wheels as well as abnormal pad wear. The effects of increased gaps and violations of the conditions for the BLT adjustment are: 1) the braking efficiency decreases and the train safety deteriorates; 2) the probability of damage to the BLT increases and the lever gears can tilt; 3) hinge elements in the BLT can be damaged due to vibration in operation; and 4) pads are displaced relative to the rolling surfaces of wheels due to increased gaps between the pad and a wheel when braking.

The operational factors include:

- damage to the device M 1180.000 of the BLT of wagon bogies due to a malfunction of the lock and stretching of the bracket; it results in the disfunction of a device together with appearance of the standard clearances between the pad and the wheel. When the train is running without braking, the upper end of the pad rubs against the rolling surface of the wheel and causes harmful abrasion in its upper part. For the pads with dual wedge-shaped

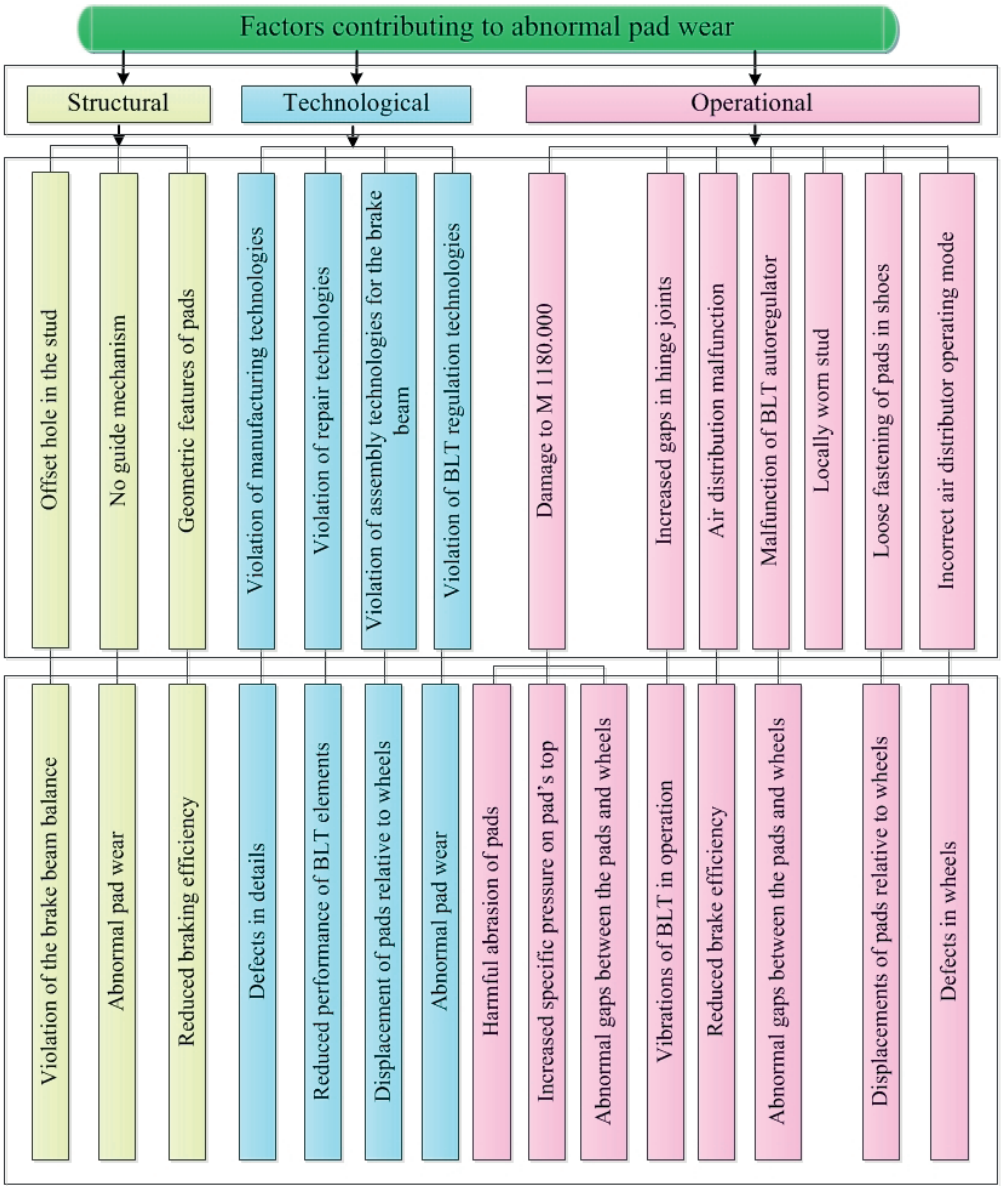

Figure 7 *The factors affecting the reliability of wagon brakes*

wear, the specific pressures in the upper part of the pad increases, and the friction temperature of the tribotechnical pairs increases at the point where the planes separate; it causes high-temperature damage to the rolling surface of the wheel;

- increased gaps in the hinge joints of the BLT of wagon bogies when the train is moving over a rail joint, a track irregularity or a rail switch result in increased displacements of the elements and their intensive wear due to vibrations from the BLT in operation;
- air distributor malfunctions cause slow brake release or failure to release the brake, which leads to an increase in the temperature of the brake pad/wheel tribotechnical pair, its increased wear and damage. In addition, a faulty air distributor can cause unauthorised brake release, which can lead to the wagon brake release and reducing the braking efficiency of the rolling stock, as well as impairing the traffic safety;
- malfunction of the BLT autoregulator leads to a violation of its dimensions in operation in accordance with the current regulatory and technical requirements, thus affecting the abnormal gaps between the pad and the wheel;
- local wear of the brake beam stud occurs due to its permanent contact with the bracket of the device M 1180.000 of the BLT of wagon bogies, which is caused by its failure and leads to dual wedge-shaped wear of the pads when the train is moving without braking;
- improper fastening of the pad in the brake shoe due to the application of non-standard fasteners, worn retaining keys or shoes can lead to increased gaps between the contacting surfaces and displacement of the pad relative to the wheel when braking;

- incorrect operation mode of the air distributor in the wagon causes excessive pressure of the brake pads on the wheels, resulting in increased wear and damage, as well as the jamming of the wheelsets and leads to slides, scrapes and other defects on the rolling surfaces of wheels.

It is important to note that the negative effects of the above-mentioned classified factors can reduce the train braking efficiency, increase energy consumption needed for the train traction, reduce the service life of the pads, damage the rolling surfaces of wheels and negatively impact the environment; they also cause the significant damage to railway infrastructure and train safety. In this regard, further research will aim at developing measures for the BLT modernisation, which will increase the mileage of wagons with composite pads and extend their residual service life over the overhaul period [29-31]. This would contribute to increase the efficiency of railway transport operation and maintenance of its position in the spectrum of the transportation process [32-35].

4 Conclusions

1. The analysis of the transport accidents on Ukraine's railways has been carried out. It has shown that from 2016 to 2023, the largest number of such accidents were caused by faults in the brake equipment, which threatened the traffic safety of wagons.

The analysis of transport accidents caused by brake equipment failures in wagons, occurred from 2002 to 2023, has shown that their peak was in 2003 (113 accidents), whereas the smallest number was recorded in 2021 (15 accidents). However, these statistics are not encouraging, given that wagon fleet of Ukrzaliznytsia has been significantly reduced.

The statistical data on malfunctions of mechanical systems of the wagon bogies brake equipment was investigated. It was found that out of 5,702 brake lever transmission (BLT) elements examined, the largest percentage of failures occurred due to abnormally worn composite brake pads and amounted to 93.5%. The locking brackets of the device for the parallel retraction of brake shoes also suffer significant damage during the operation of wagons, which amounted to 57.2%, whereas the cases of worn brake beam studs amounted to 66.3%. In addition, one of the main faults in the BLT of bogies is inclined vertical levers of the brace beam, which amounted to 67.7%. All the above-mentioned faults in the BLT have a direct impact on the abnormal wear of wagon brake pads.

2. A systemic approach was used to determine the factors contributing to abnormal wear of pads in the BLT of wagons. The factors mentioned can lead to the deterioration in the braking efficiency of trains, increased energy consumption needed for train traction, shortened useful service life of the pads, damage to the rolling surfaces of wheels, and negative impact on the environment.

The proposed classification of factors affecting the BLT reliability could help to develop recommendations for the design of modern wagon brake structures. This would reduce operating costs during the freight transportation, as well as increase traffic safety of trains by modernizing the design of the mechanical part of bogie brakes.

Acknowledgment

This publication was supported by the Cultural and Educational Grant Agency of the Ministry of Education of the Slovak Republic under the project KEGA 024ZU-4/2024: Deepening the knowledge of university students in the field of construction of means of transport by carrying out professional and scientific research activities in the field. It was also supported by the Slovak Research and Development Agency of the Ministry of Education, Science, Research and Sport under the project VEGA 1/0513/22: Investigation of the properties of railway brake components in simulated operating conditions on a flywheel brake stand. "Funded by the EU NextGenerationEU under the Recovery and Resilience Plan for Slovakia under the project No. 09I03-03-V01-00131".

Conflicts of interest

The authors declare that they have no known competing financial interests or personal relationships that could have appeared to influence the work reported in this paper.

References

[1] PANCHENKO, S., GERLICI, J., VATULIA, G., LOVSKA, A., RYBIN, A., KRAVCHENKO, O. Strength assessment of an improved design of a tank container under operating conditions. *Communication - Scientific Letters of the University of Zilina* [online]. 2023, **25**(3), B186-B193. ISSN 1335-4205, eISSN 2585-7878. Available from: https://doi.org/10.26552/com.C.2023.047

[2] SOUKUP, J., SKOCILAS, J., SKOCILASOVA, B., DIZO, J. Vertical vibration of two axle railway vehicle. *Procedia Engineering* [online]. 2016, **177**, p. 25-32. ISSN 1877-7058. Available from: https://doi.org/10.1016/j.proeng.2017.02.178

[3] CABAN, J., NIEOCZYM, A., GARDYNSKI, L. Strength analysis of a container semi-truck frame. *Engineering Failure Analysis* [online]. 2021, **127**, 105487. ISSN 1350-6307, eISSN 1873-1961. Available from: https://doi.org/10.1016/j.engfailanal.2021.105487

[4] DIZO, J., BLATNICKY, M. Investigation of ride properties of a three-wheeled electric vehicle in terms of driving safety. *Transportation Research Procedia* [online]. 2019, **40**, p. 663-670. ISSN 2352-1457, eISSN 2352-1465. Available from: https://doi.org/10.1016/j.trpro.2019.07.094

[5] DIZO, J. Analysis of a goods wagon running on a railway test track. *Manufacturing Technology* [online]. 2016, **16**(4), p. 667-672. ISSN 1213-2489, eISSN 2787-9402. Available from: https://doi.org/10.21062/ujep/x.2016/a/1213-2489/MT/16/4/667

[6] RADZIKHOVSKY, A. A., OMELYANENKO, I. A., TIMOSHINA, L. A. Systems approach to designing bogies for freight cars with increased axle loads (in Russian). *Wagon Fleet*. 2008, **8**, p. 10-16. ISSN 1994-4756.

[7] VOLOSHYN, D. I., AFANASENKO, I. M., DEREVYANCHUK, Y. V. To the issue of improving the design of the brake lever transmission of the hopper car (in Ukrainian). *Bulletin of the Eastern Ukrainian National University named after Volodymyr Dahl.* 2018, **2**(243), p. 54-59. ISSN 1998-7927, eISSN 2664-6498.

[8] BUREIKA, G., MIKALIUNA, S. S. Research on the compatibility of the calculation methods of rolling-stock brakes. *Transport* [online]. 2008, **23**(4), p. 351-355. ISSN 1648-4142, eISSN 1648-3480. Available from: https://doi.org/10.3846/1648-4142.2008.23.351-355

[9] LIUDVINAVICIUS, L., LINGAITIS, L. P. Electrodynamic braking in high-speed rail transport. *Transport* [online]. 2007, **22**(3), p. 178-186. ISSN 1648-4142, eISSN 1648-3480. Available from: https://doi.org/10.3846/16484142.2007.9638122

[10] OSENIN, Y. Y. Improving the braking characteristics of rolling stock by ensuring stable operational properties of the disc brake: autoref (in Ukrainian). Thesis. Kyiv: SE "State NDC Railway Transport of Ukraine". 2014.

[11] ZHANG, Y., CHEN, Y., HE, R., SHEN, B. Investigation of tribological properties of brake shoe materials - phosphorous cast irons with different graphite morphologies. *Wear* [online]. 1993, **166**(2), p. 179-186. ISSN 0043-1648, eISSN 1873-2577. Available from: https://doi.org/10.1016/0043-1648(93)90260-S

[12] SAFRONOV, O. M. Application of computer modeling for a refined evaluation of the braking efficiency of freight cars (in Ukrainian). *Collection of Scientific Works of the State University of Infrastructure and Technologies: Series "Transport Systems and technologies"*. 2018, **32**(2), p. 61-75. ISSN 2617-9059.

[13] MAZUR, V. L., NAIDEK, V. L., POPOV, E. S. Comparison of cast iron and composite brake pads with cast iron inserts for railway rolling stock (in Ukrainian). *Metal and Casting of Ukraine* [online]. 2021, **29**(2), p. 30-39. ISSN 2077-1304. Available from: https://doi.org/10.15407/scin15.04.005

[14] SHARMA, R. C., DHINGRA, M., PATHAK, R. K. Braking systems in railway vehicles. *International Journal of Engineering Research and Technology* [online]. 2015, **4**(01), p. 206-211. eISSN 2278-0181. Available from: https://doi.org/10.17577/IJERTV4IS010360

[15] SARIP, S. Design development of lightweight disc brake for regenerative braking - finite element analysis. *International Journal of Applied Physics and Mathematics* [online]. 2013, **3**(1), p. 52-58. eISSN 2010-362X. Available from: https://doi.org/10.7763/IJAPM.2013.V3.173

[16] SIRENKO, K. A., MAZUR, V. L. Analysis of the effect of brake pad material on the formation of defects on the rolling surface of railway wheels (in Ukrainian). *Metal and Casting of Ukraine* [online]. 2024, **2**(32), p. 57-63. ISSN 2077-1304. Available from: https://doi.org/10.15407/steelcast2024.02.008

[17] VAKKALAGADDA, M. R. K., SRIVASTAVA, D. K., MISHRA, A., RACHERLA, V. Performance analyses of brake blocks used by Indian Railways. *Wear* [online]. 2015, **328-329**, p. 64-76. ISSN 0043-1648, eISSN 1873-2577. Available from: https://doi.org/10.1016/j.wear.2015.01.044

[18] VERNERSSON, T. Thermally induced roughness of tread braked railway wheels. Part 1: brake rig experiments. *Wear* [online]. 1999, **236**(1-2), p. 96-105. ISSN 0043-1648, eISSN 1873-2577. Available from: https://doi.org/10.1016/S0043-1648(99)00260-4

[19] VERNERSSON, T., LUNDEN, R. Wear of brake blocks for in-service conditions - influence of the level of modelling. *Wear* [online]. 2014, **314**(1), p. 125-131. ISSN 0043-1648, eISSN 1873-2577. Available from: https://doi.org/10.1016/j.wear.2013.12.008

[20] JOVANOVIC, R., MILUTINOVIC, D. Modern ways for preventing the damages caused by the railway vehicle solid wheel fractures. In: VI International Scientific Conference of Railway Experts: proceedings. 1999. p. 333-318.

[21] MILUTINOVIC, D., TASIC, M., JOVANOVIC, R. Thermal load as a primary cause for the fracture of the block-braked solid wheel. *Railways*. 1999, **11-12**, p. 477-484. ISSN 1867-9668.

[22] VINEESH, K. P., VAKKALAGADDA, M. R. K., TRIPATHI, A. K., MISHRA, A., RACHERLA, V. Non-uniformity in braking in coaching and freight stock in Indian Railways and associated causes. *Engineering Failure Analysis* [online]. 2016, **59**, p. 493-508. ISSN 1350-6307, eISSN 1873-1961. Available from: https://doi.org/10.1016/j.engfailanal.2015.11.023

[23] Freight wagons. Maintenance and repair system according to technical condition: STP 04-010:2018: approved on JSC "Ukrzaliznytsia" dated August 8, 2019 (in Ukrainian). No. 519.
[24] Analysis of the state of traffic safety in the structure of JSC "Ukrzaliznytsia" in 2019 (in Ukrainian). Kiev: Joint-Stock Company "Ukrainian Railway", Department of Traffic Safety, 2019.
[25] ELYAZOV, I., RAVLYUK, V., RYBIN, A., HREBENIUK, V. Determination of forces in the elements of the brake rigging of bogies of freight cars. *E3S Web of Conferences* [online]. 2020, **166**(66), 07004. eISSN 2267-1242. Available from: https://doi.org/10.1051/e3sconf/202016607004
[26] RAVLYUK, V., RAVLIUK, M., HREBENIUK, V., BONDARENKO, V. Research of the calculation scheme for the brake lever transmission and construction of the load model for the brake pads of freight cars. *IOP Conference Series Materials Science and Engineering* [online]. 2019, **708**(1), 012026. ISSN 1757-899X. Available from: https://doi.org/10.1088/1757-899X/708/1/012026
[27] PANCHENKO, S., GERLICI, J., VATULIA, G., LOVSKA, A., RAVLYUK, V., RYBIN, A. Method for determining the factor of dual wedge-shaped wear of composite brake pads for freight wagons. *Communications - Scientific Letters of the University of Zilina* [online]. 2024, **26**(1), p. B31-B40. ISSN 1335-4205, eISSN 2585-7878. Available from: https://doi.org/10.26552/com.C.2024.006
[28] KUSTOVSKA, O. V. *Methodology of the system approach and scientific research: a course of lectures* (in Ukrainian). Ternopil: Economic Opinion, 2005. ISBN 966-654-159-9.
[29] PANCHENKO, S., GERLICI, J., LOVSKA, A., RAVLYUK, V. The service life prediction for brake pads of freight wagons. *Communications - Scientific Letters of the University of Zilina* [online]. 2024, **26**(2), p. B80-B89. ISSN 1335-4205, eISSN 2585-7878. Available from: https://doi.org/10.26552/com.C.2024.017
[30] RAVLYUK, V. H., MYKHALKIV, S. V., RYBIN, A. V., DEREVIANCHUK, I. V., PLAKHTIY, O. A. Forecasting of wear of pads of modernized brake system devices of bogies of freight cars using ARIMA models. *Scientific Bulletin of the National Mining University* [online]. 2020, **6**, p. 48-54. ISSN 2071-2227, eISSN 2223-2362. Available from: https://doi.org/10.33271/nvngu/2020-6/048
[31] DIZO, J., BLATNICKY, M., HARUSINEC, J., SUCHANEK, A. Assessment of dynamics of a rail vehicle in terms of running properties while moving on a real track model. *Symmetry* [online]. 2022, **14**(3), 536. eISSN 2073-8994. Available from: https://doi.org/10.3390/sym14030536
[32] VATULIA, G., LOVSKA, A., PAVLIUCHENKOV, M., NERUBATSKYI, V., OKOROKOV, A., HORDIIENKO, D., VERNIGORA, R., ZHURAVEL, I. Determining patterns of vertical load on the prototype of a removable module for long-size cargoes. *Eastern-European Journal of Enterprise Technologies* [online]. 2022, **6**(7), p. 21-29. Available from: https://doi.org/10.15587/1729-4061.2022.266855
[33] GERLICI J., LOVSKA A., VATULIA G., PAVLIUCHENKOV M., KRAVCHENKO O., SOLCANSKY S. Situational adaptation of the open wagon body to container transportation. *Applied Sciences* [online]. 2023. **13(15).** 8605. ISSN 1729-3774, eISSN 1729-4061. Available from: https://doi.org/10.3390/app13158605
[34] STOILOV, V., SLAVCHEV, S., MAZNICHKI, V., PURGIC, S. Method for theoretical assessment of safety against derailment of new freight wagons. *Applied Sciences* [online]. 2023, **13**, 12698. eISSN 2076-3417. Available from: https://doi.org/10.3390/app132312698
[35] MYSLINSKI, A., CHUDZIKIEWICZ, A. Power dissipation and wear modeling in wheel-rail contact. *Applied Sciences* [online]. 2024, **14**, 165. eISSN 2076-3417. Available from: https://doi.org/10.3390/app14010165

IMPROVING THE ENERGY EFFICIENCY OF THE EXPLOSIVE PULSE DURING DRILLING AND BLASTING OPERATIONS TO INCREASE THE QUALITY OF CRUSHING AND CONDITIONS FOR CONVEYOR DELIVERY OF OVERBURDEN ROCKS IN QUARRIES AND SECTIONS

Tasbulat Monbolovich Igbaev[1], Nurlan Asylkhanovich Daniyarov[2], Adilbek Kazbekovich Kelisbekov[3,*], Arsen Zakirovich Akashev[4]

[1]NJSC Kokshetau University SH. Ualikhanov, Kokshetau, Republic of Kazakhstan
[2]Corporate University of Personnel Services of Kazakhmys Corporation LLP, Karaganda, Republic of Kazakhstan
[3]Department of Transport and Logistics Systems, NJSC Karaganda University named after. E. A. Buketov, Karaganda, Republic of Kazakhstan
[4]Department of Industrial Transport named after. Professor A. N. Daniyarov, NJSC Karaganda Technical University named after Abylkas Saginov, Karaganda, Republic of Kazakhstan

*E-mail of corresponding author: akelisbekov@mail.ru

Nurlan A. Daniyarov 0000-0002-4476-4569, Adilbek K. Kelisbekov 0000-0001-8857-8162, Arsen Z. Akashev 0000-0001-5316-4146

Resume

Widespread application of advanced transportation technologies in conditions of open-pit mining with the use of high-capacity belt conveyors is limited by the need for additional crushing of overburden rocks and minerals. Accordingly, the quality of crushing of rock mass, the output of oversize during drilling and blasting operations at quarries and open-pit operations significantly affect the possibility of using flow and cyclic-flow technologies with the use of conveyor transport. In this paper is presented a method of increasing the energy efficiency of the explosive pulse in drilling and blasting operations by means of developed gas pedal designs to improve the quality of crushing and conditions of conveyor delivery of rock mass.

Article info

Received 8 September 2024
Accepted 27 January 2025
Online 28 February 2025

Keywords:

open-pit mining
cyclic-in-line technologies
conveyor transport
overburden
crushing of rock mass
accelerators
blast wave pulse

ISSN 1335-4205 (print version)
ISSN 2585-7878 (online version)

Available online: https://doi.org/10.26552/com.C.2025.024

1 Introduction

An undeniable trend in the development of the mining industry for the foreseeable future is considered to be the stable orientation of the industry towards an open method of development as providing the best economic indicators. It accounts for up to 73% of the total volume of mining in the world. For example, in the Republic of Kazakhstan, 70% of thermal coal is extracted by open-pit mining, while the main consumers are power plants (70%), industrial enterprises (20%) and the private sector (10%). Open-pit coal mining in Kazakhstan is carried out at three giant deposits (Bogatyr, Severny and Vostochny sections) in the Ekibastuz basin (Pavlodar region) and at four deposits in the Karaganda region (Borlinskoye, Shubarkolskoye, Kushokinskoye and Saryadyrskoye). The total potential for extraction of projected open-pit coal reserves in the country is estimated at 400 million tons per year, and industrial reserves suitable for open-pit mining amount to 21 billion tons [1]. The development of an open-pit mining method, characterized by a combination of preparatory, stripping and mining workings in a quarry field, is accompanied by an increase in production concentration, an increase in depth, spatial dimensions of quarries and sections, distance and complexity of transporting rock mass. At the same time, the determining indicator is the depth of quarries; in particular, the depth of the eleven

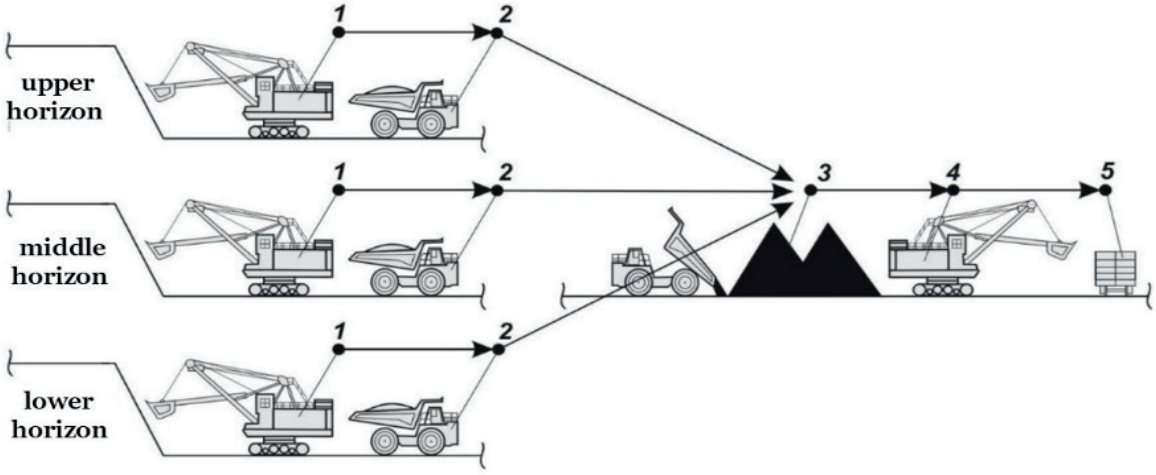

Figure 1 *Cyclic technology of coal mining at the Molodezhny section: 1 - mining excavators, 2 - BelAZ 75131 dump trucks, 3 - averaging warehouses, 4 - loading excavators, 5 - railway transport*

largest coal mines in Kazakhstan varies from 40 to 200 m.

The Molodezhny section of the Borlinsky deposit Kazakhmys Coal LLP uses the cyclic coal mining technology on three horizons - upper, middle and lower. The maximum depth of the incision is approximately 130-140 m. In the faces of mining horizons, coal is loaded by electric and hydraulic excavators into BelAZ 75131 dump trucks. Dump trucks deliver coal from the faces to the average warehouses, where it is loaded onto the railway transport, Figure 1 [2]. At the Bogatyr section, a flow-through technology for the development of minerals and overburden rocks has been implemented, including transshipment of the latter into the developed space, while rotary excavators in combination with conveyors provide an annual productivity of 50 million tons. In-line mining technology has also been introduced at the Vostochny coal mine: coal mining, transportation, averaging and shipment are carried out by four rotary complexes consisting of the SRs(k)-2000 rotary excavator, downhole and interstage loaders, connecting, lifting and main conveyors and an averaging and loading machine. For the excavation of overburden rocks, a cyclic flow technology has been introduced at the quarry, including the operation of two lines of the overburden complex, Figure 2 [3-4].

The active introduction of in-line and cyclic-in-line technologies in open-pit mining conditions is due to an increase in the depth of quarries, a progressive increase in their productivity, since cyclic technology with the delivery of rock mass by road and rail leads to a deterioration in technical and economic indicators due to an increase in the cost of production as a result of an increase in the cost of the transportation process [5]. In particular, according to the results of a number of studies conducted earlier at the Karaganda Polytechnic Institute (later - Karaganda State Technical University), it was found that when deepening a quarry for every 100 m, the cost of transportation for cyclic modes of transport increases by 1.5 times, and when using continuous modes by only 5-6% [6].

An analysis of the operation of technological equipment in open-pit mining shows that a third of the downtime is accounted for by transport due to its cyclical nature of work. In this research it was also found that the use of cyclic technologies in quarries is the most cost-effective at their depth of 150-250 m. When conducting open-pit mining operations at a depth of more than 250 m, it is economically feasible to use in-line and cyclic-in-line technologies [6].

2 Substantiation of the relevance of the problem

A characteristic feature of the use of in-line and cyclic-in-line technologies is the widespread use of conveyors, while the main type of these means of continuous transport currently in operation in quarries are belt conveyors. This is determined by their main design advantages over other types of conveyor systems - comparative simplicity of design and relatively low metal consumption. As the experience of operation shows, modern belt conveyors are capable of providing the high level of production for the largest quarries and sections, but, in general, they are suitable only for transporting loose and semi-hard rocks, and, most importantly, they are not able to move largesized loads of pieces larger than 600 mm, requiring crushing prior to transporting them, which leads to a significant increase in the cost of operating expenses [7-9].

This problem is especially relevant when transporting a large volume of overburden, the extraction of which, as a rule, is carried out in quarries by drilling and blasting. As a rule, the waste rock is

Figure 2 *Cyclic-flow technology at the Vostochny open-pit mine*

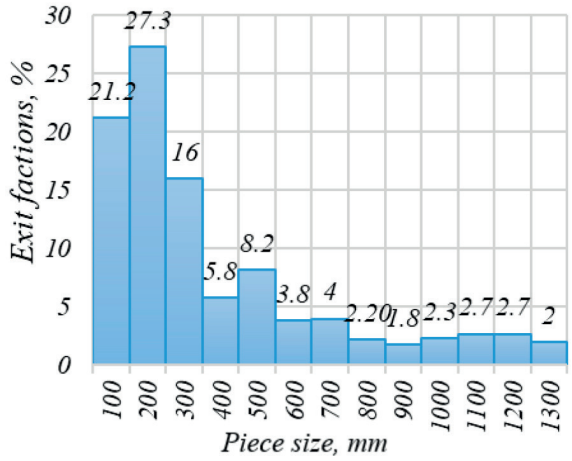

Figure 3 *Average fractional composition for 33 largest quarries based on the results of drilling and blasting operations*

too hard to be extracted without a certain number of explosions to grind the rock into smaller pieces, which can then be loaded onto a vehicle by excavators or other mechanical equipment. Figure 3 shows that the proportion of oversized material requiring additional crushing based on the results of drilling and blasting operations in quarries (with a piece size of 600 mm or more) is almost 20% of the total sample volume [10].

Thus, within the framework of implementation of cyclic-flow technology for the conditions of "Molodezhny" open-pit mine of Kazakhmys Coal LLP in Karaganda Technical University at the Department of Industrial Transport a promising technological scheme of delivery of rock mass, which can be used in the transportation of overburden and minerals in the case of increasing the depth of open-pit mining operations, presented in Figure 4: mining excavators - *1*, dump trucks BelAZ 75131 - *2*, chute for rock mass descent - *3*, intermediate averaging stockpile - *4*, bulldozer Chetra T-25 - *5*, receiving hopper NG - *6*, auger-tooth crusher SHZD - *7*, plate feeder - *8*, belt conveyors - *9-11*, waste rock dump or receiving hopper of the processing plant - *12* [11].

The rock mass from the upper and middle horizons is loaded into dump trucks BelAZ 7513, which deliver it to the chute for unloading into the receiving hopper; from the receiving hopper the rock mass flows by gravity through the chute to the site under the stack to the intermediate averaging yard. From the lower horizon, the rock mass is also loaded into dump trucks, which transport it to the averaging warehouse, from which it is shipped to the receiving hopper of the lower horizon by a Chetra T-25 bulldozer. The auger-tooth crusher, installed under the receiving hopper, crushes the mined rock mass; then it gets to the plate feeder, which transfers it further to the conveyor transport - belt conveyors, transporting it to the waste rock dumps or to

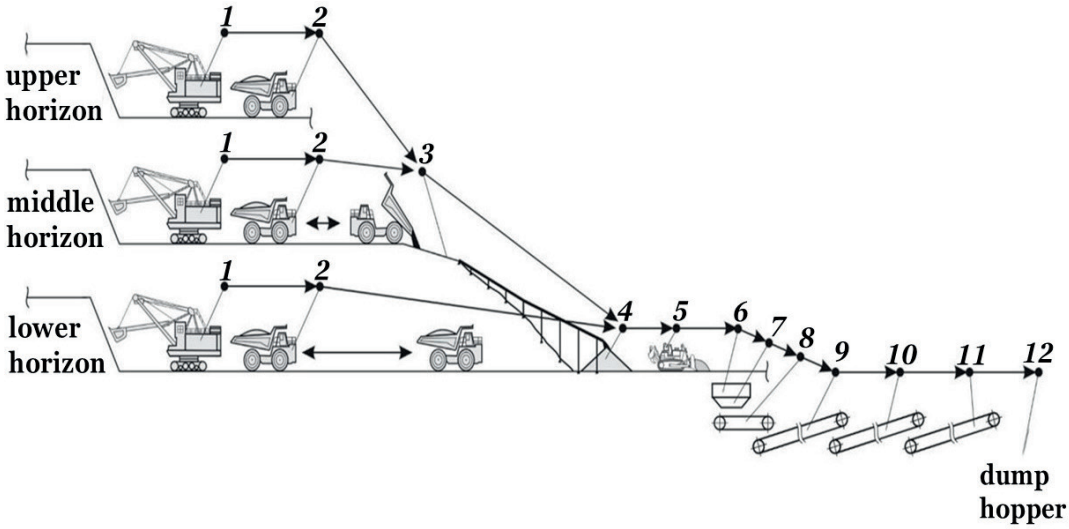

Figure 4 *Technological scheme of transportation using cyclic-flow technology at Molodezhny open pit mine of Kazakhmys Coal LLP*

the hopper of the enrichment plant. Table 1 shows the design parameters of belt conveyors, and Table 2 shows the general parameters of the conveyor line [11].

Estimated capital expenditures for implementation of this technological line also include costs for the purchase and construction of a crushing and reloading station, which, in particular, can be avoided by ensuring the necessary lumpiness of the rock mass extracted by the drilling and blasting method.

The lumpiness, quality of overburden rock mass crushing and oversize output during the blasting operations, as shown by the results of numerous studies, significantly affect the efficiency of application of flow and cyclic-flow technologies in open pit mining. To one of the first scientific researches in this direction belong the works of Baron, [12-13]. He systematized all the types of methods for measuring the lumpiness of rock mass in open pit and underground mining operations, based on the results of laboratory, polygon and production tests, analyzed various properties of explosives as criteria for their crushing ability in explosive rock removal [12-13].

In the work of Kolomnikov [14] the requirements for the coarseness of the transported material when controlling the energy of borehole charges, in the conditions of development at the mine "Muruntau" (Republic of Uzbekistan), using the cyclic-flow technology, are considered. The results of the complex research on improvement of ore crushing quality by borehole charges, based on consideration of physical and mechanical parameters of rock mass, are presented in the dissertation of Scherbich, G. V. Plekhanov St. Petersburg State Mining Institute, Russian Federation [15], which considered in detail the issues of optimizing the parameters of the drilling and blasting process to ensure a given degree of ore crushing. Optimization of blasting parameters by increasing the deceleration intervals is also presented in the work of Mityushkin et al. [16], in particular, multiple explosive loading of rock massif for a significant increase in the qualitative and quantitative indicators of the blasting process is considered.

The results of research on the control of explosion energy parameters to ensure intensive rock crushing at quarries are presented in the article by Nasirov et al. [17], which presents the experience of implementing the developed design using the turbo-explosion effect in rock crushing by borehole charges.

The influence of the detonation velocity of explosives on the degree of rock pre-destruction was considered in the work of Khokhlov et al. [18]: the issues of using explosives with reduced detonation velocity to reduce the intensity of predestruction in the zone of controlled crushing during the drilling and blasting process are presented.

One of the new publications on development of technologies aimed at improving the quality of rock crushing is a study on application of artificial intelligence and computer vision technologies to optimize the performance of the drilling and blasting complex at open-pit mining operations, Kovalchuk et al. [19]. In particular, the influence of the granulometric composition of the blasted rock mass on further stages of ore preparation was considered, the processes that affect the quantitative and qualitative indicators of the granulometric composition of the rock mass are determined.

Thus, as the analysis of the results of the above-mentioned studies, conducted within the framework of the development of methods and ways of intensification of all the processes of mining production, including loading and transportation operations, the issues of improvement and efficiency of the technology of explosive stripping, providing a given mode of crushing and compact bulk of the stripped rock mass, undoubtedly, acquire actual importance.

Table 1 *Design parameters of belt conveyors*

No. of conveyor in Figure 4	Length of the pack, m	Lift angle, deg
9	380	12
10	650	4
11	560	2

Table 2 *General parameters of the conveyor line*

No. n/a	Name	Significance
1	Hourly capacity of a conveyor line (estimated), tons/hour	1153.85
2	Hourly productivity of a conveyor line (accepted), tons/hour	1200
3	Density of cargo in loosened state, tons/m^3	1.24
4	Belt width (calculated), m	1.22
5	Belt width (accepted), mm	1400
6	Linear mass of the load on the conveyor, N/m	1308
7	Linear mass of rotating parts of the roller supports on the load branch of a conveyor, N/m	498.68
8	Linear mass of rotating parts of the roller supports on the idle branch of a conveyor, N/m	176.58

3 Theoretical basis of the study

The main phenomena accompanying explosive rebound during the mining operations - the explosion of an explosive charge in a destructible array are reduced to the following processes: detonation of the charge; expansion of the charging cavity by detonation products; mechanical interaction of detonation products with the destructible medium; propagation of shock waves and stress waves in rocks and, directly, the destruction of the mountain range. It has been established that a more uniform crushing of rocks is obtained by the explosion of borehole explosive charges with air gaps - this is explained by the interference of the shock waves, that is, a mutual increase in the resulting amplitude of waves formed during the explosion of various parts of the charge [20]. During the explosion of solid charges, as studies have shown, the rock, which is destroyed mainly due to compression forces, is crushed extremely unevenly, moreover, a large proportion of the explosion energy is spent on the re-crushing of rocks around the bottom of the charge. The separation of the charge column into separate parts and their simultaneous initiation contribute to the collision of detonation products at the locations of air gaps, which has a positive effect on the crushing of rocks.

The shape of the explosive charge also has a significant influence on the destructive effect of the explosion. In particular, it was found that using various forms of charge, or charges with recesses of various shapes (conical, spherical, parabolic, etc.), it is possible to create a cumulative effect, that is, to achieve a concentration of explosion energy that allows significantly enhancing the penetration effect of the charge on the mountain range by creating tensile and bending forces in it [21-23]. It was also found that the enhanced effect of the cumulative effect can also be obtained by placing dispersed cone-shaped caps on the detonating cord along the axis of the borehole charge. The overall effect of amplifying the explosion energy in this case is obtained from the cumulative effect of cumulative flows focused in the cone-shaped cavities into the bottom of the well, as a result of which the crushing of rock mass in the quarry is improved [24].

Determining the cumulative explosion pulses along the borehole formation presents significant difficulties because axial and radial expansion and various wave processes must be taken into account. The problem is simplified if the radial expansion of detonation products is neglected.

Explosions of charges with different shapes or notches give rise to complex wave processes associated with the collision of cumulative jets and gas flows from individual parts of the charge moving toward each other. The exact solution of the problem on the distribution of explosion parameters along the borehole in these cases is a rather complicated mathematical problem [25-26]. These difficulties are circumvented in various ways. For example, in the study of charges with air gaps, Baum et al. [27] and Baker et al. [28] propose to consider them as a solid charge, but with a greater height than that of a conventional charge at a lower density, and further, all the calculations should be carried out similarly to a solid charge. It is proposed to extend these assumptions for charges with different shapes of notches.

Let H_3 - be the height of a cylindrical charge, P_H - the initial pressure, C_H - the speed of sound in the detonation products before the onset of their expansion, and D - the diameter of the borehole. It is known that

$$P_H = \frac{1}{8}\rho_{cd}D^2,\ C_H = \sqrt{\frac{3}{8}D}\,, \tag{1}$$

where: ρ_{cd} - is the charge density.

Let x - denote the coordinate and t - denote the time of detonation product dispersal.

A rarefaction wave appears in the cross section $x = 0$ with the beginning of detonation product dispersal, which is described by the known equations of gas dynamics up to the time $t_1 = H_3/C_H$. When the isoentropic expansion of detonation products, $PV^3 = const$, is taken into account, they are of the form

$$x = (V - C)t + F(V),\ V + C = const, \tag{2}$$

where: V - is the detonation velocity,

Based on the boundary conditions: $t = 0$, $V = 0$, $x = 0$, $C = C_H$ one obtains: $F(V) = 0$, $C_H = const$.

Then, Equation (2) can be written in the form

$$x = (V - C)t,\ V + C = C_H. \tag{3}$$

Consequently, the expression $C = C_H - V$ is substituted into the first equation of the system of Equations (3) and V is found as:

$$V = \frac{x}{t} + C,\ V = \frac{1}{2}\left(C_H + \frac{x}{t}\right). \tag{4}$$

Thus, the solution of the system of Equations (2) can be written in the form

$$V = \frac{C_H}{2}\left(1 + \frac{x}{C_H t}\right), \tag{5}$$

$$C = \frac{C_H}{2}\left(1 - \frac{x}{C_H t}\right). \tag{6}$$

The pressure in the detonation products is determined from the relation

$$\frac{P_1}{P_H} = \left(\frac{C_1}{C_H}\right)^3 = \frac{1}{8}\left(1 - \frac{X}{C_H t}\right)^3. \tag{7}$$

At the moment of time $t = H_3/C_H$ the wave reaches the end of the charge, a new reflected rarefaction wave appears, the motion of which is described by the general equations of gas dynamics.

$$X = (V - C)t + F_1(V - C), \tag{8}$$

$$X = (V + C)t + F_2(V + C). \tag{9}$$

At the moment $t = H_3/C_H$ the velocity V becomes equal to 0, $x = H_3$, hence $F_1 = 0$ and

$$V - C = \frac{x}{t}. \tag{10}$$

In the section $x = -H_3$, at any moment of time $V = 0$, whence it follows that

$$F_2 = -H_3 - Ct. \tag{11}$$

Expressing $t = \frac{x}{V - C} = \frac{H_3}{C}$ from Equation (10) one finds:

$$F_2 = -2H_3 \text{ and } V + C = \frac{x + 2H_3}{t}. \tag{12}$$

The front of the reflected wave moves according to the law

$$\frac{dx}{dt} = V + C = \frac{x}{t} + \frac{2H_3}{t}. \tag{13}$$

Consequently, at $t = H_3/C_H, x = -H_3$ and $x = C_H t - 2H_3$.

Thus, the reflected wave front and the detonation product front propagate with the same velocity C_H.

Next, one has to find the pressure in the reflected wave. Taking into account that $C = H_3/t$ one obtains

$$\frac{P_2}{P_H} = \left(\frac{C_2}{C_H}\right)^3 = \left(\frac{H_3}{C_H t}\right)^3. \tag{14}$$

Equality (14) shows that the pressure in the reflected wave varies only in time. Knowing the distribution of pressure by time t and by coordinate x, one can write the total momentum:

$$J = \pi\, d_3 \int_{-H_3}^{x_2} \int_0^\infty P(x,t)dt\, dx, \tag{15}$$

where $x_2 = H_{hole} - H_3$, H_{hole} - is the height of the hole (borehole).

Let the following dimensionless parameters be introduced as:

$$\tau = \frac{tC_H}{H_3}, \alpha = \frac{x}{H_3}, \overline{P} = \frac{P}{P_H}. \tag{16}$$

Then

$$J = \frac{tC_H}{\pi\, d_3\, H_{hole}^2\, P_H} = \left(\frac{H_3}{H_{hole}}\right)^2 \int_{-1}^{\frac{x_2}{H_3}} \int_0^\infty \overline{P}\, d\tau\, d\alpha. \tag{17}$$

Since

$$C_H = \sqrt{\frac{3P_H}{\rho_{cd}}} = \frac{\sqrt{6}}{4}D, \tag{18}$$

$$J = \left(\frac{H_3}{H_{hole}}\right)^2 \int_{-1}^{\frac{H_{hole}}{H_3} - 1} \int_0^\infty \bar{P}\, d\tau\, d\alpha. \tag{19}$$

next equation (19) is integrated first by α and then by τ and the final expression for the value of the total explosion impulse along the wellbore formation is obtained:

$$J = \frac{3}{8}\frac{H_3}{H_{hole}}\left(1 + \frac{2H_3}{H_{hole}}\right) - \frac{3}{16}\left(1 - \frac{H_3}{H_{hole}}\right)^2 \ln\frac{1 + \frac{H_3}{H_{hole}}}{1 - \frac{H_3}{H_{hole}}}. \tag{20}$$

Thus, the obtained equation reflects the correlation dependence between the parameters of explosive blasting and the structural values of the borehole and it can be used in solving problems of the penetration action of the

cumulative jet and the distribution of specific explosion impulses along the borehole formation.

At the same time as experimental data show, determination of the influence of the blast wave impulse on the processes of rock mass crushing during the drilling and blasting excavation is possible only by modelling during the experimental studies, range or pilot tests in the conditions of real mining enterprises [29].

4 Experimental results

Analysis of the applied technologies of explosive stripping shows that in many cases the counter-impact of explosion products in air gaps is usually carried out at the detonation velocity of the explosive charge, which is insufficient to create a significant impulse and, accordingly, to increase the explosion energy acting on the massif to be destroyed to achieve the required lumpiness [30].

In this regard, the ideas outlined in the above works can be developed by pulsing an increase in the explosive charge explosion energy dispersed at intervals along the length of the charge. To do this, it is proposed to place the volumetric cavities of a special geometric shape (accelerators) in the explosive charge [31]. A sharp increase in the charge energy at the installation site of the cavity would take place if the explosive charge around the elongated cavity is initiated from its inner part over the entire surface simultaneously. In this case, a large mass and volume of explosives around a hollow volumetric cavity can be detonated. Modelling of explosive stripping processes with various forms of volumetric cumulative cavities was carried out in the laboratory conditions of the Department of "Rock Destruction by explosion" of the Moscow Mining Institute [30]. A mixture formed from building gypsum in various ratios with water and plexiglass was used as the test material (Table 3). As the material was being prepared, gypsum and water in the form of a mixture were poured into special molds and dried at room temperature. Samples of material with a thickness of 8 mm were prepared, the value of which was determined experimentally, taking into account the available amount of explosive to achieve the necessary cracking and crushing of the samples under consideration. The explosive charge in the thickness of the prepared material sample was formed using a PVC tube of an inner diameter of 3 mm. A constantan wire of a diameter of 0.3 mm was passed through the tubes, and then the tubes were filled with an explosive substance ammonite 6ZHV, giving them the shape of a cavity (Figure 5).

Each charge contained one cavity made of thick paper and filled with an explosive substance from the outside, which included sulfur and aluminum powder. The cavities were given various types of shapes: spherical; cones of different heights; cones connected by bases and ellipsoidal. The initiation of the explosive charge occurred as a result of passing a low-voltage current through a constantan wire. The process of explosive rebounding was recorded by high-speed photography. The actual distribution of the lumpiness of the destroyed sample on the laboratory model from the explosion of charges in various forms of the cumulative cavity is shown in Figure 6.

As a part of pilot tests, experimental explosions were carried out in the conditions of the Akzhal quarry of the Altaizoloto combine in the East Kazakhstan region with specially designed structures of one-, two- and three-cone volumetric cumulative cavities

Table 3 *Strength of samples after testing*

No. n/a	Gypsum to water ratio	Sample testing, MPa/mm		σ_c / σ_p
		for compression, σ_c	tensile, σ_p	
1	0.5 : 1	0.06	0.024	2.5
2	1 : 1	0.66	0.10	6.6
3	1.5 : 1	1.25	0.15	8.3
4	2 : 1	2.12	0.242	8.8

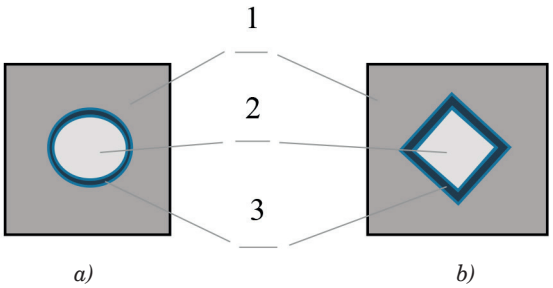

Figure 5 *Location of spherical shaped cavities in an explosive charge - a) and in the form of two cones connected by bases - b): 1 - gypsum sample, 2 - volumetric cavity, 3 - explosive charge*

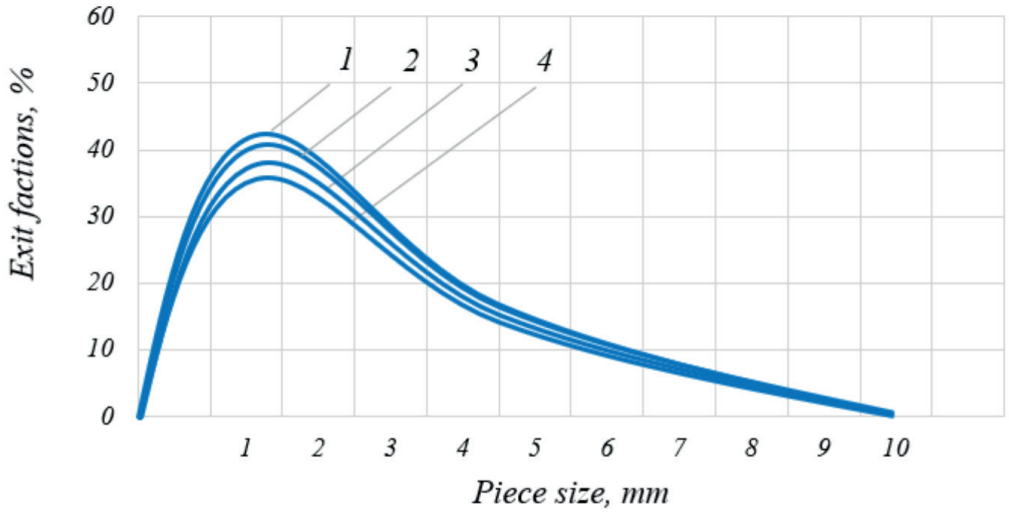

Figure 6 *Distribution of the lumpiness of the destroyed sample on a laboratory model with various shapes of the cumulative cavity: 1 - ellipse, 2 - cones connected by bases, 3 - cones of different heights, 4 - spherical shape*

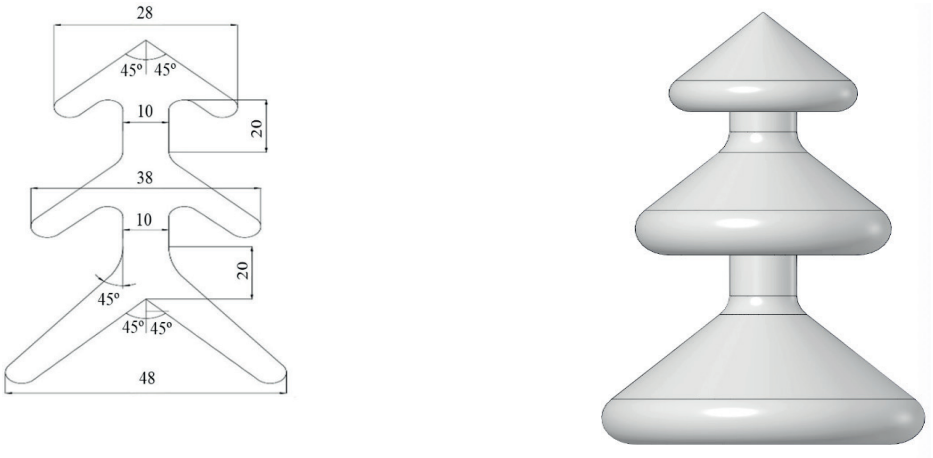

Figure 7 *Design of a three-cone cumulative cavity charge*

(accelerators) [31], Figure 7. The diameter of the wells was 150-250 mm, the depth was 3-5 m, the rock strength on the Protodyakonov scale was 13-15, the explosive used was grammonite 79/21.

The charge was formed as follows. An air partition 2, made of expanded polystyrene or polyethylene, was lowered into the well 1 (Figure 8), then a portion of explosive substance 3 was filled in, a three-cone accelerator 4 was lowered and a portion of explosive substance 3 was poured until the cavity was completely covered. Then the air partition 5 was lowered again, a portion of explosive substance 6 was filled in, a two-cone accelerator 7 was lowered and a small amount of explosive substance was poured. In the upper part of the well, similar operations were performed with a single-cone accelerator 10. Then, fuse 11 was lowered into the well on a detonating cord, which was also filled with explosives until it was completely covered. When the accelerators were installed, their cones were turned towards the fuse.

In general, for 72 exploding wells, the consumption of accelerators was 3-4 cavities per 1 well, with the upper location of the fuse, electric detonation was carried out in an orderly manner. According to the results of explosive stripping, the average size of the pieces of the chipped rock mass was mainly 90-120 mm, and the maximum diameter of the pieces was 320-450 mm (Figure 9). At the same time, as can be seen from Figure 8, with a decrease in the diameter of the well from 250 to 150 mm, the diameter of the average piece of destroyed rock mass decreased from 170-190 to 90-120 mm.

The analysis of high-speed photography data obtained in laboratory studies, as well as the results of pilot tests, in authors' opinion, confirm the previously suggested assumptions that the use of volumetric cavities (accelerators) in the explosive charge focusing the cumulative flow on the destructible medium, increases the rate of detonation of the charge and, accordingly, creates an increased pulse of the explosive

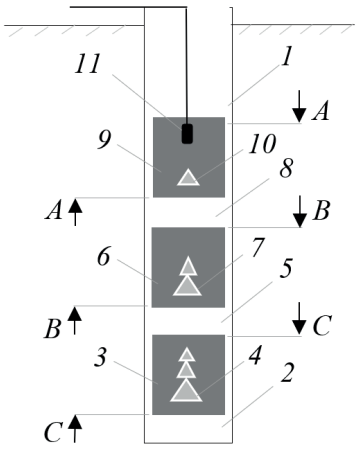

Figure 8 *Formation in a well: 1 - well, 3, 6, 9 - portions of explosives, 4, 7, 10 - accelerators, 2, 5, 8 - air barriers, 11 - fuse on a detonating cord*

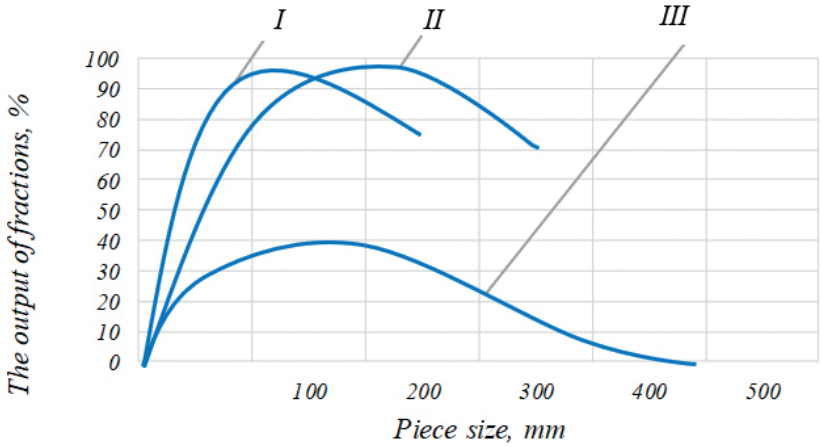

Figure 9 *Dependence of the average piece during the downhole drilling on the diameter of the well: I - 150 mm, II - 250 mm and III - the distribution of the lumpiness of the blasted rock mass*

wave, which, in the end, makes it possible to improve the quality of crushing of the test sample (rock mass).

To confirm the results obtained by the authors, the pilot experimental explosions were carried out in 2016-2019 at a number of mining facilities in Kazakhstan. At the Sarbaisky iron ore quarry of JSC "Sokolovsko-Sarbaisko Concentrating Production Association" (JSC "SSGPO", Rudnyy) at the height of the ledge of 27 m, the wells were mainly drilled 30 m deep with a re-drill of 3 m, and the delivery of explosively prepared rock mass from a considerable depth to the surface of the quarry was carried out by dump trucks of large load capacity. The cyclical nature of the technological process of transportation of rock mass using road transport, which takes considerable time to lift the ore to the surface, leads to a decrease in mining productivity.

In 2016, for experimental purposes, 10 tons of explosives were detonated at the Sarbaisky open pit using developed accelerator designs in 18 boreholes 250 mm in diameter and 23 m deep. In 2019 at the same quarry, 50 tons of explosives were detonated in 70 boreholes and almost 1,000,000 m^3 of rock mass with expected lumpiness (400-450 mm) and absence of oversize was prepared by blasting. According to the test results, the production specialists noted that the proposed drilling and blasting technology of mineral extraction promotes wider application at the open pits of SSGPO JSC of the means of transportation providing continuous delivery of ore from the bottom of the pit to the surface: conveyors, pneumatic or hydraulic transport. It was also noted that the results obtained from pilot tests, in general, reflected the correlation dependence between the parameters of explosive stripping and the design values of the hole, presented in Equation (20).

Experimental explosions with the proposed accelerator design were also conducted in conditions of underground mining, in particular, at the mine "Kvartsitka" of JSC "Altynalmas" (Stepnogorsk), developing gold-bearing ores. Total of 28 boreholes were drilled through the viscous quartzites. With the length

of the borehole up to 3 m and the number of cartridges in one borehole equal to 6, each cartridge was filled with one volume cavity. Experimental explosions during the drifting, along with a significant crushing of rock mass, also showed an increase in the borehole utilization factor to 0.94, with the existing normative value of 0.84, Figure 10.

5 Analysis of the results obtained

As is known, the basic information about the detonation process of condensed media is provided by experiment, and the criterion for the successful application of the hydrodynamic theory should be the compliance of the detonation parameters obtained experimentally with the theoretical results [29]. In this regard, the results of laboratory and pilot tests for conducting explosive stripping using volumetric cumulative cavities (accelerators) allowed us to propose the following physical model of the processes occurring during the explosion of a borehole explosive charge. During the explosion of the borehole charge shown in Figure 8, the detonation products, spreading from the fuse 11, pass through the single-cone accelerator 10 and assemble into a single cumulative flow, the speed of which is higher than the detonation velocity of explosive substance 9 to the accelerator. Such a flow has high kinetic energy and, getting into the elongated redistributive part of the accelerator 10, changes the direction of its propagation perpendicular to the surface of the concave accelerator generatrix.

The cumulative flow, while simultaneously exciting the explosion of the explosive charge located around the accelerator, increases the mass of explosives exploding per unit of time. Considering that the generatrix of the redistributive part of the accelerator 10 has an inward concavity, the voltage waves are focused outside the charge at points F (Figure 11, a).

The explosion products, approaching the air partition 8, reduce their speed, but on the way to the middle part of the charge they acquire the detonation rate of the explosive substance charge 6. When the explosion products pass through the accelerator 7 (Figure 8), they gather into an amplified two-fold cumulative flow, the speed of which is higher than the flow rate after the accelerator 10.

This enhanced cumulative flow penetrates the void of the twin accelerator 7 and explodes the explosive charge 6, directing the explosion products perpendicular to the surface of the accelerator 7, and given that its surface is concave inward, voltage waves focus at points F outside the charge (Figure 11, b). Further, the explosion products, approaching the air partition 5, reduce its speed, but when the explosive substance 3 charge is excited in its lower part, it again acquires the detonation velocity

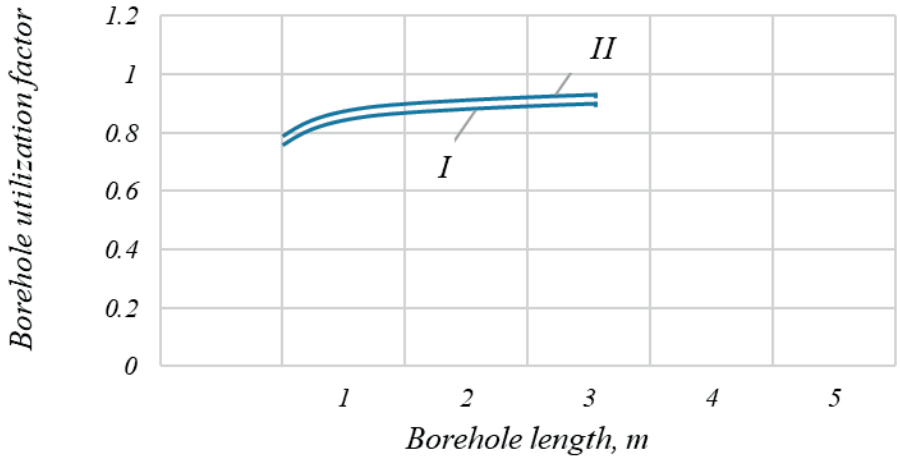

Figure 10 *Values of the borehole utilization factor during the borehole coring: I - without the use of volume cavities, II - with the use of accelerators*

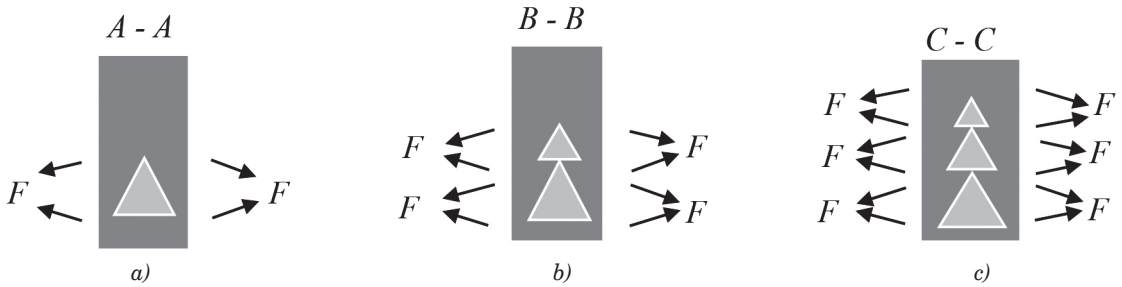

Figure 11 *Sections of the down hole explosive charge, shown in Figure 7, with one-, two- and three-cone accelerators*

of explosive substance 3. When the explosion products pass through the accelerator 4 (Figure 8), they gather again into a more amplified three-fold cumulative flow, the speed of which is higher than the flow rate after the accelerator 7. The three-fold amplified cumulative flow penetrates the void of the accelerator 4, explodes a large mass of explosive substance 3 charge around the elongated accelerator and focuses voltage waves outside the charge in the destructible array at points F (Figure 11, c). In other words, accelerators in charges, firstly, accelerate the speed of explosion products, and secondly, provide dynamic braking of explosive gases, which ensures the explosion of a larger mass of explosive charge and the reversal of the explosive pulse by 90 degrees.

6 Conclusions

Based on the results of modelling the process of explosive stripping in laboratory conditions and conducted pilot tests at a number of mining sites in Kazakhstan a method is proposed for the controlled explosive stripping of rock mass with the use of developed designs of volumetric cavities (accelerators). Due to the use of accelerators in the borehole explosive charge dynamic braking of explosion products is carried out, contributing to the emergence of localized destruction due to tensile and bending forces acting on the destroyed massif.

As a result, the specified mode of crushing of the crushed rock mass is provided (maximum lump size according to the results of tests in the conditions of mining enterprises does not exceed 450 mm), which, according to the estimation of production specialists, contributes to the possibility of wider application of flow transport means at open pits: conveyors, pneumatic and hydraulic transport.

In addition, the results of the conducted pilot tests in conditions of open-pit and underground mining showed the possibility of:

- reduction of explosive charge mass in a borehole by 32-36% in comparison to the approved passport of drilling and blasting operations by means of arrangement of air gaps in boreholes;
- reduction of drilling costs by 24-28% due to the transition to a smaller borehole diameter;
- increasing the borehole utilization factor up to 0.94.

The results of preliminary design study of implementation of the proposed technology of drilling and blasting operations and the effectiveness of cyclic-flow technology, using the belt conveyors at the Molodezhny open pit mine (Karaganda region, Republic of Kazakhstan), showed an increase in mining productivity up to 5 million tons, reducing development costs by 25-30%, and, accordingly, the possibility of effective development of deeper horizons.

Acknowledgment

The authors received no financial support for the research, authorship and/or publication of this article.

Conflicts of interest

The authors declare that they have no known competing financial interests or personal relationships that could have appeared to influence the work reported in this paper.

References

[1] AKHUNBAYEV, A. Coal industry of Kazakhstan: return to growth. *Mining and Metallurgical Industry*. 2018, **8**, p. 14-18.

[2] DANIYAROV, N. A., BALGABEKOV, T. K., AKASHEV, A. Z. Regulation of carriage flows and management of the transportation process in railway transport of JSC NC "Kazakhstan Temir Zholy". *Innovative Transport*. 2012, **1**, p. 27-32. ISSN 2311-164X.

[3] RAKISHEV, B. R. Mining industry in the light of accelerated industrial and innovative development of the Republic of Kazakhstan. *Mining Information and Analytical Bulletin*. 2012, **S1**, p. 404-415. ISSN 0236-1493.

[4] MUMINOV, R. O., KUZIEV, D. A., ZOTOV, V. V., SAZANKOVA, E. S. Performability of electro-hydro-mechanical rotary head of drill rig in open pit mining: a case-study. *Eurasian Mining* [online]. 2022, **37**(1), p. 76-80. ISSN 2072-0823. Available from: http://doi.org/10.17580/em.2022.01.16

[5] GALKIN, V. I., SHESHKO, E. E., DYACHENKO, V. P., SAZANKOVA, E. S. The main directions of increasing the operational efficiency of high productive belt conveyors in the mining industry. *Eurasian Mining* [online]. 2021, **36**(2), p. 64-68. ISSN 2072-0823. Available from: http://doi.org/10.17580/em.2021.02.14

[6] DANIYAROV, A. N. Research and establishment of operational and design parameters of quarry conveyors with a complex route for rocky rocks. Abstract of the dissertation for the degree of Doctor of Technical Sciences. Moscow: Moscow State University, 1984.

[7] ALIYEV, S. V., BREIDO, I. V., DANIYAROV, N. A., KELISBEKOV, A. K. Control of load distribution between electric drives of a multi-motor plate conveyor during non-overloading coal delivery in open-pit mining conditions. *Ugol* [online]. 2020, **9**, p. 14-17. ISSN 0041-5790, eISSN 2412-8333. Available from: http://dx.doi.org/10.18796/0041-5790-2020-9-14-17

[8] DANIYAROV, N. A., DANIYAROVA, A. E., KELISBEKOV, A. K. Professor Solod G. I. - the founder of the theory of calculation of multi-drive conveyors calculations. *Ugol* [online]. 2022, **1**, p. 63-66. ISSN 0041-5790, eISSN 2412-8333. Available from: http://dx.doi.org/10.18796/0041-5790-2022-1-63-66

[9] KELISBEKOV, A. K., DANIYAROV, N. A., MOLDABAEV, B. G. Improving the energy efficiency of operation of a multi-motor plate conveyor in the steady-state operation mode. Communications - Scientific Letters of the University of Zilina [online]. 2024, **26**(2). p. C1-C8. ISSN 1335-4205, eISSN 2585-7878. Available from: http://doi.org/10.26552/com.C.2024.022

[10] AKASHEV, Z. T., DANIYAROV, N. A., MALYBAEV, N. S. A non-expert method for evaluating career transport systems by technical level. *Heavy Engineering*. 2003, **8**, p. 18-22. ISSN 1024-7106.

[11] KUANYSHBAYEV, A., ROZHKOV, A., GORSHKOVA, N., NOGAYEV, K. Experimental studying the belt conveyor roller wear dependence on the intensity of technological dust accumulation in open pit mining. *Communications - Scientific Letters of the University of Zilina* [online]. 2023, 25(4). p. B327-B338. ISSN 1335-4205, eISSN 2585-7878. Available from: http://doi.org/10.26552/com.C.2023.071

[12] BARON, L. I. *Lumpiness and methods of its measurement*. Moscow, 1960.

[13] BARON, L. I., ROSSI, B. D., LEVCHIK, S. P. *Crushing ability of explosives for rocks*. Moscow: Institute of Mining Engineering, USSR Academy of Sciences, 1960.

[14] KOLOMNIKOV, S. S. Energy management of borehole charges in conditions of development of different-strength rock massifs at cyclic-flow technology. *Mining Information and Analytical Bulletin*. 2007, S5, p. 82-94. ISSN 0236-1493.

[15] SHCHERBICH, S. V. Improvement of ore crushing quality by borehole charges on the basis of consideration of physical and technical parameters of the rock massif. Abstract of the dissertation for a candidate of technical sciences. St. Petersburg: St. Petersburg State Mining Institute named after G. V. Plekhanov, 2009.

[16] MITYUSHKIN, Y. A., LYSAK, Y. A., PLOTNIKOV, A. Y., RUZHITSKY, A. V., SHEVKUN, G. B., LESCHINSKY, A. V. Optimization of blasting parameters by increasing the deceleration intervals. *Mining Information and Analytical Bulletin*. 2015, **4**, p. 341-348. ISSN 0236-1493.

[17] NASIROV, U. F., ZAIROV, S. S., MEKHMONOV, M. R., FATKHIDDINOV, A. U. Controlling blast energy parameters

to ensure intensive open-pit rock fragmentation. *Mining Science and Technology* [online]. 2022, 7(2), p. 137-149. eISSN 2500-0632. Available from: https://doi.org/10.17073/2500-0632-2022-2-137-149

[18] KHOKHLOV, S. V., VINOGRADOV, Y. I., MAKKOEV, V. A., ABIEV, Z. A. Effect of explosive detonation velocity on the degree of rock pre-fracturing during blasting. *Mining Science and Technology* [online]. 2024, **9**(2), p. 85-96. eISSN 2500-0632. Available from: https://doi.org/10.17073/2500-0632-2023-11-177

[19] KOVALCHUK, I. O., KOVALKOV, S. A., IVANOVA, E. A., KLEBANOV, D. A., POPLAVSKY, S. F. Application of artificial intelligence and computer vision technologies for optimization of the drilling and blasting complex at open-pit mining. *Globus. Geology and Business*. 2024, **1**(80), p. 152-155.

[20] MELNIKOV, N. V., MARCHENKO, L. N. *Explosion energy and charge design*. Moscow, 1964.

[21] BULAT, P. V. Shock and detonation waves from the point of view of the theory of interference of gas-dynamic ruptures - the task of designing the optimal configuration of shock and detonation waves. *Fundamental Research*. 2013, **10**, p. 1951-1954. ISSN 1812-7339.

[22] BAYAZITOVA, Y. R., BAYAZITOVA, A. R. Dynamics of detonation waves in an annular bubble layer. In: Trends and Prospects for the Development of Scientific Knowledge: Materials of the III International Scientific and Practical Conference: proceedings. 2012. p. 8-16.

[23] JOHNSON, G. R., HOLMQUIST, T. J. A computational constitutive model for brittle materials subjected to large strains, high strain rates and high pressures. In: *Shock Wave and High-Strain-Rate Phenomena in Materials*. Boca Raton: CRC Press, 1992. eISBN 9781003418146, p. 1075-1081.

[24] ZHARIKOV, I. F. Efficiency of management of processes of drilling and blasting preparation of a mountain range for excavation. *Explosive Business*. 2012, **108**(65), p. 82-92. ISSN 0372-7009.

[25] SINGH, P. K., ROY, M. P., PASWAN, R. K., DUBEY, R. K., DREBENSTEDT, C. blast vibration effects in an underground mine caused by open pit-mining. *International Journal of Rock Mechanics and Mining Sciences* [online]. 2015, **80**, p. 79-88. ISSN 1365-1609, eISSN 1873-4545. Available from: https://doi.org/10.1016/j.ijrmms.2015.09.009

[26] SINGH, P. K. Blast vibration damage to underground coal mines from adjacent open-pit blasting. *International Journal of Rock Mechanics and Mining Sciences* [online]. 2002, **39**(8). p. 959-973. ISSN 1365-1609, eISSN 1873-4545. Available from: https://doi.org/10.1016/S1365-1609(02)00098-9

[27] BAUM, F. A., ORLENKO, L. P., STANYUKOVICH, K. P., CHELYSHEV, V. P., SHEKHTER, B. I. *Physics of explosion*. Moscow: Publishers of Physical and Mathematical Literature, 1975.
[28] BAKER, W., COX, P., WESTINE, P., KULESZ, J., STREHLOW, R. *Explosive events. Assessment and Consequences*. Moscow: Mir, 1986.
[29] KUTUZOV, B. N. *Methods of conducting blasting operations. Part 2: Blasting in mining and industry*. Moscow: Mining Book, MGU, 2008. p. 57-92. ISBN 978-598672-197-2.
[30] IGBAEV, T. M. *Destruction of a mountain range by cumulative charges*. Almaty: Science, 1998. ISBN 5-628-02222-5.
[31] IGBAEV, T. M., DANIYAROV, N. A. Device for destruction of rocks by high-frequency explosion. Patent of the Republic of Kazakhstan 23622. 12/15/2010. Bulletin 12.

THE STRENGTH CALCULATION OF THE MODERNIZED BRAKE LEVER TRANSMISSION FOR A WAGON BOGIE

Sergii Panchenko[1], Juraj Gerlici[2], Alyona Lovska[2,*], Vasyl Ravlyuk[1]

[1]Ukrainian State University of Railway Transport, Kharkiv, Ukraine
[2]University of Zilina, Zilina, Slovak Republic

*E-mail of corresponding author: Alyona.Lovska@fstroj.uniza.sk

Sergii Panchenko 0000-0002-7626-9933,
Alyona Lovska 0000-0002-8604-1764,
Juraj Gerlici 0000-0003-3928-0567,
Vasyl Ravlyuk 0000-0003-4818-9482

Resume

The article highlights is determination of the main strength indicators of the modernized brake lever transmission for a wagon bogie. The special feature of this modernization is that the technological pin-hole in the strut is displaced by 112 ± 2 mm towards the bolster beam, i.e., in line with the pendulum joints. This helps to eliminate abnormal wear of the brake pads in operation. To substantiate the proposed modernization, the strength of the brake lever transmission was calculated. It was found that the maximum equivalent stresses were 124 MPa; they occurred in the tension member. The resulting stresses did not exceed the permissible values. Thus, the proposed modernization measures are appropriate.

This research could improve the safety of rail freight operations and profitability of the rail transport.

Article info

Received 9 December 2025
Accepted 13 February 2025
Online 18 March 2025

Keywords:

brake lever transmission
brake reliability
traffic safety
railway transport
transport mechanics

Available online: https://doi.org/10.26552/com.C.2025.027

ISSN 1335-4205 (print version)
ISSN 2585-7878 (online version)

1 Introduction

In today's competitive environment, sustainable development of the railway industry is aimed at the modernization of key elements of technical infrastructure [1-5]. Particular attention should be paid to the mechanical parts of braking systems of freight trains, which play a critical role in ensuring the traffic safety.

The braking process of a freight train is a complex multidisciplinary task, involving the interaction of various components and systems, and aimed at optimal deceleration and stopping of the rolling stock. The efficiency of braking systems and their reliable operation are crucial for reducing the risks during the transportation of goods, taking into account the high requirements for safety and stability of rail transport. Therefore, current trends in the railway transport industry include stricter requirements for braking systems, a need for their continuous modernization and improvement.

The imperfect design of the brake lever transmission (BLT) of wagon bogies has a significant impact on the braking efficiency. In the traction and idling modes, the brake pads are tilted and touch the rolling surfaces of the wheels with their upper ends. Under these conditions, unwanted friction is created, thus causing abnormal pad wear. This not only leads to an increase in operating costs for the wagon maintenance, but to an increase in traction resistance as well, which consumes additional energy resources.

Moreover, the absence of a clearance between the pad and the wheel in the upper part (Figure 1, a) leads to abrasion and a decrease in the working area, which reduces the train braking efficiency. Under this condition, the temperature of the brake pad/wheel tribotechnical surfaces increases, and this causes high-temperature damage to the wheels (Figure 1, b). Such damage can include microcracks, shelled treads and metal dislocations, which significantly shorten the service life of wheelsets and increase the cost of maintenance and replacement.

Thus, there is a need to modernize the lever transmission design of wagon brake systems to improve safety and optimize costs in the railway industry.

An analysis of scientific, technical, and advertising sources on the BLT performance of railcars has confirmed that the existing designs of brake systems

a) b)

Figure 1 *The elements of the brake pad/wheel tribotechnical assembly that are inoperable due to the BLT design features; a) without a clearance between the pad and a wheel when the brakes are released; b) high-temperature damage on the wheel surface*

of bogies described in [6-8] do not completely solve the problem of abnormal pad wear during the brake release. It is established that the developers of these systems mostly focused on auxiliary devices to counteract the forces, that affect the position of the pads according to the kinetostatic analysis of the BLT mechanism [9]. This indicates that an integrated approach is needed when designing and optimizing brake systems. The dynamics and the real operational aspects of their functioning should also be taken into account, as well as the forces that occur in the elements of the bogie's brake beams during braking.

In study [10] are analyzed the operational quality indicators of the cast iron brake pads and composite ones used for passenger and freight rolling stock. The authors considered a number of negative aspects of composite pads, in particular, their impact on the environment. In addition, the processes that cause damage to vehicle wheels due to the mechanical properties of the materials used for the pads are described. In this study the aim was to identify the cause-and-effect relationships between different types of brake pads. The study results show the impact of pad wear on environmental pollution, durability, and safety of railway transport.

In many scientific studies that were focused on the use of composite brake pads in the rolling stock the aspects related to traffic safety and their impact on the environment were emphasized. To reduce the operating costs in the railway industry, brake pads are often perceived as a commodity purchased at the lowest price while performing satisfactorily [11]. However, this approach may not ensure the lowest operating costs in the long run. The choice of material of the friction components of the pads has a direct impact on duration of the standard service life of the wheelset, the replacement of which usually significantly exceeds the cost of the BLT elements of the wagon. Thus, the economic benefit of the low initial price of pads can be considered unjustified due to the increased costs of further maintenance and repair of rolling stock.

Authors of study [12] presented the comparative indicators of the quality and performance characteristics of the cast iron brake pads as well as the composite ones. They highlighted several disadvantages of composite pads, in particular, their low thermal conductivity, which causes the thermal damage to the rolling surfaces of wheels. This, in turn, leads to an increase in operating costs associated with the repair of wheelsets. Another significant drawback is that the regulatory documents for manufacturing do not have the chemical composition of the composite mixture ingredients. This violates the current legislation of Ukraine and makes it difficult to control it. However, the authors do not mention the costs caused by the abnormal wear of composite brake pads that occurs when freight rolling stock operates without active braking.

In study [13] is presented an analysis of various braking systems, in particular those used in pad/wheel tribotechnical pairs. The authors presented the advantages of disc brakes and the feasibility of their use with conventional tribotechnical pairs. The main problem with composite brake pads used in wagons is their negative impact on the rolling surface of the wheelsets. Due to the low thermal conductivity of the pads, high temperatures occur in the contact zone with the wheels, which causes various defects on the wheel surface.

In study [14] was indicated that most international scientists focus on solving issues related to disc brakes. They analyse the strength of their parts, monitor operating parameters, and determine the temperature conditions of individual tribotechnical components of

rolling stock brake systems. This indicates a global trend towards optimizing the brake systems to increase their efficiency and reliability, reduce wear, and improve the overall performance of rolling stock.

Authors of studies [15-16] have dealt with the use of modern materials for the development of new designs of tribotechnical systems. The effectiveness of these innovations in the context of modern rolling stock has been proven. Thanks to these innovations, it is possible to increase the speed and axle load, as well as improve the efficiency of the braking system of rolling stock. However, the above studies did not pay due attention to the problems associated with abnormal wear of brake pads in freight rolling stock. Therefore, it would be advisable to analyse the factors influencing the performance of tribotechnical systems in order to increase their wear resistance and take into account modern materials used for them.

The analysis of publications [6-16] has made it possible to conclude that the problem of abnormal wear of pads used in the brake systems of railcar bogies is very urgent. The solution of it is important for ensuring the reliability and safety of the rail transport, thus further research and development is necessary.

The objective of this study was to substantiate the feasibility of using a modernized brake lever transmission on the wagon bogie 18-100.

The following tasks have been set to achieve this objective:

- to develop measures for eliminating abnormal pad wear by upgrading the BLT elements; and
- to calculate the strength of the upgraded BLT of a wagon bogie 18-100.

2 Materials and methods

In their previous works the authors [17-19] established that the main reason for abnormal wear of brake pads is the inconsistency of the force factors acting in the break lever transmission of the bogie. It can be explained by the design of the brake system on the pendulum suspension, and the tribotechnical processes that occur between the pad and the wheel when the train is moving with the brakes released.

To eliminate the harmful torque to the brake lever transmission, it is proposed to relocate the joint of the vertical arm and the brake beam strut. Based on the measurements of a typical brake beam structure, it was determined that the pin-hole in the strut should be located at a distance of 112 mm (instead of the existing 224 mm) from the outer end of the brake beam. This rather simple, but theoretically justified structural change in the location of the pin-hole in the brake beam strut can solve the problem of abnormal wear of the pads (Figure 2).

This design change makes it possible to completely eliminate the harmful torque on the brake lever transmission and the modernized brake beam will restrain the brake pads from resting on the rolling surfaces of the wheelset.

Given that the modernized brake beam is held loosely on the pendulum suspension joints by friction, it is likely that intense vibrations of the wagon's running gears may periodically cause the brake beam to tilt in one direction or another. In this case, the brake pads may tilt and touch the rolling surface of the wheels with their upper or lower parts when the brake is released.

Figure 2 *Modernized brake beam with the pin-hole in the strut moved in line with the pendulum joints*

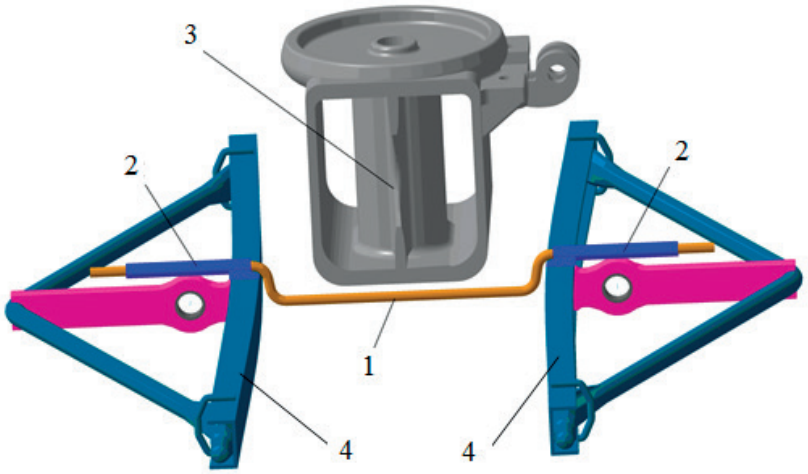

Figure 3 *The general view of the device for maintaining uniform clearances between the brake pads and the rolling surfaces of the wheelset*
1 - curved rod; 2 - cylindrical slides; 3 - bolster beam;
4 - modernized brake beams with a displaced pin-hole in the strut

To prevent the brake pads from tilting up to their partial contact with the rolling surface of the wheel, a device (Figure 3) was developed to absorb minor accidental forces from oscillations and tilts of the bogie when the train moves. This will ensure that the clearances between the pads and wheels are kept exactly even. This device has a curved guide rod 1 between the pair of modernised brake beam 4 in their middle part. The ends of this rod fit into the cylindrical slides 2, welded to the brake beam symmetrically with respect to the opening of its strut. The downward bending of the rod should be no less than the maximum possible displacement of the bolster beam 3 due to the loading of the railcar. The parts of the rod that are curved downward are located near the ends of the cylindrical slides [17-20].

When the random forces are applied to the brake beams due to intense oscillations and tilts of the wagon bogie when the train moves, the curved rod in the slides works. The forces that cause the brake beam to tilt relative to the pendulum suspensions are counteracted by the reactive forces generated between the rod and the slides. This ensures that the brake beams are constantly in balance and maintain uniform clearances between the pads and wheels when the brake is released. The bending of the rod provides space for the bolster to move downward due to the load of the wagon and simultaneously keeps it from longitudinal displacement and falling out.

3 Results and discussion

To determine the strength of the modernized brake beam with a displaced pin-hole in the strut, the corresponding calculations were performed. Due to bending moments at the end parts of the brake beam caused by the eccentric application of load at the joint of the tension member and the brake beam, the calculation was performed by the refined method including the bending deformation of the beam. The brake beam was calculated using the force method according to the diagram shown in Figure 4. The force in the tension member was taken as an extra unknown variable, i.e., the system was once statically indeterminate. Then, the canonical equation of the method of forces is as follows:

$$X_1\delta_{11} + \Delta_{1p} = 0\,, \tag{1}$$

where δ_{11} is a single displacement in the direction of the i-th link caused by the force X_1; Δ_{1F} is a displacement in the direction of the i-th link caused by the simultaneous action of the entire external load.

The basic brake beam system is shown in Figure 4. The bending moments and longitudinal forces from the force X = 1, as well as the load diagram, are shown in Figure 5.

Determining the displacement:

a) from the force X_1 = 1

$$E\delta_{11} = \frac{2l_1a^2\sin^2\beta}{3I_y} + \frac{2l_1\cos^2(\alpha+\beta)}{F_b} + \frac{2l_2}{F_c} + \frac{4\cos^2\gamma \cdot n}{F_p}\,, \tag{2}$$

where I_y is the moment of inertia of the beam relative to the vertical axis; F_b is the cross-section of the beam; F_p is the cross-section of the strut; F_c is the cross-section of the tension member; E is modulus of elasticity of the triangular component (the triangle); a is a half-length of the triangle the end joints; l_1 is length of the triangle between end joint and middle joint; l_2 is a string length; α is a tilting angle of the triangle; β is a tilting angle of the string; γ is angle formed by the spacer and the string; n is a distance from the center hinge to the point

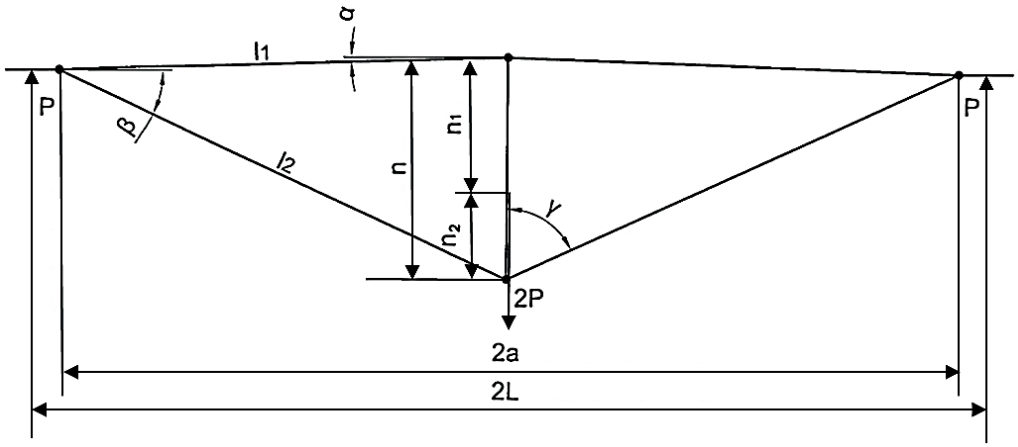

Figure 4 *The design diagram of the brake beam*

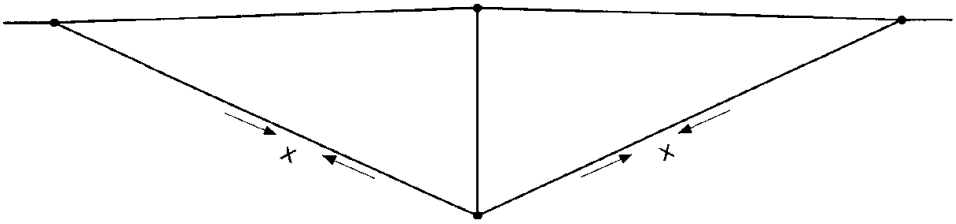

Figure 5 *The basic system of the brake beam*

of interaction of the string arms; n_1 and n_2 are segments forming the distance from the middle hinge to the point of interaction of the string arms; $2L$ is the triangle length; $2P$ is the force acting on the triangle.

b) from the load 2 P in the direction of the extra unknown value

$$E\Delta_{1p} = -\frac{a\sin\beta \cdot l_1 P}{3I_y}(3L - a) - \frac{4Ph_1\cos\gamma}{F_p}. \qquad (3)$$

The force X_1 (Figure 4) is determined from Equation (1)

$$X_1 = -\frac{\Delta_{1p}}{\delta_{11}}. \qquad (4)$$

The values included in calculation Equations (2) and (3) were taken from the design drawings of a typical brake beam:

$2L$ = 1,607 mm; h = 375.3 mm; $I_y = 20.9 \cdot 10^4$ mm^4;
$2a$ = 1.517 mm; h_1 = 208 mm; F_b = 1185 mm^2;
l_1 = 758.9 mm; cos α = 0.999 F_c = 855 mm^2;
l_2 = 845 mm; cos γ = 0.444 F_p = 1500 mm^2.

Then, based on the calculations, it was obtained:

$$E\delta_{11} = 2777.13,$$

$$E\Delta_{1p} = -6736.01P.$$

From here, follows:

$$X_1 = \frac{6736.01P}{2777.13} \cong 2.43P.$$

After determining the force X_1, the total bending moment diagram was constructed by superimposing the diagrams shown in Figure 6. In this case, the first of them is multiplied by the resulting value X_1 before o superimposing.

Based on the total bending moment diagram (Figure 7), the stresses in the brake beam elements were determined.

In the calculations it was assumed that the maximum load on the brake beam was $2P$ = 77 kN.

The tensile stress in the tension member of the brake beam is

$$\sigma = \frac{2.43P}{F_c} = \frac{2.43 \cdot 3850\text{N}}{855\,\text{mm}^2} = 11\,\text{MPa}. \qquad (5)$$

Determining the stress in the brake beam (at the end of the tension member reinforcement, i.e., at a distance of 245 mm from the support).

The slenderness of the beam was determined from the expression

$$\lambda = \frac{l_1}{\sqrt{\frac{I_{\min}}{F}}} = \frac{75.9}{\sqrt{\frac{20.9}{11.85}}} = 56.5[-]. \qquad (6)$$

The coefficient of longitudinal bending with the resulting slenderness is equal to φ = 0.87.

The stress in the rod is

$$\sigma = \frac{2.7 \cdot 3850\text{N}}{1375\text{mm}^2} + \frac{2.14 \cdot 3850\text{N}}{1185\text{mm}^2 \cdot 0.87} = 15.7\,\text{MPa}.$$

The results of the analytical calculations showed that the proposed modernization did not change the

stresses in the dangerous areas of the brake beam and, therefore, did not affect its strength.

To determine the stress distribution fields in the modernized brake lever transmission, a strength calculation was performed using the finite element method, implemented in SolidWorks Simulation [21-23]. The graphic works on creation of the brake lever transmission was reproduced in SolidWorks. Figure 8 shows a graphical model of the brake lever transmission. Since the calculations were performed as quasi-static,

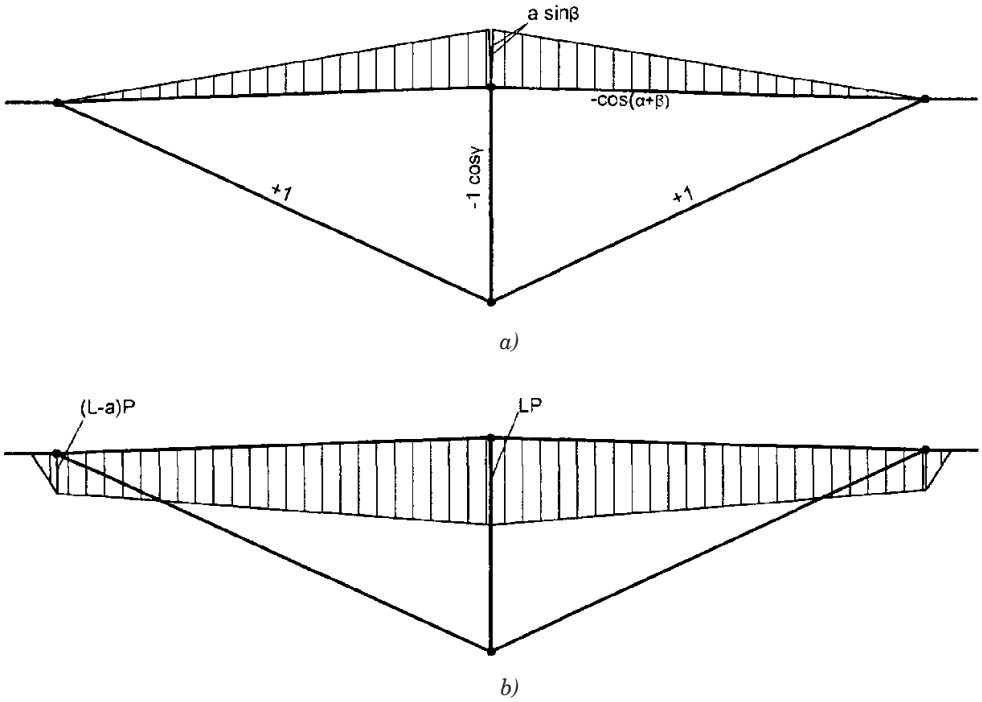

Figure 6 *The bending moment diagrams, a) from the single force X_1; b) from the external load 2P*

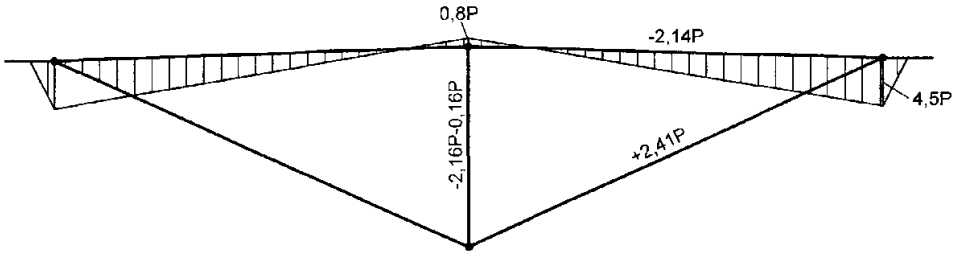

Figure 7 *The total bending moment diagram*

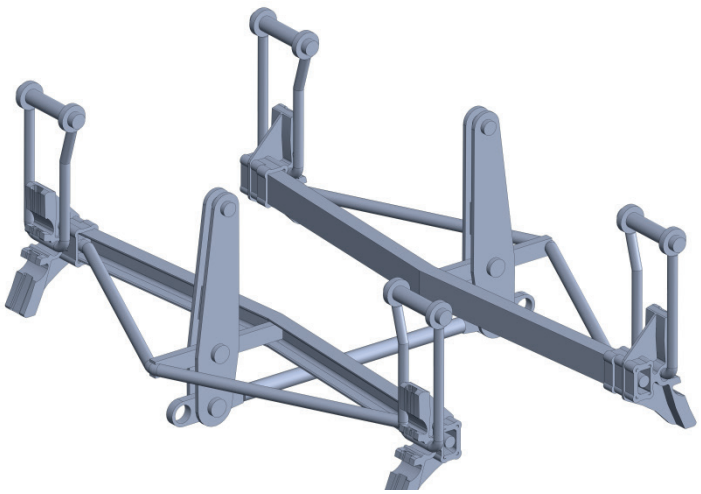

Figure 8 *The graphical model of the brake lever transmission*

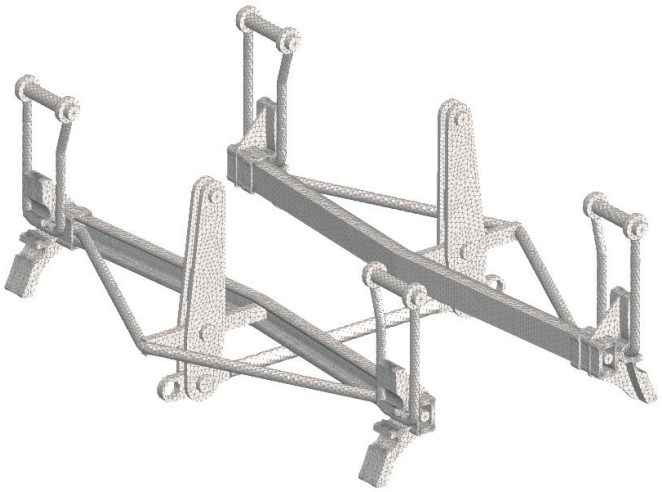

Figure 9 *The finite element model of the brake lever transmission*

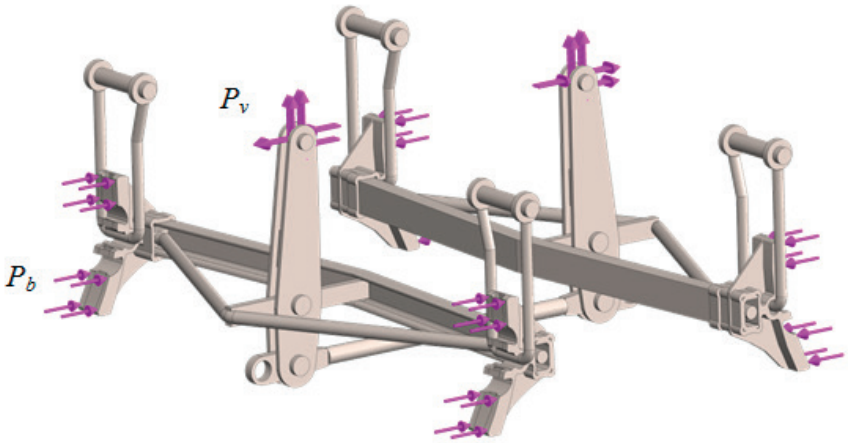

Figure 10 *The design diagram of the brake lever transmission*

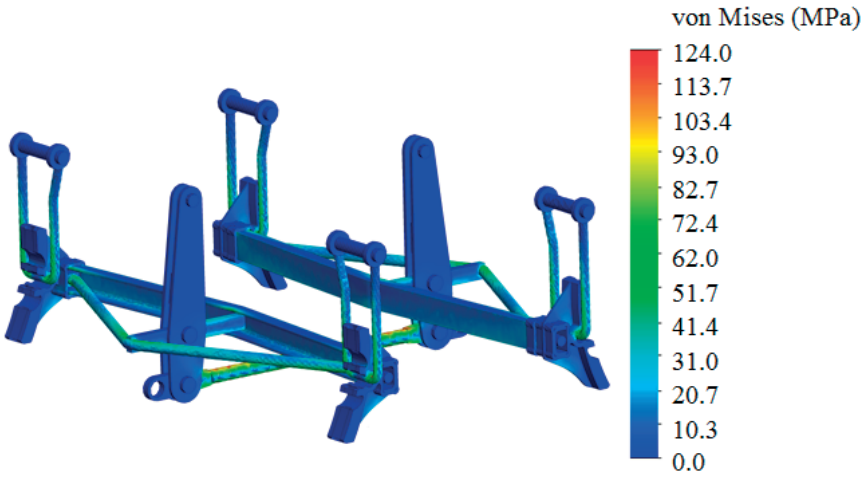

Figure 11 *The stressed state of the brake lever transmission*

the guide device was not taken into account.

The finite element model was formed by tetrahedra (Figure 9).

Their number was calculated graphically and analytically [24]. The grid had 288,115 elements and 76,296 nodes. The model was fixed by the suspension. The load was applied to the shoes P_b, as well as to the joints of the vertical arms P_v, which was decomposed into two elements taking into account the angle of application (Figure 10).

Based on the calculations performed with the von Mises criterion, the stresses in the elements of the brake lever transmission were obtained (Figure 11).

The maximum stresses, recorded in the tensile

member, were 124 MPa. Those stresses are lower than the permissible value [25], so the strength of the brake transmission is ensured. Thus, the solutions proposed in the study are appropriate.

The scientific novelty of this research is the included derived model of the strength of the brake lever transmission of the freight wagon bogie, which allows to determine the main indicators of the strength of its components under various external loads. This model can be used within the framework of the educational process of students studying in the discipline "Autobrakes of rolling stock". This model can also be used in the conditions of wagon-building enterprises when designing and modernizing the brake lever transmissions of modern rolling stock.

4 Conclusions

1. The measures aimed at eliminating abnormal pad wear by modernizing the brake lever transmission elements are proposed. The technological pin-hole in the strut is displaced by 112 ±2mm towards the bolster beam, i.e., in line with the joints of the pendulum suspensions. In addition, it is recommended to use the innovative BLT guide device, which ensures uniform clearances between the pads and wheels. Such measures to modernize the brake lever transmission elements help to balance the weight of the parts relative to the pendulum suspension and neutralize the harmful torque to the brake beams.
2. The strength of the modernized brake lever transmission of the wagon bogie 18-100 is calculated. The maximum equivalent stresses recorded in the tension member of the brake beam are 124 MPa, which is lower than the permissible value. The research shows that the proposed modernization measures are appropriate.

The research results could help in improving the safety of freight trains and increasing the profitability of the rail transport.

Acknowledgment

This publication was supported by the Cultural and Educational Grant Agency of the Ministry of Education of the Slovak Republic under the project KEGA 024ZU-4/2024: Deepening the knowledge of university students in the field of construction of means of transport by carrying out professional and scientific research activities in the field. It was also supported by the Slovak Research and Development Agency of the Ministry of Education, Science, Research and Sport under the project VEGA 1/0513/22: Investigation of the properties of railway brake components in simulated operating conditions on a flywheel brake stand. Funded by the EU NextGenerationEU under the Recovery and Resilience Plan for Slovakia under the project No. 09I03-03-V01-00131.

Conflicts of interest

The authors declare that they have no known competing financial interests or personal relationships that could have appeared to influence the work reported in this paper.

References

[1] PANCHENKO, S., GERLICI, J., VATULIA, G., LOVSKA, A., RYBIN, A., KRAVCHENKO, O. Strength assessment of an improved design of a tank container under operating conditions. *Communication - Scientific Letters of the University of Zilina* [online]. 2023, **25**(3), B186-B193. ISSN 1335-4205, eISSN 2585-7878. Available from: https://doi.org/10.26552/com.C.2023.047

[2] DIZO, J., BLATNICKY, M., HARUSINEC, J., SUCHANEK, A. Assessment of dynamics of a rail vehicle in terms of running properties while moving on a real track model. *Symmetry* [online]. 2022, **14**(3), 536. eISSN 2073-8994. Available from: https://doi.org/10.3390/sym14030536

[3] DIZO, J., BLATNICKY, M. Evaluation of vibrational properties of a three-wheeled vehicle in terms of comfort. *Manufacturing Technology* [online]. 2019, **19**(2), p. 197-203. ISSN 1213-2489 eISSN 2787-9402. Available from: https://doi.org/10.21062/ujep/269.2019/a/1213-2489/mt/19/2/197

[4] SOUKUP, J., SKOCILAS, J., SKOCILASOVA, B., DIZO, J. Vertical vibration of two axle railway vehicle. *Procedia Engineering* [online]. 2017, **177**, p. 25-32. ISSN 1877-7058. Available from: https://doi.org/10.1016/j.proeng.2017.02.178

[5] DIZO, J., BLATNICKY, M. Investigation of ride properties of a three-wheeled electric vehicle in terms of driving safety. *Transportation Research Procedia* [online]. 2019, **40**, p. 663-670. ISSN 2352-1465. Available from: https://doi.org/10.1016/j.trpro.2019.07.094

[6] BLOKHIN, E. P., ALPYSBAEV, K. T., PANASENKO, V. Y., GARKAVI, N. Y., KLIMENKO, I. V., GRANOVSKY, R. B., FEDOROV, E. F. ZK1 bogies of gondola cars built in the PRC (in Russian). *Wagon Fleet*. 2012, **9**(66), p. 12-14. ISSN 1994-4756.

[7] RADZIKHOVSKY, A. A., OMELYANENKO, I. A., TIMOSHINA, L. A. A systems approach to the design of bogies for freight cars with increased axle loads (in Russian). *Wagon Fleet*. 2008, **8**, p. 10-16.
[8] RADZIKHOVSKY, A. A., OMELYANENKO, I. A., TIMOSHINA, L. A. Brake shoe retraction device (in Russian). *Wagon Fleet.* 2009, **11-12**, p. 18-21. ISSN 1994-4756
[9] BOSOV, A. A., MYAMLIN, S. V., PANASENKO, V. Y., KLIMENKO, I. V. Ways to improve the design of a freight car bogie (in Russian). *Newsletter of the Dnipropetrovsk National University of Health Transport named after Academician V. Lazaryan.* 2009, **2**, p. 27-32. ISSN 2307-3489.
[10] MAZUR, V. L., NAYDEK, V. L., POPOV, E. C. Refinishing of cast iron and compositional with cast iron inserts of gilded pads for a dry warehouse (in Ukrainian). *Metal and Literature of Ukraine*. 2021. **2**(29), p. 30-39. ISSN 2706-5529.
[11] HODGES, T. A life-cycle approach to braking costs - International Railway Journal [online]. 2012. Available from: https://www.railjournal.com/in_depth/a-life-cycle-approach-to-braking-costs/
[12] MAZUR, V. L., SIRENKO, K. A. Economic and environmental aspects of using brake pads made of cast iron or composite material for railway transport. *Metal and Casting of Ukraine* (in Ukrainian). 2022, **3**(149), p. 54-62. ISSN 2706-5529.
[13] SHARMA, R. C., DHINGRA, M., PATHAK, R. K. Braking systems in railway vehicles. *International Journal of Engineering Research and Technology*. 2015, **4**, p. 206-211. ISSN 2278-0181.
[14] SARIP, S. Design development of lightweight disc brake for regenerative braking - finite element analysis. *International Journal of Applied Physics and Mathematics* [online]. 2013, **3**(1), p. 52-58. ISSN 2010-362X. Available from: https://doi.org/10.7763/IJAPM.2013.V3.173
[15] CRUCEANU, C., OPREA, R., SPIROIU, M., CRACIUN, C., ARSENE, S. Computer aided study regarding the influence of filling characteristics on the longitudinal reaction within the body of a braked train. In: Recent Advances in Computer: 13th WSEAS International Conference on Computers: proceedings. 2009. p. 531-537.
[16] CRUCEANU, C. Train braking, reliability and safety in railway [online]. In: *Reliability and safety in railway*. PERPINYA, X. (Ed.). 2012. ISBN 978-953-51-0451-3, eISBN 978-953-51-6187-5. Available from: https://doi.org/10.5772/37552
[17] RAVLYUK, V., RAVLIUK, M., HREBENIUK, V., BONDARENKO, V. Process features and parametric assessment of the emergence of the excessive wear for the brake pads of freight car bogies. *IOP Conference Series: Materials Science and Engineering* [online]. 2019, **708**, 012025. ISSN 1757-899X. Available from: https://doi.org/10.1088/1757-899X/708/1/012025
[18] PANCHENKO, S., GERLICI, H., LOVSKA, A., RAVLYUK, V., DIZO, J., HARUSINEC, J. Study on the strength of the brake pad of a freight wagon under uneven loading in operation. *Sensors* [online]. 2014, **24**(2), 463. eISSN 1424-8220. Available from: https://doi.org/10.3390/s24020463
[19] PANCHENKO, S., GERLICI, J., VATULIA, G., LOVSKA, A., RAVLYUK, V., RYBIN, A. Method for determining the factor of dual wedge-shaped wear of composite brake pads for freight wagons. *Communications - Scientific Letters of the University of Zilina* [online]. 2023, **26**(1), p. B31-B40. ISSN 1335-4205, eISSN 2585-7878. Available from: https://doi.org/10.26552/com.C.2024.006
[20] ELYAZOV, I., RAVLYUK, V., RYBIN, A., HREBENIUK, V. Determination of parameters of abnormal wear of brake pads of freight cars. *E3S Web of Conferences* [online]. 2020, **166**, 07004. eISSN 2267-1242. Available from: https://doi.org/10.1051/e3sconf/202016607004
[21] PUSTYLGA, S. I., SAMOSTYAN, V. R. AND KLAK, Y. V. Engineering graphics in SolidWorks: Training manual. - Lutsk: Veza, 2018, 172 p. [In Ukrainian].
[22] VATULIA, G., LOVSKA, A., PAVLIUCHENKOV, M., NERUBATSKYI, V., OKOROKOV, O., HORDIIENKO, D., VERNIGORA, R., ZHURAVEL, I. Determining patterns of vertical load on the prototype of a removable module for long-size cargoes. *Eastern-European Journal of Enterprise Technologies* [online]. 2022, **6/7**(120), p. 21-29. ISSN 1729-3774, eISSN 1729-4061. Available from: https://doi.org/10.15587/1729-4061.2022.266855
[23] GERLICI, J., LOVSKA, A., VATULIA, G., PAVLIUCHENKOV, M., KRAVCHENKO, O., SOLCANSKY, S. Situational adaptation of the open wagon body to container transportation. *Applied Sciences* [online]. 2023, **13**(15), 8605. eISSN 2076-3417. Available from: https://doi.org/10.3390/app13158605
[24] KONDRATIEV, A., POTAPOV, O., TSARITSYNSKYI, A., NABOKINA, T. Optimal design of composite shelled sandwich structures with a honeycomb filler. In: *Advances in design, simulation and manufacturing IV. DSMIE 2021. Lecture notes in mechanical engineering* [online]. IVANOV, V., TROJANOWSKA, J., PAVLENKO, I., ZAJAC, J., PERAKOVIC, D. (Eds.). Cham: Springer, 2021. ISBN 978-3-030-77718-0, eISBN 978-3-030-77719-7, p. 546-555. Available from: https://doi.org/10.1007/978-3-030-77719-7_54
[25] DSTU 7598:2014. Freight wagons. General requirements for calculations and design of new and modernized wagons of 1520 mm track (non-self-propelled). Kiev, Ukraine: UkrNDNTS, 2015.

REDUNDANT CONSTRAINTS IN CRANE DISC BRAKE MECHANISM: EFFECT AND DISPOSAL PERSPECTIVES

Vladyslav Protsenko[1], Volodymyr Malashchenko[2], Mykhaylo Babii[3], Valentyn Nastasenko[3], Roman Protasov[4], František Brumerčík[5,*], Marek Macko[5]

[1]Faculty of Engineering and Transport, Kherson National Technical University, Kherson, Ukraine
[2]Institute of Mechanical Engineering and Transport, Lviv Polytechnic National University, Lviv, Ukraine
[3]Faculty of Marine Engineering, Kherson State Maritime Academy, Kherson, Ukraine
[4]Institute of Applied Mechanics and Mechatronics, Faculty of Mechanical Engineering, Slovak University of Technology in Bratislava, Bratislava, Slovakia
[5]Department of Design and Machine Elements, Faculty of Mechanical Engineering, University of Zilina, Zilina, Slovakia

*E-mail of corresponding author: frantisek.brumercik@fstroj.uniza.sk

Vladyslav Protsenko 0000-0002-3468-4952,
Mykhaylo Babii 0000-0002-0560-2081,
Roman Protasov 0000-0003-1611-0610,
Marek Macko 0009-0001-4079-6846
Volodymyr Malashchenko 0000-0001-7889-7303,
Valentyn Nastasenko 0000-0002-0330-1138,
František Brumerčík 0000-0001-7475-3724,

Resume

In this paper is considered a promising design of the braking disk mechanism of a construction crane. The analysis of the kinematics of the brake pad drive has shown that due to redundant links in the brake pad drive mechanism the latter are not able to self-align. This leads to uneven braking torque during the smooth braking, overloads and deterioration of the positioning accuracy of the load suspended on the cable. Based on the methods of analyzing the kinematics of complex mechanisms, two variants of modernization without redundant links are proposed. Both variants can be realized without changing the kinematics of the mechanism, but they differ in the complexity of the joint manufacturing technology and depend on the design and dimensional limitations of the brake.

Article info

Received 23 September 2024
Accepted 19 February 2025
Online 21 October 2025

Keywords:

disc brake
redundant constraint
mechanism
friction torque
maintainability
self-alignment

Available online: https://doi.org/10.26552/com.C.2025.029

ISSN 1335-4205 (print version)
ISSN 2585-7878 (online version)

1 Introduction

Lifting machine brake mechanisms are designed to reduce the kinetic energy of their mechanisms during changes in movement modes and holding loads or crane elements and are responsible elements on which the safety of operation and the lives of personnel depend. Therefore, increasing the reliability of brakes is a reserve for improving the safety of the operation of lifting machines.

Nowadays, the drum-type brakes are widespread in cranes, the characteristic drawback of which is overheating, which determines a certain amount of modern scientific research in the field of their dynamics and materials for manufacturing their elements [1-2]. However, disc-type mechanisms, which cool better and provide high values of braking forces, are more promising. The disc brake elements are highly stressed, which requires ensuring an even distribution of forces between their elements during operation in the presence of manufacturing errors, wear, or thermal grooving.

The presence of redundant constraints in the mechanisms contributes to the increase in the unevenness of the load distribution between the parts [3-4]. This can lead to the destruction of parts [5], increased requirements for manufacturing and assembly accuracy [6], and an increase in mechanical losses [7]. There are not many works dedicated to the study of the structure and elimination of redundant constraints in crane brake mechanisms. For example, the lever mechanisms of crane-type drum-pad brakes with electrohydraulic and electromagnetic actuators were considered in [8], but these elements themselves were not taken into account when compiling the structural diagram of the brake mechanism. In work [9], this gap in the study of crane-type drum-pad brakes is partially filled, but

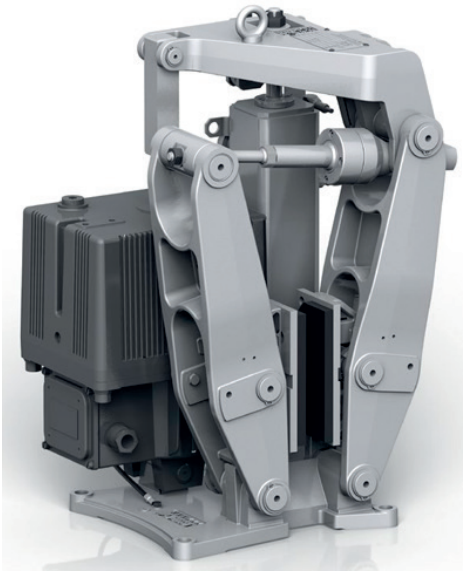

Figure 1 *Disc brake Vulkan general view [10]*

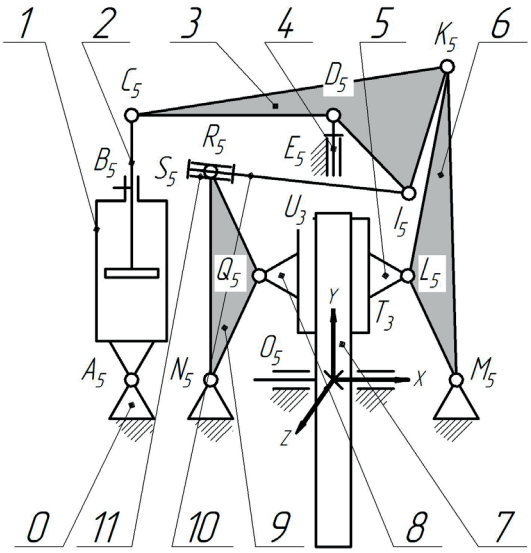

Figure 2 *Structural diagram of basic brake mechanism from Figure 1*

the structure of disc brakes remains underresearched today.

2 Methodology

Consider the structure of the Vulkan disc brake mechanism (Figure 1, Figure 2). It contains cylinder 1 of the electrohydraulic pusher attached to base 0, in which rod 2 is installed with the possibility of axial movement.

Rod 2 is hingedly connected to rocker 3, which can rotate on axis 4, and is hingedly connected to the right lever 6 of a pad 5. Disk 7 is installed with the possibility of rotation on base 0 and has the possibility of interaction of its ends with the flat surfaces of pads 5 and 8. Block 8 is hingedly fixed on the left lever 9, which is hingedly installed on base 0. The connection of the rocker 3 and the left lever 9 is provided by a rod 11, which is connected to it through a hinge formed by a sleeve 10.

In the disc brake mechanisms, the brake discs have some runout due to manufacturing and installation inaccuracies. The schematic position of the brake disc relative to the pads, at which the runout occurs, is shown in (Figure 3). In addition, some taps may not be used for a certain period of time, as a result of which corrosion occurs on the disc surface, which can also be uneven - less near the brake pads, and more in the most exposed areas. As a result of the above features, in the smooth braking mode, a variable clamping force occurs between the pads and the disc, which leads to an uneven braking torque. In special cases, the runout of the brake disc can be so great that it leads to its surfaces touching the brake pads when the brake is open, (Figure 4). In any case, the runout of the brake mechanism reduces the accuracy and smoothness of the braking process, creates an increased load on its parts and reduces their service life. This problem can be solved in several ways. The first is to increase the manufacturing accuracy of the disc and parts for its installation in the mechanism, as well as to protect the entire brake assembly from dust and moisture. Another option is to install the brake pads on the levers or install the pressure levers on the brake frame in such a way that they are dynamically self-aligned relative to the surface of the disc. To do that, it is necessary to analyze the existing types of joints in the reference mechanism using methods from the theory of machines or kinematic of machines [11-13] to determine the kinematic mobility of its elements - the so-called redundant links. The number of moving links and kinematic pairs is the determined.

The described disk brake mechanism contains eleven movable links (n = 11). Number of 5-class kinematic pairs here is P_5 = 14 (A_5, B_5, C_5, D_5, E_5, K_5, I_5, L_5, M_5, N_5, O_5, Q_5, R_5, S_5), number of 3-class kinematic pairs is P_3 = 2 (T_3, U_3), numbers of 4, 2 and 1-class kinematic pairs are $P_4 = P_2 = P_1 = 0$.

The total kinematic pairs number is:

$$P = P_5 + P_4 + P_3 + P_2 + P_1 = 14 + 0 + 3 + 0 + 0 = 16. \quad (1)$$

The sum of kinematic pairs movabilities is :

$$f = 1P_5 + 2P_4 + 3P_3 + 4P_2 + 5P_1 = 1 \times 14 + 2\times 0 + + 3 \times 2 + 4 \times 0 + 5 \times 0 = 20. \quad (2)$$

Number of independent locked circuits by Gohman formula [14] is:

$$k = P - n = 16 - 11 = 5. \quad (3)$$

Independent locked circuits are following - $N_5Q_5U_3O_5N_5$; $M_5L_5T_3O_5M_5$; $A_5B_5C_5D_5E_5A_5$; $N_5S_5R_5I_5K_5M_5N_5$; $E_5D_5I_5R_5S_5N_5E_5$.

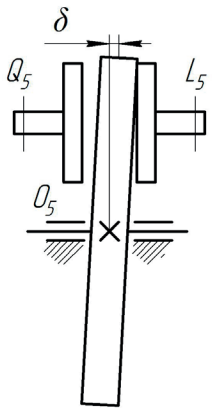

Figure 3 *Braking disk end beating δ influence*

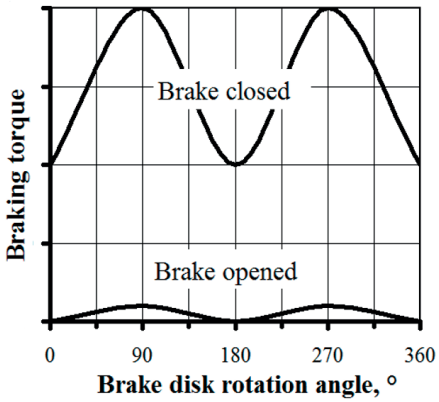

Figure 4 *Approximate influence of the disc beating on the brake friction torque in redundant constraints presence*

Table 1 *Circuit method application to basic brake mechanism (Figure 2)*

Circuit	Planar movabilities f_p	Non-planar movabilities f_n
$N_5Q_5U_3O_5N_5$	f_x' f_y' f_z''	f_x'' f_y'' f_z'
$M_5L_5T_3O_5M_5$	Ø U NQ	W_b U Ø U
$A_5B_5C_5D_5E_5A_5$	Ø T ML	TO Ø T
$N_5S_5R_5I_5K_5M_5N_5$	Ø B AC	Ø E Ø
$E_5D_5I_5R_5S_5N_5E_5$	Ø Ø K I S	R Ø Ø
	Ø Ø D	Ø Ø Ø
	$W = 1$, $q = 11$	

Total mechanism mobility by Voinea and Atanasiu equation [15-16] is:

$$W = f - \sum r_i = 20 - (3 + 3 + 4 + 4 + 5) = 1, \quad (4)$$

where: r_i - independent locked circuits axis ranks.

Thus, total mechanism mobility is:

$$W = W_b + W_l = 1 + 0 = 1, \quad (5)$$

where: W_b = 1 - basic mechanism mobility (disc 7 rotation),
W_l = 0 - local links mobilities.

Then, the redundant constraints number in basic variant, by Somov and Malyshev formula is:

$$q_{SM} = W + 5P_5 + 4P_4 + 3P_3 + 2P_2 + P1 - 6n = \\ = 1 + 5 \times 14 + 4 \times 0 + 3 \times 2 + 2 \times 0 + \\ + 0 - 6 \times 11 = 11. \quad (6)$$

Redundant constraints number, by Ozols formula, [17] is:

$$q_{OZ} = W + 6k - f = 1 + 6 \times 5 - 20 = 11. \quad (7)$$

Thereby, the total redundant constraints number in the analyzed mechanism $q = q_{SM} = q_{OZ} = 11$.

Using the contour method confirms the presented calculations (Table 1)

The identified redundant constraints prevent the self-alignment of brake pads on the ends of the brake discs and make it possible to overload the links of the mechanism (Table 2 and Table 3).

The most dangerous among identified redundant constraints belong to power circuits q_1 and q_2 which initiate the main disadvantage of the brake mechanism - the impossibility of brake pads on disc self-alignment.

3 Results and discussion

The main way to eliminate the detected redundant connections, without intentionally introducing errors into the design and worsening the brake performance, is to add mobilities to the mechanism contours by increasing the classes of kinematic pairs. The first variant is the implementation of the 4-th class pin-spherical pairs L_4 and Q_4 instead of rotary ones (L_5, Q_5) at the points of connection of blocks 5 and 8 with levers 6 and 9, as well as modification of C_3, D_3, K_3, R_3 pairs to the 3-rd class spherical pairs and conversion of I_5 pair to the 4-th class cylindrical pair I_4 (Figure 5).

In this variant, with an unchanged total number of links, kinematic pairs, and circuits, the number of kinematic pairs of the 5-class became P_5 = 7 (A_5, B_5,

E_5, M_5, N_5, O_5, S_5), number of 4-class kinematic pairs $P_4 = 3$ (I_4, L_4, Q_4), 3-class kinematic pairs $P_3 = 6$ (C_3, D_3, K_3, R_3, T_3, U_3), 2 and 1-class kinematic pairs number $P_4 = P_2 = P_1 = 0$.

Table 2 *Redundant constraints presence in basic disc brake mechanism consequences*

Redundant constraint	Redundant Constraint presence influence	Practice way of redundant constraint influence leveling	Leveling absence consequences
1	2	3	4
q_1	Impossibility of pads self-aligning around *Y* axis ($f_y'' = 0$).	Control and limitation of the end beating of the brake disc and the thickness of the pads in the plane *XZ*. This leads to an increase in the labor-intensiveness of brake maintenance.	Pads axes loading by sign variable bending moment and its levers by torque in *XZ* plane. Creating periodically changing torque in the brake shaft.
q_2			
q_3	Impossibility of circuit $A_5B_5C_5D_5E_5A_5$ assembling without tension around *X* axis ($f_x'' = 0$) in the presence of an angular error in the drilling of hinge holes or errors in of the mechanism aggregation.	Implementation of increased radial gaps in kinematic pairs *A, C, and D*. This leads to delayed brake activation.	Impossibility of mechanism assembling and brake operation without parts deformation in *YZ* and *XZ* plane.
q_4	Impossibility of circuit $A_5B_5C_5D_5E_5A_5$ assembling without tension along *Z* axis ($f_z' = 0$) in the presence of an error in the manufacture of parts in terms of thickness or displacement of the basic surfaces in the *YZ* plane or errors of the mechanism aggregation.	Implementation of increased axial gaps in kinematic pairs *A, C, D,* or radial gap in *E* kinematic pair. This leads to delayed brake activation.	
q_5	Impossibility of circuit $N_5S_5R_5I_5K_5M_5N_5$ assembling without tension around *Y* axis ($f_y'' = 0$) in the presence of an angular error in the drilling of hinge holes or errors in of the mechanism aggregation.	Implementation of increased radial gaps in kinematic pairs *N, R, I, K, M*. This leads to delayed brake activation.	Impossibility of mechanism assembling and brake operation without parts deformation in *YZ* and *XZ* plane.
q_6	Impossibility of circuit $A_5B_5C_5D_5E_5A_5$ assembling without tension along *Z* axis ($f_z' = 0$) in the presence of an error in the manufacture of parts in terms of thickness or displacement of the basic surfaces in the *YZ* plane or errors of the mechanism aggregation.	Implementation of increased axial gaps in kinematic pairs *N, R, I, K, M*.	

Table 3 *Redundant constraints presence in basic disc brake mechanism consequences - continuation*

Redundant constraint	Redundant constraint presence influence	Practice way of redundant constraint influence leveling	Leveling absence consequences
1	2	3	4
q_7	Impossibility of circuit $E_5D_5I_5R_5S_5N_5E_5$ assembling without tension along *X* and *Y* axes ($f_x' = 0, f_y' = 0$) in the presence of errors in the location of the hinge holes in the *XY* plane or errors in the mechanism aggregation.	Implementation of increased radial gaps in kinematic pairs *E, D, I, R, S, N,* or axial gap in *E* kinematic pair. This leads to delayed brake activation.	Impossibility of mechanism assembling and brake operation without parts deformation in *XY* plane.
q_8			
q_9	Impossibility of circuit $E_5D_5I_5R_5S_5N_5E_5$ assembling without tension around *X* and *Y* axes ($f_x'' = 0, f_y'' = 0$) in the presence of an angular error in the drilling of hinge holes.	Implementation of increased radial gaps in kinematic pairs *N, S, R, I, K, M, N*. This leads to delayed brake activation.	Impossibility of mechanism assembling and brake operation without parts deformation in *XY*, *YZ*, and *XZ* plane.
q_{10}			
q_{11}	Impossibility of circuit $E_5D_5I_5R_5S_5N_5E_5$ assembling without tension along the *Z* axis ($f_z' = 0$) in the presence of an error in the manufacture of parts in terms of thickness or displacement of the basic surfaces in the *YZ* plane.	Implementation of increased axial gaps in kinematic pairs *N, S, I,* or radial gap in *E*, *R* kinematic pairs. This leads to delayed brake activation.	

The sum of kinematic pairs movabilities:

$$f = 1P_5 + 2P_4 + 3P_3 + 4P_2 + 5P_1 = 1 \times 7 + 2 \times 3 + 3 \times 6 + 4 \times 0 + 5 \times 0 = 31. \quad (8)$$

Total mechanism mobility, by Voinea and Atanasiu equation, is:

$$W = f - \sum r_i = 31 - 5 \times 6 = 1 \quad (9)$$

Total mechanism mobility is:

$$W = W_b + W_l = 1 + 0 = 1, \quad (10)$$

where: W_b = 1 - basic mechanism mobility (disc 7 rotation),
W_l = 0 - local links mobilities (the lack of local mobility of the sleeve 10 can be ensured by boring a hole under the axis S_5 outside the center of the sphere R_3).

Then, redundant constraints number in basic variant, by Somov and Malyshev formula, is:

$$q_{SM} = W + 5P_5 + 4P_4 + 3P_3 + 2P_2 + P_1 - 6n = = 1 + 5 \times 7 + 4 \times 3 + 3 \times 6 + 2 \times 0 + + 0 - 66 \times 11 = 0. \quad (11)$$

Redundant constraints number by Ozols formula

$$q_{OZ} = W + 6k - f = 1 + 6 \times 5 - 31 = 0. \quad (12)$$

The application of the circuit method for the variant 1 structural diagram is shown in Table 4, confirms the obtained results.

The disadvantage of the first variant is the use of pin-spherical pairs L_4 and Q_4 since it is structurally quite difficult to do this, and it is not possible to use spherical pairs here, since it can give pads 5 and 8 local mobility, which in turn can cause their rotation around the X axis and partial release from contact with the ends of the brake discs along their entire length. A good option in this case is to leave pairs L_5 and Q_5 as 5-class rotary ones.

That is why variant 2 of mechanism improvement can be spherical pairs C_3, K_3, R_3, M_3, N_3, and cylindrical pair I_4 implementation (Figure 6).

In this version, with an unchanged total number of links, kinematic pairs, and circuits, the number of kinematic pairs of the 5-class became P_5 = 8 (A_5, B_5, D_5, E_5, L_5, O_5, Q_5, S_5), number of 4-class kinematic pairs P_4 = 1 (I_4), 3-class kinematic pairs P_3 = 7 (D_3, K_3, M_3, N_3, R_3, T_3, U_3), 2 and 1-class kinematic

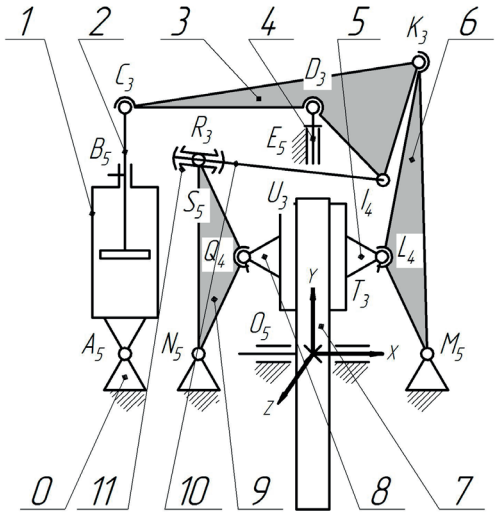

Figure 5 *Modified by variant 1 brake mechanism structural diagram*

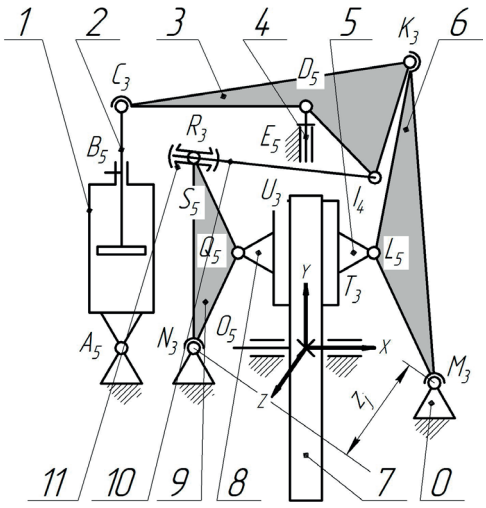

Figure 6 *Modified by variant 2 brake mechanism structural diagram*

Table 4 *Circuit method application to modified by variant 1 brake mechanism (Figure 5)*

Circuit	Planar movabilities f_p	Non-planar movabilities f_n
$N_5Q_4U_3O_5N_5$	f_x' f_y' f_z'' Ø U NQ Ø T ML	f_x'' f_y'' f_z' W_b U Q U TO L T
$M_5L_4T_3O_5M_5$	Ø B AC	C CE Ø
$A_5B_5C_3D_3E_5A_5$	Ø Ø IK S	K K I
$N_5S_5R_3I_4K_3M_5N_5$	Ø Ø DR	DR DR Ø
$E_5D_3I_4R_3S_5N_5E_5$		
W = 1, q = 0		

pairs number $P_4 = P_2 = P_1 = 0$.

The sum of kinematic pairs movabilities is:

$$f = 1P_5 + 2P_4 + 3P_3 + 4P_2 + 5P_1 = 1 \times 8 + 2 \times 1 + 3 \times 7 + 4 \times 0 + 5 \times 0 = 31. \quad (13)$$

Total mechanism mobility, by Voinea and Atanasiu equation, is:

$$W = f - \sum r_i = 31 - 5 \times 6 = 1 \quad (14)$$

Total mechanism mobility is:

$$W = W_b + W_l = 1 + 0 = 1, \quad (15)$$

where: W_b = 1 - basic mechanism mobility (disc 7 rotation),
W_l = 0 - local links mobilities.

Then redundant constraints number in basic variant, by Somov and Malyshev formula, is:

$$q_{SM} = W + 5P_5 + 4P_4 + 3P_3 + 2P_2 + P_1 - 6n = 1 + 5 \times 8 + 4 \times 1 + 3 \times 7 + 2 \times 0 + 0 - 6 \times 11 = 0. \quad (16)$$

Redundant constraints number, by Ozols formula, is:

$$q_{OZ} = W + 6k - f = 1 + 6 \times 5 - 31 = 0. \quad (17)$$

The application of the circuit method is shown in Table 5, confirms the obtained results.

The stiffness of the structure can be increased by installing the kinematic pairs M and N at a distance z_j along the Z axis.

4 Conclusion

Theoretical studies of the existing crane disc brake mechanism have been performed, and the following conclusions have been drawn:

1. Structural analysis of the kinematics of the brake pad drive mechanism showed that the mechanism has 11 redundant constraints. These constraints do not allow the brake pads to self-adjust relative to the brake disc surface. Due to that, in the event of a brake disc beating, the braking torque will not be constant.
2. The analysis identified angular constraints as the predominant challenge in the kinematics of the mechanism's constraints (joints). To mitigate the risk of jamming (or to ensure guaranteed mobility), it is necessary to manufacture these joints with either high accuracy of the mating parts, which results in an increase in price, or, conversely, to create an increased gap in the joint, which in turn increases the brake response time due to the movement of the mating parts in the joints with a gap from one extreme position to another. Concurrently, the presence of these gaps can diminish the service life of the joints, thereby increasing the impact loads they experience. That, in turn, can lead to a reduction in their fatigue strength, particularly in the drive levers.
3. A particular group of restrictions imposed on the drive mechanism can impede the ability of the brake pads to self-adjust relative to the brake disc surface. Such contact can lead to inconsistent braking torque within a single revolution, resulting in diminished smoothness and accuracy in load positioning. Furthermore, in instances of substantial brake disc beating or malfunctioning of the brake pad retraction mechanism, the pads may inadvertently come into contact with the disc surface. This phenomenon contributes to a decline in the smoothness and accuracy of movement of the load suspended on the cable, thereby reducing the service life of the brake mechanism. It also leads to accelerated wear, overheating, and increased dynamic loads.
4. In this paper, the authors proposed two design solutions for the kinematics and, consequently, the design of the brake pad drive mechanism. These solutions allow for elimination of excessive restrictions that prevent the pads from self-installing relative to the pressure levers and the surface of the brake disc. The first option proposes the use of pin spherical pads. The primary benefit of this approach

Table 5 *Circuit method application to modified by variant 2 brake mechanism (Figure 6)*

Circuit	Planar movabilities f_p	Non-planar movabilities f_n
$N_3Q_5U_3O_5N_3$	f_x' f_y' f_z'' Ø U NQ Ø T ML	f_x'' f_y'' f_z' W_b U Q U TO L T
$M_3L_5T_3O_5M_3$	Ø B AC	C CE Ø
$A_5B_5C_3D_5E_5A_5$	Ø Ø IK S	K K I
$N_3S_5R_3I_4K_3M_3N_3$	Ø Ø DR	DR DR Ø
$E_5D_5I_4R_3S_5N_3E_5$		
	$W = 1, q = 0$	

is that it necessitates only a modification to the pad mount to the pressure levers. However, a notable drawback is the complexity of implementing such a mount, particularly with regard to its strength and manufacturing technology. The necessity of a compact, durable joint underscores the challenges associated with this approach. The second option involves a substantial redesign of the brake mechanism, entailing the installation of the pressure levers on spherical joints, necessitating a corresponding modification to the brake mechanism's frame. This approach offers the benefit of preserving the original design of the replaceable brake pads.

5. Both proposed design solutions can be implemented on the disk brake of the crane without altering the mechanism's operational principle. It is noteworthy that the Vulcan crane disc brake utilizes solely cylindrical joints, which, in addition to their manufacturability, offer the benefit of a two-support design. Conversely, the implementation of a spherical joint is only feasible as a cantilever design. From the perspectives of strength, fatigue, tribology, manufacturing technology, and installation procedure, this type of joint necessitates a series of research and development endeavors in either of the two design solutions.

Acknowledgement

This article was funded in the context of the project KEGA 027ŽU-4/2024 supported by the Ministry of Education, Research, Development and Youth of the Slovak Republic.

Conflicts of interest

The authors declare that they have no known competing financial interests or personal relationships that could have appeared to influence the work reported in this paper.

References

[1] YEVTUSHENKO, A., TOPCZEWSKA, K., KUCIEJ, M. Analytical determination of the brake temperature mode during repetitive short-term braking. *Materials* [online]. 2021, **14**, 1912. eISSN 1996-1944. Available from: https://doi.org/10.3390/ma14081912

[2] UNGUREANU, M., MEDAN, N., UNGUREANU STELIAN, N., NADOLNY, K. Tribological aspects concerning the study of overhead crane brakes. *Materials* [online]. 2022, **15**, 6549. eISSN 1996-1944. Available from: https://doi.org/10.3390/ma15196549

[3] SYDORENKO, I., KRAVTSOV, E., PROKOPOVYCH, I. Reducing the reliability of the equipment as a result of the reduction of the culture of production. *Proceedings of Odessa Polytechnic University* [online]. 2019, **3**(59), p. 5-13. ISSN 2076-2429, eISSN 2223-3814. Available from: https://doi.org/10.15276/opu.3.59.2019.01

[4] ZALYUBOVSKII, M.G., PANASYUK, I.V. On the study of the basic design parameters of a seven-link spatial mechanism of a part processing machine. *International Applied Mechanics* [online]. 2020, **56**, p. 54-64. ISSN 1063-7095, eISSN 1573-8582. Available from: https://doi.org/10.1007/s10778-020-00996-x

[5] PROTSENKO, V., BABIY, M., NASTASENKO, V., PROTASOV, R. Marine diesel high-pressure fuel pump driving failure analysis. *Strojnicky casopis / Journal of Mechanical Engineering* [online]. 2021, **71**(2), p. 213-220. ISSN 0039-2472, eISSN 2450-5471. Available from: https://doi.org/10.2478/scjme-2021-0031

[6] PROTSENKO, V., NASTASENKO, V., BABIY, M., PROTASOV, R. Marine ram-type steering gears maintainability increasing. *Strojnicky casopis / Journal of Mechanical Engineering* [online]. 2022, **72**(2), p. 149-160. ISSN 0039-2472, eISSN 2450-5471. Available from: https://doi.org/10.2478/scjme-2022-0025

[7] PROTSENKO, V. O., BABIY, M. V., NASTASENKO, V. O., BILOKON, A. O. Ram-type steering gear lever mechanism improvement perspectives. *Transport Development*. 2021, **1**(8), p. 78-90. ISSN 2616-7360.

[8] SMIRNOV, G. F., SHTITSKO, P. I., IVANOVA, A. P. Redundant constraints in crane drum-pad brakes. *Lifting and Transport Technique*. 2007, **2**(22), p. 101-114. ISSN 2311-0368.

[9] SAMOYLENKO, L. K., PROTSENKO V. O. About drum-pad brake structure and reliability increase. *Herald of Kherson State Maritime Institute*. 2010, **2**(3), p. 211-216. ISSN 2313-4763.

[10] Technical data electrohydraulic disk brake FEHD-G2 - Vulkan [online]. Available from: https://www.vulkan.com/en/products/detail/electrohydraulic-disc-brake

[11] ECKHARDT, H. *Kinematic design of machines and mechanisms.* New York: McGraw-Hill, 1998, ISBN 0-07-018953-6.

[12] MARGHITU, D. B. *Kinematic chains and machine components design* [online]. Elsevier Academic Press, 2005. ISBN 978-0-12-471352-9. Available from: https://doi.org/10.1016/B978-0-12-471352-9.X5000-7

[13] SINGH, S. *Theory of machines: kinematics and dynamics*. India: Pearson, 2012. ISBN 9789332509788.

[14] WITTENBURG, J. *Kinematics. Theory and applications* [online]. Berlin, Heidelberg: Springer, 2016. ISBN 978-3-662-48486-9, eISBN 978-3-662-48487-6. Available from: https://doi.org/10.1007/978-3-662-48487-6

[15] VOINEA, R., ATANASIU, M. Contributions to the geometric theory of screws / Contributions a la teorie geometrique des vis (in Romanian). *Bulletin of the Bucharest Polytechnic Institute* / *Buletinul Institutului Politehnic Bucuresti*. 1959, **21**(3), p. 69-90. ISSN 0020-4242.
[16] WALKER, K. *Applied mechanics for engineering technology.* Essex: Pearson, 2008. ISBN 978-1-292-02736-4.
[17] UICKER, J., PENNOCK, G., SHIGLEY J. *Theory of machines and mechanisms*. New York: Oxford University Press, 2017, ISBN 9780190264482.

INTERNET OF VEHICLES SECURITY IMPROVEMENT BASED CONTROLLER AREA NETWORK AND ARTIFICIAL INTELLIGENCE

Ibraheem Hatem Mohammed

Department of Computer Communications Engineering, Al-Rafidain University College, Baghdad, Iraq

*E-mail of corresponding author: ibraheemdoser77@gmail.com

Ibraheem Hatem Mohamed 0000-0002-7362-7870

Resume

The Internet of Vehicle (IoV) is revolutionizing the automobile sector by allowing vehicles to interact between them and with roadside infrastructure. The Controller Area Network (CAN) is a vital component of such Autonomous vehicles (AVs), allowing communication between various Electronic Control Units (ECUs). However, the CAN protocol's intrinsic lack of security renders it opens to a variety of cyber-attacks, posing substantial hazards to both safety and privacy. This research proposes a defence mechanism for the real-time threat detection. It investigates the use of deep learning with multi-layer perceptron to improve the security of CAN networks inside the IoV framework. The suggested method is highly effective in identifying and mitigating potential risks, as evidenced by extensive testing on real-world CAN datasets.

Article info

Received 23 August 2024
Accepted 13 January 2025
Online 29 January 2025

Keywords:

autonomous vehicle
Internet of Vehicles (IoV)
Controller Area Network (CAN)
cyber security
deep learning
vehicular communication systems

Available online: https://doi.org/10.26552/com.C.2025.017

ISSN 1335-4205 (print version)
ISSN 2585-7878 (online version)

1 Introduction

With the latest technological developments, autonomous vehicles (AVs) that were formerly deemed science fiction have become a reality. Despite the fact that it is still in its early stages of development, the concept of autonomous vehicles is gaining global acceptance [1]. Autonomous cars are capable of sensing their environment and operating independently of people. A passenger is not required to drive the automobile at any time, nor is their presence within the vehicle required. An autonomous vehicle can go anywhere a conventional car can go and accomplish all the functions carried out by a competent human driver.

The applicability of a proposed solution to CVs or AVs depends on the specific nature of the proposed solution in terms of driving function, which can be classified hereunder:

- Conventional vehicles (non-AVs) participating in IoV rely on their human drivers for decision-making. The IoV solutions for these vehicles typically focus on" information sharing", warnings, or driver assistance, e.g., alerting drivers to nearby accidents or real-time traffic updates.
- Autonomous vehicles (AVs), on the other hand, can process the IoV data to directly execute actions such as rerouting or autonomous braking without human intervention.

According to the Society of Automotive Engineers (SAE), automation in autonomous cars can be categorized into six separate levels, ranging from SAE Level 0 (fully manual) to SAE Level 5 (entirely autonomous) [2-3]. Table 1 gives a description of these levels.

Although customers are not yet able to acquire fully autonomous vehicles, we are already in the phase of partially automated automobiles [3]. The Internet of Vehicles (IoV), an interconnected network of autonomous vehicles, roadside infrastructure, and components that communicate and interact with one another using wireless technology, is derived from the Internet of Things (IoT), with the objective of improving the effectiveness, efficiency, and safety of autonomous vehicles [4-5].

The electrical and electronic system of autonomous vehicles is a scattered and complicated network of Electronic Control Units (ECUs), sensors, and actuators. ECUs, which are computing units, are required to operate a specific subsystem and make critical autonomous driving decisions. They must interact with one another and exchange sensitive data using a set of standard protocols. The CAN bus is regarded as the de facto standard for the in-vehicle communication

Table 1 *SAE levels of driving automation*

SAE Level	Description
0	The driver is the one who controls the entire vehicle. In the form of alerts, such as lane departure or blind spot warnings, driver aid is offered.
1	With one autonomous function to help, the driver has complete control over the car. Adaptive cruise control, for example, uses automated acceleration and braking to maintain a safe distance from oncoming traffic. Alternatively, automated steering can be used, which involves the assistance of lane centering and other features to keep the car moving at a consistently high speed.
2	The driver has complete control over how the vehicle performs, with assistance from two automated operations such as steering, braking, and acceleration.
3	The car may function autonomously under a set of predetermined configurations, and the driver can take control of the vehicle at any time.
4	The vehicle may operate autonomously under specified settings, eliminating the need for the driver to oversee it. The car is extremely close to being totally autonomous.
5	At this level, the car is supposed to be completely autonomous and capable of operating without restrictions. There is no need for the driver to supervise it.

network, and it is ubiquitously used in almost all the automobiles [1, 6-7].

The remaining sections of this article are organized as follows. In Section 2 the relevant background knowledge is introduced. In Section 3 is discussed related work and their limitations. In Section 4, the specific design details of the intrusion detection model are described, while the performance evaluation is shown in Section 5, followed by the conclusion in Section 6.

2 Background knowledge

The power train, chassis and safety, body and comfort, and telematics and infotainment domains are the four main segments of an autonomous vehicle's internal communication system [8]. The airbag control, anti-lock braking, suspension, and Advanced Driver Assistance System, which perform real-time, safety-critical operations, are included in the Chassis and Safety domain. The Body and Comfort domain includes operations that do not frequently need real-time processing, such as in-vehicle climate control, seat control, door, window, or light control. The remote communication, information, and entertainment services are managed by the Telematics and infotainment domain. Each domain's performance and reaction time requirements vary depending on the function performed. Figure 1 depicts how these domains are integrated via various standards, like CAN, Media Oriented Systems Transport (MOST), and Local Interconnect Network (LIN). The CAN Bus protocol is most commonly used in the internal communication network of vehicles to support the aforementioned operations [9-14].

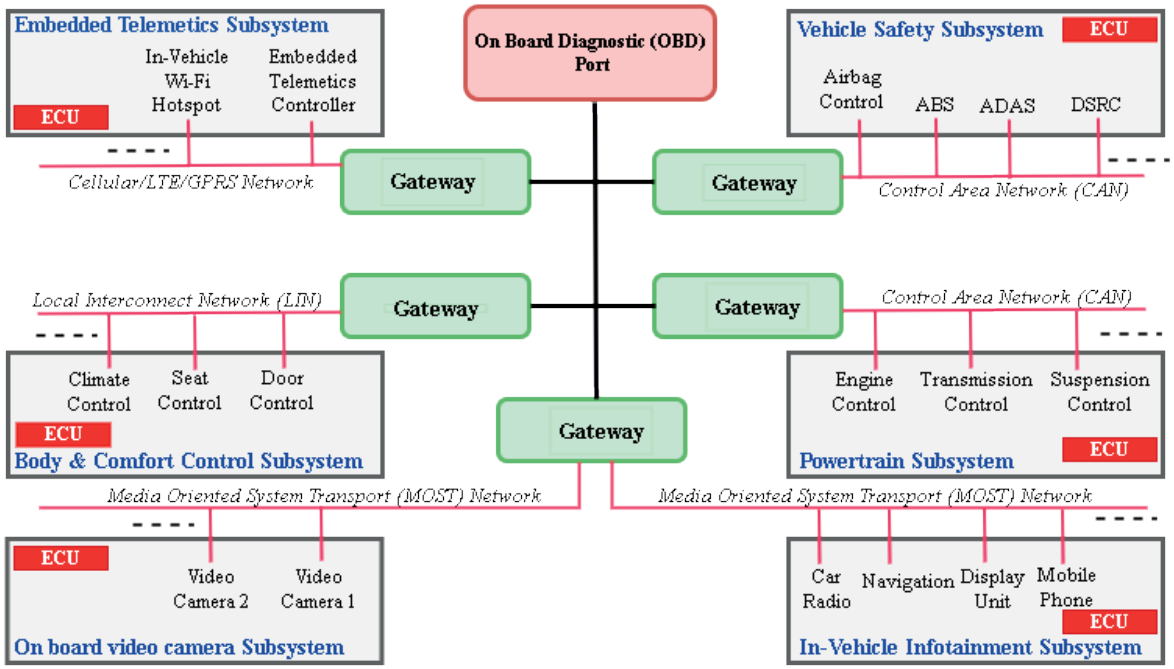

Figure 1 *In-Vehicle sub-systems adapted from [9]*

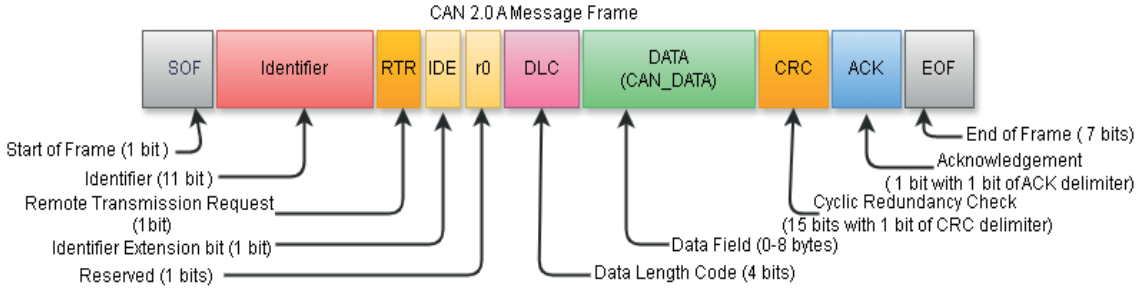

Figure 2 *The CAN frame structure*

Table 2 *Attacks executed and analysed on IoV subsystem*

Ref.	Attack Surface	Impact
Eisenberth et al. [15]	Keyless entry system	Control the door lock, unlock, and the engine
Koscher et al. [16]	Interfaces Infotainment using OBD-II/ USB port	CAN Bus injection, full access to the vehicle
Miller et al. [17]	OBD-II port	Control brakes, wheels, and get access to the CAN Bus of a real vehicle
Petit et al. [18]	LiDAR, Cameras Sensors	Signal jamming
Zorz et al. [19]	OBD-II Cellular Dongle	CAN Bus injection in Real vehicle
Palanca et al. [20]	OBD-II interface	DoS attack on CAN Bus
Woo et al. [21]	OBD-II interface	Replay, impersonation attack using the smartphone application
Nie et al. [22]	Wi-Fi, GSM	Replay, impersonation using access to CAN network using browser exploit
Mukherjee et al. [23]	OBD-II port	DoS attack by compromise ECU using the data link layer exploit

Figure 2 depicts the CAN data frame, which begins with an 1-bit Start of Frame (SOF) field, followed by an Arbitration field containing an 11- or 29-bit Identifier (ID) (CAN 2.0A has an 11-bit ID, whereas CAN 2.0B is the extended format with a 29-bit ID), and an 1-bit Remote Transmission Request (RTR).

Cybercriminals can get access to the internal communication network of the targeted vehicle using the aforementioned interfaces and carry out a range of attacks, including "replay", "DoS", or "spoofing" attacks [11]. Table 2 shows a list of effective attacks undertaken and analysed by various researchers on the IoV subsystem.

3 Literature review

Encryption, authentication, protocol stack redesign, and intrusion detection systems are among the suggested security options for the CAN Bus protection [8]. Some studies in recent years have focused on encryption techniques to secure the CAN system. However, adopting similar algorithms may need extra hardware or modifications to current ECUs. Intrusion detection methods that do not need changes to the network protocol or hardware are a better alternative for security inside AVs [7]. Researchers have utilised a range of ways to identify the CAN bus intrusions, including rule-based, machine learning-based, and other technologies. The authors of the article [24] present a deep learning-based Convolutional Neural Network (CNN) model for protecting the CAN bus in autonomous vehicles. The findings are also compared to various traditional methods; among them, the deep learning system achieves excellent accuracy. The study conducted in [25], describes another deep learning-based intrusion detection model that utilizes Long Short-Term Memory (LSTM) and CNNs network models. LSTM is a type of recurrent neural network (RNN) architecture used in deep learning, particularly for analysing sequential or time-series data, whereas identical research has been done by authors in [12, 26-29]. These studies have shown that standard CAN network data is growing increasingly sophisticated, and neural network-based models, particularly deep learning models, are the most effective way to handle the identified weaknesses in IoV security [30].

The majority of DNN-based solutions were built using the Convolutional Neural Networks (CNN) and Recurrent Neural Networks (RNN), which are extensively utilised to solve complicated problems in computer vision, text processing, audio recognition and classification, and so on. Due to their complexity, the DNNs often take a long time to train on input data.

They also require powerful computers with specialized processing units like Tensor, and Neural Processing Units. In this study, the deep learning-based IDS for CAN bus networks is presented, which outperforms previous work due to its simpler and more optimized network model.

4 Defence mechanism

To detect and categorize various assaults on autonomous vehicles by recognizing abnormal CAN network traffic patterns, the Multi-Layer Perceptron (MLP) based deep learning model is presented that may be deployed as an extra CAN Bus node, such as an OBD-2 dongle. It is more affordable and practical, and there is no need to modify the CAN Bus. It can detect and identify several types of attacks on the IoV CAN network. In Section 4.1 are described the methods to mitigate identified threats in the proposed IoV defence solution, while in Section 4.2 are described the realistic and most recent dataset used to train the model, whereas in section 4.3 is described the structure of the suggested solution.

4.1 Methods to mitigate identified threats in the proposed IoV defence solution

The proposed deep learning-based defence mechanism (e.g., using CNNs and LSTMs) provides an effective approach to intrusion detection. However, as IoV networks are highly dynamic and interconnected, they are susceptible to a wide range of cyber threats, such as DoS attacks, spoofing, man-in-the-middle attacks, data manipulation, and more.

This section outlines potential attack mitigation techniques that could complement or enhance the proposed solution to improve security within IoV systems.

4.2 Description of the dataset

In this study, the Canadian Institute for Cyber security (CIC) IoV2024 dataset is used [31-32]. It is a benchmark dataset; generated using a testbed of the real vehicle, to encourage the development of innovative security solutions for IoV processes, and it is published on the CIC dataset homepage. It contains traces for normal as well as five attack scenarios: DoS, "spoofing-steering wheel", "spoofing-RPM", "spoofing-GAS", and "spoofing-SPEED" attack, carried out by leveraging the unique characteristics of the CAN protocol in a real testbed of a Ford automobile equipped with all ECUs [31]. The original dataset was cleaned to eliminate noise (irrelevant data) and extract a specific amount of samples for each class to maintain the dataset balanced and in a format suitable for Deep Neural Networks [33-37]. Table 3 shows the class and sample's information, while Table 4 shows the retrieved features. The dataset is subsequently divided into training and testing datasets. The data is divided into 60:40 ratios, which means that 60% is utilised for model training and 40% is used for model validation.

4.3 Proposed deep learning model and experimental setup

Multi-Layer Perceptron (MLP), which serves as the foundation for this deep learning approach, is a neural network with multiple hidden layers. It is best suited for regression or classification problems in which inputs are allocated to a class. The neurons (or nodes) are arranged in different layers, as illustrated in Figure 3, and are connected to every neuron in the next layer, so the output of one neuron becomes the input of the next. Each connection between neurons has a weight, which is one of the variables that change throughout training. The weight of the link influences how much information is sent between neurons. Once a neuron gets inputs from all the other neurons linked to it, the output (y) is determined using the formula provided in Equation (1).

$$y = \sum_{i=1}^{N} (x_i * w_i) + b\,, \tag{1}$$

where x_i is an input of the neuron, w_i is the associated weight, and b is the bias. The output value (y) is then given to the activation function $g(y)$, which introduces nonlinearity into the neuron's output. Finally, the model employs the backpropagation algorithm to update the weights of the input layer based on the error at the output layer.

The proposed MLP-based deep learning model consists of an input layer, an output layer, and two dense hidden layers. The model receives input that is extracted from the data packet transmitted over the internal communication channel of the vehicle. Due to 153 features being extracted from the in-vehicle network traffic, the same number of neurons is inserted in the first layer. It is followed by the two dense hidden layers of two and eight neurons, respectively. Since the CAN network traffic is to be classified into six classes (TARGET LABEL in Table 4), the output layer is made up of completely linked six neurons. The model has a total of 386 trainable parameters. Figure 4 depicts the layer relationships, while Table 5 provides the model's summary.

The activation functions in MLP are critical for generating complex decisions and predictions. This article uses the ReLU activation function in the intermediate layers, which operates by performing a basic mathematical operation on the input value. If the input value is higher than or equal to zero, the output is the same as the input. If the input value is negative, the

Table 3 *Number of samples collected for each class*

S. No.	Class	# of Samples
1	BENIGN	80000
2	DoS	74660
3	SPOOFING_GAS	9991
4	SPOOFING_RPM	54899
5	SPOOFING_SPEED	24950
6	SPOOFING_STEERING_WHEEL	19976
	TOTAL	264476

Table 4 *Features extracted from the dataset*

S. No.	Features	Description
1	ID	Arbitration ID
2 to 9	"DATA_0" to "DATA_7"	1st to 8th byte of data transmitted through CAN data frame
10	LABEL	Type of traffic (Benign/Malicious)
11	TARGET LABEL	Six Specific Class of the traffic ("Benign", "DoS", "Spoofing_GAS", "Spoofing_RPM", "Spoofing_SPEED", and "Spoofing_STEERING_WHEEL")

Table 5 *Proposed MLP Model Summary*

Layer	Shape of the Output	Number of Parameters	Activation function
dense_136 (Dense)	(None, 2)	308	Rectified Linear Units (ReLU)
dense_137 (Dense)	(None, 8)	24	Rectified Linear Units (ReLU)
dense_138 (Dense)	(None, 6)	54	Softmax
Total parameters: 386 (1.51 KB) Trainable parameters: 386 (1.51 KB) Non-trainable parameters: 0 (0.00 Byte) Optimizer: "Adam", Loss function: "categorical_crossentropy", Performance Metrics: "Accuracy"			

result is zero. The mathematical representation of the ReLU function is as follows:

$$f(x) = \max(0,x). \tag{2}$$

The output layer employs the softmax activation function, which transforms the raw output scores of the model into probabilities, facilitating the distribution of these probabilities across various classes. This transformation is mathematically represented by:

$$Soft\max(Z_i) = \frac{e^{Z_i}}{\sum_{j=1}^{K} e^{Z_j}}. \tag{3}$$

Here, Z_i represents the input value for the Softmax function and is the output value of the node for i-th class at the output layer. K is the total number of nodes at the output layer.

Cross entropy measures the difference between the predicted probability and the true probability. Multiclass Cross-Entropy Loss, also known as categorical cross-entropy, is used as a loss function in the proposed deep-learning model. The loss function is mathematically represented by:

$$L = -\frac{1}{N}\sum_{i=1}^{N}\sum_{j=1}^{K}(y_{i,j}\log(p_{i,j})). \tag{4}$$

Here, N is the number of instances in the dataset, K is the number of classes, $y_{i,j}$ is the true output for the i-th sample and j-th class, and $p_{i,j}$ is the predicted probability for i-th sample and j-th class. The Adam optimizer, which stands for "Adaptive Moment Estimation", is employed to iteratively minimize the loss function during training.

5 Results and comparative analysis

In the domain of deep learning, a perfect fit model is desired since it assures strong generalization and consistent performance on new data. Overfitting and underfitting, on the other hand, provide unreliable results and poor generalization. A well-performing deep learning model should have training and validation loss curves that converge to a comparable, low data point.

Table 6 *Training and Validation efficiency of the proposed model*

Epoch	Tr_loss	Tr_accuracy	Val_loss	Val_accuracy
	1.4293	0.4142	1.1413	0.4878
	1.0016	0.4883	0.8921	0.4884
	0.8277	0.4973	0.7646	0.5072
	0.6848	0.6311	0.5988	0.7578
	0.5273	0.7775	0.4573	0.8402
	0.3966	0.8415	0.3480	0.8423
	0.3133	0.8789	0.2821	0.9425
	0.2539	0.9430	0.2272	0.9428
	0.2022	0.9431	0.1805	0.9428
	0.1628	0.9594	0.1486	0.9805
	0.1366	0.9809	0.1274	0.9805
	0.1187	0.9809	0.1123	0.9805
	0.1056	0.9809	0.1010	0.9805
	0.0956	0.9809	0.0922	0.9805
	0.0877	0.9809	0.0850	0.9805
	0.0811	0.9809	0.0790	0.9805
	0.0757	0.9809	0.0739	0.9805
	0.0710	0.9809	0.0696	0.9805
	0.0670	0.9809	0.0658	0.9806
	0.0635	0.9809	0.0625	0.9806
	0.0604	0.9809	0.0595	0.9806
	0.0577	0.9809	0.0570	0.9806
	0.0553	0.9809	0.0547	0.9806
	0.0532	0.9809	0.0527	0.9806
	0.0514	0.9811	0.0509	0.9808
	0.0497	0.9811	0.0494	0.9809
	0.0483	0.9811	0.0480	0.9809
	0.0470	0.9811	0.0468	0.9809
	0.0459	0.9811	0.0457	0.9809
	0.0449	0.9812	0.0447	0.9809
	0.0439	0.9812	0.0435	0.9809
	0.0423	0.9812	0.0415	0.9809
	0.0399	0.9812	0.0387	0.9809
	0.0367	0.9812	0.0353	0.9809
	0.0333	0.9973	0.0318	0.9999
	0.0298	0.9999	0.0283	0.9999
	0.0265	0.9999	0.0251	0.9999
	0.0234	0.9999	0.0222	0.9999
	0.0207	0.9999	0.0196	0.9999
	0.0184	0.9999	0.0174	0.9999

Tr_loss: Training Loss; Tr_accuracy: Training Accuracy; Val_loss: Validation Loss; Val_accuracy: Validation Accuracy

This shows that the model is generalizing properly and not overfitting or underfitting. Analysing the behaviour of these curves during the training gives vital insights into the model's learning process and aids in making the required changes to increase performance. Table 6 shows the training and validation losses reported for each epoch throughout the simulation, which are also represented in Figure 5. The convergence of the training and validation loss curves demonstrates that the suggested model is learning the core trends in the data and generalizing successfully to the validation set. It indicates that the model is neither overfitting nor underfitting, as well.

Evaluating the performance of a deep learning model incorporates a series of procedures and metrics that offer a full picture of how well the model is doing.

Figure 6 depicts the confusion matrix obtained as a consequence of the simulation and used to calculate accuracy, precision, recall, and F1-score. Precision and recall are measures used to assess the effectiveness of a classification model, particularly in the cases with unbalanced classes or where different types of classification errors have varying costs.

The performance evaluation metrics, shown in Table 7, can be produced using Equations (5) to (8), where α, β, γ, and μ denote True Positive, True Negative, False Positive, and False Negative, respectively.

Precision and recall should both be high, however, they should be used in conjunction with other assessment measures like accuracy and F1-score to have a thorough view of a classifier's performance. The F1-score, which is the harmonic mean of the Precision and Recall values, provides a more balanced assessment of the model's performance.

$$Accuracy = \frac{\alpha + \beta}{\alpha + \beta + \gamma + \mu}, \tag{5}$$

$$Precision\,(P) = \frac{\alpha}{\alpha + \gamma}, \tag{6}$$

$$Recall\,(R) = \frac{\alpha}{\alpha + \mu}, \tag{7}$$

$$F1_{score}(F1) = 2 * \frac{Precesion * Recall}{Precesion + Recall}. \tag{8}$$

The results from the Confusion matrix (Figure 6) and Tables 7, 8, and 9 show that the proposed deep learning model can detect and classify an attack on an autonomous vehicle's CAN network with an average Recall of 0.999927477, Precision of 0.999930671, and F1-Score of 0.999929069. The model performed better than the benchmark research [31] in terms of accuracy, recall, precision, and F1-Score. It also outperformed previous studies [24] with the highest accuracy of 99.99%. Achieving an average accuracy of 99.99% is an impressive feat, but it is important to provide transparency regarding the factors that contributed to this result and to discuss any potential limitations or biases. To clarify achieved results some succeeded points can be addressed such as: dataset quality and size, model architecture, training process, evaluation metrics.

On the other hand, there are some potential limitations and biases that can be summarized due to: dataset bias concerning both causes (class imbalance or synthetic data), overfitting risk, limited attack types, real-world conditions, model complexity and deployment feasibility.

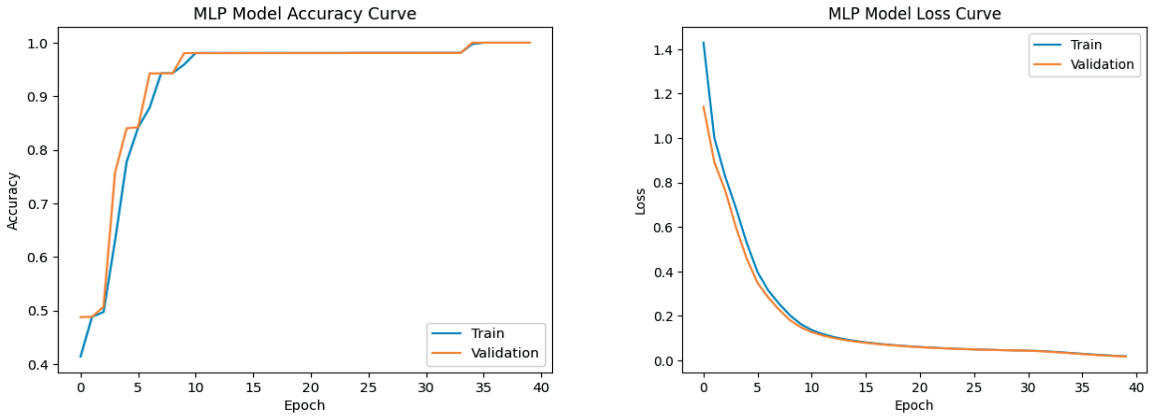

Figure 5 *(a) Accuracy curve, (b) Loss curve*

Actual	BENIGIN	31997	1	0	2	0	0
	DOS	0	29865	0	0	0	0
	SPOOFING_GAS	0	0	3996	0	0	0
	SPOOFING_RPM	0	0	0	21958	2	0
	SPOOFING_SPEED	0	0	0	0	9980	0
	SPOOFING_STEERING_WHEEL	0	0	0	2	0	7988
		BENIGIN	DOS	SPOOFING_GAS	SPOOFING_RPM	SPOOFING_SPEED	SPOOFING_STEERING_WHEEL
		Predicted					

Figure 6 *Confusion Matrix*

Table 7 *Recall, Precision, and F1-Score values for the proposed model*

Class	Recall	Precision	F1-Score
BENIGN	0.99990625	1	0.999953123
DoS	1	0.999966517	0.999983258
SPOOFING_GAS	1	1	1
SPOOFING_RPM	0.999908925	0.999817867	0.999863394
SPOOFING_SPEED	1	0.999799639	0.99989981
SPOOFING_STEERING_WHEEL	0.999749687	1	0.999874828
Macro Average	0.999927477	0.999930671	0.999929069

Table 8 *Proposed solution vs. the benchmark study*

Ref.	Accuracy	Recall	Precision	F1-Score
Neto et al. [31]	95%	0.68	0.74	0.63
Proposed Model	99.99%	0.999927477	0.999930671	0.999929069

Table 9 *Proposed solution vs. related work*

Ref.	Solution Type	Attack type	(Avg. Accuracy)
Sudhakar et al. [38]	Deep learning (CNN)	Malware	98.63%
Ahmed et al. [24]	Deep learning (CNN)	DoS, Fuzzy	96%
Neto et al. [31]	Deep learning (MLP)	DoS, Spoofing	95%
Proposed Model	Deep learning (MLP)	DoS, Spoofing	99.99%

6 Conclusion and scope for future work

The CAN protocol is a key component of the internal communication network of autonomous. However, the protocol's inherent lack of security makes it susceptible to a wide range of cyber threats, posing significant risks to both the safety and privacy of the driver, passenger or the vehicle itself.

This paper has explored the effectiveness of the DL-based approach to enhance the security of internal communication networks of autonomous vehicles in the IoV framework. A novel deep-learning based defence mechanism is proposed that provides the real-time threat detection. The findings highlight the potential of deep learning to significantly enhance the security of CAN networks in IoV, contributing to safer and more reliable vehicular communication systems.

The simulation results indicate that the proposed DL-based model is capable of successfully detecting and classifying attacks (DoS and spoofing) on the CAN network of an autonomous vehicle, with an average Recall of 0.999927477, Precision of 0.999930671, and F1-Score of 0.999929069. The proposed model outperformed benchmark studies and other related work in terms of accuracy, recall, precision, and F1-Score, achieving the highest accuracy of 99.99%. Future work should focus on improving the scalability of the proposed system and integrating it with broader IoV security frameworks to provide a holistic defence strategy.

Acknowledgment

The authors received no financial support for the research, authorship and/or publication of this article.

Conflicts of interest

The authors declare that they have no known competing financial interests or personal relationships that could have appeared to influence the work reported in this paper.

References

[1] ISLAM, R., REFAT, R. U. D. Improving CAN bus security by assigning dynamic arbitration IDs. *Journal of Transportation Security* [online]. 2020, **13**(1-2), p. 19-31. ISSN 1938-7741, eISSN 1938-775X. Available from: https://doi.org/10.1007/s12198-020-00208-0

[2] O.-R. A. D. (ORAD) Committee. Taxonomy and definitions for terms related to driving automation systems for on-road motor vehicles. SAE International, 2021.

[3] GERSHON, P., SEAMAN, S., MEHLER, B. REIMER, B., COUGHLIN, J. Driver behavior and the use of automation in real-world driving. *Accident Analysis and Prevention* [online]. 2021, **158**, 106217. ISSN 0001-4575, eISSN 1879-2057. Available from: https://doi.org/10.1016/j.aap.2021.106217

[4] SHARMA, N. CHAUHAN, N., CHAND, N. Security challenges in Internet of Vehicles (IoV) environment. In: 2018 First International Conference on Secure Cyber Computing and Communication ICSCCC: proceedings [online]. IEEE. 2018. eISBN 978-1-5386-6373-8, p. 203-207. Available from: https://doi.org/10.1109/ICSCCC.2018.8703272

[5] ASWAL, K., DOBHAL, D. C., PATHAK, H. Comparative analysis of machine learning algorithms for identification of BOT attack on the Internet of Vehicles (IoV). In: 2020 International Conference on Inventive Computation Technologies ICICT: proceedings [online]. IEEE. 2020. eISBN 978-1-7281-4685-0, p. 312-317. Available from: https://doi.org/10.1109/ICICT48043.2020.9112422

[6] ZHAO, Q., CHEN, M., GU, Z., LUAN, S., CAN bus intrusion detection based on auxiliary classifier GAN and out-of-distribution detection. *ACM Transactions on Embedded Computing Systems* [online]. 2022, **21**(4), p. 1-30. ISSN 1539-9087, eISSN 1558-3465. Available from: https://doi.org/10.1145/3540198

[7] SUN, H., HUANG, W., WENG, J., LIU, Z., TAN, W., HE, Z., CHEN, M., WU, B., LI, L., PENG, X. CCID-CAN: cross-chain intrusion detection on CAN bus for autonomous vehicles. *IEEE Internet of Things Journal* [online]. 2024, p. 26146 - 26159. eISSN 2327-4662. Available from: https://doi.org/10.1109/JIOT.2024.3393122

[8] ALIWA, E., RANA, O., PERERA, C., Cyberattacks and countermeasures for in-vehicle networks. *ACM Computing Surveys* [online]. 2022, **5**(1), p. 1-37. ISSN 0360-0300, eISSN 1557-7341. Available from: https://doi.org/10.1145/3431233

[9] ZHANG, T., ANTUNES, H., AGGARWAL, S. Defending connected vehicles against malware: challenges and a solution framework. *IEEE Internet of Things Journal* [online]. 2014, **1**(1), p. 10-21. eISSN 2327-4662. Available from: https://doi.org/10.1109/JIOT.2014.2302386

[10] CHEN, S.-H., LIN, C.-H. R. Evaluation of DoS attacks on vehicle CAN bus system. In: *Recent advances in intelligent information hiding and multimedia signal processing. Vol. 110* [online]. PAN, J.-S., ITO, A., TSAI, P.-W., JAIN, L. C. (Eds.). Cham: Springer International Publishing, 2019. ISBN 978-3-030-03747-5, eISBN 978-3-030-03748-2, p. 308-314. Available from: https://doi.org/10.1007/978-3-030-03748-2_38

[11] JO, H. J., CHOI, W. A Survey of attacks on controller area networks and corresponding countermeasures. *IEEE Transactions on Intelligent Transportation Systems* [online]. 2022, **23**(7), p. 6123-6141. ISSN 1524-9050, eISSN 1558-0016. Available from: https://doi.org/10.1109/TITS.2021.3078740

[12] HANSELMANN, M., STRAUSS, T., DORMANN, K., ULMER, H. CANet: An unsupervised intrusion detection system for high dimensional CAN bus data. *IEEE Access* [online]. 2020, **8**, p. 58194-58205. eISSN 2169-3536. Available from: https://doi.org/10.1109/ACCESS.2020.2982544

[13] LIU, J., ZHANG, S., In-vehicle network attacks and countermeasures: challenges and future directions. *IEEE Network* [online]. 2017, **31**(5), p. 50-58. ISSN 0890-8044, eISSN 1558-156X. Available from: https://doi.org/10.1109/MNET.2017.1600257

[14] BOZDAL, M. SAMIE, M., ASLAM, S., JENNIONS, I. Evaluation of CAN bus security challenges. *Sensors* [online]. 2020, **20**(8), 2364. eISSN 1424-8220. Available from: https://doi.org/10.3390/s20082364

[15] EISENBARTH, T. KASPER, T., MORADI, A., PAAR, C., SALMASIZADEH, M., SHALMANI, M. T. M. On the power of power analysis in the real world: a complete break of the KeeLoq code hopping scheme. In: 28th Annual International Cryptology Conference Advances in Cryptology-CRYPTO 2008: proceedings [online]. Springer. 2008. ISBN 978-3-540-85173-8, eISBN 978-3-540-85174-5, p. 203-220. Available from: https://doi.org/10.1007/978-3-540-85174-5_12

[16] KOSCHER, K., CZESKIS, A., ROESNER, F., PATEL, S., KOHNO, T., CHECKOWAY, S., MCCOY, D., KANTOR, B., ANDERSON, D., SHACHAM, H., SAVAGE, S. Experimental security analysis of a modern automobile. In: 2010 IEEE Symposium on Security and Privacy: proceedings [online]. IEEE. 2010. ISSN 1081-6011, eISSN 2375-1207, ISBN 978-1-4244-6894-2, eISBN 978-1-4244-6895-9, p. 447-462. Available from: https://doi.org/10.1109/SP.2010.34

[17] VALASEK, C., MILLER, C. Remote exploitation of an unaltered passenger vehicle. *Black Hat USA*. 2015, **2015**(S91), p. 1-91.

[18] PETIT, J., STOTTELAAR, B., FEIRI, M., KARGL, F. Remote attacks on automated vehicles sensors: experiments on camera and lidar. *Black Hat Eur*. 2015, **11**(2015), 995.

[19] ZORZ, Z. Backdooring connected cars for covert remote control - help net security. 2018. Retrieved August, 2020.

[20] PALANCA, A., EVENCHICK, E., MAGGI, F., ZANERO, S. A stealth, selective, link-layer denial-of-service attack against automotive networks. In: 14th International Conference, Detection of Intrusions and Malware, and Vulnerability Assessment DIMVA 2017: proceedings [online]. 2017. Springer. 2017. ISBN 978-3-319-60875-4, eISBN 978-3-319-60876-1, p. 185-206. Available from: https://doi.org/10.1007/978-3-319-60876-1_9

[21] WOO, S., JO, H. J., LEE, D. H. A practical wireless attack on the connected car and security protocol for in-vehicle CAN. *IEEE Transactions on Intelligent Transportation Systems* [online]. 2014, **16**(2), p. 993-1006. ISSN 1524-9050, eISSN 1558-0016. Available from: https://doi.org/10.1109/TITS.2014.2351612

[22] NIE, S., LIU, L., DU, Y. Free-fall: hacking tesla from wireless to can bus. *Defcon*. 2017, p. 1-16.

[23] MUKHERJEE, S., SHIRAZI, H., RAY, I., DAILY, J., GAMBLE, R. Practical DoS attacks on embedded networks in commercial vehicles. In: 12th International Conference Information Systems Security ICISS 2016: proceedings [online]. 2016. Springer. 2016. ISBN 978-3-319-49805-8, eISBN 978-3-319-49806-5, p. 23-42. Available from: https://doi.org/10.1007/978-3-319-49806-5_2

[24] AHMED, I., JEON, G., AHMAD, A. Deep learning-based intrusion detection system for internet of vehicles. *IEEE Consumer Electronics Magazine* [online]. 2023, **12**(1), p. 117-123. ISSN 2162-2248, eISSN 2162-2256. Available from: https://doi.org/10.1109/MCE.2021.3139170

[25] ALLADI, T., KOHLI, V. CHAMOLA, V., YU, F. R. A deep learning based misbehavior classification scheme for intrusion detection in cooperative intelligent transportation systems. *Digital Communications and Networks* [online]. 2023, **9**(5), p. 1113-1122. ISSN 2468-5925, eISSN 2352-8648. Available from: https://doi.org/10.1016/j.dcan.2022.06.018

[26] HOSSAIN, M. D., INOUE, H. OCHIAI, H., FALL, D., KADOBAYASHI, Y. LSTM-Based intrusion detection system for in-vehicle Can bus communications. *IEEE Access* [online]. 2020, **8**, p. 185489-185502. eISSN 2169-3536. Available from: https://doi.org/10.1109/ACCESS.2020.3029307

[27] SONG, H. M., WOO, J., KIM, H. K. In-vehicle network intrusion detection using deep convolutional neural network. *Vehicular Communications* [online]. 2020, **21**, 100198. eISSN 2214-210X. Available from: https://doi.org/10.1016/j.vehcom.2019.100198

[28] ZHANG, J., LI, F., ZHANG, H., LI, R., LI, Y. Intrusion detection system using deep learning for in-vehicle security. *Ad Hoc Networks* [online]. 2019, **95**, 101974. ISSN 1570-8705, eISSN 1570-8713. Available from: https://doi.org/10.1016/j.adhoc.2019.101974

[29] ZHOU, A., LI, Z., SHEN, Y. Anomaly detection of CAN bus messages using a deep neural network for autonomous vehicles. *Applied Sciences* [online]. 2019, **9**(15), 3174. eISSN 2076-3417. Available from: https://doi.org/10.3390/app9153174

[30] MANSOURIAN, P., ZHANG, N., JAEKEL, A., KNEPPERS, M. Deep learning-based anomaly detection for connected autonomous vehicles using spatiotemporal information. *IEEE Transactions on Intelligent Transportation Systems* [online]. 2023, **24**(12), p. 16006-16017. ISSN 1524-9050, eISSN 1558-0016. Available from: https://doi.org/10.1109/TITS.2023.3286611

[31] NETO, E. C. P., TASLIMASA, H., DADKHAH, S., IQBAL, S., XIONG, P., RAHMAN, T., GHORBANI, A. A. CICIoV2024: advancing realistic IDS approaches against DoS and spoofing attack in IoV CAN bus. *Internet of Things* [online]. 2024, **26**, 101209. ISSN 2543-1536, eISSN 2542-6605. Available from: https://doi.org/10.1016/j.iot.2024.101209

[32] NETO, E. C. P., TASLIMASA, H., DADKHAH, S. IQBAL, S., XIONG, P., RAHMANB, T., GHORBANI, A. A. CIC IoV dataset 2024 [online]. Canadian Institute for Cybersecurity, 2024. Available from: https://www.unb.ca/cic/datasets/iov-dataset-2024.html

[33] SPITALOVA, Z. Vehicle-to-everything communication. *Communications - Scientific Letters of the University of Zilina* [online]. 2023, **25**(1), p. 24-35. ISSN 1335-4205, eISSN 2585-7878. Available from: https://doi.org/10.26552/com.C.2023.017

[34] SABIHA, A. D., KAMEL, M. A., SAID, E., HUSSEIN, W. M. Path planning algorithm based on teaching-learning-based-optimization for an autonomous vehicle. *Communications - Scientific Letters of the University of Zilina* [online]. 2022, **24**(2), p. C33-C42. ISSN 1335-4205, eISSN 2585-7878. Available from: https://doi.org/10.26552/com.C.2022.2.C33-C42

[35] MORGOS, J., KLCO, P., HRUDKAY, K. Artificial neural network based MPPT algorithm for modern household with electric vehicle. *Communications - Scientific Letters of the University of Zilina* [online]. 2022, **24**(1), p. C18-C26. ISSN 1335-4205, eISSN 2585-7878. Available from: https://doi.org/10.26552/com.C.2022.1.C18-C26

[36] DANKO, M., HANKO, B., DRGONA, P. Optimized control of energy flow in an electric vehicle based on GPS. *Communications - Scientific Letters of the University of Zilina* [online]. 2021, **23**(1), p. C7-C14. ISSN 1335-4205, eISSN 2585-7878. Available from: https://doi.org/10.26552/com.C.2021.1.C7-C14

[37] KAPOOR, J., PATHAK, A., RAI, M., MISHRA G. R. Vehicle cabin noise cancellation model using pre-filter for improved convergence rate and better stability. *Communications - Scientific Letters of the University of Zilina* [online]. 2023, **25**(1), p. C1-C12. ISSN 1335-4205, eISSN 2585-7878. Available from: https://doi.org/10.26552/com.C.2023.003

[38] SUDHAKAR, KUMAR, S. An emerging threat fileless malware: a survey and research challenges. *Cybersecurity* [online]. 2020, **3**(1), 1. eISSN 2523-3246. Available from: https://doi.org/10.1186/s42400-019-0043-x

ENHANCED BUCK CONVERTER WITH UNIVERSAL MODEL FOR THE SWITCHED VOLTAGE REGULATORS

Dobroslav Kováč*, Irena Kováčová

Department of Theoretical and Industrial Electrical Engineering, Faculty of Electrical Engineering and Informatics, Technical University of Kosice, Kosice, Slovak Republic

*E-mail of corresponding author: dobroslav.kovac@tuke.sk

Dobroslav Kováč 0000-0002-9930-9272, Irena Kováčová 0000-0003-0482-6646

Resume

This article presents the enhancement and refinement of a simulation model for an integrated universal switched voltage regulator compatible with PSPICE software. The model enables users to create representations of any specific type of switched voltage regulator currently available on the market. The described regulator model is practically applied in widely used configurations of buck converters, including applications in transportation. The accuracy of the regulator model is verified by comparing the simulated waveforms of the converter to those provided in its datasheet. Additionally, the model is employed for the design and simulation analysis of buck converter circuits, with extended current and voltage ranges for their output parameters. In the context of improving the performance of such converters, particular attention is given to enhancing their electromagnetic compatibility.

Article info

Received 29 January 2025
Accepted 25 February 2025
Online 12 March 2025

Keywords:

buck converter
simulation model
extended parameters

Available online: https://doi.org/10.26552/com.C.2025.026

ISSN 1335-4205 (print version)
ISSN 2585-7878 (online version)

1 Introduction

The efficient utilization of alternative energy sources is highly relevant in today's energy-intensive era, which has resulted in significant attention being directed toward the field of direct current (DC) power conversion. For this purpose, power semiconductor converters are primarily used, with simulation software considered as one of the most effective development tools in their design [1-6]. The use of integrated switched voltage regulators has greatly simplified the design and construction of the DC power supplies, which are widely utilized, including in transportation. However, a broader range of simulation models for these components is unfortunately lacking. Based on the configuration of such converters, these integrated regulators can be categorized into several groups. The largest group consists of switched regulators designed for step-down (buck) converters, with a manufacturer-recommended connection presented in Figure 1 [7-10].

This configuration includes not only the integrated switched regulator circuit but the additional external components essential for its operation, as well.

2 Regulator model

Based on the key catalog parameters of existing switched voltage regulators, designed for the buck DC-DC converters, a conceptual and universal block diagram can be developed. This diagram is presented in Figure 2.

A universal simulation model of the regulator [11] was developed based on this diagram. This model can be simplified as follows, resulting in a more streamlined, accurate, and efficient design, which subsequently reduces simulation time.

.SUBCKT 2576M Vin On_Off GND FB Vout; Name of subcircuit and parameters
+ PARAMS: Vref=1.23 Imax=3.7 f=52000; Default setting: Vref, Imax, f, Rsw
+ Rsw=0.019 Dmax=0.9 Umax=40 Delay=0u; Dmax, Umax, Delay
VA1 12 60; Ammeter A
V+5 9 GND 5; Power supply + 5V for logical circuits
VG 19 GND DC 0 AC 1 0; Frequency generator with parameters:

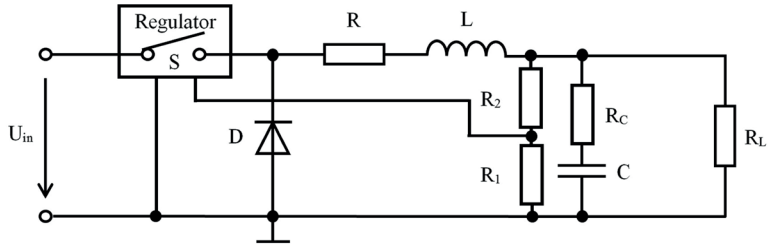

Figure 1 *Configuration of a buck converter with an integrated switched voltage regulator*

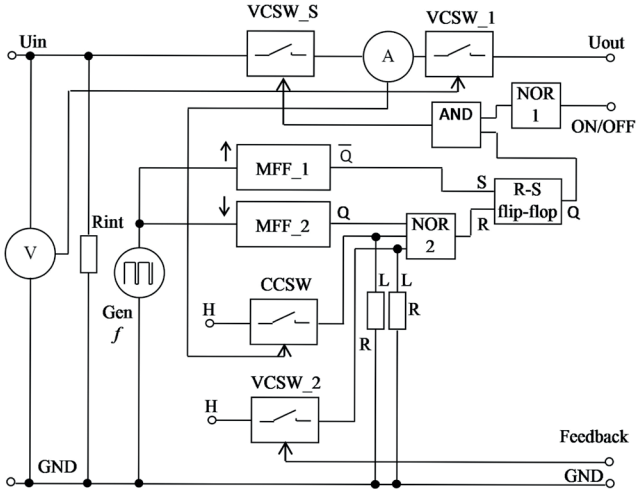

Figure 2 *Block diagram of the proposed universal switched voltage regulator*

+ PWL (0,0) ({Delay} 0); Delay, Dmax, f
+ REPEAT FOREVER (0,0) (10N 5)
+ (+{Dmax/f} 5)(+10N 0)(+10N 0)
+ (+{1/f-Dmax/f} 0) (+10N 0)
+ ENDREPEAT
U7 INV 9 GND On_Off 6 7404 IO_STD; Inverter (INV) (NOR 1)
U5 AND(2) 9 GND 7 6 8 7408 IO_STD; (AND)
SW3 9 10 FB GND SW1; Voltage controlled switch 2 (VCSW_2)
R2 GND 10 390; Resistor R
HCCV+5 11 GND VA1 10; Conversion: switch S current to voltage
SW2 9 13 11 GND SW2; Switch controlled by S current (CCSW)
R1 13 GND 390; Resistor R
SW0 60 Vout Vin GND SW4; Voltage controlled switch 1 (VCSW_1)
SW1 Vin 12 8 GND SW3; Voltage controlled switch S (VCSW_S)
U6 NOR(3) 9 GND 15 13 10 16 7427 IO_STD; (NOR 2)
U4 NAND(2) 9 GND 7 16 17 7400 IO_STD; NAND - part of (R-S flip-flop)
U3 NAND(2) 9 GND 18 17 7 7400 IO_STD; NAND - part of (R-S flip-flop)
XU2 19 19 9 15 20 GND 9 74121; Monostable flip-flop 2 (MFF_2)
XU1 GND GND 19 21 18 GND 9 74121; Monostable flip-flop 1 (MFF_1)

.MODEL SW1 VSWITCH (Ron=0 Roff=1G Von={Vref} Voff={Vref-0.0000001})
.MODEL SW2 VSWITCH (Ron=0 Roff=1G Von={10*Imax} Voff={10*Imax-0.01})
.MODEL SW3 VSWITCH (Ron={Rsw} Roff=1G Von=1.8 Voff=1.79)
.MODEL SW4 VSWITCH (Ron=0 Roff=1000G Von={Umax} Voff={Umax+0.1})
.MODEL 7404 UGATE
.MODEL 7408 UGATE
.MODEL 7427 UGATE
.MODEL 7400 UGATE
.ENDS

.SUBCKT 74121 A1 A2 B Q Q_Neg GND VCC; Subcircuit of monostable flip-flop 74121
U2 INV VCC GND A1 30 7404 IO_STD; Inverter
U3 NAND(2) VCC GND 30 B 29 7400 IO_STD; NAND
U4 JKFF(1) VCC GND; JK flip-flop
+ VCC 27 29 VCC GND 23 24 7476 IO_STD
U5 INV VCC GND 29 28 7404 IO_STD; Inverter
U6 NAND(2) VCC GND 28 23 25 7400 IO_STD; NAND
U7 JKFF(1) VCC GND; JK flip-flop
+ 23 31 25 GND VCC 27 26 7476 IO_STD
U8 INV VCC GND 24 Q 7404 IO_STD; Inverter
U9 INV VCC GND 23 Q_Neg 7404 IO_STD; Inverter
.MODEL 7476 UEFF
.ENDS

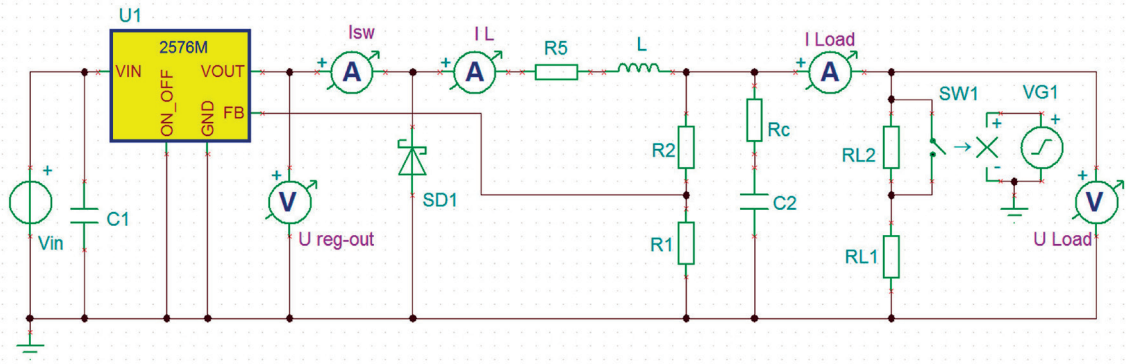

Figure 3 *Circuit diagram of the configuration under investigation in the TINA program*

The accuracy and functionality of the LM2576-ADJ regulator model can be validated by incorporating it into a buck converter circuit with a dynamically variable resistive load, configured with the following parameters: L = 100 µH, R5 = 200 mΩ, Vin = 40 V, R1 = 2 kΩ, R2 = 22.39 kΩ, C1 = 100 µF, C2 = 1 mF, Rc = 40 mΩ, RL1 = 5 Ω, RL2 = 32.5 Ω, as shown in Figure 3. The diode SD1 was selected as the MBR360.

For the simulation, the TINA software (Toolkit for Interactive Network Analysis) [12] was employed. This program is fully compatible with the globally recognized PSPICE software, including its libraries and operational rules [13].

A comparison of the results obtained through simulation to those reported in the datasheets, both under constant load and with a step change in load, is presented in Figure 4.

A correlation of the waveforms clearly demonstrates that the model accurately approximates the behavior of the real component in both static and dynamic operating modes.

The advantages of using the proposed simulation model for the switched voltage regulator can be illustrated through a comparison to existing models, although such models are relatively few in number. The most widely used model is the LM2576ADJ simulation model, available on the Texas Instruments website [14]. In terms of model simplicity, its description spans 125 lines, whereas the newly proposed model is described in only 38 lines. Regarding computation speed, this is, of course, dependent on the hardware of the computer used and the settings of the simulation software. Therefore, analyzing the absolute time savings is not meaningful. However, a relative analysis is possible. Specifically, a simulation analysis of the circuit shown in Figure 3 was performed on the same machine, using the same software, and under identical conditions. The comparison of computation times revealed that the use of the newly proposed model resulted in calculation times that were half of those of the analysis employing the LM2576ADJ model from the Texas Instruments website.

The limitations of the proposed simulation model lie in its inability to include the thermal conditions of the voltage regulator in the circuit analysis, as well as in the fact that the user is constrained by the properties of the individual simulation elements used in constructing the switched regulator model. These limitations, however, are general constraints inherent to the use of PSPICE simulation software, which restricts its application in any electrical circuit simulation. The same holds true for the impact of component parameter tolerances on the model's performance.

This validation of the model enables its application in designing circuits that extend the output parameters of a buck converter beyond its catalog specifications. Additionally, it leverages the significant advantages of the regulator in the form of an integrated circuit, including its relatively low cost, wide availability, and high level of integration, which incorporates control, regulation, and protection circuits for the converter.

3 Increase in the output current of a buck converter with a switched voltage regulator

The first option involves the parallel arrangement of separate converters with regulators. The current division between the regulators is inversely proportional to the ratio of their inductances, meaning that a higher inductance results in a lower current for the corresponding converter. When identical regulators are used in both converters connected in parallel, selecting the same inductance values is advantageous, as it ensures even current distribution. Additionally, it is beneficial to use a single common diode (SD1), two separate summing diodes (SD2 and SD3), and a shared feedback control (FB). To obtain simulation results, the LM2576 switched regulator model will be employed. Due to the limitations of the simulation (since the oscillators of the individual real controllers are not time-synchronized), the time course of controller U1 is shifted by 10 µs relative to controller U2. The wiring diagram of the simulated circuit is presented in Figure 5.

The circuit parameters are as follows: L1 = L2 = 100 µH, R3 = R5 = 460 mΩ, Vin = 40 V, R1 = 1 kΩ, R2 = 6.12 kΩ, C1 = 100 µF, C2 = 1 mF, Rc = 181 mΩ. Diodes SD1, SD2, and SD3 were selected as MBR360.

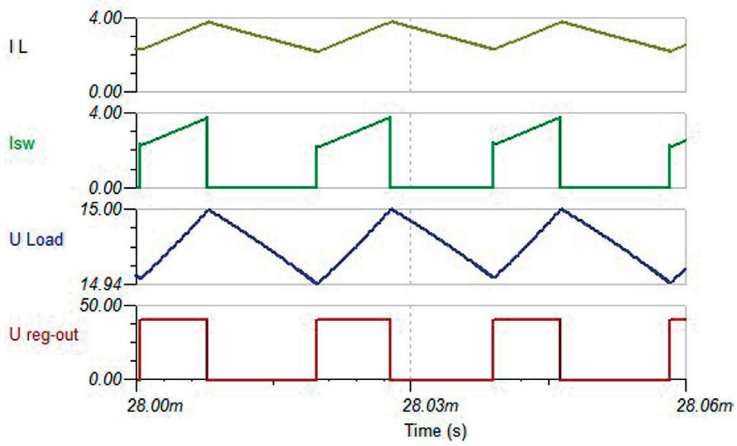

a)

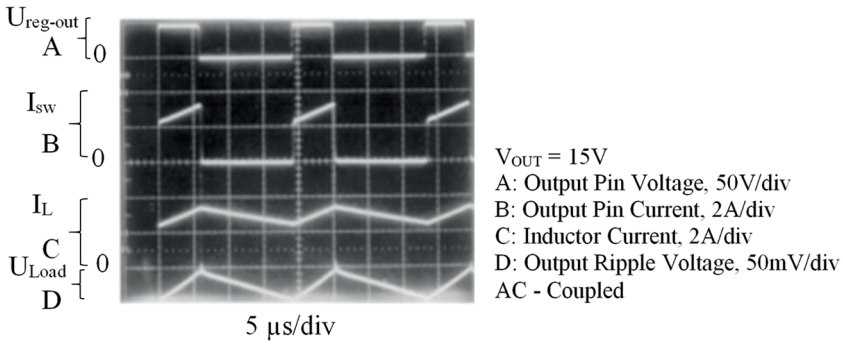

b)

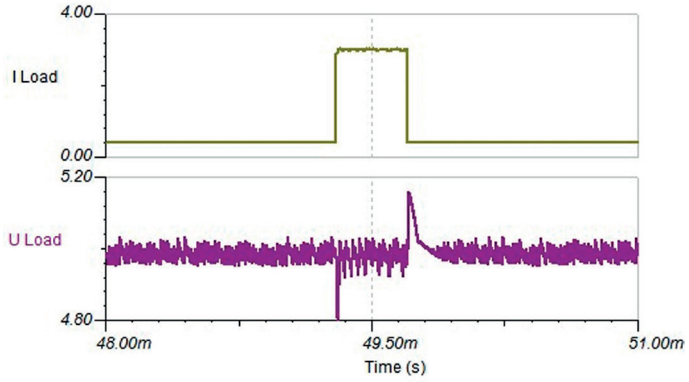

c)

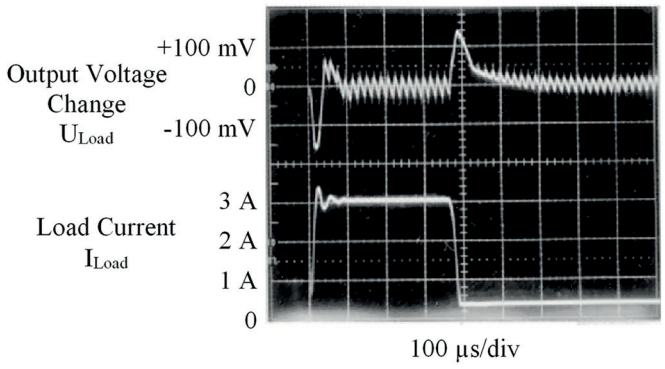

d)

Figure 4 *Key parameters of the converter: a) static results obtained through simulation at constant load; b) results from the manufacturer's datasheet for the LM2576-ADJ at constant load; c) results obtained through simulation during the step change in load; d) results from the manufacturer's datasheet for the LM2576-ADJ during the step change in load*

The load resistors have values of RL_1 = 1 Ω and RL_1 = 1.5 Ω. The main waveforms of the investigated circuit, obtained through simulation, are shown in Figure 6.

The results obtained from the measurements are presented in Figure 7.

The second method for increasing the output current of the buck converter is to incorporate a bipolar transistor (BT) into the circuit, as shown in Figure 8.

The total maximum allowable current of the converter is given by the following expression:

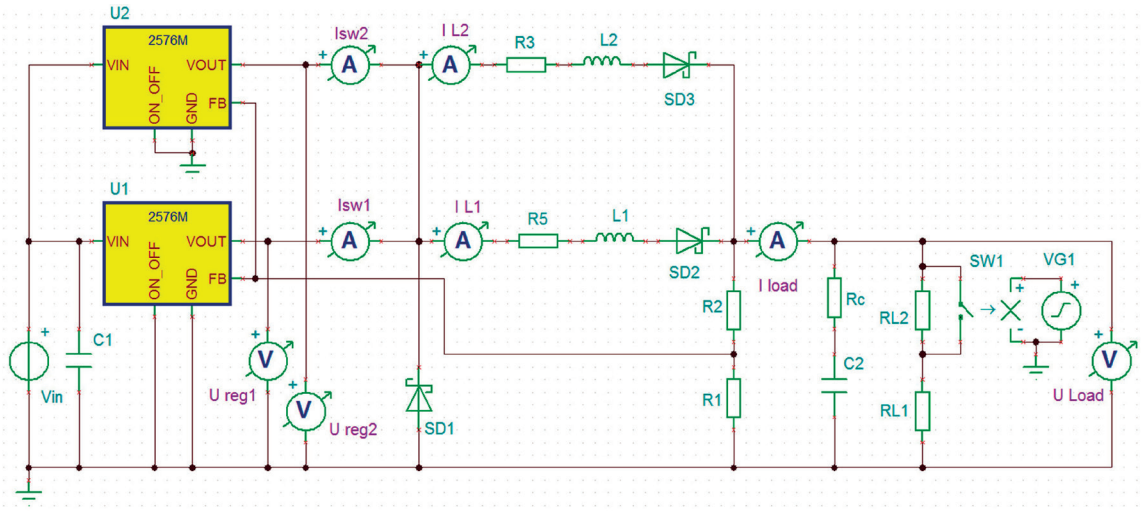

Figure 5 *Simulated parallel configuration of converters with separate regulators under a step change in load*

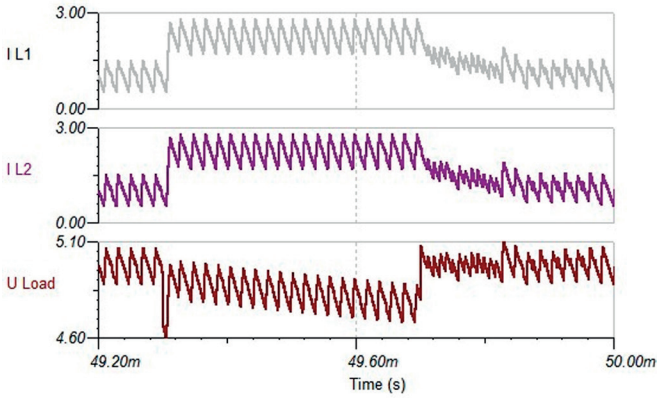

Figure 6 *Main waveforms of the parallel connection of converters with separate regulators under a step change in load, obtained through simulation in the TINA program*

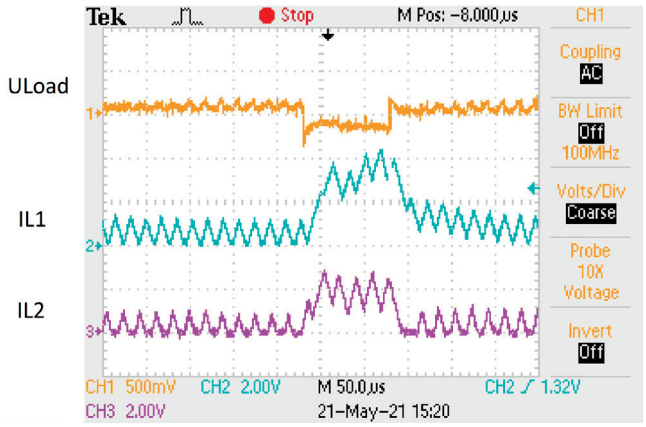

Figure 7 *Measured waveforms of the parallel-connected converters with separate regulators under a step change in load (current scale: 1 V = 1 A)*

$$I_{cmax} = (1 + h_{21E})I_{max}\,, \tag{1}$$

where:
I_{max} is the maximum allowable current of the regulator used,
h_{21E} is the current gain of the bipolar transistor.

The circuit parameters are as follows: L = 100 µH, R3 = 460 mΩ, Vin = 40 V, R1 = 1 kΩ, R2 = 6.12 kΩ, C1 = 100 µF, C2 = 1 mF, Rc = 181 mΩ. The SD1 diode used is of the MBR360 type. The load resistors have values of RL1 = 0.6 Ω and RL2 = 2 Ω. The results obtained from simulating the circuit are shown in Figure 9, while the

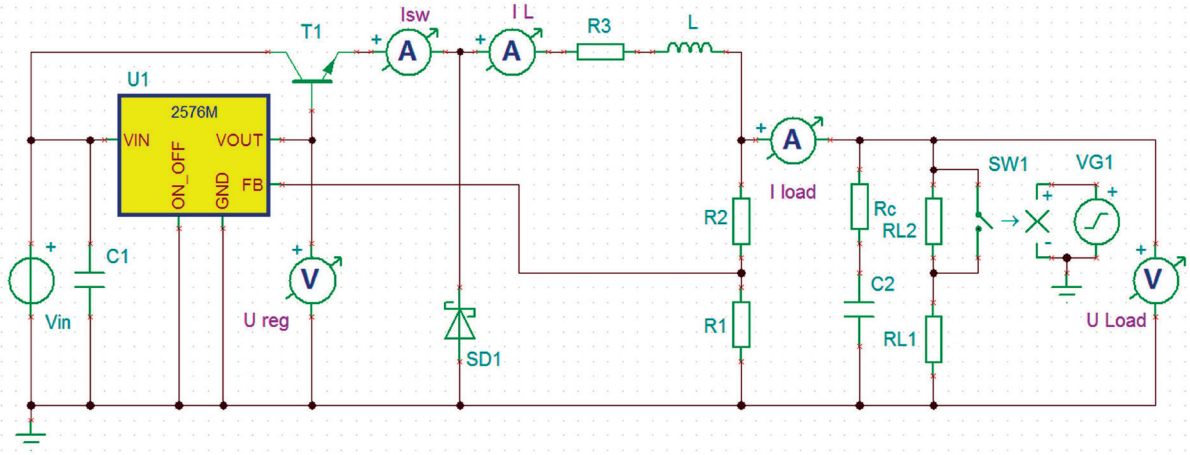

Figure 8 *Wiring diagram of the switching regulator with output current extension using a bipolar junction transistor*

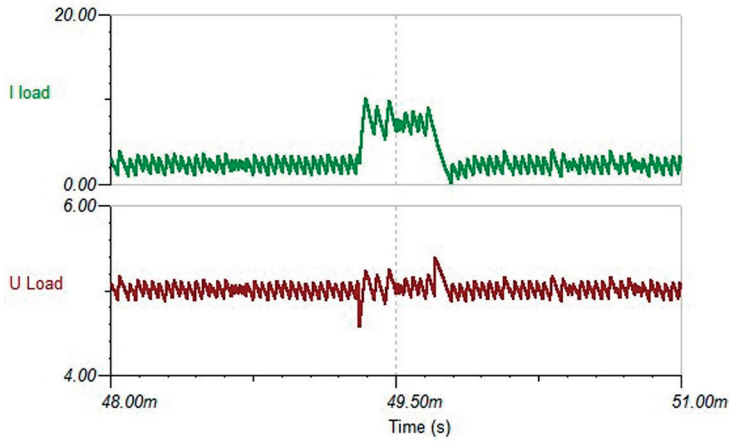

Figure 9 *Voltage and load current waveforms of the switched voltage regulator using a bipolar transistor during a step change in load, obtained through simulation in the TINA program*

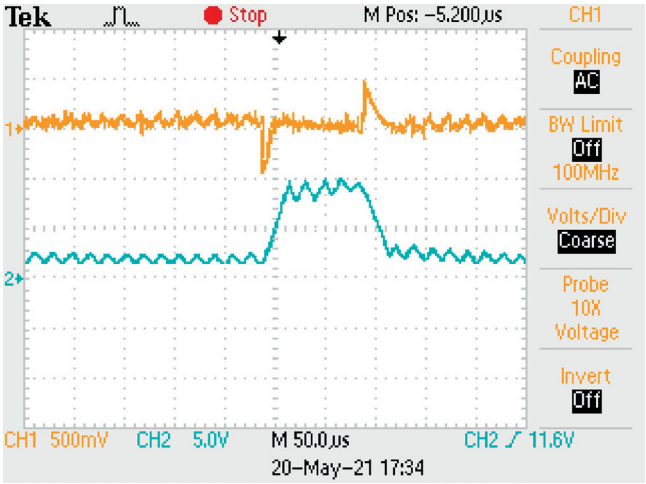

Figure 10 *Voltage and load current (blue) of the switched voltage regulator using a bipolar transistor during a step change in load, obtained through measurement (current scale: 1 V = 1 A)*

verification results, obtained from measurements on a laboratory sample of the transducer, are presented in Figure 10.

Based on the aforementioned considerations, it can be concluded that both analyzed solutions are practically applicable when an increased output current from the converter is required. In terms of output voltage regulation, the more effective, though costlier, option involves using multiple regulators connected in parallel. The simpler alternative, which employs a switching bipolar transistor (BT), is less expensive but offers lower output voltage regulation quality. Additionally, due to the switching speed of the BT, this solution is suitable only for regulators with lower switching frequencies.

4 Increase in the output voltage of a buck converter using the switched voltage regulator

To demonstrate a potential increase in the voltage and current output parameters of a switched voltage regulator, the LM2574 regulator type [10] was chosen. Its advantages include affordability, compact size, integrated current limiting, and a built-in voltage regulator. However, its limitations include a maximum current of 0.5 A and a voltage limit of 40 V. These limitations can be overcome by employing the circuit shown in Figure 11 [15].

The connection is based on the integrated circuit (IC) LM2574, which generates the control pulses for the converter based on the output voltage, obtained from the resistive divider R2 and R1. This voltage is compared with the reference voltage U_{ref} = 1.23 V. According to the datasheet, the resistance value of R1 should range from 1 kΩ to 5 kΩ. The required output voltage is set by potentiometer R2, as described by:

$$R_2 = R_1\left(\frac{U_{out}}{U_{ref}} - 1\right). \tag{2}$$

The reduced supply voltage for the regulator and the isolated DC-DC converter (TRACO) is achieved using a Zener stabilizer, implemented with components R13, Z2, and C3. A similar stabilizer, formed by elements R6, Z3, and C4, generates a 5V supply for the output side of the optical isolator 6N137, whose input LED is driven by the output signal VOUT from the LM2574. Since the optocoupler inverts the signal, it must be inverted again and amplified using transistor T5. The resulting control signal is impedance-matched by the complementary transistor pair T2 and T4 and passed through resistor R12 to the gate of the power switching transistor MOSFET (or IGBT) T1, which is dimensioned for the required higher voltage and current. Current limitation in the circuit is achieved using the sensing diode D1, where the voltage across it in the closed state corresponds to the current flowing through the switch. This voltage triggers the opening of transistor T3, generating a signal that corresponds to the current magnitude on the resistor divider R7 and R14. This signal is then connected to the ON/OFF control input of the LM2574 regulator, which is switched off when the voltage exceeds the threshold value of 1.4 V, as specified in the datasheet. The allowable current of transistor T1 can be adjusted using trimmer R5, thereby ensuring current limitation for the entire converter.

It is also important to note that DC-DC converters can operate in two modes:

- CCM (Continuous Conduction Mode): The current i_{L3} supplied by the inductor to the load when the switch S is open is always greater than zero.

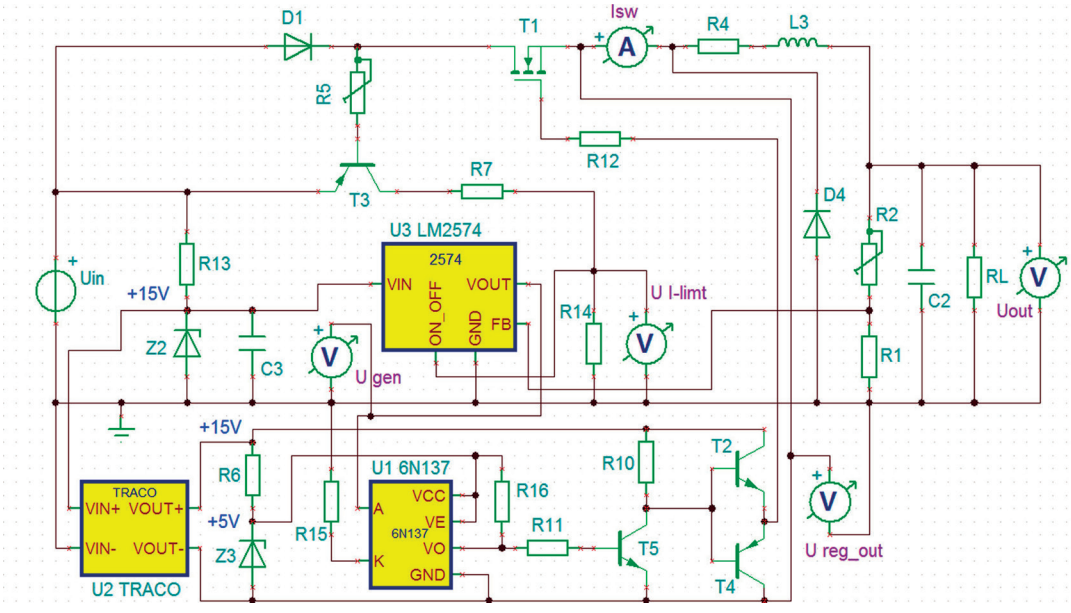

Figure 11 *Configuration of a buck DC-DC converter with the LM2574-ADJ, extending its current and voltage limits*

- DCM (Discontinuous Conduction Mode): The current i_{L3} is zero at certain points during the switching period.

The mode in which the converter operates primarily depends on the inductance value L of the inductor L3, the duty cycle D, and the switching frequency f. The inductance value that defines the boundary between CCM and DCM is given by the following relation for a buck DC-DC converter [16]:

$$L_b = \frac{(1-D)R_L}{2f}. \tag{3}$$

For L > L_b, the converter operates in Continuous Conduction Mode (CCM). Based on the operational

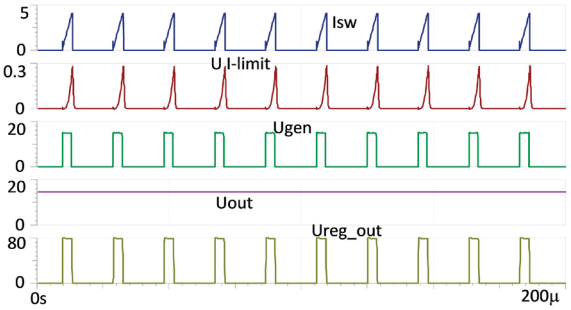

a)

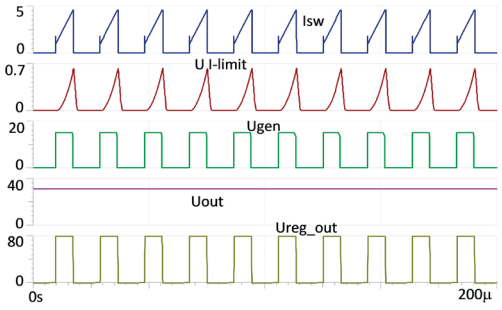

b)

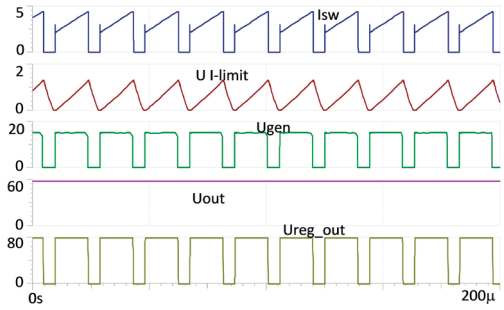

c)

Figure 12 *Converter waveforms obtained from the simulation in the TINA program: a) Uout=14.3 V, b) Uout=31 V, c) Uout=58 V*

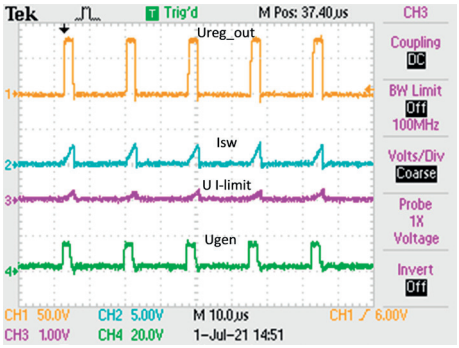

a)

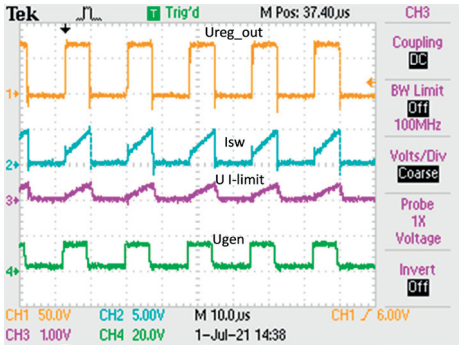

b)

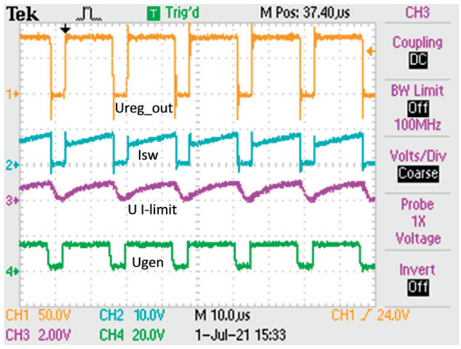

c)

Figure 13 *Converter waveforms obtained through measurement: a) Uout=14.3 V, b) Uout=31 V, c) Uout=58 V*

principle of the regulator, it is evident that when using a switched voltage regulator, the duty cycle (D) varies, which in turn alters the mode of operation of the converter, transitioning between CCM and Discontinuous Conduction Mode (DCM). The current i_C flowing through the capacitor C2 induces a small ripple in the output voltage U_{out}. To limit this ripple to the desired value U_{ripple}, the capacitance of capacitor C2 must meet a minimum value, as given by [16]:

$$C_{\min} = \frac{(1-D)U_{out}}{8U_{ripple}Lf^2}. \quad (4)$$

The waveforms obtained from the simulation in the TINA program for three different output voltage values are shown in Figure 12. The corresponding measurement results from the converter circuit are presented in Figure 13. The key component values of the converter are as follows: Uin = 80 V, f = 52 kHz, R1 = 1 kΩ, R2 = 10.62 kΩ (24.2 kΩ, 46.15 kΩ), R4 = 360 mΩ , L3 = 330 µH, C2 = 470 µF, RL = 11 Ω. The maximum inverter switching current has been set to 8 A.

The measured output voltage-current (V-I) characteristics of the converter, for the output voltages Uout = 14.3 V, Uout = 31 V and Uout = 58 V, are shown in Figure 14.

An example of the laboratory implementation of the described converter is shown in Figure 15. A comparison of the results obtained from both simulation and measurement demonstrates good agreement in the waveforms, highlighting the practical applicability of the proposed configuration. Utilizing the cost-effective LM2574 circuit, along with the addition of several other components, it is relatively straightforward to configure a buck DC-DC converter capable of delivering power in the hundreds of watts, with an output voltage that can reach several hundred volts.

5 Recommendations for enhancing the EMC of a buck DC-DC converter

An important consideration in the design of a buck converter is electromagnetic compatibility [17]. From this perspective, the most critical component is the inductance L, implemented as a technical coil, which serves as a source of electromagnetic emissions. These emissions can significantly affect the operation of nearby electrical and electronic equipment. The critical nature of this component arises not only from the relatively high switching frequencies but, more importantly, from the high switching currents. This issue is clearly illustrated in Figure 16, which shows the magnetic field generated by both a toroidal and a cylindrical coil when subjected to a harmonic current with an amplitude of 10 A and a frequency of f = 52 kHz.

The results of the magnetic field distribution were

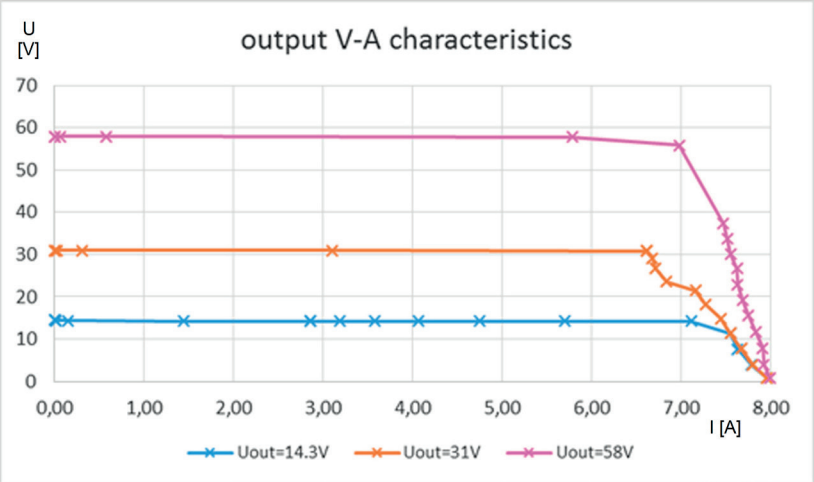

Figure 14 *Measured output voltage-current (V-I) characteristics of the converter*

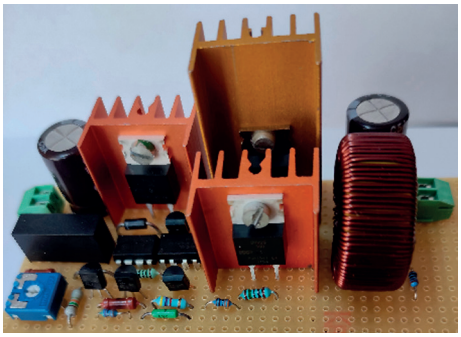

Figure 15 *Demonstration of the laboratory prototype of the converter*

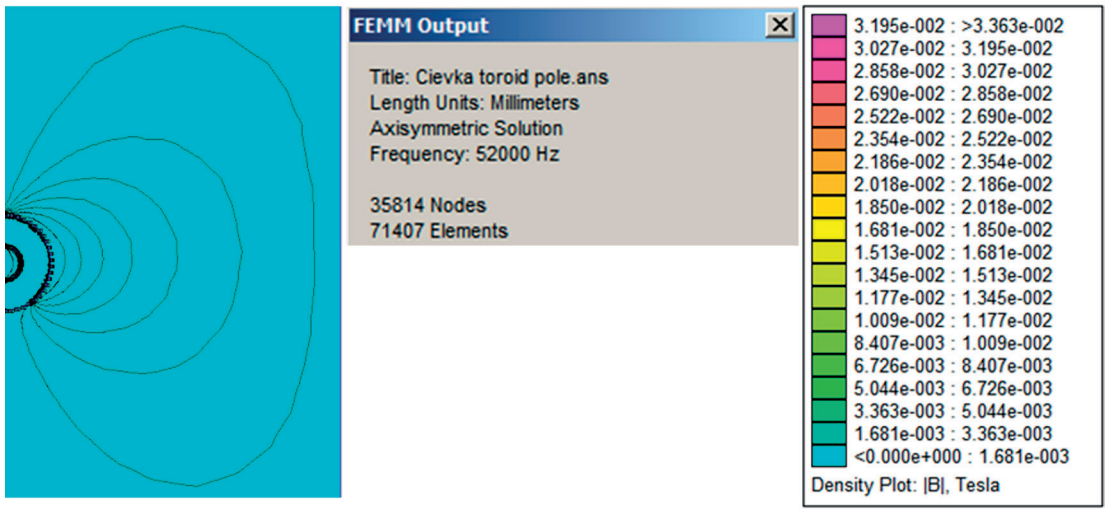

a)

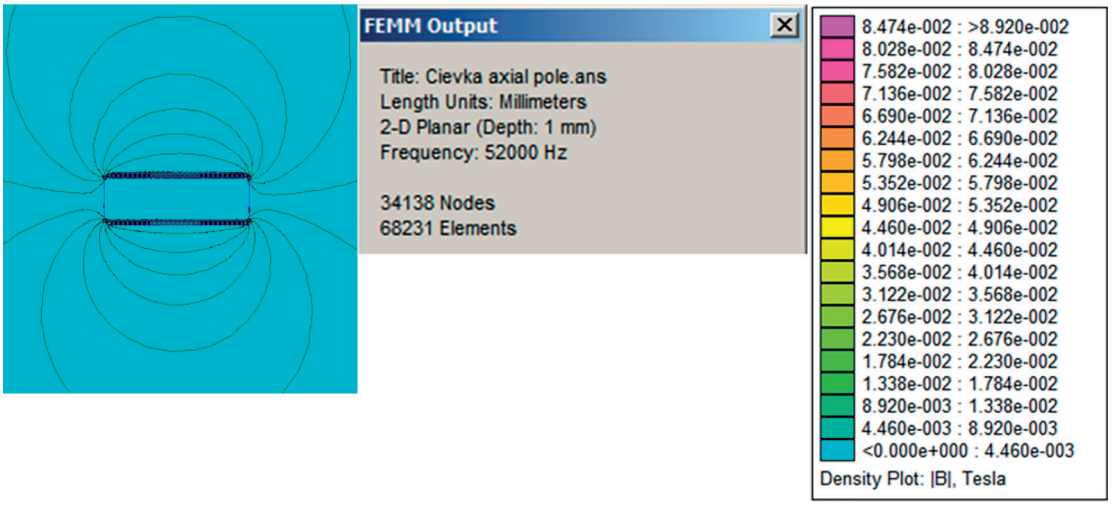

b)

Figure 16 *Radiated magnetic field of the coil: a) toroidal, b) axial*

obtained using the FEMM simulation program [18], which utilizes the finite element method. To mitigate the radiation, it is sufficient to shield the coil with 0.3 mm thick aluminum foil [19]. This solution is illustrated in Figure 17.

The simulations demonstrate that substantial improvements in the electromagnetic compatibility of the buck DC-DC converters can be achieved by shielding the technical coil with 0.3 mm-thick aluminum foil.

6 Conclusion

By comparing Figures 4a) and 4b), an overview of the accuracy of the static parameters in the converter, using the improved and simplified regulator model, is obtained, showing an agreement of 95%. Similarly, the accuracy of the dynamic parameters is assessed through Figures 4c) and 4d), where the results demonstrate approximately 93% agreement. This is an excellent outcome, particularly considering that accuracy is influenced not only by the regulator model but by the realism of the models for the external components (MOSFET, diode), as well.

The presented universal model of the switching voltage regulator is based on the equivalence of its typical properties, which significantly simplifies the model. Unlike existing regulator models, it allows for easy modification of individual parameters, providing a more accurate reflection of the characteristics of the actual components used, particularly when components are employed multiple times in a single configuration.

Using this model, recommended configurations of switching regulators were tested to enhance the output power of a buck DC-DC converter. These configurations included parallel regulator connections, the addition of a switching bipolar transistor, and the use of external MOSFET or IGBT transistors. The results obtained from measurements conducted on laboratory samples of the converters demonstrate their practical applicability, offering low costs and compact

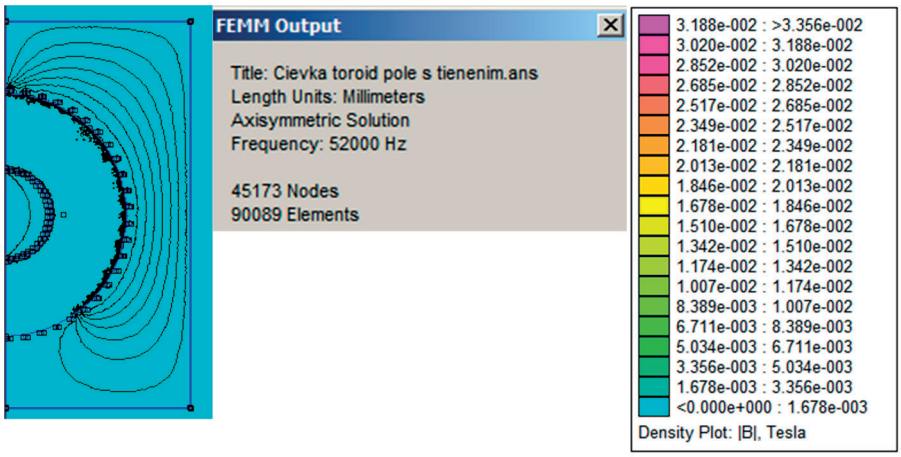

a)

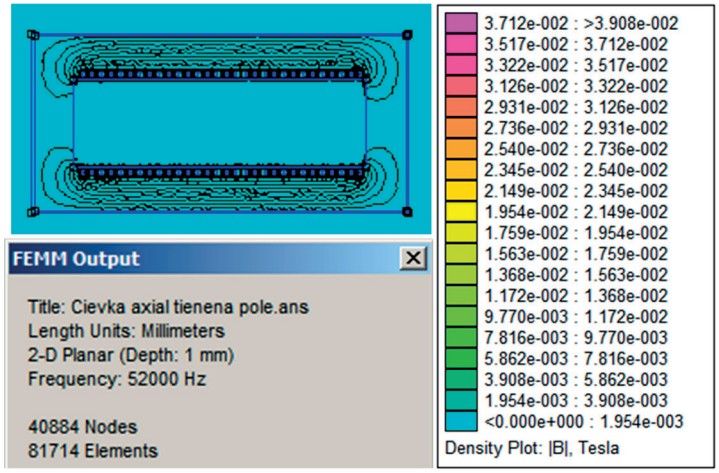

b)

Figure 17 *Radiated magnetic field of an aluminum-shielded coil to a thickness of 0.3 mm: a) toroidal, b) axial*

dimensions. The improvement of the converter's output parameters is fundamentally determined by the limiting characteristics of the external components connected to the regulator. In the case of increasing the output current through the parallel connection of switched regulators, the limiting factor is primarily the number of regulators, particularly in terms of spatial arrangement. When increasing the output current by adding a bipolar transistor circuit, the limitations are imposed by the maximum output current of the integrated regulator, the current amplification factor of the bipolar transistor, and, ultimately, its frequency characteristics, which must be compatible with the frequency of the integrated regulator. However, it is important to note that even in this configuration, the converters can be further connected in parallel if additional current increase is needed. For increasing the output voltage of the converter, the proposed configuration is constrained by the maximum allowable drain-source voltage (u_{DS}) of the used MOSFET transistor, its frequency parameters (which must match the integrated regulator's frequency characteristics), and the power losses in the Zener stabilizer circuit or the TRACO converter, which are used to generate the low-voltage supply for the switched regulator and additional logic circuits.

A significant contribution of this study is the simulation evidence demonstrating a substantial improvement in the electromagnetic compatibility (EMC) of the constructed converters. This improvement was achieved through the straightforward application of shielding foil around the primary source of radiation - the technical coil.

Acknowledgment

The authors received no financial support for the research, authorship and/or publication of this article.

Conflicts of interest

The authors declare that they have no known competing financial interests or personal relationships that could have appeared to influence the work reported in this paper.

References

[1] BERES, M., KOVAC, D., VINCE, T., KOVACOVA, I., MOLNAR, J., TOMCIKOVA, I., DZIAK, J., JACKO, P., FECKO, B., GANS, S. Efficiency enhancement of non-isolated DC-DC interleaved buck converter for renewable energy sources. *Energies* [online]. 2021, **14**(14), 4127. eISSN 1996-1073. Available from: https://doi.org/10.3390/en14144127

[2] WANG, L., ZHANG, D., DUAN, J., GU, R. Research on high-performance multiphase DC-DC converter applied to distributed electric propulsion aircraft. *IEEE Transactions on Transportation Electrification* [online]. 2023, **9**(3), p. 3545-3563. EISSN 2332-7782. Available from: https://doi.org/10.1109/TTE.2022.3207142

[3] YAMA, O., KHYZHNIAK, T., BONDARENKO, O. Analysis of modified non-isolated DC-DC converters and solutions to improve their characteristics. In: IEEE 4th KhPI Week on Advanced Technology: proceedings [online]. 2023. eISBN 979-8-3503-9553-2, p. 1-6. Available from: https://doi.org/10.1109/KhPIWeek61412.2023.10312965

[4] FRIVALDSKY, M., PCOLA, M., BIEL, Z., KUCERA, R., FRANKO, M., HOLCEK, R. Node ringing reduction of synchronous buck converter. *Communications - Scientific Letters of the University of Zilina* [online]. 2023, **25**(3), p. C48-C55. ISSN 1335-4205, eISSN 2585-7878. Available from: https://doi.org/10.26552/com.C.2023.054

[5] LYU, Y., SANUSI, B. N., OUYANG, Z. Modeling and analysis of coupling effect in four legged core for multi-phase buck converter. In: IEEE Applied Power Electronics Conference and Exposition: proceedings [online]. 2023. eISBN 978-1-6654-7539-6, eISSN 2470-6647, p. 3307-3313. Available from: https://doi.org/10.1109/APEC43580.2023.10131131

[6] SIMCAK, J., FRIVALDSKY, M., RESUTIK, P. The power analysis of semiconductor devices in multi-phase traction inverter topologies applicable in the automotive industry. *Communications - Scientific Letters of the University of Zilina* [online]. 2024, **26**(3), p. C21-C38. ISSN 1335-4205, eISSN 2585-7878. Available from: https://doi.org/10.26552/com.C.2024.034

[7] MOBAYEN, S., BAYAT, F., LAI, CH.-CH., TAHERI, A., FEKIH, A. Adaptive global sliding mode controller design for perturbed DC-DC buck converters. *Energies* [online]. 2021, **14**(14), 1249.e ISSN 1996-1073. Available from: https://doi.org/10.3390/en14051249

[8] Datasheet LM2576 - Texas Instruments [online] [accessed 2024-10-18]. Available from: https://www.ti.com/lit/ds/symlink/lm2576.pdf?ts=1626045022539&ref_url=https%253A%252F%252Fwww.google.com%252F

[9] Design tools and simulation - Texas Instruments [online] [accessed 2024-10-11]. Available from: https://www.ti.com/product/LM2576

[10] Datasheet LM2574 - Texas Instruments [online] [accessed 2024-10-18]. Available from: https://www.ti.com/lit/ds/snvs104f/snvs104f.pdf?ts=1626064117944&ref_url=https%253A%252F%252Fwww.google.com%252F

[11] KOVAC, D., VINCE, T., BERES, M., MOLNAR, J., DZIAK, J., JACKO, P., KOVACOVA, I. A universal PSpice simulation model of a switched buck voltage regulator. *Energies* [online]. 2022, **15**(15), 8209. eISSN 1996-1073. Available from: https://doi.org/10.3390/en15218209

[12] TINA-TI SPICE-based analog simulation program - Texas Instruments [online] [accessed 2024-10-21]. Available from: https://www.ti.com/tool/TINA-TI

[13] PSpice reference guide [online] [accessed 2024-10-21]. Available from: https://www.seas.upenn.edu/~jan/spice/PSpice_ReferenceguideOrCAD.pdf

[14] LM2576 unencrypted PSpice transient model - Texas Instruments [online] [accessed 2024-10-21]. Available from: https://www.ti.com/product/LM2576#design-development

[15] KOVAC, D., KOVACOVA, I., SCHWEINER, D. Wiring for extending the current and voltage load capacity of a switched voltage regulator [online]. Slovak patent No. 289249. Industrial Property Office of the SR, 2024. Available from: https://wbr.indprop.gov.sk/WebRegistre/Patent/Detail/129-2019?csrt=9841336417737460554

[16] RASHID, M. H. *Power electronics handbook*. 3. ed. Elsevier Inc., 2011. ISBN 978-0-12-382036-5.

[17] KOVACOVA, I., KOVAC, D. Electromagnetic coupling - EMC of electrical systems. *Journal on Communications Antenna and Propagation* [online]. 2014, **4**(2), p. 51-57. ISSN 2039-5086, eISSN 2533-2929. Available from: https://www.praiseworthyprize.org/jsm/index.php?journal=irecap&page=article&op=view&path%5B%5D=0103

[18] FEMM application [online] [accessed 2024-10-07]. Available online: https://www.femm.info/wiki/HomePage

[19] KUBIK, Z., SKALA, J. Shielding effectiveness simulation of small perforated shielding enclosures using FEM. *Energies* [online]. 2016, **9**(3), p.1-12. eISSN 1996-1073. Available from: https://doi.org/10.3390/en9030129

MATHEMATICAL MODELLING OF HYBRID POWERTRAIN SYSTEMS FOR IMPROVED ENERGY EFFICIENCY

Oleg Lyashuk[1,*], Victor Aulin[2], Roman Rohatynskiy[1], Ivan Gevko[1], Andriy Gypka[1], Dmytro Mironov[1], Volodymyr Martyniuk[3,4], Artur Lutsyk[1], Nadia Denysiuk[5]

[1]Department of Automobiles, Ternopil Ivan Puluj National Technical University, Ternopil, Ukraine
[2]Department of Maintenance and Repair of Machines, Central Ukrainian National Technical University, Kirovohrad, Ukraine
[3]Administration and Social Sciences Faculty, WSEI University, Lublin, Poland
[4]Administrative and Financial Management Department, Lviv Polytechnic National University, Lviv, Ukraine
[5]Department of Ukrainian and Foreign Languages, Ternopil Ivan Puluj National Technical University, Ternopil, Ukraine

*E-mail of corresponding author: oleglashuk@ukr.net

Oleg Lyashuk 0000-0003-4881-8568,
Roman Rohatynskiy 0000-0001-8536-4599,
Andriy Gypka 0000-0002-7565-5664,
Volodymyr Martyniuk 0000-0003-4139-0554,
Nadia Denysiuk 0000-0001-8197-2183
Victor Aulin 0000-0002-9658-2492,
Ivan Gevko 0000-0001-5170-0857,
Dmytro Mironov 0000-0002-5717-4322,
Artur Lutsyk 0009-0003-3938-9228,

Resume
The development and simulation of a mathematical model for a hybrid powertrain vehicle, aiming to optimize its energy efficiency and dynamic performance is presented in this study. Implemented in MATLAB/Simulink, the model captures the dynamic interactions between the hybrid system's components, including the internal combustion engine, electric motor, and battery. By conducting a full factorial experiment, the specific power of the hybrid vehicle was analyzed, revealing the critical influence of factors such as driving speed, road gradient, and battery state of charge. The proposed model demonstrated a discrepancy of 4-11% between the simulated and experimental results, confirming its adequacy for forecasting energy consumption and operational range. These findings offer valuable insights for enhancing the hybrid vehicle performance and sustainability through precise energy management strategies.

Article info
Received 30 September 2024
Accepted 27 February 2025
Online 19 March 2025

Keywords:
hybrid power plant
drive
electric motor
transmission
generator
car

Available online: https://doi.org/10.26552/com.C.2025.028

ISSN 1335-4205 (print version)
ISSN 2585-7878 (online version)

1 Introduction

Recent years have been characterized by high growth rates of the global automobile fleet, causing the increase in oil consumption and emissions of harmful substances with exhaust gases. Improving the fuel efficiency and reducing emissions is a priority in the design of automobiles. These problems can be solved by the improvement of the design of internal combustion engines (ICE), the use of alternative fuels (biofuels, natural gas, etc.) [1-2], and the increase in the energy efficiency of automobiles. The use of electric and hybrid power plants (HPP) in road transport is particularly noteworthy.

The production of hybrid buses is a global trend in the bus industry. Many global manufacturers, in particular North American ones, most actively participate in the development of hybrid power plants and buses in cooperation with major energy companies and national laboratories such as EPRI, General Electric, NREL, INEEL, ISE Research, and others. Design and production are carried out in accordance with the government program "The 21st Century Truck Program (21CT)" and the program of US Department of Energy (DOE) "Advanced Heavy Vehicle Hybrid Propulsion System R&D Program (Heavy Hybrid Program)". In 2002, at the request of the US Department of Energy, the NREL National Laboratory analyzed the development of hybrid trucks and buses of various types in order to determine the concept of designing hybrid

power plants for urban and suburban transport. In this study [3], the authors analysed the optimisation of timetables and scheduling for electric buses. They proposed a new approach that combines scheduling and traffic planning to improve service quality and reduce operating costs. Using the case of a university bus route in Montreal, the authors developed a mathematical model and algorithm that takes into account passenger waiting time and seat availability. As a result, the proposed approach significantly improved service and reduced costs compared to the existing schedule.

Keseev (2023) [4] conducted a comprehensive gap analysis in the classification of eco-friendly vehicle categories, emphasizing the environmental and economic benefits of hybrid electric vehicles (HEVs) and plug-in hybrid electric vehicles (PHEVs) over the battery electric vehicles (BEVs) for diverse driving conditions. The findings highlight that HEVs and PHEVs are more versatile and economically viable, especially in urban and extra-urban environments, whereas BEVs are mainly effective in city driving due to infrastructure and battery limitations. However, this research did not extensively address the modelling and simulation of hybrid powertrain systems to optimize performance parameters such as energy consumption and vehicle dynamics. This gap underlines the need for advanced mathematical models to enhance hybrid vehicle efficiency.

The authors of this study [5] offered a detailed analysis of the sizing of powertrain components in commercially available electrified vehicles, focusing on internal combustion engines, electric motors, and battery capacities across HEV, PHEV, and BEV models. The research identified how the powertrain components are dimensioned to meet specific performance requirements, such as acceleration and driving range, using data-driven methodologies. However, the static sizing approaches, without exploring dynamic simulation or optimization of powertrain operations under varying driving conditions were primarily emphasized in this study. This gap highlights the need for comprehensive modelling that incorporates dynamic performance and energy management strategies.

In the study [6] authors investigated the power loss analysis of semiconductor devices in multi-phase traction inverter topologies for automotive applications. The research compared traditional two-level Voltage Source Inverters (VSI) to advanced three-level Neutral Point Clamped (NPC) and T-type NPC (T-NPC) inverters, using PLECS and MATLAB simulations. The findings demonstrate that T-NPC inverters offer superior efficiency and reduced power losses, particularly at higher switching frequencies. However, authors primarily focuse on inverter topology optimization without addressing how these advancements impact the overall energy management and dynamic performance of hybrid powertrains. This limitation underscores the need for integrated modelling of hybrid vehicle systems.

The authors of this study note that the introduction of the HPP will significantly improve the environmental and economic performance of a vehicle. The papers [7-11] provide a justification for the need to create vehicles for urban passenger transportation with a hybrid power plant. The authors underline that combining the positive qualities of an internal combustion engine and a traction electric drive of a vehicle allows obtaining advantages over a traditional design by increasing environmental friendliness, cutting fuel consumption, improving dynamic properties, and increasing the efficiency of the power plant. In [12], the authors analyzed current innovations in electric vehicles (EVs) for the energy transition. They emphasised the importance of EVs in reducing dependence on fossil fuels and reducing carbon dioxide emissions. The latest technologies, market trends and challenges related to the development of EFVs, as well as prospects for future development were covered in this study. The main focus was on technological improvements, the expansion of charging infrastructure and policy support required for the widespread adoption of EVs.

The system “HPP - automobile - road” is considered in [13]. This approach requires the development of models for each component of the system. Currently, there are various models of HPP, the automobile, and the road. Specific method was applied for designing models that describe the dynamics of automobile movement, design features, and road conditions [14]. However, the generalizing features among the HPP models could not be distinguished; thus, the assessment of indicators by this method is ambiguous. In [15], the authors analyzed the use of hybrid reinforcement learning models to optimise the charging and discharging of lithium-ion batteries in electric vehicles. They integrated the deep Q-learning and active criticism algorithms into the battery management systems. This improves the battery efficiency, performance and service life. The models have been tested in simulations and experimental environments, demonstrating the ability to adapt to changes in battery health and adhere to complex operational constraints.

When studying the performances of automobiles with HPP [16], the maximum power was assumed decisive for determining the choice of series or parallel HPP layout scheme. The parallel one was assumed suitable for power up to 150 kW, typically for passenger cars. The series scheme was assumed suitable for power plant capacities greater than 150 kW, such as heavy-duty vehicles. The choice based on power is not used today. As technology is constantly evolving, the usefulness of a series or parallel scheme has become less significant with the advent of mixed control algorithms for HPP. Therefore, all the processes and traction-and-speed properties of vehicles could be better optimized. Based on the above, the rational parameters of the hybrid power plant should be selected for the automobiles of M3 category with consideration of the

control algorithm, provided the required indicators of specific power consumption of the hybrid vehicle be ensured.

2 Materials and methods

A vehicle with HPP is a complex mechatronic system with coordinated operation of electrical, mechanical, and thermal units. When modelling a vehicle with HPP, the simulation of the control object and the control algorithm should be carried out in a single environment. Such simulation allows optimizing the entire system. To provide effective modelling, a balance between calculation accuracy and modelling speed should be maintained. To quickly execute the model, fast iterations, i.e., not very accurate, are required at some stages of development. There are several approaches to modelling.

One of them is the modelling from the power plant (PP) to the drive of the drive wheels (DDW) [17-18]. The principle of modelling from PP to DDW is shown schematically in Figure 1.

This method is used in cases when there is a need to quickly execute the model with a small number of simulation iterations and their low accuracy. Although this method minimizes the number of options for model calculations, it contains a number of uncertainties regarding the input parameters, which can critically affect the accuracy of the calculations.

The method of modelling from DDW to PP is more rational (Figure 2), as the operating conditions are known at the initial stage of the design. Therefore, the general requirements for electrical, mechanical, thermal units, and the control system of the car's power plant could be substantiated; the energy and technical and economic indicators of the unit could also be predicted.

Having specified the operating mode (i. e., in the form of a change in the speed of the car over time and the dynamic radius of the wheel), the power, torque and angular velocity could be determined and then created on DDW shaft. Therefore, having specified the efficiency value of the transmission, the moment of shafts inertia, the transmission ratio (or a series of transmission ratios) of DDW, the power, torque and rotation frequency, created by the automobile PP, are determined. Then, having accepted the previous values of the PP efficiency, the power provided by PP could be determined. The obtained power value of PP allows choosing the optimal power distribution parameters between the PP units to meet the given operating mode. This approach to designing automobiles with HPP is methodologically more justified. It allows selecting and substantiating the values of the maximum power of the power plant, the distribution of power between the internal combustion engine and the electric motor, the amount of energy required for the driving cycle, the capacity and power of the battery, and fuel consumption. It is also possible to select optimal conditions for the transition between states (modes) of the power plant. In addition, it allows minimizing the number of calculation options and eliminating a number of uncertainties that complicate the design process. That is why this approach was chosen to implement the mathematical model of the hybrid.

In this paper, the principle of modelling a hybrid car with a sequential power plant configuration is considered. A hybrid car with a serial configuration scheme is structurally simpler (and therefore simpler from the point of view of modelling its operation) than a hybrid car with a parallel scheme, since only an electric motor is used as a driving component. The structural scheme of an automobile with HPP, which has the main functional elements and input/output signals of each of them, is considered in the paper (Figure 3).

The main functional elements are the automobile rechargeable battery (BAT), the drive of driving wheels (DDW) of a rear axle, the internal combustion engine (ICE), the motor/generator (M/G), the gearbox (GC), rear drive wheels (WL), the GC control unit (GCU) and automatic control system (ACS). The latter combines the control logic (CL) and control circuits for the internal combustion engine and electric motor, which consist of

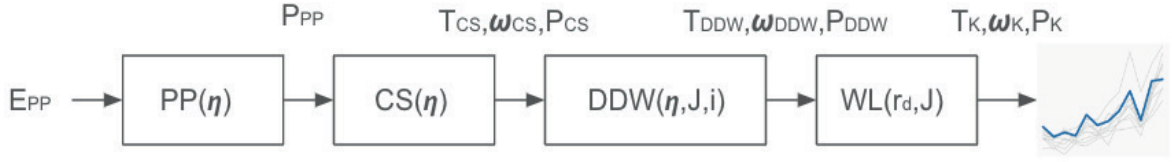

Figure 1 *Structural scheme of an automobile with HPP modelled from PP to DDW*

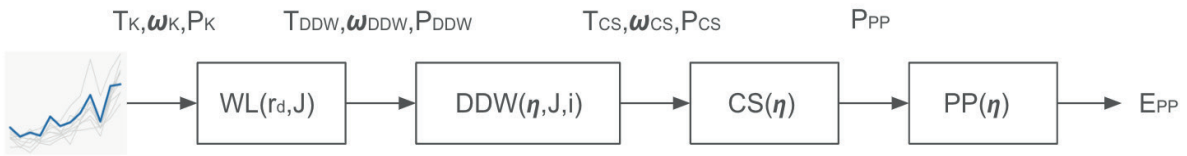

Figure 2 *Structural scheme of an automobile with HPP modelled from DDW to PP*

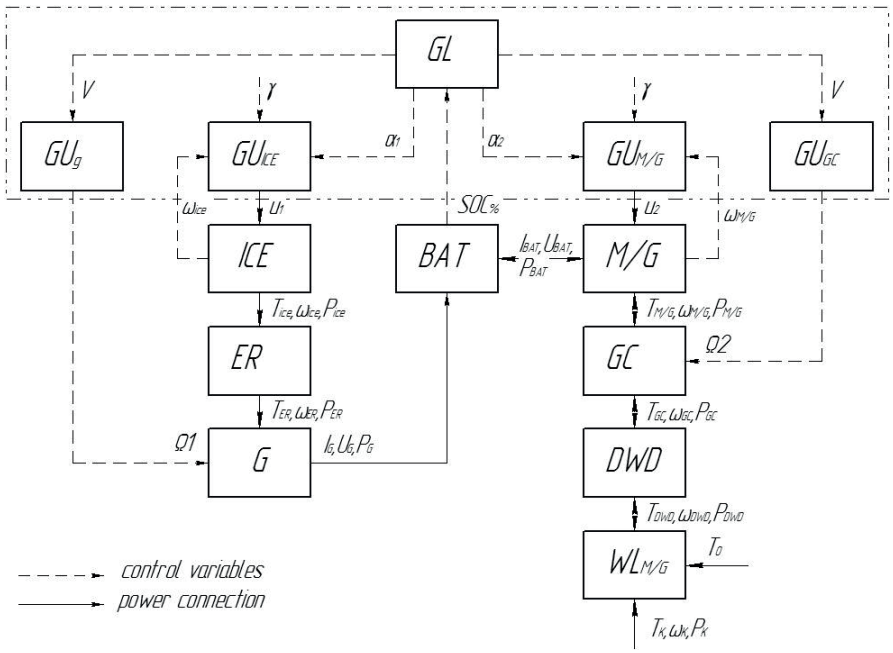

Figure 3 *Considered structural scheme of an automobile with HPP*

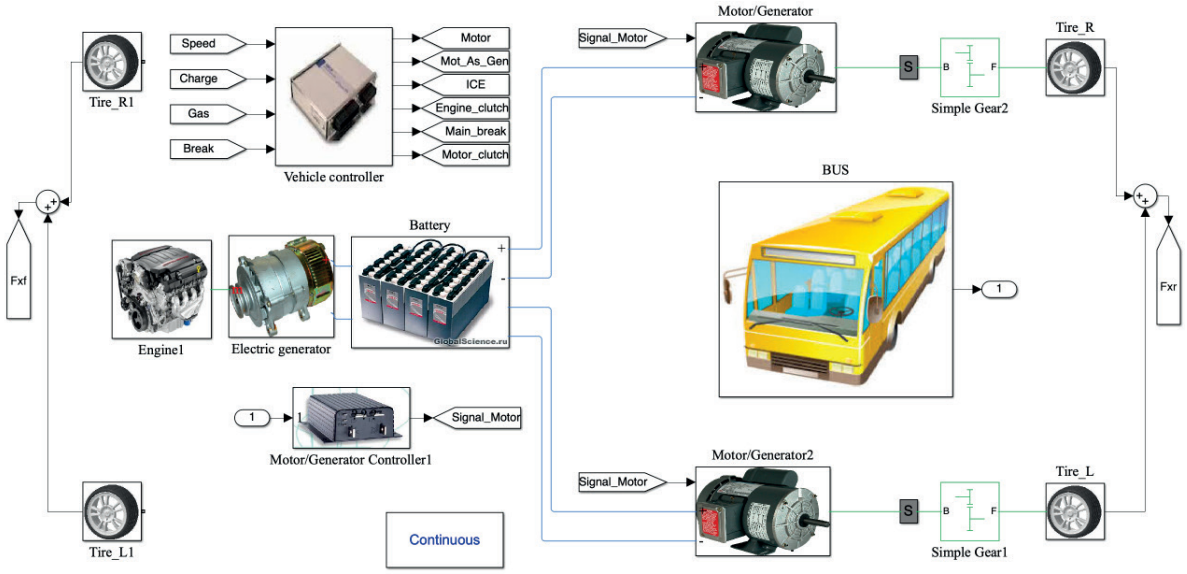

Figure 4 *Simulink model of an automobile with HPP of a serial type*

the control unit *ICE-CU*$_{ICE}$ and the electric motor control unit - $CU_{M/G}$.

The control logic forms the control signals α_1, α_2, which are sent to the CU_{ICE} and $CU_{M/G}$; the output signals of the latter are u_1 and u_2, which represent the control action on the ICE and M/G

The power of the battery P_{BAT}, which is proportional to the voltage U_{BAT} and the current I_{BAT}, ensures the operation of the M/G in traction mode. When working in the traction mode, M/G creates mechanical power $P_{M/G}$, which is proportional to torque $T_{M/G}$ and angular velocity $\omega_{M/G}$, and is transmitted to DDW. The power on the driving wheels P_{WL} is determined by the power P_{DDW}, which, in turn, depends on the current value of the torque of the drive of the driving motor T_{DDM}, the angular velocity P_{DDM}, and the moment of the resistance forces T_o. In the braking mode, the M/G converts the mechanical energy from the DDW into electrical energy and charges the battery.

The ICE is used exclusively to recharge the batteries. When operating, the ICE generates mechanical power P_{ICE}, which is proportional to the torque T_{ICE} and angular velocity P_{ICE}, and is transmitted to the generator G. The power at the generator is determined by the power of the engine reducer P_{ER}, which, in turn, depends on the current value of the torque T_{ER}, the angular velocity $\omega_{ER,}$ and the moment of resistance forces T_O. The generated energy is supplied from the generator to the battery.

To model an automobile with HPP, a control

algorithm was considered using the MatLab Simulink environment. In accordance with the structural scheme of the vehicle with HPP, the mathematical model is presented in Figure 4. The mathematical model was developed using the current recommendations [19-20].

The mathematical model of a car with a sequential type HPP consists of the main blocks: Engine - diesel engine model; MG - model of electric motor /generator; Battery - battery model; Front Transmission - front beam model; Rear Transmission - rear axle model; Longitudinal Vehicle Dynamics - model of a longitudinal dynamics of vehicle movement; Wheel - four blocks that model the wheels of the car; Vehicle controller - model of the vehicle operating mode control system; Engine Controller - model of the diesel engine control unit; MG Controller - model of the electric motor - generator control unit.

When developing a mathematical model that describes the dynamics of a vehicle with HPP in various modes of power plant operation, the elastic and deformable properties of the transmission, as well as possible slippage of the drive wheels when the vehicle is moving, were not taken into account. When modelling the internal combustion engine, thermodynamic processes were not taken into account, as well. The battery capacity with a maximum permissible discharge of 70% of the total capacity was assumed sufficient to complete the driving cycle. Additionally, the model set the parameters of the road surface. The road was chosen to be flat and straight. The longitudinal slope of the road was set to +5%. The maximum transverse curvature of the road was 1.5%. The test cycle for modelling was the European urban driving cycle ECE 15 [21], lasting 195 s.

A model of a petrol engine with angular velocity control is under study in this paper. The input parameter of the ICE model is the throttle valve opening. The parameters that define the engine model are maximum power, angular velocity at maximum power, and maximum angular velocity of the crankshaft.

Current angular velocity value ω_i is a feedback to the motor model input. The angular speed of the motor is limited: $\omega_{\min} \le \omega_i \le \omega_{\max}$. The maximum engine power $P_{\max}$ corresponds to ω_P thus, $P_{\max} = f(\omega_P)$. The equation that determines the maximum torque [17]:

$$T_{\max} = \frac{P_{\max}}{\max}. \tag{1}$$

A well-known relationship is used to describe the dependence of the power of an internal combustion engine on the angular velocity of the crankshaft:

$$P(\omega) = P_{\max}\left[p_1\frac{\omega_i}{\omega_N} + p_2\left(\frac{\omega_i}{\omega_N}\right)^2 + p_3\left(\frac{\omega_i}{\omega_N}\right)^3\right], \tag{2}$$

where p_1, p_2, p_3 - Leiderman coefficients; ω_N - the nominal (rated) angular velocity of the crankshaft

The electric motor model is a model of a brush motor with torque feedback control [13]. This block represents the dependence of torque on angular velocity $T_m(\omega_m)$. Applying a well-known relation, the dependence $T_m(\omega_m)$ is converted into a voltage and current dependence $U_m(I_m)$:

$$\begin{cases} I_m = T_m/(k\Phi_m) \\ E_m = k\omega_m\Phi_m \\ U_m = E_m + I_m\sum R_m \end{cases}, \tag{3}$$

where k - motor design factor; Φ_m - magnetic flux; R_m - resistance; E_m- electromotive force (EMF); $\sum R_m$ - total winding resistance.

The model ensures the output of a certain torque at a certain speed, the values of which are predefined, when the block parameters are set.

The battery model is a dynamic model of the parameters of a lithium-ion battery [17]. The model is divided into two main components - the charge model and the discharge model.

Discharge model $i^* > 0$:

$$f_1(it, i^*, i) = U_0 - K\cdot\frac{Q}{Q-it}\cdot i^* - \\ -K\cdot\frac{Q}{Q-it}\cdot it + A\cdot\exp(-B\cdot it), \tag{4}$$

Charge model $i^* < 0$:

$$f_2(it, i^*, i) = U_0 - K\cdot\frac{Q}{it+0.1Q}\cdot i^* - \\ -K\cdot\frac{Q}{Q-it}\cdot it + A\cdot\exp(-B\cdot it), \tag{5}$$

where U_0 - rated EMF of the battery (V); K - polarization constant (A×H^{-1}) or polarization resistance (Ω); i*- low frequency dynamic current (A); i - battery current (A); it - instantaneous battery capacity (A×H); Q - maximum battery capacity (A×H); A - exponential voltage (V); B - exponential capacity (A×H).

The front axle DDW model (Figure 5) consists of the main blocks: Variable ratio transmission - gearbox unit; Gearboxlever - gearbox control system; Simple gear1 - block that simulates the main gear; Front differential - block that models the differential; Blocks that model the effect of the moment of mechanisms inertia.

The transmission unit is represented as a gearbox that dynamically transmits angular velocity and torque between the two axes, depending on the set gear ratio. If one ignores the change in angular velocity due to shaft stiffness and mechanical losses, the model can be represented by the equations:

$$\omega_B = u_{FB}(t)\omega_F, \tag{6}$$

$$T_F = u_{FB}(t)T_B, \tag{7}$$

where ω_B i ω_F - angular velocities of the input and output shafts, respectively; T_B and T_F - torque on the primary and secondary shafts, respectively; $u_{FB}(t)$ - gear ratio of the gearbox, which changes over time depending on driving conditions.

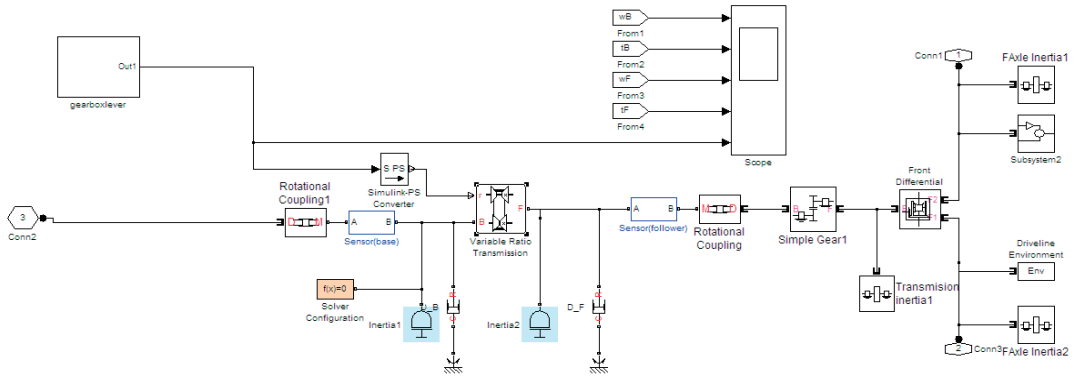

Figure 5 *Simulink front axle DDW model*

Based on the changes in angular velocity due to shaft torsion, the instantaneous change in time between angular velocities over time is calculated as

$$d\phi/dt = u_{FB}(t)\omega_F - \omega_B, \tag{8}$$

where ϕ - shaft twist angle.

The torque is determined as:

$$T_B = -k_P - k_V d\phi/dt, \tag{9}$$

where k_p and k_V - empirical coefficients.

The torque loss in the box is calculated using the formula:

$$T_{loos} = T_F(1-\eta_g), \tag{10}$$

where η_g - gearbox efficiency.

Taking into account mechanical losses, the resulting model is developed:

$$u_{FB}(t)T_B - T_F - T_{loss} = 0. \tag{11}$$

The control system is modelled to evaluate and optimize the interaction between the various components of the hybrid, such as the internal combustion engine (ICE), electric motor and traction battery. The control system model is integrated into a general model of a vehicle with a sequential type of HPP. The control object and control algorithm are modelled in a single Stateflow environment, which is used to model and simulate combinatorial and sequential decision-making logic based on machine states and flowcharts. The Vehicle controller is a sequential control unit based on the theory of finite state machines. The proposed model uses a deterministic finite state machine Q, which is represented by five components:

$$Q = f(S, \Sigma, \delta_i, s_0, R), \tag{12}$$

where S - set of states; Σ - set of input characters; δ_i - transition function; s_0 - initial state; R - set of final states.

The arguments of the transition function δ_i are the current state and the input signal, and the value is the new state. If s is the state and λ is the input state, then $\delta_i(s,\lambda)$ - is the state p.

The control logic model has two main states, one of which has two sub-states, and the other has three sub-states, two of which also have two sub-states. The formula is deduced:

$$Q = \begin{bmatrix} s_1(s_{11}, s_{12}\{s_{121}, s_{122}\}), \\ s_2(s_{21}, s_{22}\{s_{221}, s_{222}\}), \\ c_1(j_1, j_2, j_3, j_4\{r_1, r_2\}), \\ c_2(i_1, i_2, i_3, i_4\{l_1, l_2\}), \\ \delta_i, \\ s_{21}, \end{bmatrix} \tag{13}$$

where s_1, s_2 - main states; s_{11}, s_{12} - sub-states of the main state s_1; s_{121}, s_{122} - sub-states of state s_{12}; s_{21}, s_{22}, s_{23} - sub-states of the main state s_2; s_{221}, s_{222} - sub-states of state s_{22}; c_1 - condition of transition from state s_1 to state s_2; c_2 - condition of transition from state s_2 to state s_1; j_1 - condition of entry into state s_{11}; j_2 - condition of entry into state s_{12}; j_3 - condition of transition from state s_{11} to s_{12}; j_4 - condition of transition from state s_{12} to s_{11}; r_1 - condition of transition from state s_{121} to s_{122}; r_2 - condition of transition from state s_{122} to s_{121}; i_1 - condition of entry into state s_{21}; i_2 - condition of entry into state s_{22}; i_3 - condition of transition from state s_{21} to s_{22}; i_4 - condition of transition from state s_{22} to s_{21}; l_1 - condition of transition from state s_{221} to s_{222}; l_2 - condition of transition from state s_{222} to s_{221}.

Based on Moore's model, the logic is described:

$$\begin{aligned} &s_1, c_1 \mapsto s_2; s_2, c_2 \mapsto s_1; \\ &s_{11}, j_1 \mapsto s_{11}; s_{11}, j_3 \mapsto s_{12}; s_{12}, j_2 \mapsto s_{12}; s_{12}, j_4 \mapsto s_{11}; \\ &s_{121}, r_1 \mapsto s_{122}; s_{122}, r_2 \mapsto s_{121}; \\ &s_{21}, i_1 \mapsto s_{21}; s_{21}, i_3 \mapsto s_{22}; s_{22}, i_2 \mapsto s_{22}; s_{22}, i_4 \mapsto s_{21}; \\ &s_{221}, l_1 \mapsto s_{222}; s_{222}, l_2 \mapsto s_{221}. \end{aligned} \tag{14}$$

The control logic is implemented using the Stateflow tool in the MatLab Simulink environment. Figure 6 shows a block diagram of the control algorithm.

The implemented control algorithm should be further considered. Figure 7 shows

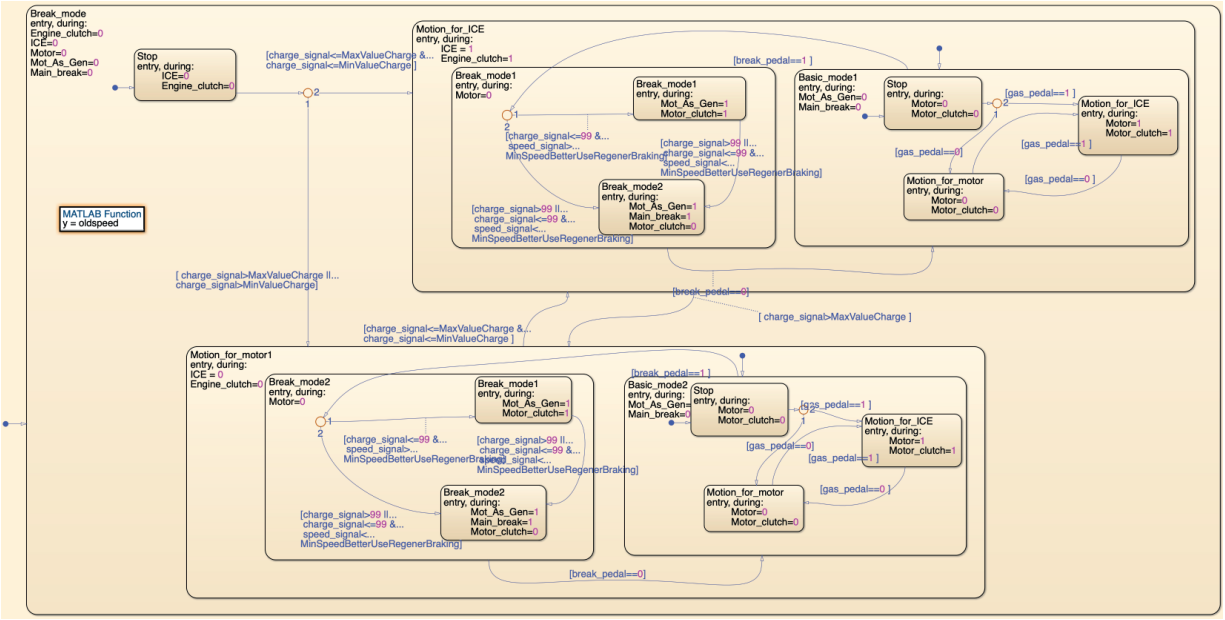

Figure 6 *Block diagram of the algorithm for controlling the power plant of an automobile with HPP*

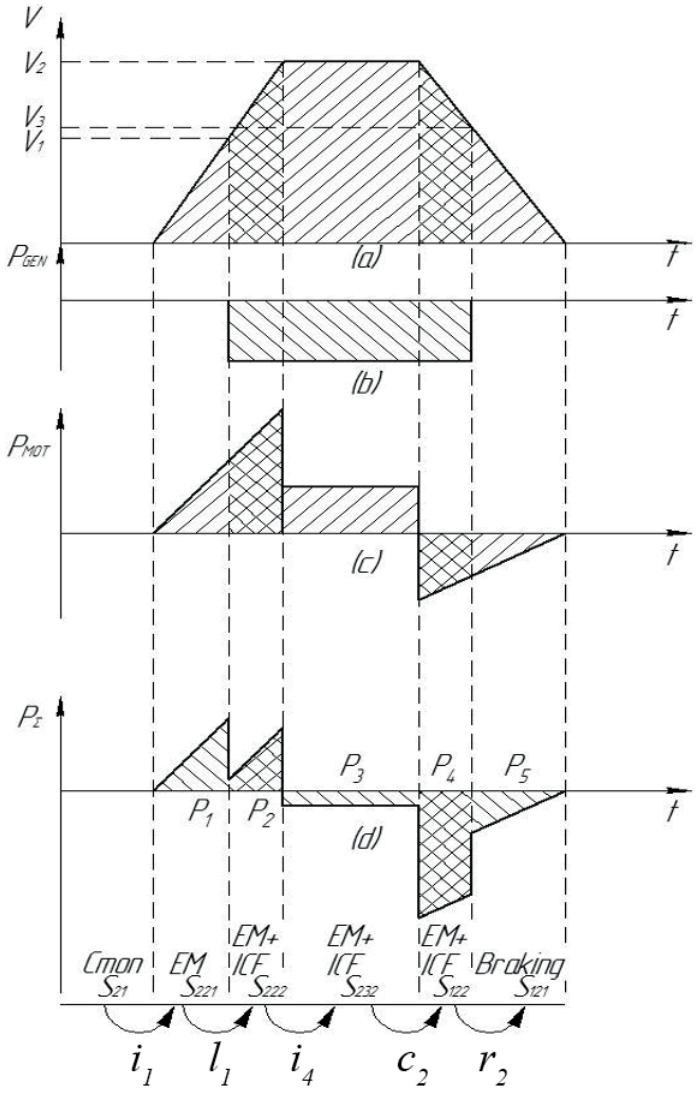

Figure 7 *Scheme of movement modes and transition conditions when an automobile with HPP is moving: a) dependence of automobile speed on time; b) dependence of the power generated by the generator on time; c) dependence of required power for automobile speed mode on time; d) dependence of total power consumed by an automobile on time*

a diagram of the movement modes and transition conditions when an automobile with HPP is moving.

The accepted notation is used in the MatLab Simulink environment. Input signals: gas - accelerator pedal signal (1, 0); break - brake pedal signal (1, 0); Charge - signal about the amount of battery power; Speed - vehicle speed; Output signals: Motor - the electric motor drives the wheels of the vehicle and charges the battery during regenerative braking (on/off) → (1, 0); Mot_As_Gen - electric motor in generator mode for regenerative braking, (on/off) → (1, 0); ICE - internal combustion engine, (on/off) → (1, 0); Engine_clutch - internal combustion engine clutch, (on/off) → (1, 0); Main_break - service brake system (on/off) → (1, 0); Motor_clutch - clutch of the electric motor to the wheel drive, (on/off) → (1, 0).

The basic control logic of a power plant of an automobile with HPP of a serial type has two main modes: (s_2) - basic mode (movement with ICE running) (Figure 8), (s_1) - additional mode (movement with ICE off) (Figure 9). The transition from mode (s_2) to mode (s_1) is carried out when the condition (c_1) is met, which indicates that the battery charge has reached a certain value. The transition from mode (s_1) to mode (s_2) is carried out when the condition (c_2) is met, which indicates that the battery discharge is below the minimum permissible value. The block diagram of the control algorithm in the additional mode (s_1) is shown in Figure 7, where the parking mode occurs; the process of steady or accelerated movement of a vehicle is controlled; and braking with a regenerative braking system takes place.

The transition to the additional mode occurs when the battery is charged to 100%, if the conditions (c_1) is met, from any mode. In this mode, the internal combustion engine and, accordingly, the generator, are turned off. In this mode, the logic can be considered in two ways.

The fulfilment of conditions (r_1) or (r_2) indicates that the brake pedal is pressed, and the driving speed is greater than the minimum permissible value, from which it is advisable to start regenerative braking (the speed is calculated depending on the driving cycle for each automobile specifically). There is a transition to mode (s_{121}) or (s_{221}), respectively, in which the operation of the motor/generator in engine mode is stopped and regenerative braking is activated.

Based on the developed model of hybrid car control, the simulation modelling of the hybrid's operation was performed. The simulation results for the main components of the hybrid (internal combustion engine, traction battery, and electric motor) are shown in Figures 10-12.

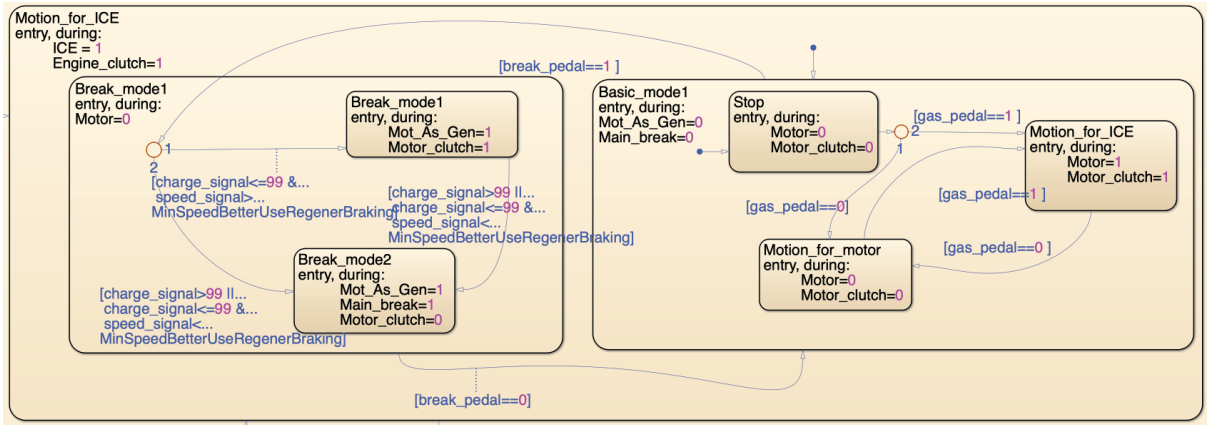

Figure 8 *Block diagram of the control algorithm in the main mode*

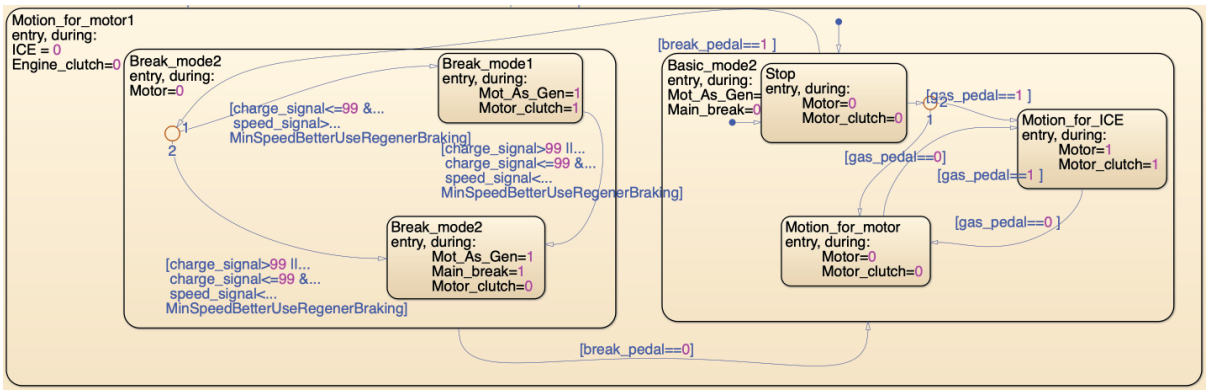

Figure 9 *Block diagram of the control algorithm in additional mode*

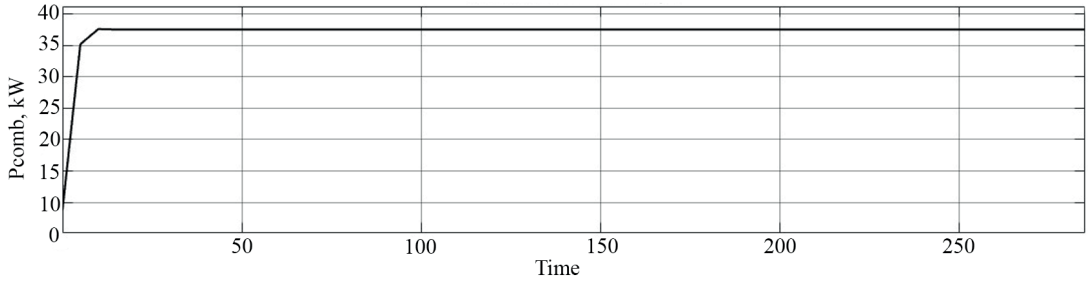

Figure 10 *Power of an internal combustion engine according to simulation in the Simulink environment*

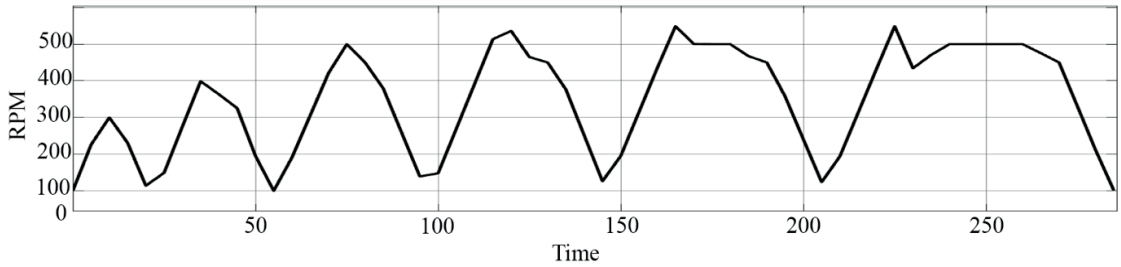

Figure 11 *Electric motor speed according to simulation in the Simulink environment*

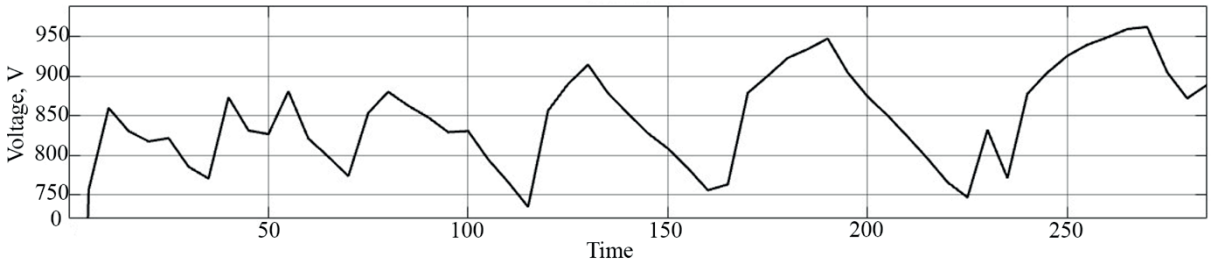

Figure 12 *Battery voltage according to simulation in the Simulink environment*

The graph in Figure 10 shows the power output of an internal combustion engine (ICE) at different points in time during a Simulink simulation. The visible power fluctuations reflect the different modes of the vehicle operation, including acceleration and steady state driving. This data helps to assess the efficiency of the engine in different driving conditions.

The graph in Figure 11 illustrates the changes in motor speed during the simulation. The speed changes according to the different driving modes of a vehicle, including acceleration, steady-state driving, and regenerative braking. This information is key to understanding the efficiency of the motor in different operating conditions.

The graph in Figure 12 shows the change in the voltage across the battery (during the simulation). The voltage fluctuates depending on the processes of charging and discharging the battery that occur during different modes of operation of a hybrid vehicle.

Additionally, the model of the hybrid vehicle control algorithm, proposed in this paper, was compared to the models of the control algorithms based on fuzzy logic [3, 7]. To test the effect of the two control algorithms on the energy characteristics of a hybrid vehicle, a road slope of 5% was set. The comparison was performed for three different modes of hybrid operation: electric motor operation, operation from a combination of an electric motor and an internal combustion engine, and operation from an internal combustion engine. Table 1 shows the results of modelling the operation of a hybrid vehicle using the developed control algorithm and the control algorithm based on fuzzy logic.

As shown in Table 1, when the hybrid vehicle is operating in the ”By EM” mode, the developed algorithm provides a 6% higher maximum engine power and a 5% higher electric motor speed compared to the fuzzy logic-based algorithm. The voltage also increases by an average of 4.5%, indicating the better energy efficiency and stability.

Similar results were obtained in the “By EM and ICE” mode - here, the developed algorithm provides a wider range of engine power, with a maximum value of 6% higher. The voltage increases by an average of 3.4%, and the motor speed increases by 6%. This results in more efficient energy use and better performance.

In the brake mode, the developed algorithm provides a 7% higher maximum motor power, a 4.6% higher voltage on average, and a 7% higher motor speed.

***Table 1** Energy characteristics of a hybrid vehicle*

No.	Driving modes	Developed algorithm	Algorithm based on fuzzy logic
		Internal combustion engine (kW)	
1	By EM	up to 262	up to 246
2	By EM and ICE	110	103
3	Brake mode	up to 175	up to 163
		Voltage (V)	
1	By EM	33.1	31.6
2	By EM and ICE	34.5	33.3
3	Brake mode	41.5	39.5
		Electric motor speed (RPM)	
1	By EM	9.8	9.3
2	By ICE	3.4	3.2
3	By EM and ICE	2.8	2.6

This indicates the better energy efficiency and energy recovery during braking.

A comparative analysis of the two strategies for controlling the torque distribution shows that the developed hybrid vehicle control algorithm outperforms the fuzzy logic-based algorithm in all the analyzed driving modes. It provides higher motor power, higher voltage, and higher electric motor speed. This indicates a higher energy efficiency and stability of the hybrid vehicle under the control of the developed algorithm compared to the fuzzy logic-based algorithm.

An equally important parameter of a hybrid vehicle's operation is the specific power [22]. Evaluating and optimizing the factors that influence the specific power of a hybrid vehicle is important from the perspective of hybrid vehicle performance, as it affects the acceleration and overall dynamic performance of a vehicle, as well as its overall efficiency and economy. To assess the factors that influence the specific power of a hybrid, a regression mathematical model of the vehicle specific power was developed. To form the regression model, the method of planning a multivariate experiment was applied.

When developing an experiment plan, optimality criteria and scope of research come to the fore. In this context, it becomes clear that the optimal plan should be two-level (since the emphasis is on the linear model), with orthogonality and the possibility of rotation. At the first stage of conducting a full factorial experiment, the selection of factors and response functions and the area of their definition is performed [23]:

$$\begin{aligned} y_{\min} \le y \le y_{\max}, \\ x_{\min} \le x \le x_{\max}. \end{aligned} \tag{15}$$

To simplify the recording of experimental conditions and the processing of experimental data, the coding of factors is performed. For this purpose, zero levels for each factor x_{io} and intervals of their variation x_i are selected in the field of determining factors. The upper x_{ib} and lower x_{in} factor levels are calculated in natural values [23]:

$$\begin{aligned} x_{ib} = x_{io} + x_i, \\ x_{ib} = x_{io} - x_i. \end{aligned} \tag{16}$$

Then, the transition to the dimensionless coordinate system is performed:

$$x_j = \frac{K_j \tilde{x}_j - K_{jo} \tilde{x}_{jo}}{I_j}, \tag{17}$$

where x_j - coded value of the factor, $K_j \tilde{x}_j$ - natural value of the factor, $K_{jo} \tilde{x}_{jo}$ - natural value of the main level, I_j - variation interval, j - number of the factor. For quality factors with two levels, one level is +1, and the other is - 1, the order of the levels does not matter.

The next step is to develop an experiment-planning matrix by recording the coded values of the factors and the resulting response function for each experiment. A complete factorial experiment implements all the unique combinations of levels of n independent variables, each of which varies at two levels. The number of such combinations is $N = 2^n$, if n is the number of factors. The developed experiment-planning matrix must satisfy the requirements [24]:

1) Symmetry relative to the center of the experiment

$$\sum_{i=1}^{N} x_{ji} = 0, \tag{18}$$

where j - number of the factor, N - number of experiments, j = 1,2,.....k.

2) Rationing condition

$$\sum_{i=1}^{N} x_{ji}^2 = N. \tag{19}$$

This is a consequence of the fact that the values of the factors in the matrix are set +1 and -1.

3) Orthogonality of the planning matrix

$$\sum_{i=1}^{N} x_{ji} \cdot x_{iu} = 0, \ j \ne u \ \ j = 0,1,2,.....,k. \tag{20}$$

4) Rotativity means that the points in the planning matrix are selected so that the accuracy of predicting

the values of the optimization parameter is the same at equal distances from the center of the experiment and does not depend on the direction.

In the resulting matrix of the experiment, the columns of controlled variables form the plan of the experiment. In addition, the full-factorial experiment (FFE) matrix includes a column with a fictitious factor x_o at the +1 level, which is needed to calculate the coefficient b_o of the regression equation [25]. The results of the experiment are recorded in the last column of the matrix. The response function in this case is the value Y, which takes the values $y_1, y_2, y_3,..., y_n$.

After conducting the FFE, the results are processed at the next stage [26]:

1) Calculation of the reproducibility variance estimation

$$S^2_{(y)} = \frac{\sum_1^N (y_i - \bar{y})^2}{N-1}, \quad (21)$$

where $\bar{y}$ - mathematical expectation of the response function, $N-1$ - the number of degrees of freedom.

2) Definition of regression coefficients

$$b_j = \frac{\sum_{i=1}^N y_i \cdot x_{ji}}{N}, \; b_0 = \bar{y}. \quad (22)$$

3) Checking the significance of regression coefficients.

$$S^2_{\{bj\}} = \frac{S^2_{\{y\}}}{N}, \; \Delta b_j = \pm t \cdot S_{\{bj\}}, \quad (23)$$

where t - tabular value of the Student's criterion for the number of degrees of freedom, at which $S2^2_{\{bj\}}$ was determined; and the selected level of significance (in this case, 0.05).

The coefficient is significant if its absolute value is greater than or equal to Δb_j. Additions with insignificant coefficients are excluded from the equation.

4) Testing the adequacy of the model.

$$F = \frac{S^2_{ad}}{S^2_{\{y\}}}, \quad (24)$$

where F - Fisher's criterion. Then, $F_{calcul} \langle F_{tabl}$; f - number of degrees of freedom, $f = N - (k+1)$; S^2_{ad} - variance of adequacy:

$$S^2_{ad} = \frac{\sum_{i=1}^N (y_i - \hat{y}_i)^2}{f}, \quad (25)$$

where $\hat{y}_i$ - value of the response function calculated by the regression equation; y_i - value of the response function obtained as a result of the experiment.

If a simple linear model turns out to be inadequate, additional methods are applied to improve adequacy: changing the limits of factor variation, shifting the center of the plan, or completing the experimental design. The latter approach involves the transition to orthogonal central compositional plans of higher order experiments.

3 Results and discussion

To obtain a mathematical model of the power change of a hybrid vehicle, a full factorial experiment was conducted. The specific power of the hybrid vehicle P was used as the response function. The main operational indicators and their change limits for obtaining P were determined (Table 2).

Based on the criteria of optimality and the number of factors, the plan of the full factorial experiment of the first order of type 2^4 was selected; and the planning matrix of the full factorial experiment was formed (Table 3), which consists of 16 experiments. The planning matrix contains the values of the factors in all the possible combinations. In the experiment matrix, the 2nd to 5th columns correspond to the factor values, the 6th column is the system response value, and the first column contains units corresponding to the unit coefficients of the free term of the model.

To unify the various physical factors and the response of the system, the transformation of dimensional physical values into dimensionless qualitative ones was performed using the Harington's desirability function [26].

Table 2 *Limits of changes in performance indicators*

Parameter	Moving speed, km/h	t of environment, C	Slope angle of the road surface, %	State of charge (SOC), %
Basic level	25	10	2.5	87.5
Variations	20	20	2.5	12.5
Upper level	45	30	5	100
Lower level	5	-10	0	75

Table 3 *Fragment of the planning matrix of a full factorial experiment*

Experiment number	x_0	x_1	x_2	x_3	x_4	P
1	1	0.780	0.421	0.780	0.765	0.665
2	1	0.780	0.390	0.780	0.765	0.663
3	1	0.375	0.421	0.780	0.765	0.554

Table 4 *Fragment of the coded planning matrix of a full factorial experiment*

Experiment number	1	2	3
x0	1	1	1
x1	1	1	-1
x2	1	-1	1
x3	1	1	1
x4	1	1	1
x1x2	1	-1	-1
x1x3	1	1	-1
x1x4	1	1	-1
x2x3	1	-1	1
x2x4	1	-1	1
x3x4	1	1	1
x1x2x3	1	-1	-1
x1x2x4	1	-1	-1
x1x3x4	1	1	-1
x2x3x4	1	-1	1
x1x2x3x4	1	-1	-1
P	0.665	0.653	0.554

Table 5 *Fragment of the coded planning matrix of the orthogonal central-composite plan of the second order*

Experiment number	1	2	3	4
x0	1	1	1	1
x1	1	1	-1	-1
x2	1	-1	1	-1
x3	1	1	1	1
x4	1	1	1	1
$x1^2$-α	0.2	0.2	0.2	0.2
$x2^2$-α	0.2	0.2	0.2	0.2
$x3^2$-α	0.2	0.2	0.2	0.2
$x4^2$-α	0.2	0.2	0.2	0.2
x1x2	1	-1	-1	1
x1x3	1	1	-1	-1
x1x4	1	1	-1	-1
x2x3	1	-1	1	-1
x2x4	1	-1	1	-1
x3x4	1	1	1	1
x1x2x3	1	-1	-1	1
x1x2x4	1	-1	-1	1
x1x3x4	1	1	-1	-1
x2x3x4	1	-1	1	-1
x1x2x3x4	1	-1	-1	1
P	0.665	0.653	0.554	0.544

At the next stage, to simplify the solution of the system, factors were normalized according to Equation (17). In addition, the planning matrix of the full factorial experiment is completed with rows of interaction of factors between themselves (rows 2-16) (Table 4).

The developed matrix satisfies the requirements in Equations (18)-(20). The specific power model of a hybrid vehicle, obtained because of a full factorial experiment, can be presented in the form of a general equation:

$$P = b_0 + b_1 \cdot x_1 + b_2 \cdot x_2 + b_3 \cdot x_3 + b_4 \cdot x_4 + \\ + b_5 \cdot x_1 \cdot x_2 + ... + b_{11} \cdot x_1 \cdot x_2 \cdot x_3 + \\ + b_{15} \cdot \cdot x_1 \cdot x_2 \cdot x_3 \cdot x_4. \quad (26)$$

The regression coefficients are determined according to Equation (22). The regression coefficients, whose value is equal to or greater than the confidence interval, are considered statistically significant and included in the final equation. As a result, the following regression equation was deduced:

$$P = 0.5104 + 0.0466 \cdot x_1 + 0.0588 \cdot x_2 + \\ + 0.0486 \cdot x_3 \quad . \quad (27)$$

The model was tested for adequacy by the Fisher's test according to Equation (24). The estimated value of Fisher's criterion F_{calcul} = 2.009633495, table F_{table} = 1.8874. Since the condition $F_{calcul} < F_{table}$ is not fulfilled, the model in Equation (27) cannot be considered adequate.

Based on the obtained results, it was decided to complete the plan of the full factorial experiment to the orthogonal central-compositional plan of the second order without losing information about the previous experiments (Table 5).

Analogous transformations with the planning matrix of the orthogonal central-composite plan of the second order allow obtaining the following regression equation:

$$P = 0.53476 + 0.0451 \cdot x_1 + 0.04368 \cdot x_3 + \\ + 0.03265 \cdot x_4 - 0.02975 \cdot x_2^2. \quad (28)$$

The model was tested for adequacy. The calculated value of the Fisher's criterion F_{calcul} = 1.632. For the given parameters of the experiment, F_{table} = 1.96. Based on the adequacy test, the model obtained is considered adequate (F_{calcul} = 0.0994 < F_{table} = 1.53).

Additionally, the model was tested by conducting experimental measurements with recording the values of statistically significant influence factors and the response function, and by calculating the value of the response function using a mathematical model. The object of the experimental study was a car with hybrid module (Figure 13).

The road tests were designed to verify the adequacy of the developed model in Equation (28) based on the conducted research and to refine it by accounting for factors present in real-world driving conditions. The testing program involved determining the kinematic and energy parameters of a hybrid-powered vehicle during straight-line motion under various driving modes with different energy sources. The tests were conducted in compliance with European standards EH 1986-2:2001 [27] and EH 1986-1 [28]. The testing equipment met the requirements of Directive 91/441/EEC. The test track was flat, straight, free of obstacles, and without wind barriers. The longitudinal slope of the test road did not exceed ±2%, while the maximum transverse curvature was limited to 1.5%. The driving cycle followed the European urban driving cycle ECE 15, with a total duration of 195 seconds.

The results of experimental measurements and

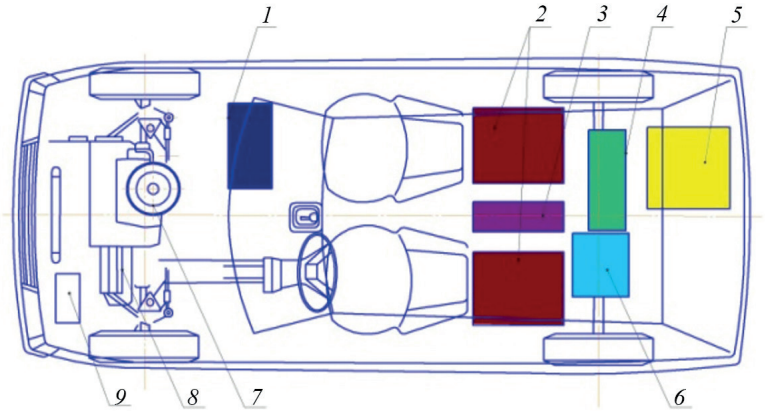

Figure 13 *Configuration of a vehicle with a hybrid powertrain system: 1 - control and data acquisition unit; 2 - traction battery pack (72 V); 3 - power converter unit; 4 - electric motor; 5 - fuel tank; 6 - rear axle transmission; 7 - internal combustion engine (ICE); 8 - front axle transmission; 9 - on-board battery (12 V)*

Table 6 *Fragment of the results of experimental measurements and modelling of the specific power of the hybrid*

Exp. No.	Moving speed, km/h	Ambient temperature, °C	Slope angle, %	SOC, %	Experimental Power, kW	Calculated Power, kW	Discrepancy, %
1	29.3	22.3	0.6	91.6	146.96	131.6	10.45
2	11.8	2.2	2.5	82.8	127.51	121.62	4.62
3	7.6	-6.1	0.2	88.0	143.95	136.22	5.37
4	43.0	17.4	4.5	88.7	139.48	133.46	4.32
5	43.6	7.6	1.3	79.6	109.79	102.9	6.28

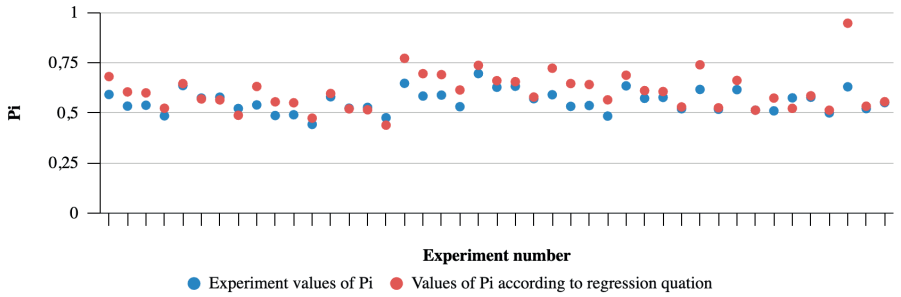

Figure 14 *Specific power of a hybrid vehicle according to the experiment data and regression equation in the "Electric vehicle: mode*

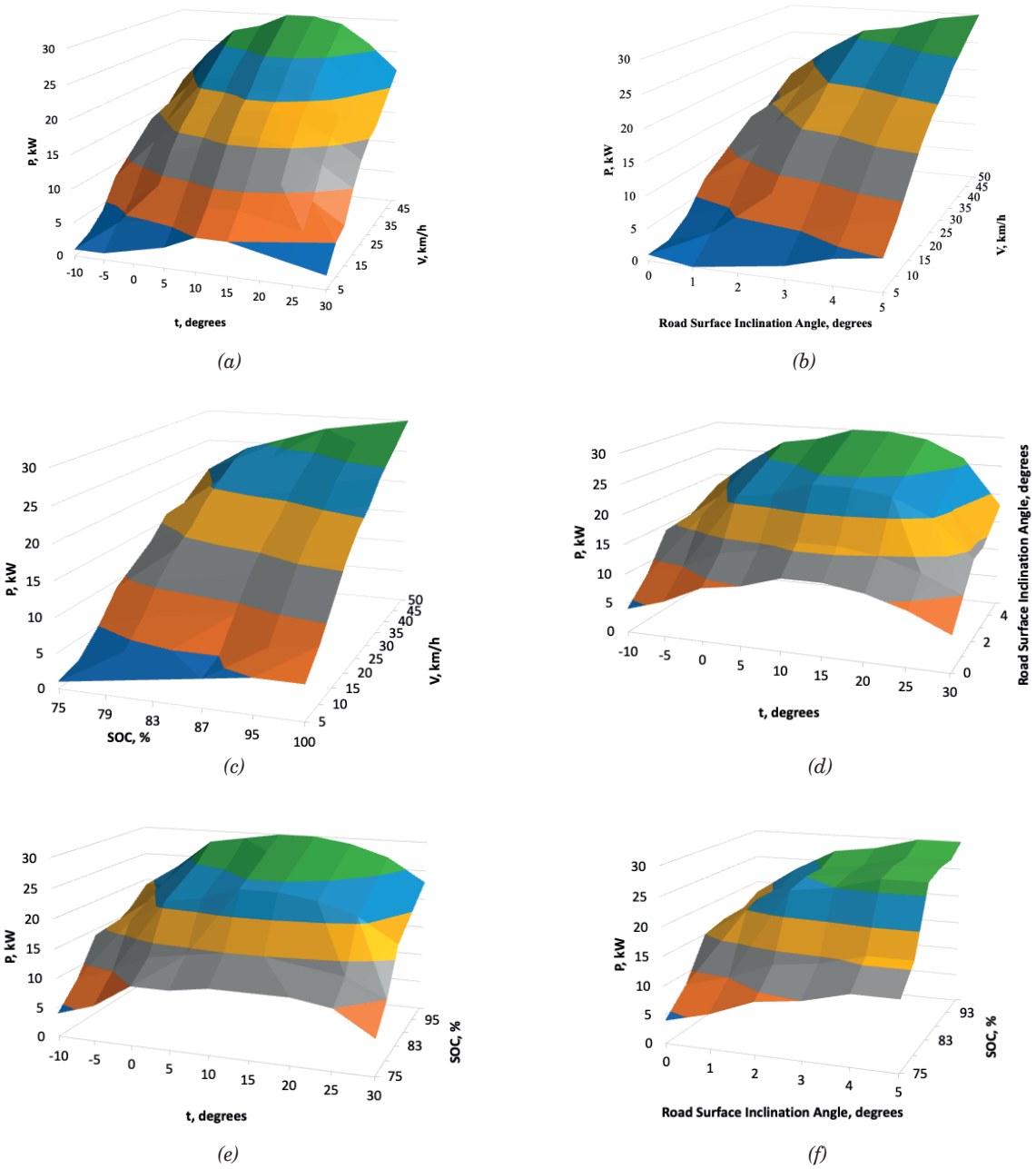

Figure 15 *Response surfaces of the model of specific power of a hybrid vehicle when factors change: a) "driving speed" and "environment t"; b) "driving speed" and "road surface angle"; c) "driving speed" and "SOC"; d) "environment t" and "road surface angle"; d) " environment t" and "SOC"; e) "road surface slope angle" and "SOC"*

modelling of the specific power of the hybrid in the "Electric vehicle" mode are shown in Table 6.

Based on the results of the experiment and the regression equation for different modes of operation of the hybrid installation (Figure 14), the difference between the values of specific power is 4 to 11%. The above mentioned indicates the adequacy of the results obtained.

To determine the nature of the influence of the selected performance indicators on the value of the specific power of a hybrid vehicle, the response surfaces of the model were developed with the alternate fixation of two factors at zero level and the change of two other factors (Figure 15).

Having analyzed the regression Equation (28) and the response surfaces of the model, the nature of the influence of the hybrid vehicle's performance on the change in specific power was determined. If the value of such factors as "driving speed", "road surface slope angle", and "SOC" (the regression coefficients of these factors have a positive sign) increases and the value of the factor "environment *t*" (the regression coefficient of the factor has a negative sign) decreases, the value of specific power *P* increases, as well. If the values of the above factors change in the opposite direction, the value of the specific power, on the contrary, would approach the minimum value.

Additionally, the transition from normalized to non-normalized factors was performed by the inverse transformation according to Equation (17) to obtain a polynomial model of the specific power of a hybrid vehicle suitable for use in forecasting tasks. After performing the transformation, an expression is deduced:

$$P = 0.53476 + 0.0621 \cdot x_1 + 0.0676 \cdot x_3 + \\ + 0.0545 \cdot x_4 - 0.0373 \cdot x_2^2. \quad (29)$$

The obtained polynomial models of the specific power of a hybrid vehicle with normalized and non-normalized factors, can be used as a basis for developing an automated system for monitoring the electric part of a hybrid vehicle. Additionally, these models can be used to estimate and predict the energy consumption of the electric part of the hybrid, as well as the vehicle range in the traction battery mode. Thus, the values of factors should be substantiated into the model in Equation (29); and the predicted value P can be applied to calculate the energy consumption of a hybrid vehicle and estimate the range of a trip in the battery mode. Additionally, based on a real data obtained during the vehicle operation, the model can be further adjusted to improve its accuracy and reliability.

4 Conclusion

A mathematical model and an algorithm for optimizing the operation of HPP (hybrid power plant), implemented in the MATLAB/Simulink environment, are considered in the paper. To assess the influence of energy and traction-speed parameters on the specific power of a hybrid vehicle, a regression equation was deduced by conducting a full factorial experiment. Based on the regression equation, the nature of the influence of HPP operational parameters on the change in the specific power of the unit is determined.

Having analyzed the values of the coefficients of the regression equation terms, a list of factors that greatly influence the change in the specific power of the vehicle with HPP was obtained. Therefore, the impact of operational factors on the specific power of a hybrid vehicle could be evaluated. This fact in turn can influence the acceleration and overall dynamic performance of a vehicle, as well as its overall efficiency and economy, and can significantly improve the driving range of a hybrid on a single battery charge. Adequacy of the developed mathematical model for determining the energy and traction-speed indicators of the vehicle movement with HPP was confirmed with a discrepancy of results within 4 to 11% in driving modes under the electric motor operation.

Acknowledgment

The authors received no financial support for the research, authorship and/or publication of this article.

Conflicts of interest

The authors declare that they have no known competing financial interests or personal relationships that could have appeared to influence the work reported in this paper.

References

[1] KUSZNIER, J. Influence of environmental factors on the intelligent management of photovoltaic and wind sections in a hybrid power plant. *Energies* [online]. 2023, **16**, 1716. eISSN 1996-1073. Available from: https://doi.org/10.3390/en16041716

[2] MORENO-GAMBOA, F., ESCUDERO-ATEHORTUA, A., NIETO-LONDONO, C. Alternatives to improve performance and operation of a hybrid solar thermal power plant using hybrid closed Brayton cycle. *Sustainability* [online]. 2022, **14**, 9479. eISSN 2071-1050. Available from: https://doi.org/10.3390/su14159479

[3] YALCIN S, HERDEM, M. S. Optimizing EV battery management: advanced hybrid reinforcement learning models for efficient charging and discharging. *Energies* [online]. 2024, **17**(12), 2883. eISSN 1996-1073. Available from: https://doi.org/10.3390/en17122883

[4] KESEEV, V. P. Gap analysis in eco categories, electric vehicle comparison and solutions to global transport challenges. *Communications - Scientific Letters of the University of Zilina* [online]. 2023, **25**(1), p. B34-B44. ISSN 1335-4205, eISSN 2585-7878. Available from: https://doi.org/10.26552/com.C.2023.008

[5] SANJARBEK, R., MAVLONOV, J., MUKHITDINOV, A. Analysis of the powertrain component size of electrified vehicles commercially available on the market. *Communications - Scientific Letters of the University of Zilina* [online]. 2024, **24**(1), p. B74-B86. ISSN 1335-4205, eISSN 2585-7878. Available from: https://doi.org/10.26552/com.C.2022.1.B74-B86

[6] SIMCAK, J., FRIVALDSKY, M., RESUTIK, P. The power analysis of semiconductor devices in multi-phase traction inverter topologies applicable in the automotive industry. *Communications - Scientific Letters of the University of Zilina* [online]. 2024, **26**(3), p. C21-C38. ISSN 1335-4205, eISSN 2585-7878. Available from: https://doi.org/10.26552/com.C.2024.034

[7] GAO, D. W., MI, C., EMADI. A. Modelling and simulation of electric and hybrid vehicles. *Proceedings of the IEEE* [online]. 2006, **95**(4), p. 729-745. ISSN 0018-9219, eISSN 1558-2256. Available from: https://doi.org/10.1109/JPROC.2006.890127

[8] LIN, C. C., FILIPI, Z., WANG, Y., LOUCA, L., PENG, H., ASSANIS, D., STEIN, J. Integrated feed-forward hybrid electric vehicle simulation in Simulink and its use for power management studies. SAE Technical Paper 2001-01-1334. 2001 Available from: https://doi.org/10.4271/2001-01-1334

[9] GAO, W. Performance comparison of a hybrid fuel cell-battery powertrain and a hybrid fuel cell-ultracapacitor powertrain. *IEEE Transactions on Vehicular Technology* [online]. 2005, **54**(3), p. 846-855. ISSN 0018-9545, eISSN 1939-9359. Available from: https://doi.org/10.1109/TVT.2005.847229

[10] GAO, W., PORANDLA. S. Design optimization of a parallel hybrid electric powertrain. In: 2005 IEEE Vehicle Power and Propulsion Conference [online]. IEEE. 2005. ISBN 0-7803-9280-9, ISSN 1938-8756, p. 530-535. Available from: https://doi.org/10.1109/VPPC.2005.1554609

[11] ONODA, S., EMADI. A. PSIM-based modelling of automotive power systems: conventional electric and hybrid electric vehicles. *IEEE Transactions on Vehicular Technology* [online]. 2004, **53**(2), p. 390-400. ISSN 0018-9545, eISSN 1939-9359. Available from: https://doi.org/10.1109/TVT.2004.823500

[12] JIANG, B.-H., HSU, C.-C., SU, N.-W., LIN, C.-C. A review of modern electric vehicle innovations for energy transition. *Energies* [online]. 2024; **17**(12), 2906. eISSN 1996-1073. Available from: https://doi.org/10.3390/en17122906

[13] ZARIPOV, R. Y., GAVRILOV, P., KARKU, A. D., SERIKPAEV, T. M. Ways to reduce the toxicity of diesel exhaust gases / Sposoby snijenia toksıchnosti vyhlopnyh gazov dizelnogo topliva [in Russian]. *Nauka i tekhnika Kazakhstana / Science and technology of Kazakhstan*. 2019, **1**, p. 75-84. ISSN 2788-8770.

[14] SHARMA, D., JIBHAKATE, LONARE, P. G., SAH, T., B. M., PANDEY, R. Study and modelling of hybrid MILD vehicle. *International Journal for Scientific Research and Development*. 2015, **3**(01), p. 272-274. ISSN 2321-0613.

[15] ALAMATSAZ, K, QUESNEL, F, EICKER, U. Enhancing electric shuttle bus efficiency: a case study on timetabling and scheduling optimization. *Energies* [online]. 2024, **17**(13), 3149. eISSN 1996-1073. Available from: https://doi.org/10.3390/en17133149

[16] YAN, X., ZHANG, H., LI, X., LI, Y., XU, L. Control strategy of torque distribution for hybrid four-wheel drive tractor. *World Electric Vehicle Journal* [online]. 2023, **14**, 190. eISSN 2032-6653. Available from: https://doi.org/10.3390/wevj14070190

[17] CHENG, R., DONG, Z. Modelling and simulation of plug-in hybrid electric powertrain system for different vehicular application. In: 2015 IEEE Vehicle Power and Propulsion Conference (VPPC): proceedings [online]. IEEE. 2015. eISBN 978-1-4673-7637-2. Available from: https://doi. org/10.1109/vppc.2015.7352976

[18] ADACHI, S., YOSHIDA, S., MIYATA, H., KOUGE, T., INOUE, D., TAKAMIYA, Y., NAGAUNE, F., KOBAYASHI, H., HEINZEL, T., NISHIURA, A. Automotive power module technologies for high-speed switching. In: International Exhibition and Conference for Power Electronics, Intelligent Motion, Renewable Energy and Energy Management: proceedings. 2016. p 1-7.

[19] DHAWAN, R., GUPTA, S., HENSLEY, R., HUDDAR, N., IYER, B., MANGALESWARAN, R. The future of mobility in India: challenges and opportunities for the auto component industry [online]. Available from: https://www.mckinsey.com/industries/automotive-and-assembly/our-insights/the-future-of-mobility-in-india-challenges-and-opportunities-for-the-auto-component-industry#/

[20] SINGH, S. Global electric vehicle market looks to power up in 2018 - Forbes [online], Available from: https://www.forbes.com/sites/sarwantsingh/2018/04/03/global-electric-vehicle-market-looks-to-fire-on-all-motors-in-2018/

[21] CHEN, H., SONG, Z., ZHAO, X., ZHANG, T., PEI, P., LIANG, CH. A review of durability test protocols of the proton exchange membrane fuel cells for vehicle. *Applied Energy* [online]. 2018, **224**, p. 289-299. ISSN 0306-2619, eISSN 1872-9118. Available from: https://doi.org/10.1016/j.apenergy.2018.04.050

[22] TARNAPOWICZ, D., GERMAN-GALKIN, S., NERC, A., JASKIEWICZ, M. Improving the energy efficiency of a ship's power plant by using an autonomous hybrid system with a PMSG. *Energies* [online]. 2023, **16**, 3158. eISSN 1996-1073. Available from: https://doi.org/10.3390/en16073158

[23] AULIN, V., ROGOVSKII, I., LYASHUK, O., TITOVA, L., HRYNKIV, A., MIRONOV, D., VOLIANSKYI, M., ROGATYNSKYI, R., SOLOMKA, O., LYSENKO, S. Comprehensive assessment of technical condition of vehicles during operation based on Harrington's desirability function. *Eastern-European Journal of Enterprise Technologies* [online]. 2024, **1**(3(127), p. 37-46. ISSN 1729-3774, eISSN 1729-4061. Available from: https://doi.org/10.15587/1729-4061.2024.298567

[24] O'KEEFE, R., ROACH, J. W. Artificial intelligence approach to simulation. *Journal of the Operational Research Society* [online]. 1987, **38**, p. 713-722. ISSN 0160-5682, eISSN 1476-9360. Available from: https://doi.org/10.2307/2582843

[25] MILLS, K. L., FILLIBEN, J. J., HAINES, A. L. Determining relative importance and effective settings for genetic algorithm control parameters. *Evolutionary Computation* [online]. 2015, **23**(2), p. 309-342. ISSN 1063-6560, eISSN 1530-9304. Available from: http://dx.doi.org/10.1162/EVCO_a_00137

[26] MIRONOV, D., LYASHUK, O., HEVKO, I., HUPKA, A., SLOBODIAN, L., HEVKO, B., KHOROSHUN, R. Development of a model of a generalized diagnostic indicator of the technical condition of the vehicle chassis using mathematical methods of the theory of experiment planning. *Advances in Mechanical Engineering and Transport* [online]. 2023, **2**(21), p. 135-144. ISSN 2313-5425. Available from: https://doi.org/10.36910/automash.v2i21.1218

[27] EN 1986-2:2001. Electrically propelled road vehicles. Measurement of energy performances. Part 2: Thermal electric hybrid vehicle. Brussels, Belgium: European Standard for Electrically Propelled Vehicles, 2001.

[28] EN 1986-1:1997. Electrically propelled road vehicles. Measurement of energy performances. Part 1: Pure electric vehicle. Brussels, Belgium: European Standard for Electrically Propelled Vehicles, 1997.

DEVELOPING A SPEED-BASED CONGESTION SEVERITY INDEX USING THE CLUSTERING TECHNIQUE FOR DEVELOPING COUNTRIES

Malaya Mohanty, Satya Ranjan Samal*, Kundan Samal

School of Civil Engineering, Kalinga Institute of Industrial Technology (KIIT) Deemed to be University, Bhubaneswar, Odisha, India
*E-mail of corresponding author: satya.samalfce@kiit.ac.in

Malaya Mohanty 0000-0002-6116-782X, Satya Ranjan Samal 0000-0001-8675-453X, Kundan Samal 0000-0003-2142-0656

Resume

A novel approach for traffic congestion assessment has been presented using percentile speeds as key indicators, focusing on urban roads. By evaluating the 98th, 85th, and 15th percentile speeds, authors of the research developed a congestion severity index, offering a more precise and intuitive method for analyzing traffic flow compared to traditional travel time-based indices. Key congestion indices, such as the Planning Time Index (PTI) and Travel Time Index (TTI) were compared to percentile speeds, revealing a significant association with the 15th and 85th percentile speeds. The K-means clustering technique was applied to classify congestion severity into three levels, validated by a high silhouette value indicating the robust clustering. The study's speed-based congestion severity index provides a practical and efficient framework for real-time congestion management, particularly in heterogeneous traffic environments.

Article info

Received 8 October 2024
Accepted 31 January 2025
Online 17 February 2025

Keywords:

traffic congestion
percentile speed
k-mean clustering
silhouette value
congestion severity index

Available online: https://doi.org/10.26552/com.C.2025.020

ISSN 1335-4205 (print version)
ISSN 2585-7878 (online version)

1 Introduction

Traffic congestion is a growing concern globally, affecting both developed and developing countries. The rapid increase in vehicular traffic, coupled with insufficient infrastructure, has led to excessive delays for road users, negatively impacting economic productivity, environmental sustainability, and public health. The development of any country, particularly a nation like India, heavily relies on its transportation infrastructure. With the rapid rise in vehicle numbers, the current road infrastructure is struggling to handle the increased traffic demand, resulting in widespread congestion [1-5]. In developing countries, traffic congestion has become a major challenge for road users. Typically, congestion occurs when current traffic demand surpasses the capacity of existing roadways. This not only extends the travel time, but also negatively impacts human health, contributing to a deteriorating traffic environment [6-8]. The rise in population, the increasing number of vehicles, and the migration of people from rural to urban areas are the primary factors contributing to traffic congestion [9]. Traffic congestion increases driver stress, which can lead to road accidents [10]. Faulty traffic infrastructure, especially in developing countries, such as poorly designed speed humps, an abundance of three-wheelers, and reckless driving behavior, all contribute to prolonged congestion [11-17]. Due to congestion, the Level of Service (LOS) of the road decreases drastically during the peak hours [18]. Understanding the congestion dynamics is crucial for effective traffic management, as it helps implement targeted measures to reduce congestion, enhancing both road safety and traffic flow.

Traditional methods of assessing congestion, such as the Planning Time Index (PTI) and Travel Time Index (TTI), primarily focus on travel times. While these indices provide useful insights, they may not fully capture the complexities of urban traffic, particularly in heterogeneous environments like those found in many Indian cities. Congestion indices, such as TTI and PTI, are widely used around the world to evaluate traffic congestion [19-23]. Despite its fundamental importance, speed has not been directly factored into the

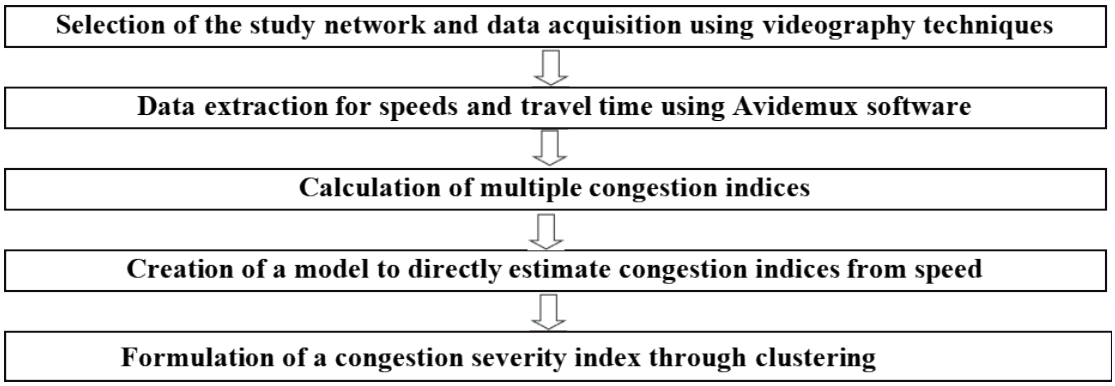

Figure 1 *Flowchart illustrating the research framework*

calculation of congestion indices, while the speed affects travel times, essential for determining these indices. The traditional method relies on average and off-peak travel times, as well as the 95th percentile travel time, neglecting the 15th percentile speed. This 15th percentile speed is particularly significant as it reflects the speeds of the slowest vehicles in the traffic flow, making it a vital indicator of congestion. In this study, clustering techniques were utilized to categorize levels of congestion based on percentile speeds. Clustering techniques were extensively employed to categorize the severity congestion intensity. Clustering is a common technique used to organize specified data into groups, depends on the Euclidean distances between the input information [24-29].

In this study is introduced an alternative approach to evaluating traffic congestion by leveraging percentile speeds, specifically the 98th, 85th, and 15th percentiles, as more direct indicators of congestion severity. By analyzing the speed data, the research aim was to develop a congestion severity index that provides a more intuitive and accurate reflection of traffic flow conditions. In the study are also compared the traditional congestion indices to the speed-based metrics, finding that the 15th and 85th percentile speeds have a stronger correlation with congestion than the 98th percentile. Additionally, K-means clustering is employed to classify congestion into distinct levels, further enhancing the practicality of this speed-based approach for real-time congestion management. This novel methodology offers an enhanced ideas of urban traffic dynamics and serves as a valuable strategy for alleviating congestion in cities with complex traffic patterns.

2 Study framework

The framework is a critical component of any research for achieving the desired results. The current study follows the approach outlined below, as illustrated in Figure 1.

3 Selection of the road network and data collection

To evaluate the traffic congestion, data was collected from various arterial roads. Bhubaneswar, recognized as a tier-II smart city featuring a population of approximately 1.5 million, was chosen for its representation of tier-II cities across India, sharing similar demographic characteristics. The study was focused on selecting the most critical roads for analysis. The road surfaces were mainly bituminous pavements, and the data collection took place during mostly sunny weather, with occasional partial cloud cover.

The speed data and travel time data were obtained from field-recorded videos. Cameras were used for recording data at different times of the day. The time it took for vehicles to cross specific road segments was tracked, allowing for the calculation of their travel time and speeds. The recorded videos were reviewed on a monitor using Avidemux, a free video editing software, and the necessary data, such as the 15th, 85th, and 98th percentile speeds, along with average, 95th percentile, and off-peak travel times, were calculated during this process to meet the study's objectives.

4 Congestion indices

The primary congestion indices, as highlighted in several literature sources are listed below along with their standard formulas or expressions.

$$\text{Planning Time Index} = 95^{\text{th}} \text{ Percentile Travel Time/Off-Peak Travel Time} \quad (1)$$

$$\text{Travel Time Index (TTI)} = \text{Mean Travel Time/Off-Peak Travel Time} \quad (2)$$

$$\text{Buffer Time Index (BTI)} = (95^{\text{th}} \text{ Percentile - Mean Travel Time})/\text{Mean Travel Time} \quad (3)$$

This study was conducted specifically at mid-block

sections under a heterogeneous traffic environment, necessitating modifications to the definitions of congestion indices to suit the study's characteristics. In this research, average travel time, 95th percentile travel time, and off-peak travel time were calculated from the collected travel time data. Based on this data, various congestion indices were computed, and the results were compared to different percentile speeds. A model was then developed to directly estimate congestion index values without relying on travel time data. Finally, a range of congestion index values corresponding to different severity levels was identified using a clustering technique.

5 Results and discussions

Travel times and speeds were derived from the captured videos. As detailed in the "Data Collection and Research Framework" sections, speed and travel time data were gathered for analysis. Key metrics such as the 15th, 85th, and 98th percentile speeds, as well as average, 95th percentile, and off-peak travel times, were estimated and used for further analysis.

These travel times were extracted and analyzed to determine various congestion indices. A combination of quantitative and descriptive analyses was then applied to investigate the traffic congestion. The study focused on three key congestion indices: the Planning Time Index (PTI), the Travel Time Index (TTI), and the Buffer Time Index (BTI), to assess the level of congestion.

The methodology used provides an accurate and dependable means of assessing the traffic congestion by considering real-world traffic flow parameters. The summarized data in Table 1 outlines the various congestion indices calculated using the field data.

The study utilized two congestion indices, namely the PTI and TTI, for assessing congestion levels. The Buffer Time Index (BTI) was omitted from this analysis because initial calculations revealed that it does not sufficiently account for variations in the 95th and 15th percentile travel times throughout both extremely high and moderate traffic volumes. This limitation may stem from the fact that the PTI and TTI relate travel times to off-peak or-free flowing conditions, while the BTI compares travel times to the average travel time. This could introduce bias, particularly in scenarios where there is a significant number of vehicles traveling at either slow or high speeds.

It is important to recognize that many traffic metrics are derived from fundamental parameters like speed, flow, and density. Congestion indices, for instance, are typically based on travel time, which serves as an indirect indicator of speed. Among these factors, operating speed is a critical measure for evaluating the traffic flow and has well-established practical applications in real-world traffic analysis. Given the direct relationship between the speed and congestion, it becomes simpler and more intuitive to assess and analyze traffic congestion using speed data rather than relying on travel time. This is because speed offers a more immediate reflection of traffic conditions, enabling a clearer and more efficient evaluation of congestion levels.

Standard speed calculations, such as the 15th, 85th, and 98th percentile values for a given road, are essential for establishing lower and upper speed limits, as well as determining the design speed. These percentile values serve as benchmarks for safe driving speeds and help guide speed limit policies. Therefore, it is logical to correlate various congestion indices with percentile speeds, as this enhances the overall evaluation of traffic congestion, particularly in areas more susceptible to congestion, by linking it directly to fundamental traffic parameters. For example, the 15th percentile speed is typically used to define the lower speed limit, while the 85th percentile speed represents the upper limit. This range is crucial because around 70% of road users generally drive within these speeds, making them a reliable indicator of traffic behavior. When the two roads have similar 85th percentile speeds but differ in their 15th percentile speeds, this discrepancy reveals differences in traffic flow conditions. Consider two roads, Road 1 and Road 2, both of which have an 85th percentile speed of 38 km/h. However, Road 1 has a 15th percentile speed of 22 km/h, whereas Road 2 has a 15th percentile speed of 11 km/h. This difference suggests that a larger proportion of vehicles on Road 2 travel at lower speeds, indicating heavier congestion or more variability in vehicle speeds. Thus, despite having the same 85th percentile speed, Road 2 is more prone to congestion because more vehicles are operating at reduced speeds. Percentile speeds, particularly the 15th and 85th, are therefore essential in congestion assessment. They not only highlight the variability in traffic flow across different road segments, but also help to identify areas where congestion is more likely to occur. Roads with significant gaps between these two percentile values may exhibit greater congestion issues, as they suggest a broader range of vehicle operating speeds and, potentially, a higher number of slower-

Table 1 *Congestion indices for the selected road network*

Stretch	PTI (%)	TTI (%)	BTI(%)
Stretch 1	200.10	171.50	34.29
Stretch 2	182.23	147.81	26.30
Stretch 3	170.00	126.89	37.66
Stretch 4	140.09	102.91	40.01

Table 2 *Percentile speeds (98th, 85th, and 15th) for different road stretches, [km/h]*

Stretch	98th	85th	15th
Stretch 1	23.9	21.1	15.05
Stretch 2	36.8	27.1	17.90
Stretch 3	38	31.90	21
Stretch 4	50.90	40.80	25.40

Table 3 *Pearson correlation between percentile speeds and congestion indices*

		98th Per. Speed	85th Per. Speed	15th Per. Speed	TTI (%)	PTI (%)
98th Per. Speed	Pearson Correlation	1	0.951**	0.910*	-0.857*	-0.811*
	Sig. (1-tailed)		0.003	0.014	0.030	0.045
85th Per. Speed	Pearson Correlation	0.951**	1	0.973**	-0.944**	-0.910*
	Sig. (1-tailed)	0.003		0.001	0.008	0.014
15th Per. Speed	Pearson Correlation	0.910*	0.973**	1	-0.979**	-0.960**
	Sig. (1-tailed)	0.014	0.001		0.001	0.004
TTI (%)	Pearson Correlation	-0.857*	-0.944**	-0.979**	1	0.986**
	Sig. (1-tailed)	0.030	0.008	0.001		0.000
PTI (%)	Pearson Correlation	-0.811*	-0.910*	-0.960**	.0986**	1
	Sig. (1-tailed)	0.045	0.014	0.004	0.000	

** Significant at 5% significance level

* Significant at 10% significance level

moving vehicles. By associating congestion indices with these percentile speeds, the evaluation becomes more accurate and meaningful, offering a direct link between the congestion severity and key traffic speed parameters.

In this study, the 15th, 85th, and 98th cumulative percentile speed curves were computed for several road stretches. These curves represent the speed distribution across different percentiles of vehicles on the road. After determining these percentile speeds, the identified congestion indices were compared to them, to assess how well the current congestion indices reflect these key speed percentiles. In addition to this comparison, in the study is introduced a novel method of evaluating traffic congestion using percentile speeds, which led to the creation of a congestion severity index, a new metric designed to quantify congestion based on speed variations. Table 2 presents a visual summary of the cumulative percentile speed curves, showcasing the differences observed across various road stretches. This approach helps to better understand how speed distribution relates to congestion, offering a more precise means of evaluating road performance in terms of congestion levels.

The analysis of different percentile speeds, i.e., 98th, 85th, and 15th, reveals a consistent decreasing trend as traffic volume increases. This pattern corresponds to the expected behavior observed in established congestion indices. To further explore the relationship between these percentile speeds and the congestion indices, a Pearson correlation analysis was conducted, specifically examining the correlation between the congestion indices (TTI and PTI) and the 98th, 85th, and 15th percentile speeds. The Pearson correlation analysis assesses the strength and direction of the linear relationship between the congestion indices and the speed percentiles. The results, summarized in Table 3, offer insights into whether there is a statistically significant connection between these variables, helping to understand how well the congestion indices are aligned with the percentile speeds. This correlation helps to validate the effectiveness of percentile speeds in reflecting traffic congestion levels.

The results from the Pearson correlation analysis yielded some unexpected findings. Notably, the PTI and TTI exhibited a significant association with the 15th and 85th percentile speeds, contrasted to the 98th percentile speeds. This observation indicates that TTI and PTI can be effectively estimated directly from either the 15th or 85th percentile speeds, suggesting that these two percentile speeds offer more accurate insights for congestion evaluation than the 98th percentile speed. This highlights the practical utility of focusing on these speeds when assessing the congestion levels.

Table 4 presents the generalized linear regression equations for estimating TTI and PTI directly from the percentile speeds, along with the associated p-values and R-squared values for each independent parameter. As shown, each equation shows statistical significance at a 95% confidence interval (or 5% level of significance), as the p-values for the models are below 0.05 under every instance, except for the equations related to TTI and PTI when using the 98th percentile speed. This

Table 4 *Applying linear regression models for estimating TTI and PTI*

Developed model	p-value	R-Square
TTI = 366.036 - 5.865 X (98th Per. Speed)	0.064 > 0.05	0.75
TTI = 349.011 - 6.831 X (85th Per. Speed)	0.014 < 0.05	0.86
TTI =358.615 - 10.907 X (15th Per. Speed)	0.004 < 0.05	0.96
PTI = 532.833 - 8.767 X (98th Per. Speed)	0.078 > 0.05	0.66
PTI = 511.943 - 10.243 X (85th Per. Speed)	0.040 < 0.05	0.84
PTI = 527.645 - 17.143 X (15th Per. Speed)	0.008 < 0.05	0.91
X represents multiplication		

Figure 2 *Silhouette metric for clusters*

indicates that the relationship between TTI, PTI, and percentile speeds is significant, except in the case of the 98th percentile speed. Additionally, the R-squared values for these equations are all above 0.65, implying that the models explain a considerable proportion of the variability in the data, making them reliable for predicting congestion indices from percentile speeds.

While average and 95th percentile travel times are commonly used to evaluate congestion indices, it is significant to note that stronger R-squared values are observed when these indices are derived from the 85th and 15th percentile speeds. This finding highlights the potential to estimate congestion indices based solely on speed data, eliminating the need to calculate travel times. However, it is important to recognize that relying solely on congestion indices may not provide a complete picture, especially in scenarios with severe congestion. A comprehensive congestion assessment should incorporate both percentile speeds and congestion indices to accurately reflect traffic conditions. The values of the 98th, 85th, and 15th percentile speeds provide valuable insights into actual traffic flow patterns. The results indicate a strong correlation between these percentile speeds and congestion indices. In light of this, a congestion severity index could be developed using the values of the 98th, 85th, and 15th percentile speeds, effectively making traditional congestion index calculations redundant. This approach allows for a more direct and efficient assessment of traffic congestion levels.

In this study, clustering techniques were applied to classify the congestion levels according to percentile speeds. Clustering is a widely used method for grouping data points into a specified number of clusters by evaluating the Euclidean distances between them. The K-means algorithm, commonly used for large datasets with normally distributed data, was selected for this research. It divides the dataset into a predetermined number of clusters (K), based on the Euclidean distance, a method of calculating the straight-line distance between the two points between data points. The algorithm assigns each point to the nearest cluster center (called a centroid), and this process is repeated iteratively until the centroids stabilize, ensuring that each point is placed in the most suitable cluster. The challenge with K-means, however, lies in selecting the correct number of clusters (K). To address this, the study adopted a two-step clustering process. A two-step clustering approach was first employed to identify the optimal number of clusters. The first step involves an algorithm that can estimate the optimal number of clusters based on the input data, rather than pre-defining the number.

Once the optimal number of clusters is identified, the K-means algorithm is applied in the second step to finalize the clustering. After the clustering is performed, the quality of these clusters are validated with the help of silhouette values. A silhouette value measures how similar a data point is to its assigned cluster compared to other clusters. Silhouette is used for interpretation and validation of the internal consistency of data within a cluster [28]. Previous studies [24, 29] have concluded that silhouette could be used to define the number of clusters (K) for clustering analysis. A few studies [28-29] identified that silhouette width index performed well in many comparative experiments. The silhouette value ranges from -1 to 1, with higher values indicating well-defined clusters where the data points are closer to their assigned cluster center and farther from other clusters. In this analysis, the high silhouette value (0.89 as shown in Figure 2) demonstrates that the percentile speed data were effectively grouped, confirming the accuracy and reliability of the clustering process. For traffic engineers, this validation holds significant practical value. By ensuring that the clusters represent distinct congestion levels, engineers can confidently interpret the results and apply them to real-world scenarios. Additionally, a robust clustering approach ensures that the proposed congestion severity index can be effectively used to prioritize interventions, allocate resources, and design the traffic management strategies that address specific congestion challenges. The high silhouette value thus reinforces the applicability of the methodology in assisting traffic engineers to make data-driven decisions aimed at improving traffic flow, enhancing road safety, and minimizing the environmental and economic impacts of congestion.

In the present study, high silhouette value of 0.89 suggests that three clusters provide the best representation for the data in this context. In this research, silhouette values were calculated to determine the quality of clustering, with a particular focus on identifying how well data points were grouped. As shown in Figure 2, the obtained silhouette value was 0.89, which is considered very high. A value of 0.89 indicates that the clusters are well-separated, meaning that the data points within each cluster are highly similar, while the points across clusters are quite distinct. This level of clarity and separation suggests a robust clustering outcome. The analysis determined that three clusters provide the most accurate and meaningful classification of congestion levels based on the percentile speed data. The silhouette value of 0.89 signified that three clusters best represented the dataset, ensuring a precise and reliable classification system for congestion severity, which can guide traffic management and decision-making in real-world scenarios.

Table 5 presents the final cluster centers, which is the direct output from the clustering analysis. The values from Table 5 have been utilized to define the ranges for congestion severity index, which is provided in Table 6. Table 6 illustrates the traffic conditions based on the average speeds of the 98th, 85th, and 15th percentiles for a specific road segment. When these average speeds exceed 44.15 km/h, 35.15 km/h, and 22.43 km/h, respectively, the traffic flow is considered smooth, indicating that there is no congestion. This situation is classified as Congestion Level 0. Conversely, in the case where the mean speed of the 98th percentile falls between 44.15 km/h and 30.65 km/h, the 85th percentile speed ranges from 35.15 km/h to 25.30 km/h, and the 15th percentile speed is between 22.43 km/h and 17.25 km/h, the traffic is categorized as mildly congested. This scenario marks the onset of congestion and is designated as Congestion Level 1. Finally, when the average speeds

Table 5 *Final cluster centers derived from K-means clustering.*

	Cluster Centers		
	1	2	3
98th Per. Speed	50.90	37.40	23.9
85th Per. Speed	40.80	29.50	21.1
15th Per. Speed	25.40	19.45	15.05

Table 6 *Congestion Index formulated through clustering*

98th Per. Speed (km/h)	85th Per. Speed (km/h)	15th Per. Speed (km/h)	Level of congestion severity	Remarks
> 44.15	>35.15	>22.43	Level 0	Free-flowing traffic/Uncongested roads
44.15-30.65	35.15-25.30	22.43-17.25	Level 1	Reasonable Traffic Flow/Mild-to-Moderate Congestion (Road users unable to operate at their desired speed)
<23.90	<21.10	<15.05	Level 2	Overwhelming traffic/Extreme traffic congestion (Vehicles traveling at significantly reduced speeds)

for the 98th, 85th, and 15th percentiles drop below 23.90 km/h, 21.10 km/h, and 15.05 km/h, respectively, it signifies a state of extreme traffic congestion. In this case, the traffic flow can be described as overwhelming, indicating a severe level of congestion.

In the real-world conditions, it is unlikely that the exact speed ranges specified in the proposed congestion severity index will always be maintained consistently. The suggested speed thresholds are tailored for heterogeneous traffic environments and offer a more holistic approach to assessing congestion. This method goes beyond relying solely on congestion index values, providing a more nuanced evaluation of traffic flow and congestion levels by accounting for the variability in traffic patterns. Consequently, these levels present a practical framework for understanding and managing congestion in diverse traffic conditions.

The present study introduces an innovative approach to traffic congestion assessment by utilizing percentile speeds - specifically the 98th, 85th, and 15th percentiles - as direct indicators of congestion severity. Unlike the traditional methods that rely on travel times (e.g., TTI and PTI) and neglect critical speed variations, in this method the 15th percentile speed was highlighted as the key metric reflecting the slowest vehicles, offering a more comprehensive view of congestion.

Using the K-means clustering, congestion levels were categorized into distinct groups based on speed data, providing a practical framework for real-time traffic management. The findings demonstrate stronger correlations between the 15th and 85th percentile speeds and congestion severity compared to traditional indices, showcasing the superiority of this speed-based methodology in capturing urban traffic dynamics, particularly in heterogeneous environments.

6 Conclusion

In this study, a novel framework is proposed for the traffic congestion assessment using percentile speed metrics, specifically the 98th, 85th, and 15th percentiles, to develop a congestion severity index. Applied to urban roads in Bhubaneswar, India, the research highlights the limitations of traditional congestion indices like the Travel Time Index (TTI) and Planning Time Index (PTI) in isolation and emphasizes the predictive power of percentile speeds.

The summary of key findings are as follows.

- Percentile Speed Metrics for Congestion Assessment: The 98th, 85th, and 15th percentile speeds were identified as reliable indicators of traffic congestion, surpassing traditional indices like TTI and PTI in precision
- Correlation and Sensitivity: Strong correlations were observed between the 15th and 85th percentile speeds and congestion indices, with the 15th percentile speed showing the highest sensitivity.
- Clustering and Congestion Levels: K-means clustering revealed three congestion levels with clear speed thresholds:
  - ❑ Smooth Traffic: Speeds > 44.15 km/h (98th), 35.15 km/h (85th), 22.43 km/h (15th).
  - ❑ Moderate Congestion: Speeds in intermediate ranges.
  - ❑ Severe Congestion: Speeds < 23.90 km/h (98th), 21.10 km/h (85th), 15.05 km/h (15th).
- Congestion Severity Index: A robust severity index was developed using percentile speed data, providing a simpler and more intuitive approach for congestion evaluation.
- Practical Implications: This framework eliminates reliance on complex travel time data, making it highly suitable for heterogeneous traffic environments and real-world traffic management.

This approach offers a practical, intuitive alternative to traditional travel time-based methods, particularly in heterogeneous traffic environments, facilitating efficient traffic management and policy-making.

Acknowledgment

The authors received no financial support for the research, authorship and/or publication of this article.

Conflicts of interest

The authors declare that they have no known competing financial interests or personal relationships that could have appeared to influence the work reported in this paper.

References

[1] PADIATH, A., VANAJAKSHI, L., SUBRAMANIAN, S. C., MANDA, H. Prediction of traffic density for congestion analysis under Indian traffic conditions. In: 12th International IEEE Conference on Intelligent Transportation Systems ITSC 2009: proceedings [online]. IEEE. 2009. ISBN 9781424455195, p. 78-83. Available from: https://doi.org/10.1109/ITSC.2009.5309716

[2] SAMAL, S. R., DAS, A. K. Evaluation of traffic congestion parameters under heterogeneous traffic condition: a case study on Bhubaneswar City [online]. In: *Transportation research. Lecture notes in civil engineering. Vol. 45.* MATHEW, T. M., JOSHI, G. J., VELAGA, N. R., ARKATKAR, S. (Eds.). Singapore: Springer, 2020.

ISBN 978-981-32-9041-9, eISBN 978-981-32-9042-6, ISSN 2366-2557, eISSN 2366-2565, p. 675-684. Available from: https://doi.org/10.1007/978-981-32-9042-6_53

[3] DUBEY, P. P., BORKAR, P. Review on techniques for traffic jam detection and congestion avoidance. In: 2015 2nd International Conference on Electronics and Communication Systems ICECS 2015: proceedings [online]. IEEE. 2015. eISBN 978-1-4799-7225-8, p. 434-440. Available from: https://doi.org/10.1109/ECS.2015.7124941

[4] SAMAL, S. R., KUMAR, P. G., SANTHOSH, J. C., SANTHAKUMAR, M. Analysis of traffic congestion impacts of urban road network under Indian condition. *IOP Conference Series: Materials Science and Engineering* [online]. 2020, **1006**(1), 012002. ISSN 1757-8981, eISSN 1757-899X. Available from: https://doi.org/10.1088/1757-899X/1006/1/012002

[5] UDDIN, A. Traffic congestion in Indian cities: challenges of a rising power. Naples: Kyoto of the Cities, 2009.

[6] SAMAL, S. R., MOHANTY, M., SANTHAKUMAR, S. M. Adverse effect of congestion on economy, health and environment under mixed traffic scenario. *Transportation in Developing Economies* [online]. 2021, **7**(2), p. 1-10. ISSN 2199-9287, eISSN 2199-9295. Available from: https://doi.org/10.1007/s40890-021-00125-4

[7] MAHMUD, K., GOPEAND, K., CHOWDHURY, S. M. Possible causes and solutions of traffic jam and their impact on the economy of Dhaka City. *Journal of Management and Sustainability* [online]. 2012, **2**(2), p. 112-135. ISSN 1925-4725, eISSN 1925-4733. Available from: https://doi.org/10.5539/jms.v2n2p112

[8] SAMAL, S. R., MOHANTY, M., GORZELANCZYK, P. Exploring the traffic congestion and improving travel time reliability measures in heterogeneous traffic environments: a focus on developing countries. *Communications - Scientific Letters of the University of Zilina* [online]. 2023, **25**(4), D91-D102. ISSN 1335-4205, eISSN 2585-7878. Available from: https://doi.org/10.26552/com.C.2023.074

[9] DOWNS, A. Stuck in traffic: coping with peak-hour traffic congestion. Brookings Institution Press, 2000. ISBN 081571923X.

[10] HENNESSY, D. A., WIESENTHAL, D. L. Traffic congestion, driver stress, and driver aggression. *Aggressive Behavior: Official Journal of the International Society for Research on Aggression* [online]. 1999, **25**(6), p. 409-423. eISSN 1098-2337. Available from: https://doi.org/10.1002/(SICI)1098-2337(1999)25:6<409::AID-AB2>3.0.CO;2-0

[11] MOHANTY, M., RAJ, Y., ROUT, S., TIWARI, U., ROY, S., SAMAL, S. R. Operational effects of speed breakers: a case study in India. *European Transport / Trasporti Europei* [online]. 2021, **81**(1), p. 1-10. ISSN 1825-3997. Available from: https://doi.org/10.48295/ET.2021.81.1

[12] SAMAL, S. R., MOHANTY, M., BISWAL, D. R. A review of effectiveness of speed reducing devices with focus on developing countries. *Transactions on Transport Sciences* [online]. 2022, **13**(1), p. 65-73. ISSN 1802-9876. Available from: https://doi.org/10.5507/tots.2021.018

[13] SAMAL, S. R., MOHANTY, M., BISWAL, D. R. Operational effectiveness of speed humps in urban areas - a review. In: Recent Developments in Sustainable Infrastructure ICRDSI-2020: proceedings [online]. Springer. Vol. 2. 2020. ISBN 978-981-16-7508-9, eISBN 978-981-16-7509-6, p. 841-850. Available from: https://doi.org/10.1007/978-981-16-7509-6_66

[14] SAMAL, S. R., MOHANTY, M., GIREESH KUMAR, P., SANTHAKUMAR M, M. Evaluation of functional effectiveness of speed humps in accordance to IRC specifications. In: 2nd International Conference on Sustainable Construction Technologies and Advancements in Civil Engineering ScTACE 2021: proceedings [online]. Springer. 2022. ISBN 978-981-19-0188-1, eISBN 978-981-19-0189-8, p. 105-114. Available from: https://doi.org/10.1007/978-981-19-0189-8_9

[15] MOHANTY, M., PATTANAIK, M. L., SAMAL, S. R. Assessing the impact of three-wheelers on traffic flow in India: a case study using ANN. *Communications - Scientific Letters of the University of Zilina* [online]. 2024, **26**(3), A50-A65. ISSN 1335-4205, eISSN 2585-7878. Available from: https://doi.org/10.26552/com.C.2024.033

[16] SAMAL, S. R. MOHANTY, M., GORZELANCZYK, P. Exploring lane changing dynamics: A comprehensive review of modelling approaches, traffic impacts, and future directions in traffic engineering research. *Transactions on Transport Sciences* [online]. 2024, **15**(2), p. 54-68. ISSN 1802-9876. Available from: https://doi.org/10.5507/tots.2024.005

[17] MOHANTY, M., SAMAL, S. R. Role of young drivers in road crashes: a case study in India. *European Transport / Trasporti Europei*. 2019, **74**(1), p. 1-9. ISSN 1825-3997.

[18] KUMAR, P. G., SAMAL, S. R., PRASANTHI, L., BHAVITHA, V., DEVI, J. M. Level of service of urban and rural roads - a case study in Bhimavaram. *IOP Conference Series: Materials Science and Engineering* [online]. 2020, **1006**(1), 012018. ISSN 1757-899X. Available from: https://doi.org/10.1088/1757-899X/1006/1/012018

[19] LYMAN, K., BERTINI, R. L. Using travel time reliability measures to improve regional transportation planning and operation. *Transportation Research Record: Journal of the Transportation Research Board* [online]. 2008, **2046**(1), p. 1-10. ISSN 0361-1981, eISSN 2169-4052. Available from: https://doi.org/10.3141/2046-01

[20] SAMAL, S. R., MOHANTY, M., SELVARAJ, M. S. Assessment of traffic congestion under Indian environment-a case study. *Communications - Scientific Letters of the University of Zilina* [online]. 2022, **24**(4), p. D174-D182. ISSN 1335-4205, eISSN 2585-7878. Available from: https://doi.org/10.26552/com.C.2022.4.D174-D182

[21] RAO, A. M., RAO, K. R. Measuring urban traffic congestion-a review. *International Journal for Traffic and Transport Engineering* [online]. 2012, **2**(4), p. 286-305. ISSN 2217-544X, eISSN 2217-5652. Available from: http://dx.doi.org/10.7708/ijtte.2012.2(4).01

[22] MOHANTY, M., SARKAR, B., PATTANAIK, M. L., SAMAL, S. R., GORZELANCZYK, P. Development of congestion severity index for uncontrolled median openings utilising fundamental traffic parameters and clustering technique: a case study in India. *International Journal of Intelligent Transportation Systems Research* [online]. 2023, **21**(3), p. 461-472. ISSN 1348-8503, eISSN 1868-8659. Available from: https://doi.org/10.1007/s13177-023-00365-1

[23] HE, F., YAN, X., LIU, Y., AND MA, L. A traffic congestion assessment method for urban road networks based on speed performance index. *Procedia Engineering* [online]. 2016, **137**, p. 425-433. ISSN 1877-7058. Available from: https://doi.org/10.1016/j.proeng.2016.01.277

[24] ROUSSEEUW, P. J. Silhouettes: A graphical aid to the interpretation and validation of cluster analysis. *Journal of Computational and Applied Mathematics* [online]. 1987, **20**, p. 53-65. ISSN 0377-0427, eISSN 1879-1778. Available from: https://doi.org/10.1016/0377-0427(87)90125-7

[25] YADAV, J., SHARMA, M. A review of K-mean algorithm. *International Journal of Engineering Trends and Technology (IJETT).* 2013, **4**(7), p. 2972-2976. ISSN 2231-5381.

[26] SAMAL, S. R., MOHANTY, M., GORZELANCZYK, P. Perception based level of service for speed humps in mixed traffic conditions - a case study in India. *Communications - Scientific Letters of the University of Zilina* [online]. 2024, **26**(1), p. D11-D26. ISSN 1335-4205, eISSN 2585-7878. Available from: https://doi.org/10.26552/com.C.2024.010

[27] BOORA, A., GHOSH, I., CHANDRA, S. Assessment of level of service measures for two-lane intercity highways under heterogeneous traffic conditions. *Canadian Journal of Civil Engineering* [online]. 2017, **44**(2), p. 69-79. ISSN 1208-6029. Available from: https://doi.org/10.1139/cjce-2016-0275

[28] MOHAPATRA, S. S., BHUYAN, P. K., RAO, K. V. Genetic algorithm fuzzy clustering using GPS data for defining level of service criteria of urban streets. *European Transport/Trasporti Europei*. 2012, **52**, p. 1-18. ISSN 1825-3997.

[29] ARBELAITZ, O., GURRUTXAGA, I., MUGUERZA, J., PEREZ, J.M. PERONA, I. An extensive comparative study of cluster validity indices. *Pattern Recognition* [online]. 2013, **46**(1), p. 243-256. ISSN 0031-3203, eISSN 1873-5142. Available from: https://doi.org/10.1016/j.patcog.2012.07.021

REVISITING PCU VALUES OF VARIOUS VEHICLES IN MIXED TRAFFIC CONDITIONS: ESTIMATION AND COMPARISON

Amir Ali Khan*, Sachin Dass

Deenbandhu Chhotu Ram University of Science and Technology, Murthal, Sonipat, India

*E-mail of corresponding author: amirm640@gmail.com

Amir Ali Khan 0000-0002-3309-9831, Sachin Dass 0000-0003-1015-4807

Resume

This study is an attempt to derive and to compare the Passenger Car Unit (PCU) values of vehicle types present in the stream, obtained using the Chandra's method, homogeneous coefficient method, speed-based modelling, and multiple linear regression method. Using the data collected from five sites of Sonipat City with varying traffic and geometric characteristics, it was found that Chandra's method is the best method to derive the PCU values in heterogeneous traffic conditions on divided urban roads. The PCU values obtained from Chandra's method are closer to IRC (Indian Roads Congress) code values. The PCU value of e-rickshaw was also estimated in this study, and it was found that it is smaller than one using the Chandra's method. The result of the comparison of obtained PCU values and values given in the IRC code points to conclusion that the IRC codes pertaining to PCU values need revision.

Article info

Received 30 August 2024
Accepted 12 February 2025
Online 6 March 2025

Keywords:

PCU
Chandra's method
IRC
comparison
speed-based modelling

Available online: https://doi.org/10.26552/com.C.2025.025

ISSN 1335-4205 (print version)
ISSN 2585-7878 (online version)

1 Introduction

The passenger car unit (PCU) is an equivalency factor assigned to each kind of a vehicle in the flow, to convert each vehicle category to a single homogeneous unit. It is critical to establish the Passenger Car Unit (PCU) values for each vehicle type for the building and analysis of various traffic facilities, as well as for managing the traffic control. The adoption of appropriate PCUs for diverse vehicle types will accurately quantify the homogenous volume of traffic in the mixed transportation environment. There are various approaches available for estimating the PCUs for each vehicle category, namely, Chandra's Method [1], Homogeneous Coefficient Method [2], Headway Method [3], Multiple Linear Regression [4-5], Speed based Modelling [6], Density method [7], Huber's Method [8], Simulation technique [9-10]. However, different methods are used for different traffic and roadway conditions.

In this study, the PCU values of each vehicle category were derived and compared to the values given in the IRC (Indian Roads Congress) code (IRC: 106-1990). The PCU value for e-rickshaw was developed in this study, as well. E-rickshaw is a new vehicle type. It is a substitute for cycle rickshaw and is different from auto rickshaws in terms of speed and capacity. Auto-rickshaw has relatively higher speed because it is powered by fuel (CNG, petrol or diesel), the while e-rickshaw is driven by a battery. E-rickshaws are gaining popularity, especially in Asian developing countries like India, Bangladesh etc. because of low operating and maintenance costs. The PCU value of this type of vehicle is not available in the literature. Chandra's method, homogeneous coefficient method, speed-based modelling, and multiple linear regression methods were used to derive PCU values of vehicle types present in the stream. It is a case study of Sonipat City. Five sites of varying traffic and geometric parameters were selected, and by videography method, classified speed and volume data were collected and processed with the help of a VLC media player. The aims of this study were as follows.

1. To derive the PCU values of vehicle types present in the stream using different methods.
2. To compare the PCU values derived using different methods.
3. To compare the PCU values with the values given in IRC: 106-1990 and other literature.
4. To derive the PCU value of e-rickshaw (PCU value of e-rickshaw is not available in the IRC code)

The results of this study will benefit planners and

engineers in dealing with heterogeneous traffic, and it will also be helpful in revising the IRC code pertaining to PCU values.

2 Review of published research

Dhananjaya et al. (2023) applied Chandra's method to get the passenger car unit of vehicle types for four different stretches in Sri Lanka's Colombo district. Field surveys were used to collect data, speed and vehicle area. Obtained results were compiled and compared to existing values with the goal of proposing a fresh set for generalized transport investigations in the nation of Sri Lanka [11].

Zero et al. (2022) collected data on passenger car unit for various vehicle types in Erbil City under mixed traffic conditions. Results showed significant variations in passenger car unit with traffic volume and roadway width. Buses had a PCU value of 2.92, similar to Iraq but different from the UK. Highway capacity increased with shoulder areas, positively affecting passenger car unit for vehicle types. Passenger car units were evaluated using Headway, Density, and Homogeneous Coefficient methods [12].

Ali et al. (2021) used Chandra's method and modified it (the modified version of Chandra's method uses average headway along with the average speed and projected rectangular area) for the estimation of PCUs on NHs (National Highways) as:

$$(PCU)_a = Headway\ factor \times Area\ Factor \times \\ \times Speed\ Factor. \quad (1)$$

It was concluded that the Modified Chandra Method gives a higher value for more vehicle types [13].

The PCE (Passenger Car Equivalency of e-rickshaw was developed by Khan and Singh (2021) using Chandra's method of PCE determination and speed-based modelling on urban roads of Sonepat city of Haryana. Parameters considered for this study were the speed of vehicles, traffic volume, traffic composition, and average rectangular area of vehicles present in the stream. It was concluded that PCE of e-rickshaw changes with the change in traffic parameters. The PCE value of e-rickshaw increases positively with the composition of e-rickshaw and decreases as the traffic volume builds up in the stream. However, carriageway width has no significant impact on the PCE of e-rickshaw [14].

Ballari (2020) reviewed various research with respect to methods of estimation of passenger car units in terms of the trucks with different performance measures at the midblock sections [15].

Dasani et al. (2020) used different methods, namely Chandra's method, homogeneous coefficient method, headway method, and multiple linear regression method, to estimate dynamic equivalency factor (DEF) (a term used for Passenger car unit) for different vehicles on mid-block sections of Porbandar city. The study's characteristics included headway, the width of the road, the composition of traffic, and average speed. It was found that the Headway method yields higher dynamic equivalency factor values for MAV (Multi-Axle vehicle), truck, and bus and lower values for bike and autos than IRC standards, the Multiple Linear Regression method produces values for LCVs (Light Commercial Vehicles) that are almost identical to IRC standards, and the Homogenization Coefficient method produces equivalent values for all classes of vehicles. Chandra's approach produces outcomes that are more similar to IRC codes [2].

Sharma and Biswas (2021) examined passenger car units on city roads. They examined various methods for determining the PCU or PCE values and demonstrated how their effectiveness varies depending on the field situation. The estimated PCU values proposed in various research were also highlighted in the current paper. Some researchers suggested static PCU values, while others investigated its dynamic facets [16].

Pooja et al. (2019) examined methods for estimating PCU or PCE values. This paper provided an in-depth examination of methods for estimating the PCU/PCE values for homogeneous and heterogeneous conditions. An attempt was made to identify the limitations of existing PCU estimation methods and to identify potential solutions to these limitations [17].

Parth et al. (2018) calculated dynamic PCU/PCE for vehicles on urban roads with varying traffic conditions. In the current study is shown the dynamic nature of passenger car unit values on two different roads with highly varying traffic conditions. Using Chandra's method, the PCU values were calculated for both roads. Both roads' PCU factors were found to be extremely sensitive to changes in the traffic stream, whether in terms of traffic composition or traffic volume. The type of road also has an impact on it [18].

The PCU values using data from six highway locations of Andra Pradesh were calculated and compared by Rao and Yadav (2018). The speed and area of vehicles were considered to derive PCU values. Speed volume relations were also developed to check the effect of traffic parameters. The obtained PCU values were later compared to the recommended values of IRC: 106-1990 [6].

Barve and Sugandhi (2017) examined a highway-capable passenger car unit (PCU). They attempted to cover the most critical and recent research work in the advancement of PCE or PCU in both homogeneous and heterogeneous traffic conditions. In this study authors addressed and gathered multiple methods for estimating the PCU values. For the calculation of PCU, each method has its own set of factors, such as traffic conditions, geometric factors, headway time, speed, delay, and so on. The PCE or PCU values were found to vary based on traffic situation [19].

Mondal et al. (2017) estimated PCU or PCE values for mixed traffic streams on Kolkata's urban arterials. Author aimed to determine the passenger car unit values for various vehicle categories under non-homogenous traffic conditions on the mid-block section of inter-city arterials, as well as evaluate the variation of PCE values to different traffic stream parameters. Based on the variation of passenger car unit or equivalency, mathematical relationships were developed and validated using statistical analysis [20].

Table 1 *Summary of past research related to PCU estimation*

Author	Year	Method Used	Nature of Traffic	Type of road	No of Sites	Country of Study	Traffic Parameters considered
Dhananjaya et al. [11]	2023	Chandra's method	Mixed	Urban road	4	Sri Lanka	Speed
Zero et al. [12]	2022	Headway, Density and Homogeneous Coefficient method	Mixed	Urban road	5	Iraq	Speed, Volume
Ali et al. [13]	2021	Chandra's method and Modified Chandra's method	Mixed	National Highway	1	Pakistan	Headway, Speed
Dasani et al. [2]	2020	Chandra's method, Homogenization coefficient method, Multiple regression method and Headway method	Mixed	Urban road	3	India	Speed, composition and headway
Vijay et al. [31]	2019	Chandra's method	Mixed	2 lane Highway	12 sites	India	Speed
Rajesh and Rao [32]	2018	Chandra's method and speed-volume relationship	Mixed	2 lane urban road	3	India	Speed and Volume
Parth et al. [18]	2018	Chandra's method	Mixed	Urban road	2	India	Speed, Volume and Composition
Chand [21]	2016	Chandra's method, Density method, and Headway method	Mixed	Plain and hilly roads	2	India	Speed, headway and Density

Table 2 *Summary of past research related to PCU estimation*

Author	Year	Method Used	Nature of Traffic	Type of road	No of Sites	Country of Study	Traffic Parameters considered
Dhamaniya and Chandra [22]	2016	Chandra's method and speed-volume relationship	Mixed	Urban road	8	India	Speed, Volume and Composition
Shalkamy et al. [33]	2015	Chandra's method	Mixed	2 lane rural road	6	Egypt	Speed
Khanorkar and Ghodmare [27]	2014	Chandra's method and speed-volume relationship	Mixed	2 lane highway	4	India	Speed and Volume
Kumar et al. [34]	2018	Area Occupancy method, TRRL definition	Mixed	Multilane	8	India	V/C ratio
Biswas et al. [35]	2017	Kriging based approach	Mixed	Six lane divided road	1	India	Speed
Jassal et al. [36]	2025	Axle based mapping approach	Mixed	Two lane dual carriageway	1	India	Speed and Flow
Behzadi and Shakibaei [37]	2016	Headway and Density method	Mixed	Urban roads	1	Iran	Density, headway and speed
Sugiarto et al. [38]	2018	Time occupancy method	Mixed	Roundabout	1	Indonesia	Time occupancy
Subotic et al. [39]	2016	Time Headway	Mixed	Two lane roads	3	Serbia	Headway

Chand (2016) determined and compared the Passenger Car Unit (PCU) values on both hilly and plain urban roads. In this paper author considered a 3.2 km long section of a road in Visakhapatnam city, of which 1.9 km is plain and 1.3 km is hilly. PCE values were estimated using different methods. In both plain and hilly terrains, Chandra's method was found to produce more accurate results [21].

Simultaneous Equations and Chandra's method were used by Dhamaniya and Chandra (2016) to estimate dynamic Passenger Car Units on city roads. To illustrate the dynamic nature of the passenger car unit factor, data obtained on eight city road roads in India were analyzed. To determine the speed of different vehicles, all vehicles in the stream of traffic were classified into five categories, and simultaneous equations were developed. The PCU/PCE values obtained by using Chandra's method and simultaneous equations are very similar. Passenger car unit values for a vehicle were found to increase with the vehicle's share in the traffic stream [22].

Mahidadiya and Juremalani (2016) examined the global scenario for PCU estimation. A literature review on PCU or PCE values was discussed in this work. The majority of papers in this field concentrate on evaluating PCU at particular parts of the road as well as at intersections. The PCU or PCE values have been observed to fluctuate in response to traffic patterns. PCU values have not been calculated universally, taking into consideration all effects such as gradient, shoulder condition, road roughness, vehicle percentage, and share of slow-moving vehicles [23].

Nokandeh et al. (2016) used the method proposed by Chandra and simultaneous equations based on linear regression to derive passenger car unit values for highly heterogeneous situations [24].

The status of highway capacity research was described by Chandra (2015) in India on all types of highways. This paper presented a view of capacity-related studies [25].

In India, Mardani et al. (2015) calculated the Passenger Car Unit (PCU) values of vehicle types on undivided interurban roads. The purpose of this study was to investigate the influence of carriageway width on passenger car unit of various vehicle types. Data were obtained from ten stretches of various Indian roads. According to the findings, the PCU or PCE value for a type of vehicle tends to vary with traffic volume and composition, as well as the carriageway width of the street that is used [26].

Khanorkar and Ghodmare (2014) developed passenger car unit values for vehicles operating in mixed traffic on congested highways in cities. Data in this study were gathered using videography at 5 stretches of the two-lane highways in and around Nagpur to measure the effects of lane width and shoulder condition on the capacity of the 2-lane highways. Chandra's method was used to calculate PCU or PCE values. The PCU or PCE value of a vehicle was found to alter significantly depending on the traffic volume and roadway width based on a study of traffic volume and roadway conditions. It was discovered that as lane width increases, so does the PCU or PCE value of a vehicle type. The PCU or PCE is linearly changed as a function of the lane width [27].

Khanorkar et al. (2014) estimated the effect of lane width on the capacity on congested highways of Nagpur city with heterogeneous traffic. Data for this research were obtained at six locations to measure the influence of lane width and shoulder condition on the capacity. The PCU or PCE values for various vehicle types were determined separately for each of the selected locations. The newly calculated equivalency values differed significantly from the IRC code values [28].

Minh et al. (2005) used a modified version of Chandra's method. They considered a motorcycle as a base vehicle instead of a car due to the high proportion of motorcycles in the stream. The PCU values of a vehicle types were derived as:

$$(PCU)_a = \frac{V_{mc}/V_a}{A_{mc}/A_a}, \tag{2}$$

where: V and A are the speed and area, respectively, and mc and a stand for motorcycle and vehicle type "a", respectively, [29].

Omar et al. (2020) review the methods of PCU estimation. In this study, publications devoted to works on PCU estimation were summarised and different methods were discussed in detail [30].

A summary of some past research pertaining to PCU estimation is shown in Tables 1-2.

3 Data collection and methodology

The methodology followed in this study is presented in Figure 1. Five different road sections of Sonipat city with different carriageways and shoulder widths were selected to calculate the PCU values of vehicles present in the stream using Chandra's method, Homogeneous Coefficient method, Speed-based modelling, and multiple linear regression method. Description of the selected sites is presented in Table 3. All selected sections are located in the main city Sonipat. The estimated population of Sonipat city is 382000. This city is in the Haryana state of India and is located at just 46 km distance from Delhi (Capital of India).

For the data collection, three hour-long videos were captured from the selected road sections, and desired data (classified volume and speed of vehicle types) were extracted using the VLC media player. Data collection was done for every 15-minute interval. The composition of different types of vehicles observed on these sites is shown in Figure 2. The speed of vehicles was calculated by measuring the time taken by the vehicle to cross

a section of predefined length. Speed and volume data for site 1 is presented in Figure 3. Similarly, data from other sites were collected and interpreted. Speed ratios of car with respect to other vehicle types are presented in Table 4. The length and width of vehicle types were also noted. Area ratios of standard vehicle (car) with respect to different types of vehicles, which is required for Chandra's method, and length ratios of standard vehicle (car) with respect to different types of vehicles , which is required for the Homogeneous Coefficient method, are presented in Table 5. Data was collected on sunny days. Stretches selected to collect data were away from any intersections and other obstructions like parking, pedestrian flow etc. The composition of cycles in the stream ranges from 2.49% to 6.77% and their movement was mostly in singles. The share of bike, auto-rickshaw and e-rickshaw is ranged from 43.24% to 70.83%.

Table 3 *Description of Selected Sites*

Site	Carriageway Width (m)	Shoulder Width (m)	Location
1	6.71	Raised footpath	29°00'05"N, 77°00'22"E
2	4.11	2.54	29°00'13"N, 77°01'44"E
3	6.75	Raised footpath	28°59'47"N, 77°00'31"E
4	7.2	5.80	28°59'22"N, 77°02'15"E
5	4.73	1.75	28°58'40"N, 77°01'45"E

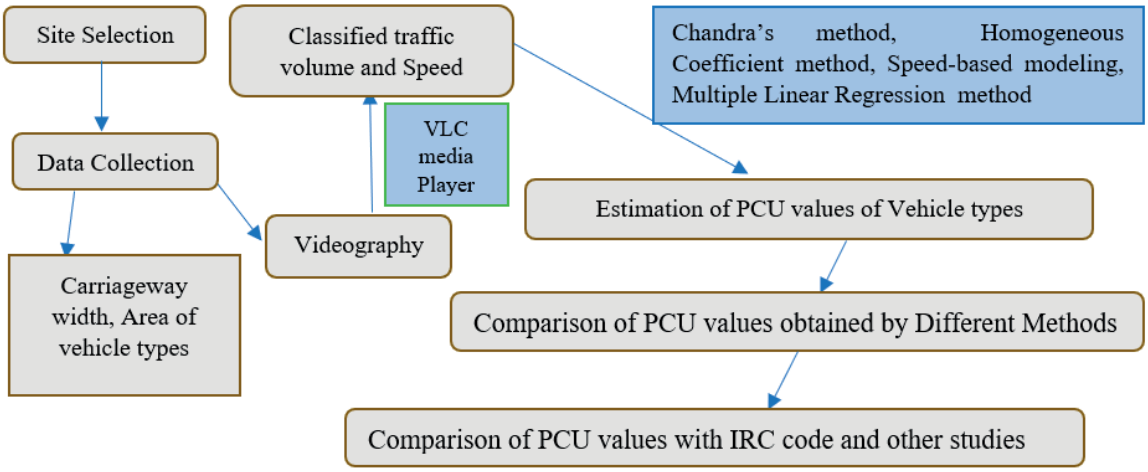

Figure 1 *Followed methodology for this study*

Table 4 *Speed ratios of vehicle types*

Site	Vc/Vb	Vc/Var	Vc/Ver	Vc/Vl	Vc/Vcy	Vc/Vbs	Vc/Vtr	where, V = Speed
1	0.974	1.105	1.571	1.164	2.320	1.123	1.917	c = car, b = bike,
2	1.016	1.027	1.487	1.155	2.281	1.019	1.374	ar = auto-rickshaw,
3	1.050	1.081	1.617	1.136	2.259	1.013	1.522	er = e-rickshaw, l = LCV,
4	1.054	1.231	1.499	1.116	2.034	1.080	1.265	cy = cycle, bs = bus,
5	0.977	1.106	1.396	1.050	1.966	1.116	1.344	tr = truck

Table 5 *Area and length ratio of vehicle types*

Area Ratios		Length Ratios		Notations
Ac/Ab	4.621	Lc/Lb	1.989	A, L are area and length of vehicles respectively.
Ac/Aar	1.196	Lc/Lar	1.163	C = car, b = bike, ar = auto-rickshaw, er = e-rickshaw, l = LCV,
Ac/Aer	1.971	Lc/Ler	1.333	cy = cycle, bs = bus, and tr = truck.
Ac/Al	0.418	Lc/Ll	0.610	
Ac/Acy	6.269	Lc/Lcy	1.958	
Ac/Abs	0.218	Lc/Lbs	0.368	
Ac/Atr	0.307	Lc/Ltr	0.496	

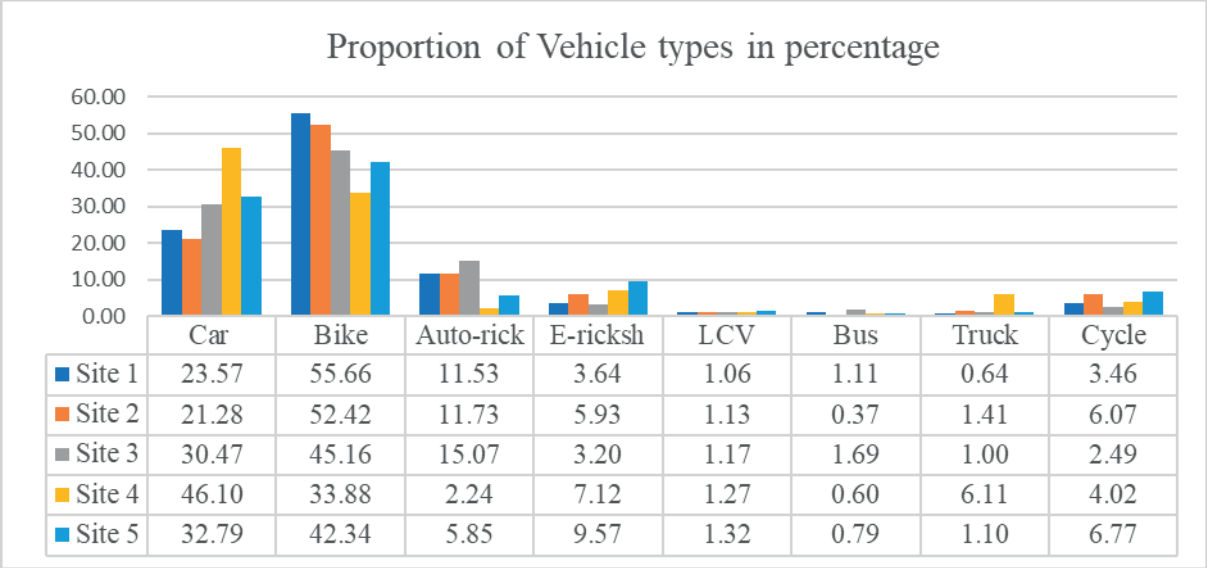

	Car	Bike	Auto-rick	E-ricksh	LCV	Bus	Truck	Cycle
Site 1	23.57	55.66	11.53	3.64	1.06	1.11	0.64	3.46
Site 2	21.28	52.42	11.73	5.93	1.13	0.37	1.41	6.07
Site 3	30.47	45.16	15.07	3.20	1.17	1.69	1.00	2.49
Site 4	46.10	33.88	2.24	7.12	1.27	0.60	6.11	4.02
Site 5	32.79	42.34	5.85	9.57	1.32	0.79	1.10	6.77

Figure 2 *Proportion of Vehicle types on different sites in percentage*

Intervals	Speed of Vehicle types (in m/s)								Volume of Vehicle types							
	V_c	V_b	V_{ar}	V_{er}	V_l	V_{cy}	V_{bs}	V_{tr}	Nc	Nb	Nar	Ner	Nl	Ncy	Nbs	Ntr
1 interval	9.65	10.17	7.96	6.28	7.68	4.33	9.12	5.71	93	213	44	10	8	8	4	2
2 interval	8.63	10.11	8.63	5.55	8.02	3.91	0.00	5.39	107	224	46	13	3	15	0	2
3 interval	9.77	9.40	7.71	5.67	7.69	3.86	8.20	0.00	92	243	45	10	2	13	2	0
4 internal	9.77	10.25	7.94	6.07	6.73	4.16	8.84	5.39	85	192	46	10	1	16	4	1
5 interval	8.71	9.09	8.02	6.30	6.98	3.87	9.20	6.46	92	233	47	16	4	16	4	3
6 interval	8.79	8.55	8.57	5.68	8.34	4.13	8.38	6.28	83	228	46	17	5	21	2	3
7 interval	9.50	8.77	8.65	6.08	7.21	3.75	8.47	5.54	101	220	48	10	3	17	2	2
8 interval	9.14	9.11	8.85	6.03	9.55	4.09	8.91	7.54	90	205	60	15	4	11	7	2
9 interval	8.59	8.69	7.87	5.41	8.44	4.35	9.67	4.90	94	237	40	21	3	16	2	3
10 interval	8.29	9.13	8.25	5.25	7.94	3.96	9.92	5.35	105	248	53	32	4	17	3	2
11 interval	9.82	8.89	8.25	5.62	7.66	3.82	7.44	0.00	111	268	43	12	4	14	5	0
12 interval	9.15	10.56	8.69	5.96	8.08	4.38	9.67	4.71	111	239	49	16	6	6	2	1
Average	9.15	9.39	8.28	5.83	7.86	4.05	8.15	4.77	97	229	47	15	4	14	3	2

Where, V is the average speed and N is the number of vehicles in each interval. And c = car, b = bike, ar = auto-rickshaw, er = e-rickshaw, l = LCV (light commercial vehicle), cy = cycle, bs = bus, and tr = truck

Figure 3 *Speed and Volume data for Site 1*

4 Estimation of PCU values of vehicle types

Data were analyzed using different methods of PCU calculation. PCU of vehicle types were determined using Chandra's method, homogeneous coefficient method, speed-based modelling, and multiple linear Regression method.

4.1 PCU determination using Chandra's method

This method was proposed by Chandra [1]. As per this method, Passenger car unit of vehicles under heterogenous traffic conditions can be calculated as:

$$(PCU)_x = \frac{Speed\ ratio\ of\ car\ vehicle\ type\ x}{Are\ ratio\ of\ car\ vehicle\ type\ x}. \quad (3)$$

The speed ratio and area ratio are given in Table 4 and Table 5, respectively. Calculated PCU values using this method are listed in Table 6 with the help of interpreted data.

4.2 PCU determination using Homogeneous coefficient method

This method was proposed by Permanent International Association of Road Congress (PIARC) [2]. This method is very similar to Chandra's method. Instead of area ratio, length ratio is used in this method. PCU can be calculated as:

$$(PCU)_x = \frac{Speed\ ratio\ of\ car\ vehicle\ type\ x}{Length\ ratio\ of\ car\ vehicle\ type\ x}. \quad (4)$$

Table 6 *Developed PCU values of vehicle types using Chandra's and Homogeneous coefficient method*

Site	Method	Passenger Car Unit values using Chandra's and homogeneous coefficient method							
		Car	Bike	Auto-rickshaw	E-rickshaw	LCV	Bus	Truck	Cycle
1	CM	1	0.211	0.921	0.797	2.765	4.754	5.175	0.37
	HCM	1	0.49	0.948	1.178	1.895	2.814	3.203	1.185
2	CM	1	0.219	0.854	0.752	2.788	4.695	4.446	0.364
	HCM	1	0.509	0.879	1.111	1.911	2.779	2.752	1.165
3	CM	1	0.227	0.904	0.816	2.437	4.622	3.703	0.36
	HCM	1	0.528	0.93	1.206	1.67	2.736	2.292	1.154
4	CM	1	0.228	1.029	0.76	2.669	4.956	4.122	0.324
	HCM	1	0.53	1.059	1.124	1.829	2.936	2.551	1.039
5	CM	1	0.211	0.924	0.708	2.513	5.119	4.377	0.314
	HCM	1	0.491	0.951	1.048	1.722	3.032	2.709	1.004

Notations: CM = Chandra's method, HCM = Homogeneous Coefficient method.

Length ratios of car to different vehicle types are given in Table 5. The PCU developed using homogeneous coefficient method is listed in Table 6.

4.3 PCU determination using Speed-based modelling

In this approach, the speed of vehicles is modelled in terms of classified volume and speed as:

$$V_x = a_0 + \sum_{x=1}^{n} a_x \frac{N_x}{V_x}. \tag{5}$$

All the selected sites have eight vehicle types in the traffic stream, so the speed of each vehicle class will be modelled as Equations (6) to (13). These equations were solved for each selected site to get the PCU values.

$$\begin{aligned} V_c = {} & a_{0-c} + a_{1-c}(n_c/V_c) + a_{2-c}(n_b/V_b) + \\ & + a_{3-c}(n_{ar}/V_{ar}) + a_{4-c}(n_{er}/V_{er}) + \\ & + a_{5-c}(n_l/V_l) + a_{6-c}(n_{cy}/V_{cy}) + \\ & + a_{7-c}(n_{bs}/V_{bs}) + a_{8-c}(n_{tr}/V_{tr}), \end{aligned} \tag{6}$$

$$\begin{aligned} V_b = {} & a_{0-b} + a_{1-b}(n_c/V_c) + a_{2-b}(n_b/V_b) + \\ & + a_{3-b}(n_{ar}/V_{ar}) + a_{4-b}(n_{er}/V_{er}) + \\ & + a_{5-b}(n_l/V_l) + a_{6-b}(n_{cy}/V_{cy}) + \\ & + a_{7-b}(n_{bs}/V_{bs}) + a_{8-b}(n_{tr}/V_{tr}), \end{aligned} \tag{7}$$

$$\begin{aligned} V_{ar} = {} & a_{0-ar} + a_{1-ar}(n_c/V_c) + a_{2-ar}(n_b/V_b) + \\ & + a_{3-ar}(n_{ar}/V_{ar}) + a_{4-ar}(n_{er}/V_{er}) + \\ & + a_{5-ar}(n_l/V_l) + a_{6-ar}(n_{cy}/V_{cy}) + \\ & + a_{7-ar}(n_{bs}/V_{bs}) + a_{8-ar}(n_{tr}/V_{tr}), \end{aligned} \tag{8}$$

$$\begin{aligned} V_{er} = {} & a_{0-er} + a_{1-er}(n_c/V_c) + a_{2-er}(n_b/V_b) + \\ & + a_{3-er}(n_{ar}/V_{ar}) + a_{4-er}(n_{er}/V_{er}) + \\ & + a_{5-er}(n_l/V_l) + a_{6-er}(n_{cy}/V_{cy}) + \\ & + a_{7-er}(n_{bs}/V_{bs}) + a_{8-er}(n_{tr}/V_{tr}), \end{aligned} \tag{9}$$

$$\begin{aligned} V_l = {} & a_{0-l} + a_{1-c}(n_c/V_c) + a_{2-l}(n_b/V_b) + \\ & + a_{3-l}(n_{ar}/V_{ar}) + a_{4-l}(n_{er}/V_{er}) + \\ & + a_{5-l}(n_l/V_l) + a_{6-l}(n_{cy}/V_{cy}) + \\ & + a_{7-l}(n_{bs}/V_{bs}) + a_{8-l}(n_{tr}/V_{tr}), \end{aligned} \tag{10}$$

$$\begin{aligned} V_{cy} = {} & a_{0-cy} + a_{1-cy}(n_c/V_c) + a_{2-cy}(n_b/V_b) + \\ & + a_{3-cy}(n_{ar}/V_{ar}) + a_{4-cy}(n_{er}/V_{er}) + \\ & + a_{5-cy}(n_l/V_l) + a_{6-cy}(n_{cy}/V_{cy}) + \\ & + a_{7-cy}(n_{bs}/V_{bs}) + a_{8-cy}(n_{tr}/V_{tr}), \end{aligned} \tag{11}$$

$$\begin{aligned} V_{bs} = {} & a_{0-bs} + a_{1-bs}(n_c/V_c) + a_{2-bs}(n_b/V_b) + \\ & + a_{3-bs}(n_{ar}/V_{ar}) + a_{4-bs}(n_{er}/V_{er}) + \\ & + a_{5-bs}(n_l/V_l) + a_{6-bs}(n_{cy}/V_{cy}) + \\ & + a_{7-bs}(n_{bs}/V_{bs}) + a_{8-bs}(n_{tr}/V_{tr}), \end{aligned} \tag{12}$$

$$\begin{aligned} V_{tr} = {} & a_{0-tr} + a_{1-tr}(n_c/V_c) + a_{2-tr}(n_b/V_b) + \\ & + a_{3-tr}(n_{ar}/V_{ar}) + a_{4-tr}(n_{er}/V_{er}) + \\ & + a_{5-tr}(n_l/V_l) + a_{6-tr}(n_{cy}/V_{cy}) + \\ & + a_{7-tr}(n_{bs}/V_{bs}) + a_{8-tr}(n_{tr}/V_{tr}), \end{aligned} \tag{13}$$

where: V = speed, n = number of vehicle (volume), a_0 = intercept, a_1, a_2, ……. , a_8 are the coefficients for car (c), bike (b), auto-rickshaw (ar), e-rickshaw (er), LCV (l), cycle (cy), bus (bs), and truck (tr), respectively.

With the help of SPSS software and Microsoft Excel, these equations were solved. After the solving, the modelled speed of different vehicles for Site 1 and the ratio of speed of car to speed of different vehicles are presented in Table 7. Then, the modelled speed is directly used for PCU determination using Chandra's method and Homogeneous coefficient method. A similar process was employed for other sites. The PCU values of vehicle types using this approach are listed in Table 8.

Table 7 *Modelled speed of vehicles and speed ratio*

Modelled Speed (m/s)		Speed ratio (car to different vehicle type)	
Vc	9.156		
Vb	9.385	Vc/Vb	0.979
Var	8.285	Vc/Var	1.107
Ver	5.822	Vc/Ver	1.573
Vl	7.863	Vc/Vl	1.17
Vcy	4.049	Vc/Vcy	2.261
Vbs	8.156	Vc/Vbs	1.123
Vtr	4.778	Vc/Vtr	1.632

Table 8 *Developed PCU values of vehicle types using Speed-based modelling*

Site	Method		Passenger Car Unit values using Speed-based modelling							
			Car	Bike	Auto-rickshaw	E-rickshaw	LCV	Bus	Truck	Cycle
1	SBM	CM	1	0.212	0.925	0.799	2.799	5.039	5.316	0.362
		HCM	1	0.492	0.952	1.181	1.918	2.844	3.29	1.158
2	SBM	CM	1	0.221	0.859	0.755	2.855	4.742	4.612	0.371
		HCM	1	0.512	0.883	1.116	1.957	2.807	2.721	1.187
3	SBM	CM	1	0.228	0.906	0.824	2.654	4.656	4.008	0.383
		HCM	1	0.529	0.932	1.221	1.819	2.756	2.481	1.226
4	SBM	CM	1	0.228	1.037	0.761	2.676	5.016	4.106	0.342
		HCM	1	0.529	1.067	1.127	1.834	2.969	2.541	1.096
5	SBM	CM	1	0.312	0.925	0.71	2.545	5.081	4.396	0.307
		HCM	1	0.725	0.952	1.052	1.819	2.756	2.481	0.983

Notations: CM = Chandra's method, HCM = Homogeneous Coefficient method, SBM = Speed based modelling

Table 9 *Obtained Regression Coefficients for Site 1*

Regression Coefficients	Obtained value
a_0	12.179
a_c	-0.003
a_b	-0.006
a_{ar}	-0.022
a_{er}	-0.036
a_{bs}	0.077
a_{tr}	-0.363
a_{cy}	0.022
a_l	0.064

Table 10 *Developed PCU values of vehicle types using Multiple Linear Regression method*

Site	Method	Passenger Car Unit values using Multiple Linear Regression Method							
		Car	Bike	Auto-rickshaw	E-rickshaw	LCV	Bus	Truck	Cycle
1	MLR	1	1.596	6.404	10.561	18.659	22.305	105.275	6.368
2	MLR	1	0.13	0.338	0.362	0.733	3.165	5.352	1.127
3	MLR	1	0.006	1.1	1.901	12.345	6.822	4.899	5.598
4	MLR	1	2.465	2.584	7.699	0.193	16.098	0.256	2.611
5	MLR	1	1.953	0.458	4.826	0.463	14.607	46.786	1.219

Notations: MLR = Multiple Linear Regression Method

4.4 PCU determination using Multiple linear regression method

This method can be used for mixed types of traffic conditions having any number of vehicle types. In this method, the average speed of car is presented in terms of classified traffic volume as Equation (14). Extended form as per the number of vehicle types in the traffic stream can be expanded as Equation (15).

$$V_c = a_0 + \sum_{x=1}^{n} a_x N_x, \tag{14}$$

$$V_c = a_0 + a_1 N_c + a_2 N_b + a_3 N_{ar} + a_4 N_{er} + \\ + a_5 N_l + a_6 N_{cy} + a_6 N_{cy} + a_7 N_{bs} + a_8 N_{tr}, \tag{15}$$

where: V = speed, N = classified volume, and a_0, a_1, ……. , a_8 are the regression coefficients. PCU of a vehicle type x can be calculated as:

$$(PCU)_x = \frac{a_x}{a_1}, \tag{16}$$

where: a_1 is the regression coefficient for car and a_x is for vehicle type x.

Equation (15) was regressed using SPSS software to calculate regression coefficients. The coefficients obtained for Site 1 are listed in Table 9. Then, the PCU values were determined using Equation (16), and are presented in Table 10.

5 Comparison of PCU values obtained from different methods

In this study, the PCU values of vehicle types were estimated using the Chandra's method, Homogeneous Coefficient method, Speed-based modelling, and multiple linear regression method. A comparison of PCU values obtained from Chandra's method, homogeneous coefficient method, and speed-based modelling is shown in Figures 4-10. Comparison of PCU values of bike, auto-rickshaw, e-rickshaw, LCV, bus, truck and cycle using different methods are shown in Figures 4, 5, 6, 7, 8, 9 and 10, respectively. From the Figures, it is clear that the PCU values of light vehicles (bike, auto-rickshaw, e-rickshaw, and cycle), estimated using Homogeneous coefficient method, are relatively higher, and PCU values of Heavy vehicles (LCV, bus, and truck) are lower than the PCU values obtained using the Chandra's method. The PCU values estimated using speed-based modelling are similar to values obtained without modelling the speed of vehicles with minor variations. The PCU values developed using multiple linear regression methods are not relevant. Out of all these methods, values obtained from Chandra's method are the most suitable.

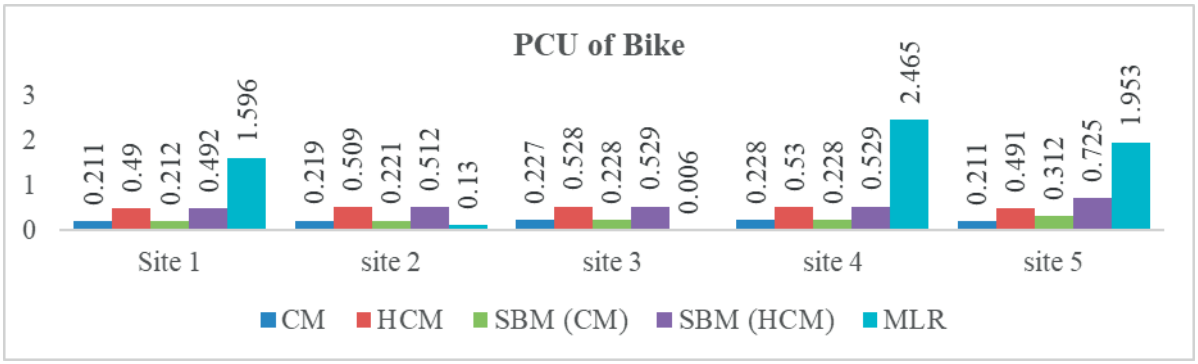

Figure 4 *Comparison of PCU values of Bikes*

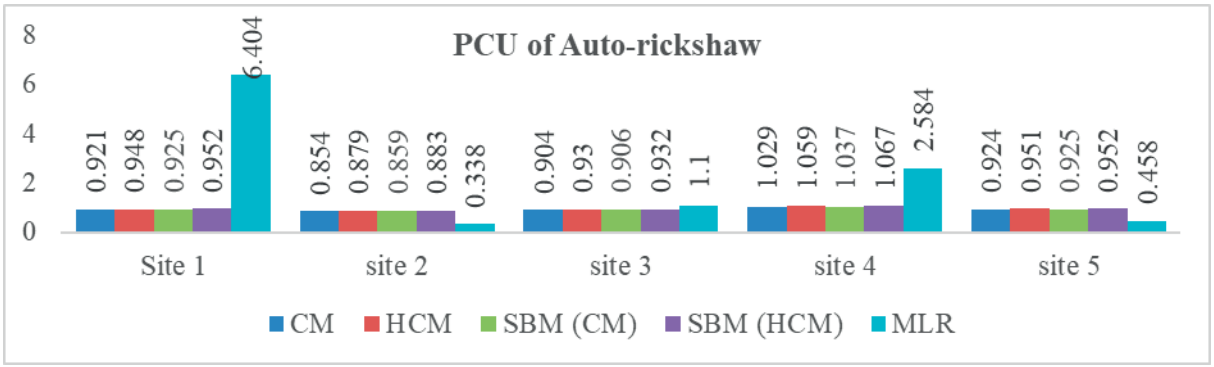

Figure 5 *Comparison of PCU values of Auto-rickshaws*

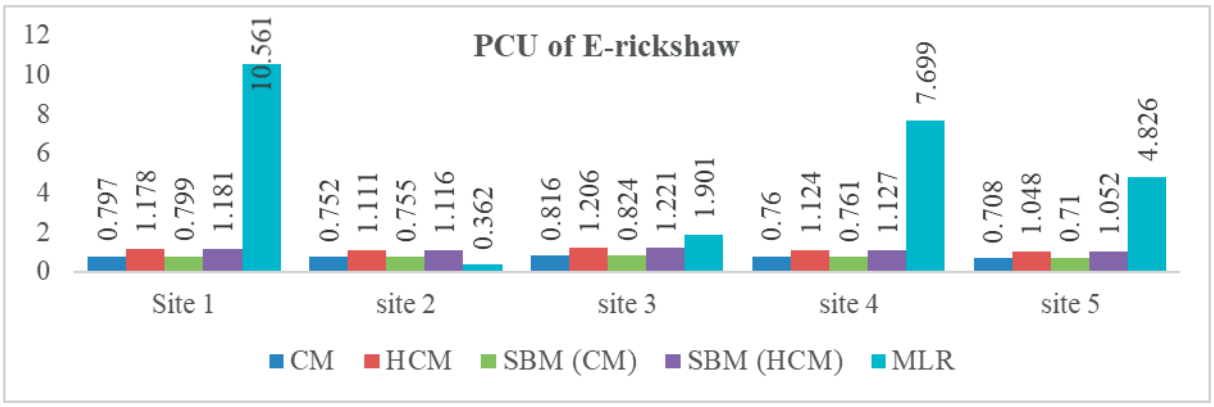

Figure 6 *Comparison of PCU values of E-rickshaws*

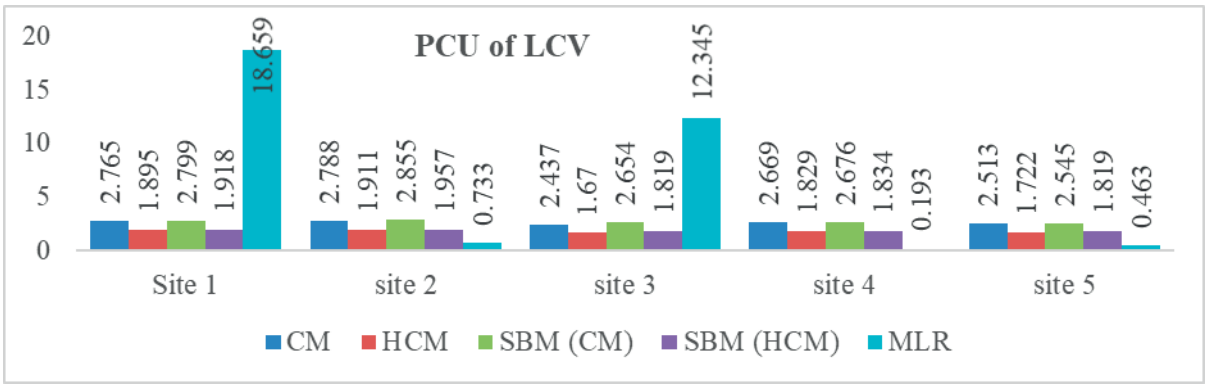

Figure 7 *Comparison of PCU values of LCVs*

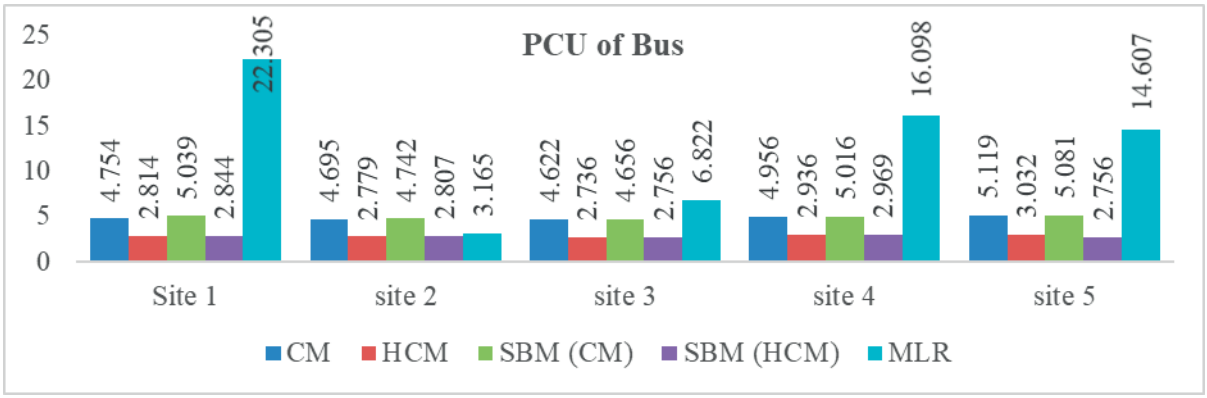

Figure 8 *Comparison of PCU values of Buses*

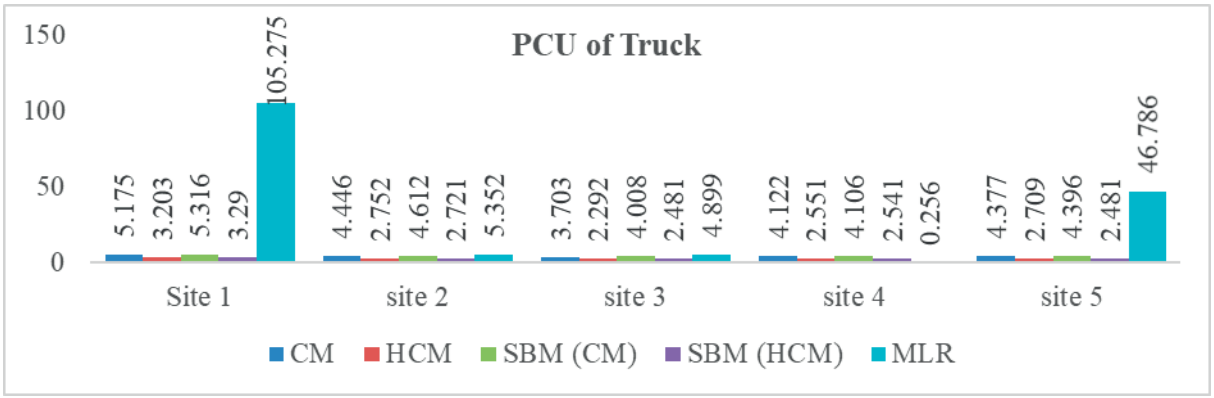

Figure 9 *Comparison of PCU values of Trucks*

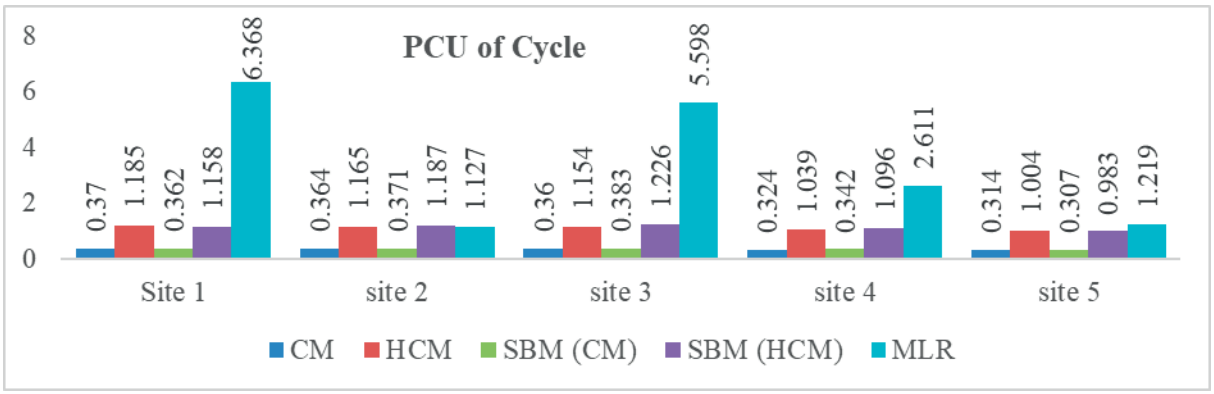

Figure 10 *Comparison of PCU values of bicycles*

Table 11 *Comparison of obtained PCU values to IRC:106-1990 and other study*

Vehicle Types	Passenger Car Unit using Chandra's Method					IRC 106:1990	Rao and Yadav 2018
	Site1	Site2	Site3	Site4	Site5		
Car	1	1	1	1	1	1	
Bike	0.211	0.219	0.227	0.228	0.211	0.5 - 0.7	0.231-0.250
Auto-rickshaw	0.921	0.854	0.904	1.029	0.924	1.2 - 2	0.963-1.04
E-rickshaw	0.797	0.752	0.816	0.76	0.708	-	-
LCV	2.765	2.788	2.437	2.669	2.513	1.4 - 2	2.74-3.02
Bus	4.754	4.695	4.622	4.956	5.119	2.2 - 3.7	5.33-5.76
Truck	5.175	4.446	3.703	4.122	4.377	2.2 - 3.7	4.19-4.52
Cycle	0.37	0.364	0.36	0.324	0.314	0.4 - 0.5	-

6 Comparison of PCU values to IRC 106:1990

A comparison between obtained PCU values using Chandra's method and values given in IRC 106:1990 is shown in Table 11. It is clear that the PCU values of bikes, auto-rickshaws, and cycles are smaller than the values given in the IRC code, while the values of LCVs, buses, and trucks are relatively higher. Rao and Yadav (2018) also obtained similar result [6].

7 Results, discussion and conclusion

The PCU of vehicle types is required to calculate capacity, signal designing, flow measurements, etc. Thus, the PCU is an important parameter and it can be calculated using many methods. In this study, PCU of every vehicle class was calculated using the Chandra's method, homogeneous coefficient method, speed-based modelling, and multiple linear regression. To calculate the PCU values, classified speed and volume data from 5 sites of Sonipat city having different traffic and geometric parameters were collected with the help of the videography method. After calculating the PCU of vehicle types, a comparison was made between values obtained from different methods (Figure 4-10), and it was found that values obtained from the Chandra's method are most suitable, while values obtained from the multiple linear regression are irrelevant. Later, the PCU values obtained from the Chandra's method and values given in IRC: 106-1990 were compared, and it was found that the PCU values obtained from the Chandra's method of slower vehicles (bike, auto-rickshaw, and cycle) are relatively lower and the PCU values of heavy vehicles (LCV, bus, and truck) are relatively higher. It can be concluded that the PCU values mentioned in IRC codes are old and outdated. A revision of the IRC code pertaining to the PCU values is required to meet technological advancements in vehicles and roads.

The PCU value of e-rickshaw obtained from this study can be used directly by urban planners to design different traffic facilities where the similar type of traffic condition prevails and more studies with different roadway and traffic conditions are required to precisely determine equivalency value of e-rickshaw.

One distinctive feature of this work is the Chandra technique, which provides a novel way to calculate Passenger Car Unit (PCU) values in mixed traffic situations. This approach can give a more realistic depiction of traffic flow and vehicle interactions, particularly in areas like India where there is a wide

variety of vehicle types. It can take into consideration various vehicle classifications, such as auto-rickshaws and e-rickshaws.

The share of bike, auto-rickshaw and e-rickshaw is ranged from 43.24% to 70.83% on the analysed locations. Bikes, rickshaws, and e-rickshaws are predominant vehicle types ply on the city roads (urban roads) of India. The shares of these vehicles are generally smaller on the rural roads. The PCU values of vehicles are different for rural and urban roads. Different sets of PCU values for rural and urban roads are available in IRC codes (Indian Roads Congress code).

There are large differences in PCU values of trucks between different measurement locations (from 3.7 to 5.180) because out of five roads, two roads were connected to highways and rest were within the city only. So, the difference in PCU values may be due to change in given conditions in the analyzed locations.

Acknowledgment

The authors received no financial support for the research, authorship and/or publication of this article.

Conflicts of interest

The authors declare that they have no known competing financial interests or personal relationships that could have appeared to influence the work reported in this paper.

References

[1] CHANDRA, S., KUMAR, V., SIKDAR, P. K. Dynamic PCU and estimation of capacity of urban roads. *Indian Highways*. 1995, **23**(4), p. 17-28. ISSN 0376-7256.

[2] DASANI, Y. R., VALA, M., PATEL, B. Estimation of dynamic equivalency factor under heterogeneous traffic condition on urban arterial road - a case study of Porbandar city. In: *Transportation research. Lecture Notes in Civil Engineering. Vol 45* [online]. MATHEW, T., JOSHI, G., VELAGA, N., ARKATKAR, S. (Eds.). Singapore: Springer, 2020. ISBN 978-981-32-9041-9, eISBN 978-981-32-9042-6, p. 465-474. Available from: https://doi.org/10.1007/978-981-32-9042-6_37

[3] WERNER, A., MORRALL, J. F. Passenger car equivalencies of trucks, buses, and recreational vehicles for two-lane rural highways. *Transportation Research Record*. 1977, **615**, p. 10-17. ISSN 0361-1981, eISSN 2169-4052.

[4] CHU, M. C., MAI, T. T., BINH, T. H., SANO, K. The delay estimation under heterogeneous traffic conditions. *Journal of the Eastern Asia Society for Transportation Studies* [online]. 2010, **8**, p. 1583-1595. eISSN 1881-1124. Available from: https://doi.org/10.11175/easts.8.1583

[5] ADAMS, C. A., ABDUL, M., ZAMBANG, M., BOAHEN, R. O. Effects of motorcycles on saturation flow rates of mixed traffic at signalized intersections in Ghana. *International Journal of Traffic and Transportation Engineering* [online]. 2015, **4**(3), p. 94-101. ISSN 2325-0062, eISSN 2325-0070. Available from: https://doi.org/10.5923/j.ijtte.20150403.03

[6] RAO, R. S., YADAV, N. Determination and comparison of PCU on urban roads under mixed traffic conditions - a case study. In: Conference Urbanization Challenges in Emerging Economies: proceedings. 2018.

[7] TIWARI, G., FAZIO, J., PAVITRAVAS, S. Passenger car units for heterogeneous traffic using a modified density method. In: 4th International Symposium on Highway Capacity: proceedings. 2000. p. 246-257.

[8] HUBER, M. J. Estimation of passenger-car equivalents of trucks in traffic stream. *Transportation Research Record*. 1982, **869**, p. 60-70. ISSN 0361-1981, eISSN 2169-4052.

[9] BAINS, M. S., PONNU, B., ARKATKAR, S. S. Modelling of traffic flow on Indian expressways using simulation technique. *Procedia - Social and Behavioral Sciences* [online]. 2012, 43, p. 475-493. ISSN 1877-0428. Available from: https://doi.org/10.1016/j.sbspro.2012.04.121

[10] ARASAN, V. T., ARKATKAR, S. S. Microsimulation study of effect of volume and road width on PCU of vehicles under heterogeneous traffic. *Journal of Transportation Engineering, Part A: Systems* [online]. 2010, **136**(12), p. 1110-1119. ISSN 2473-2907, eISSN 2473-2893. Available from: https://doi.org/10.1061/(ASCE)TE.1943-5436.0000176

[11] DHANANJAYA, D., FERNANDO, M., SILVA, M., SIVAKUMAR, T. Passenger car units for different midblock sections in Sri Lanka under mixed traffic condition. *Journal of Applied Engineering Science* [online]. 2023, **21**(2), p. 1-9. ISSN 1451-4117, eISSN 1821-3197. Available from: https://doi.org/10.5937/jaes0-36600

[12] ZERO, B. C., OMER, D. H., ALI, N. S., ABDULLA, K. Y. Development of passenger car unit (PCU) for streets in Erbil City. In: 8th IEC 2022 - International Engineering Conference: Towards Engineering Innovations and Sustainability: proceedings [online]. IEEE. 2022. eISBN 978-1-6654-7829-8, p. 149-154. Available from: https://doi.org/10.1109/IEC54822.2022.9807486

[13] ALI, M., AHMED, K., HAROON, M. Estimation of passenger car units for national highways using speed methods. In: 1st International Conference on Recent Advances in Civil and Earthquake Engineering: proceedings. 2021. p. 218-222.

[14] KHAN, A. A., SINGH, G. Development of PCU value of e-rickshaw on urban roads [online]. In: *Advances in water resources and transportation engineering. Lecture notes in civil engineering. Vol 149*. MEHTA, Y. A., CARNACINA, I., KUMAR, D. N., RAO, K. R., KUMARI, M. (Eds.). Singapore: Springer, 2021. ISBN 978-981-16-1302-9, eISBN 978-981-16-1303-6. Available from: https://doi.org/10.1007/978-981-16-1303-6_10

[15] BALLARI, S. O. Passenger car equivalent estimation methods of trucks in traffic stream. *International Journal of Recent Technology and Engineering (IJRTE)* [online]. 2020, **8**(5), p. 710-716. eISSN 2277-3878. Available from: https://doi.org/10.35940/ijrte.d9236.018520

[16] SHARMA, M., BISWAS, S. Estimation of passenger car unit on urban roads: a literature review. *International Journal of Transportation Science and Technology* [online]. 2021, **10**(3), p. 283-298. ISSN 2046-0430, eISSN 2046-0449. Available from: https://doi.org/10.1016/j.ijtst.2020.07.002

[17] RAJ, P., SIVAGNANASUNDARAM, K., ASAITHAMBI, G., RAVI SHANKAR, A. U. Review of methods for estimation of passenger car unit values of vehicles. *Journal of Transportation Engineering, Part A: Systems* [online]. 2019, **145**(6). ISSN 2473-2907, eISSN 2473-2893. Available from: https://doi.org/10.1061/jtepbs.0000234

[18] THAKKAR, P. S., GUPTE, S., JUREMALANI, J., STUDENT, P. G. Estimation of dynamic PCU of different types of vehicles on urban roads under heterogeneous traffic conditions. *Journal of Emerging Technologies and Innovative Research*. 2018, **5**(4), p.821-825. ISSN-2349-5162.

[19] BARVE, H., SUGANDHI, S. Modified passenger car unit for highway traffic: a review. *International Journal of Engineering Sciences and Research Technology* [online]. 2017, **6**(1)2, p. 584-587. ISSN 2277-9655. Available from: https://doi.org/10.5281/zenodo.1130903

[20] MONDAL, S. CHAKRABORTY, S., ROY, S. K., GUPTA, A. Estimation of passenger car unit for heterogeneous traffic stream of urban arterials: case study of Kolkata. *Transportation Letters* [online]. 2017, **15**(10), p. 1-13. ISSN 1942-7867, eISSN 1942-7875. Available from: https://doi.org/10.1080/19427867.2017.1293313

[21] CHAND, S. Comparison of passenger car units on plain and hilly urban road. In: Civil Engineering Systems and Sustainable Innovations: proceedings. 2016. ISBN 978-93-83083-78-7, p. 283-289.

[22] DHAMANIYA, A., CHANDRA, S. Conceptual approach for estimating dynamic passenger car units on urban arterial roads by using simultaneous equations. *Transportation Research Record: Journal of the Transportation Research Board* [online]. 2016, **2553**(1), p. 108-116. ISSN 0361-1981, eISSN 2169-4052. Available from: https://doi.org/10.3141/2553-12

[23] MAHIDADIYA, A. N., JUREMALANI, J. Global scenario on estimation of passenger car unit: a review. *International Journal of Scientific Research in Science, Engineering and Technology (IJSRSET)*. 2016, **2**(1), p. 341-344. ISSN 2395-1990, eISSN 2394-4099.

[24] NOKANDEH, M. M., GHOSH, I., CHANDRA, S. Determination of passenger-car units on two-lane intercity highways under heterogeneous traffic conditions. *Journal of Transportation Engineering, Part A: Systems* [online]. 2016, **142**(2). ISSN 2473-2907, eISSN 2473-2893. Available from: https://doi.org/10.1061/(ASCE)TE.1943-5436.0000809

[25] CHANDRA, S. Highway capacity research on inter-urban highways in India. *Transportation in Developing Economies* [online]. 2015, **1**(1), p. 20-24. ISSN 2199-9287, eISSN 2199-9295. Available from: https://doi.org/10.1007/s40890-015-0003-4

[26] MARDANI, N. M., CHANDRA, S., GHOSH, I. Passenger car unit of vehicles on undivided intercity roads in India. *Procedia Computer Science* [online]. 2015, **52**, p. 926-931. eISSN 1877-0509. Available from: https://doi.org/10.1016/j.procs.2015.05.167

[27] KHANORKAR, A. R. R., GHODMARE, S. D. D. Development of PCU value of vehicle under mix nature traffic condition in cities on congested highways. *International Journal of Engineering and Computer Science*. 2014, **3**(5), p. 6109-6113. ISSN 2319-7242.

[28] KHANORKAR, A. R., GHODMARE, S. D., KHODE, B. V. Impact of lane width of road on passenger car unit capacity under mix traffic condition in cities on congested highways. *Journal of Engineering Research and Applications*. 2014, **4**(5), p. 180-184. ISSN 2248-9622.

[29] MINH, C. C., SANO, K., MATSUMOTO, S. The speed, flow and density analyses of motorcycle traffic. *Journal of the Eastern Asia Society for Transportation Studies* [online]. 2005, **6**, p. 1496-1508. eISSN 1881-1124. Available from: https://doi.org/10.11175/easts.6.1496

[30] OMAR, B. S., KAR, P., CHUNCHU, M. Passenger car equivalent estimation for rural highways: methodological review. *Transportation Research Procedia* [online]. 2020, **48**, p. 801-816. ISSN 2352-1457, eISSN 2352-1465. Available from: https://doi.org/10.1016/j.trpro.2020.08.085

[31] VIJAY, B. G., KHATAVKAR, R. Comparative study of methods used for a capacity estimation on two lane undivided national highways. *Journal of Traffic and Transportation Engineering* [online]. 2019, **7**(1). ISSN 2325-0062, eISSN 2325-0070. Available from: https://doi.org/10.17265/2328-2142/2019.01.004

[32] RAJESH, K. N., RAO, R. S. Field evaluation of dynamic PCU under heterogeneous traffic conditions. *International Journal for Research in Applied Science and Engineering Technology (IJRASET).* 2018, **6**(XII), p. 35-41. eISSN 2321-9653.

[33] SHALKAMY, A., SAID, D., RADWAN, L. Influence of carriageway width and horizontal curve radius on passenger car unit values of two-lane two-way rural roads. *Civil and Environmental Research*. 2015, **7**(3), p. 157-167. ISSN 2224-5790, eISSN 2225-0514.

[34] KUMAR, P., RAJU, N., MISHRA, A., ARKATKAR, S. S., JOSHI, G. Validating area occupancy - based passenger car units and homogeneous equivalent concept under mixed traffic conditions in India. *Journal of Transportation Engineering, Part A: Systems* [online]. 2018, **144**(10). ISSN 2473-2907, eISSN 2473-2893. Available from: https://doi.org/10.1061/jtepbs.0000184

[35] BISWAS, S., CHAKRABORTY, S., CHANDRA, S., GHOSH, I. Kriging-based approach for estimation of vehicular speed and passenger car units on an urban arterial. *Journal of Transportation Engineering, Part A: Systems* [online]. 2017, **143**(3). ISSN 2473-2907, eISSN 2473-2893. Available from: https://doi.org/10.1061/JTEPBS.0000031

[36] JASSAL, K., ASCE, S. M., SHARMA, U., PH, D., INGALE, V. Axle-based mapping approach for vehicle classification in heterogeneous traffic. *Journal of Transportation Engineering, Part A: Systems* [online]. 2025, **151**(4), p. 1-8. ISSN 2473-2907, eISSN 2473-2893. Available from: https://doi.org/10.1061/JTEPBS.TEENG-8524

[37] BEHZADI, G., SHAKIBAEI, F. Determination of passenger car equivalent for bus in urban roads using AIMSUN (case study: Emam reza avenue, amol city). *International Research Journal of Engineering and Technology (IRJET)*. 2016, 03(06), p. 2360-2364. ISSN 2395-0056, eISSN 2395-0072.

[38] SUGIARTO, S., APRIANDY, F., FAISAL, R., SALEH, S. M. Measuring passenger car unit (PCU) at four legged roundabout using time occupancy data collected from drone. *Aceh International Journal of Science and Technology* [online]. 2018, **7**(2), p. 77-84. ISSN 2503-2348, eISSN 2088-9860. Available from: https://doi.org/10.13170/aijst.7.2.8587

[39] SUBOTIC, M., TUBIC, V., MARIC, B. PCE in analysis models of the number of following vehicles on a two-lane road. *International Journal for Traffic and Transport Engineering* [online]. 2016, **6**(1), p. 25-37. ISSN 2217-544X, eISSN 2217-5652. Available from: https://doi.org/10.7708/ijtte.2016.6(1).03

UNIVERSITY
OF ŽILINA

In its over 70 years of successful existence, the University of Žilina (UNIZA) has become one of the top universities in Slovakia.

Scientific conferences

organized by University of Žilina

TRANSCOM 2025
Date and venue: 21 - 23 May 2025, High Tatras (SK)
Contact: transcom@uniza.sk
Web: http://www.transcom-conference.com/

Conference InvEnt 2025
(Invention Enterprises 2025)
Date and venue: 16 - 18 June 2025, Štrbské Pleso (SK)
Contact: invent.invent@fstroj.uniza.sk
Web: https://www.priemyselneinzinierstvo.sk/
http:/www.priemyselneinzinierstvo.sk/invent2025/

Open Source Software in Education, Research and IT Solutions (OSSConf)
Date and venue: 1 - 3 July 2025, Žilina (SK)
Contact: miroslav.kvassay@fri.uniza.sk
Web: https://ossconf.fri.uniza.sk/

40th International Colloquium Advanced Manufacturing and Repair Technologies in Vehicle Industry
Date and venue: 26 - 28 May 2025,
Zuberec - Brestová (SK)
Contact: eva.tillova@fstroj.uniza.sk
Web: http://kmi2.uniza.sk/

Unconventional Technologies 2025
Date and venue: 26 - 27 June 2025,
Žilina - Budatín (SK)
Contact: jan.moravec@fstroj.uniza.sk

Horizons of Railway Transport 2025
Date and venue: 7 - 9 October 2025, Jasná (SK)
Contact: zdenka.bulkova@uniza.sk

UNIVERSITY OF ŽILINA
Science & Research Department

Univerzitná 8215/1,
010 26 Žilina,
Slovakia

Ing. Janka Macurová
tel.: +421 41 513 5143
e-mail: janka.macurova@uniza.sk

ASSESSING THE RISKS OF A FREIGHT FORWARDER ENTERING THE TRANSPORT MARKET WITH STOCHASTIC DEMAND

Vitalii Naumov[1,*], Guldana Nugymanova[2], Ihor Taran[3], Yana Litvinova[4]

[1]Transportation Systems Department, Faculty of Civil Engineering, Cracow University of Technology, Cracow, Poland
[2]Mukhametzhan Tynyshbaev ALT University, Almaty, Kazakhstan
[3]Department of Roads and Bridges, Faculty of Civil and Environmental Engineering and Architecture, Rzeszow University of Technology, Rzeszow, Poland
[4]Transport Management Department, Faculty of Mechanical Engineering, Dnipro University of Technology, Dnipro, Ukraine

*E-mail of corresponding author: vitalii.naumov@pk.edu.pl

Vitalii Naumov 0000-0001-9981-4108,
Ihor Taran 0000-0002-3679-2519,
Guldana Nugymanova 0000-0001-6035-9590,
Yana Litvinova 0000-0003-2806-4076

Resume

This research investigates freight forwarders' operational risks when entering a new transport market characterized by stochastic demand. A simulation model was developed to represent the service request flow potentially experienced by a freight forwarder in a new market. The proposed model incorporates key operational parameters such as average request interval, service tariff, and request processing time. Based on the simulation results, a regression model was developed to predict the market entry risk. The obtained model demonstrates that the risk increases with longer average request intervals between service requests and decreases with higher service tariffs. The findings provide insights for freight forwarders seeking to enter new markets. The simulation-based approach offers a practical tool for assessing operational risks and informing strategic decisions related to market entry and service pricing.

Article info

Received 22 November 2024
Accepted 22 January 2025
Online 3 February 2025

Keywords:

freight forwarding
risk assessment
transportation market
simulation model
regression analysis

Available online: https://doi.org/10.26552/com.C.2025.018

ISSN 1335-4205 (print version)
ISSN 2585-7878 (online version)

1 Introduction

The increasing interconnectedness of the global economy has elevated the significance of logistics and international cargo transportation. As the world becomes more integrated, efficient and reliable movement of goods across borders is critical for businesses to thrive. Logistics, encompassing the planning, management, and optimization of goods, information, and financial flows, plays a pivotal role in streamlining these processes. International cargo transportation, in turn, facilitates the long-distance delivery of goods, expanding market access and stimulating economic growth.

The symbiotic relationship between logistics and transportation significantly impacts a company's competitiveness and the development of international trade. To navigate the complexities of the global marketplace, effective management of logistics processes and efficient organization of cargo transportation are paramount. Globalization itself, characterized by the integration of national economies, has profound implications for the evolution of transportation and logistics operations. The surge in global trade volumes and heightened competition necessitates continuous improvement in processes and technologies to ensure the timely and reliable delivery of goods.

The dynamic nature of the transportation market is marked by uncertainty, conflict, and fluctuating goals. Numerous stochastic factors influence technological processes, and the competition for limited financial and material resources exacerbates risk. Consequently, freight forwarders, carriers, 3PL providers (Third-Party Logistics providers), and shippers face a myriad of risk situations when making decisions. By proactively considering and managing these risks, stakeholders can mitigate potential losses arising from market

fluctuations and optimize their operations. Additionally, risk assessment can serve as a valuable tool for evaluating the feasibility of administrative decisions.

This research aims to propose a methodological framework for estimating the possible risks of freight forwarding companies when a company enters a new market of transport services or changes its resources and financial policy.

The research gap addressed in this paper lies in the limited focus of existing risk assessment methods for freight forwarders on external factors, especially - parameters of nondeterministic demand. Existing methods typically concentrate on external challenges such as political instability, natural disasters, or economic downturns. Instead, this research introduces a simulation-based approach to evaluate internal operational risks specifically. By focusing on the service request flow, the study provides a more nuanced understanding of the risks of a freight forwarding business. Essentially, this research bridges the gap by shifting the focus from primarily external risks to internal operational risks, providing a more comprehensive framework for freight forwarders' risk assessment.

The paper has the following structure: the second section contains a brief review of contemporary literature related to recent trends in the freight transportation market; the third section presents the developed simulation model that allows for the estimation of risks for a forwarding company; the fourth section describes the simulation experiment, its numeric results, and results of the regression analysis completed based in the obtained data; the last part contains conclusions and directions of future research.

2 Literature review

The intense competitive landscape of the logistics market serves as a powerful catalyst for innovation. In their quest to offer superior services, companies are compelled to prioritize factors such as rapid delivery times, reliability, and operational efficiency. This relentless drive for excellence fuels the development of innovative solutions and the continuous refinement of logistics processes [1].

On a global scale, innovation encompasses both technological advancements and organizational strategies. By embracing innovation, freight forwarding companies can optimize their operations and elevate their cargo transportation capabilities to contemporary standards. Key areas of innovation include technological investments, route optimization, flexibility and adaptability, infrastructure development, sustainability and environmental consciousness, and strategic collaborations and partnerships.

The integration of modern information and communication technologies has emerged as a critical factor in enhancing the efficiency of logistics processes [2-3], which significantly influenced the estimated risks for the business entities participating in the delivery chain. Logistics Management Systems [4] enhance efficiency by automating warehouse processes [5] and enabling real-time tracking of shipments. Big data analytics and the Internet of Things [6, 7] provide valuable insights into supply chain performance, allowing for data-driven decision-making. Additionally, advanced cargo tracking systems [8] mitigate the risk of theft and loss.

Route optimization algorithms and technologies [9-10] reduce transportation costs and time, particularly critical in the face of resource shortages and rising fuel prices [11]. Furthermore, flexible supply chains [12] and backup suppliers [13] enable logistics providers to respond effectively to demand fluctuations, seasonal variations, and unforeseen disruptions [14-15].

Investments in transportation infrastructure, including roads, ports, airports, and warehouses [16-17], are essential for efficient and reliable logistics operations. These investments facilitate the smooth flow of goods and reduce transit times. As environmental concerns grow, logistics companies are increasingly adopting sustainable practices. The use of eco-friendly vehicles [18-19], energy-efficient technologies [20-21], and carbon reduction initiatives [22] can enhance a company's reputation and reduce its environmental impact.

Strong partnerships between suppliers, carriers, and distributors [23-24] can optimize resource utilization and risk management [25]. Collaborative efforts can lead to improved efficiency, cost savings, and enhanced service quality.

The dynamic nature of the logistics industry is characterized by uncertainty, conflict, and fluctuating goals [26-27]. Numerous stochastic factors, such as economic fluctuations, geopolitical events, and operational disruptions, can impact logistics operations. As the result, transport service providers, including freight forwarders, carriers, and 3PL providers, face significant risks. These risks stem from factors like demand variability [28], economic downturns [29], geopolitical tensions [30], and vehicle breakdowns [31]. Additionally, intense competition [32-33] can lead to conflicts between companies and labor unions [34].

To mitigate these risks, logistics providers must adopt a proactive approach. By considering risk factors in decision-making processes, companies can reduce potential losses and ensure business continuity. Risk assessment can also help evaluate the feasibility of strategic initiatives and identify opportunities for improvement.

One of the most frequent situations characterized with the high enterpreneur risks are the situations of entering at new market. This relates to freight

forwarding companies when they start their operations or change price politics [35].

Contemporary research in freight forwarders' risk assessment underscores the importance of proactive risk identification. The study [36] utilizing the failure mode and effects analysis method has effectively identified critical risks across the freight forwarding process, encompassing transportation, customs clearance, and documentation. The paper [37] employing a risk map within the context of service supply chains provides a valuable framework for quantitatively classifying and prioritizing risks, enabling freight forwarders to make informed decisions regarding risk mitigation strategies. The significance of implementing effective risk mitigation strategies is also highlighted in the specialized literature. The study [38] investigating the benefits of flexible pricing and hedging instruments demonstrates how proactive financial strategies can enhance the resilience and profitability of freight forwarding operations by mitigating the impact of fluctuating fuel costs. Additionally, research [39] utilizing the decision-making trial and evaluation laboratory method emphasizes the importance of understanding the interdependencies among various operational risk factors to develop targeted and effective risk response strategies.

The mentioned publications underscore the critical need for robust risk management frameworks within the international freight forwarding industry. Contemporary studies conclude that by effectively identifying, assessing, and prioritizing risks, and by implementing proactive mitigation strategies, freight forwarders can enhance their operational efficiency, mitigate potential losses, and ensure long-term success in a complex and dynamic market of transportation services.

3 Proposed simulation model

The forwarder's risk of market entry encompasses a spectrum of potential threats. This risk, essentially the likelihood of an adverse event, can manifest as a loss of resources, diminished income, or increased costs stemming from the company's chosen operational or financial strategies. In the specific context of a forwarding company venturing into the transport services market, this risk translates to the probability of encountering challenges that could hinder its success - receiving a positive profit:

$$r = 1 - prob(I_{FF} > E_{FF}) = prob(I_{FF} \leq E_{FF}), \qquad (1)$$

where:
I_{FF} and E_{FF} are income and expenses of a forwarding company within a considered period [EUR];
$prob(I_{FF} > E_{FF})$ is the probability that the forwarder's income from fulfilling requests for freight forwarding operations will exceed the costs of servicing;
$prob(I_{FF} \geq E_{FF})$ is the probability that the forwarder's income from fulfilling the requests will not exceed the servicing expenses.

To numerically assess a freight forwarder's market entry risk, one must analyze statistical data on the company's income and expenses (or profit) per a set of requests serviced during the given period. This data allows for the calculation of the probability of an event occurring, specifically when income I_{FF} is less than or equal to expenses E_{FF}. Key factors influencing this probability include the frequency of service requests (a random variable of the time interval between requests), the number of dispatchers servicing the requests' flow, and the company's service tariffs, which directly impact its income.

To investigate the relationship between demand parameters (request intervals), available resources (dispatchers count), pricing policy (service tariffs), and the associated market entry risk for a freight forwarder, a simulation model was developed to mimic the company's request fulfillment process. This model, implemented in Python and publicly accessible on GitHub [40], provides a platform for conducting experimental studies to quantify these dependencies.

The proposed software implementation of the simulation model follows the paradigm of object-oriented programming and contains the following classes:

- *Stochastic*: the class wraps the methods used to simulate random variables. The main parameters of the class allow for describing the distribution law alongside with the corresponding numeric characteristics - location, scale, and shape parameters.
- *Request*: the class represents a request for freight forwarding services. Its basic characteristics include the appearance time and a Boolean parameter that shows if a request is serviced.
- *RequestsFlow*: the class simulates the demand for forwarding services as a flow of requests. This class contains a collection of the generated requests for forwarding services, its main parameters are a stochastic variable of the interval between requests and the duration of the considered period.
- *Dispatcher*: the class represents a dispatcher of a forwarding company as an entity involved in servicing the requests. Basic fields of this class include a collection of requests serviced by a dispatcher and a stochastic variable of time needed to service a single request.
- *FreightForwarder*: the class is used to simulate the operations of a freight forwarding company. The basic parameters of this class are a collection of dispatchers and numeric financial characteristics - hourly self-costs, the tariff for services, and tax rates.

To simulate demand for forwarding services, the *generate* method of the *RequestsFlow* class was developed: for the given duration of the considered

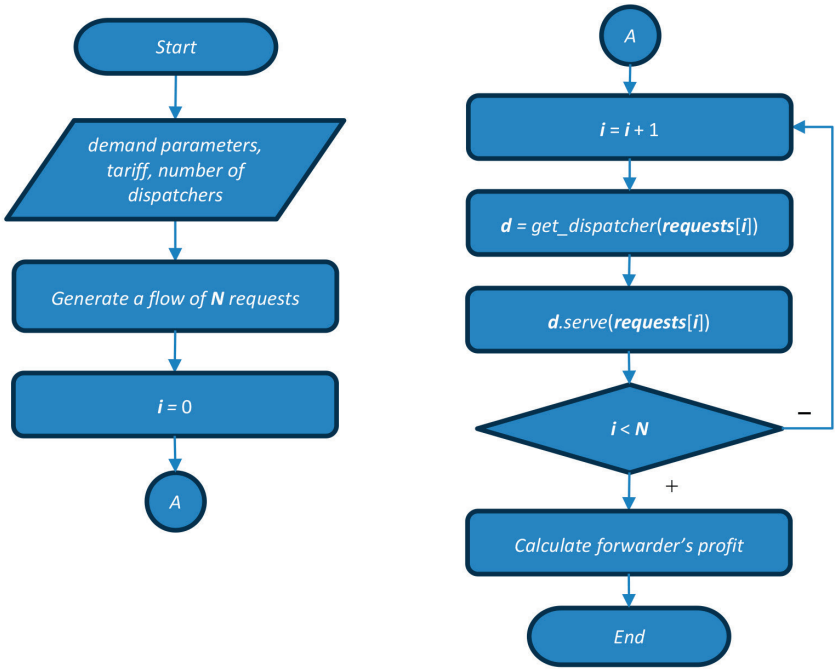

Figure 1 *Simplified algorithm of the simulation procedure*

period, the method generates a set of requests as entities of the *Request* class with the appearance time calculated based on the values of the provided variable of the requests' interval.

The simulation of the process of servicing the generated demand is run by the *serve* method of the *FreightForwarder* class with the corresponding *RequestsFlow* instance given as an argument: for each request in a flow, an available dispatcher is assigned by calling the *get_dispatcher* method, if such a dispatcher found, the *serve* method of the *Dispatcher* class is called with the request provided as an argument of this method. The *get_dispatcher* method returns a dispatcher that is not involved in servicing a request at the moment when the considered request appears. Additionally, this method finds the less busy dispatcher (a dispatcher who served the least number of requests) among the set of available dispatchers and returns it as a result. The *serve* method of the *Dispatcher* class sets the status of a request as a serviced one, adds it to the list of requests serviced by the dispatcher, and calculates the time when the dispatcher will become available after servicing the request.

The algorithm of the described above simulation procedure is presented in Figure 1.

The profit of a freight forwarding company is determined by subtracting its total expenses from its total revenue, considering taxes. This can be expressed as:

$$P_{FF} = I_{FF} - E_{FF} - VAT - PT, \tag{2}$$

where:
VAT and PT are value-added tax and profit tax, [EUR].

A freight forwarder's primary revenue comes from fees charged for services rendered. These fees can be calculated based on a fixed tariff per request:

$$I_{FF} = T_{FF} \cdot \sum_{i=1}^{N_d} S_i, \tag{3}$$

where:
T_{FF} is the tariff for services of a forwarding company, [EUR/request];
N_d is the number of dispatchers;
S_i is the number of requests serviced by the i-th dispatcher during the considered period, [requests/dispatcher].

$$E_{FF} = T_m \cdot s_h \cdot N_d, \tag{4}$$

where:
T_m is the duration of the servicing period (simulation time), [hours];
s_h are hourly self-costs of servicing requests by a dispatcher, [EUR/hour].

In this case, the value-added tax is determined based on the corresponding tax rate:

$$VAT = \delta_{VAT} \cdot \frac{I_{FF} - T_m \cdot s_{paid}}{1 + \delta_{VAT}}, \tag{5}$$

where:
δ_{VAT} is the rate for value-added tax;
s_{paid} is the hourly cost of services purchased by a freight forwarder from other companies, [EUR/hour].

Profit tax is calculated based on the net profit value as follows:

$$PT = \begin{cases} 0, & NP \le 0, \\ \delta_{PT} \cdot NP, & NP > 0, \end{cases} \tag{6}$$

where:
NP is a net profit of a forwarding company during the considered period, [EUR].

Finally, net profit can be calculated using the following formula:

$$NP = I_{FF} - E_{FF} - VAT - \frac{\delta_{VAT} \cdot T_m \cdot s_{paid}}{1 + \delta_{VAT}}. \quad (7)$$

The method *serve* of the *FreightForwarder* class returns a dictionary, containing the results of calculations for the indicators presented in Equation (2)-(7).

4 Simulation experiment results

The simulation experiment was designed to investigate the impact of key parameters on the financial performance of a freight forwarding company. Specifically, the experiment varied the following input variables:

- The average request arrival interval, modeled using an exponential distribution, ranged from 0.2 to 0.9 hours, with increments of 0.1 hours. As mentioned, it represents the average time between incoming requests for freight forwarding services.
- The freight forwarder's tariff charged per request varied from 4 to 8 EUR, with increments of 0.5 EUR. This range reflects typical market rates for freight forwarding services in Poland in the case when the requests from the specialized logistics portals are serviced.

The number of dispatchers employed by the company varied from 1 to 7. This parameter directly influences the company's capacity to handle demand. The productivity of dispatchers (reflected by the stochastic variable of servicing time) was assumed equal.

For each combination of these input variables, the simulation model was launched 1000 times to generate a statistically significant sample of outcomes. The primary outcome of interest was the probability of the company

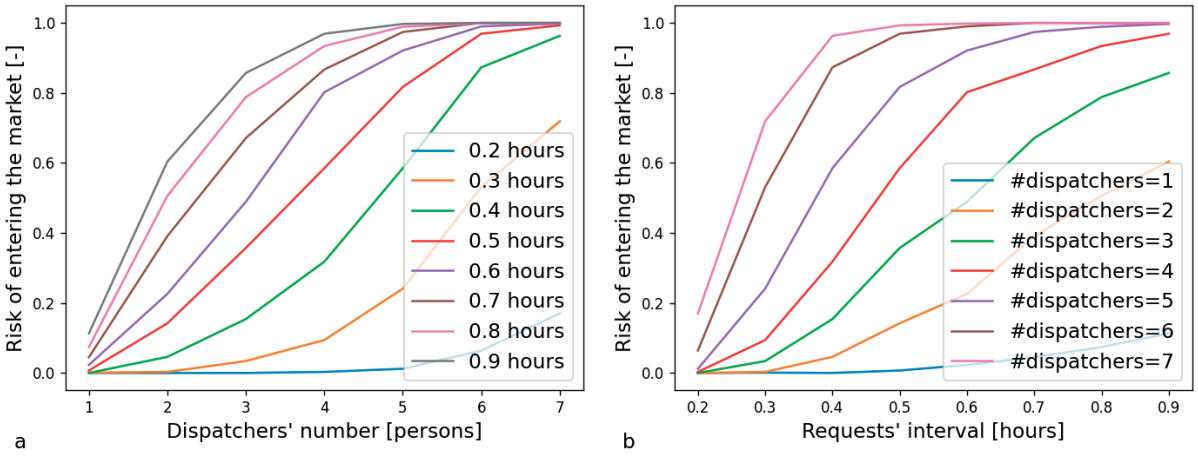

Figure 2 *Dependance of the forwarder's risk on:*
(a) the number of dispatchers (b) requests' mean interval

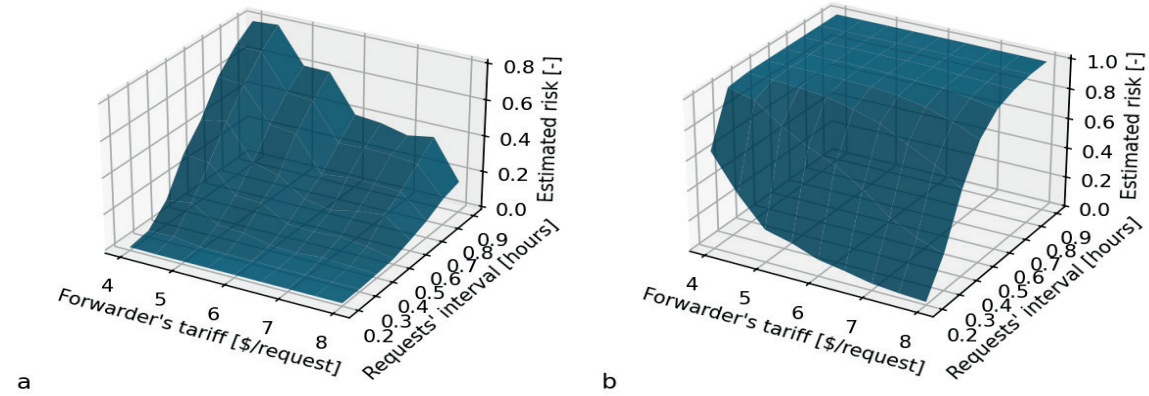

Figure 3 *Dependance of the risk on the tariff and mean interval for:*
(a) 2 dispatchers (b) 7 dispatchers

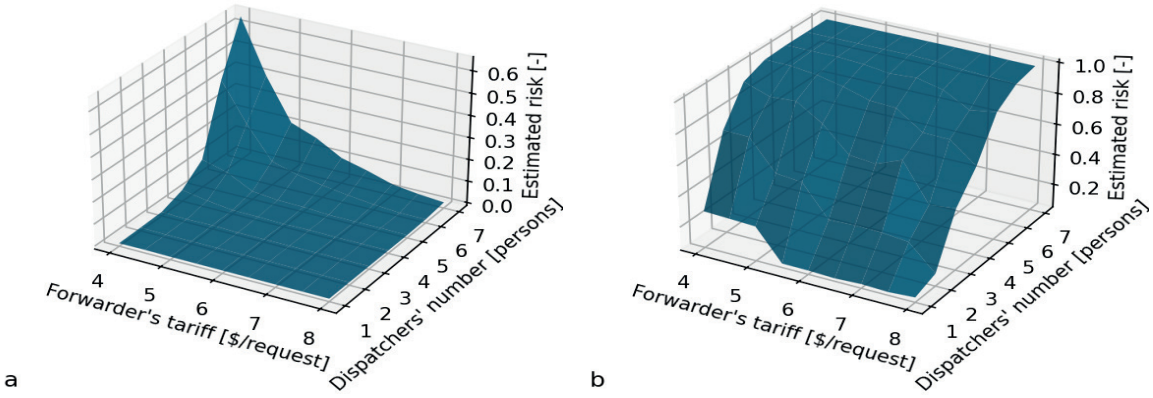

Figure 4 *Dependance of the risk on the tariff and the dispatchers' number for: (a) mean interval of 0.1 hours (b) mean interval of 0.7 hours*

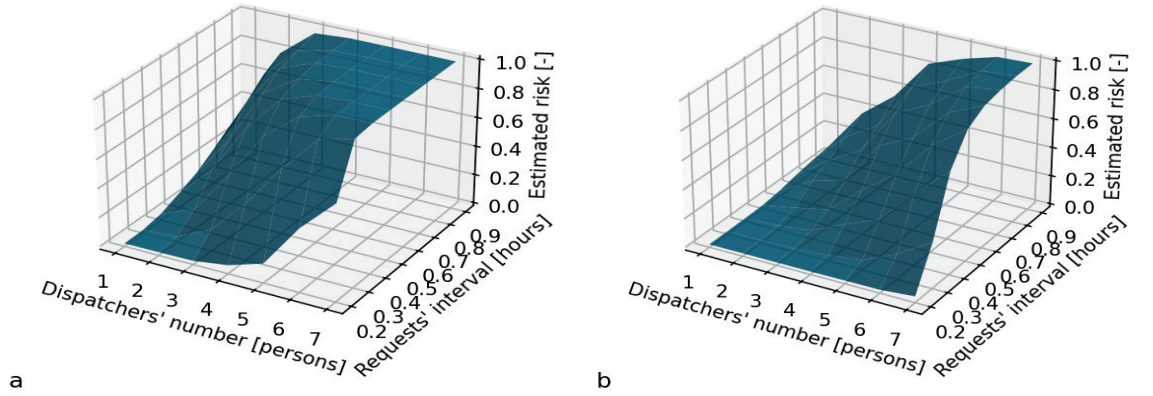

Figure 5 *Dependance of the risk on the requests' interval and the dispatchers' number for: (a) tariff of 4 EUR/request (b) tariff of 7 EUR/request*

incurring a loss, i.e., the probability that its revenue would be less than or equal to its expenses ($P_{FF} \leq 0$).

The results of the simulation experiment, focusing on a modeling period of 4 hours and a tariff of 5 EUR per request, are visually presented in Figure 2. In more detail, the obtained results are visualized in Figures 3-5.

The presented figures illustrate the complex non-linear interplay between the number of dispatchers and the average request arrival interval in determining the risk of financial loss.

5 Discussion

A key finding from the analysis is that the risk of financial loss increases as the number of dispatchers and the average request arrival interval both increase. This nonlinear relationship suggests that while adding more dispatchers can initially improve efficiency, it may also lead to overstaffing and increased costs if the volume of requests does not justify the additional labor. Furthermore, the simulation results highlight the importance of carefully balancing the company's capacity with the expected demand for its services.

To quantitatively assess the relationship $r = f(T_{ff}, N_d, \xi)$, where ξ is the average request arrival interval, a regression analysis was conducted on the simulation results. This analysis involved testing various functional forms to identify the most suitable model. The results of the regression analysis, summarized in Table 1, provide insights into the nature of the dependence between these variables.

Based on the data in Table 1, it can be argued that the most adequate dependence of the forwarder's risk from the tariff, dispatchers' number, and the mean interval is described by a model of the type $r = \beta_0 + \beta_T \cdot \ln T_{FF} + \beta_N \cdot N_d + \beta_\xi \cdot \ln \xi$. Considering the numerical values of the coefficients of the regression model, we obtain the following expression for the functional dependence of the risk of the forwarder entering the market:

$$r = 1.114 - 0.452 \cdot \ln T_{FF} + \\ + 0.131 \cdot N_d + 0.497 \cdot \ln \xi \quad . \tag{8}$$

The derived equation provides a valuable quantitative tool for assessing the impact of key operational parameters on the risk of financial loss for a freight forwarding company. By understanding the relationship between the tariff, number of dispatchers, and average request arrival interval, decision-makers can make informed choices about resource allocation and pricing strategies.

Table 1 *Impact of request intervals, dispatchers count, and tariffs on the forwarder's risk to entry the market*

Hypothesis about the type of dependence	Regression coefficients				R^2
	β_0	β_T	β_N	β_ξ	
$r = \beta_0 + \beta_T \cdot T_{FF} + \beta_N \cdot N_d + \beta_\xi \cdot \xi$	-0.127	-0.078	0.131	1.016	0.8383
$r = \beta_T \cdot T_{FF} + \beta_N \cdot N_d + \beta_\xi \cdot \xi$	-	-0.092	0.127	0.975	0.8351
$r = \beta_0 + \beta_T \cdot \ln T_{FF} + \beta_N \cdot \ln N_d + \beta_\xi \cdot \ln \xi$	1.139	-0.452	0.409	0.497	0.8506
$r = \beta_T \cdot \ln T_{FF} + \beta_N \cdot \ln N_d + \beta_\xi \cdot \ln \xi$	-	0.130	0.459	0.447	0.7335
$r = T_{FF}^{\beta T} \cdot N_d^{\beta N} \cdot \xi^{\beta \xi}$	38.191	-3.387	2.788	4.729	0.6919
$r = \beta_0 \cdot T_{FF}^{\beta T} \cdot N_d^{\beta N} \cdot \xi^{\beta \xi}$	-	-1.527	2.946	4.572	0.6772
$r = \beta_0 + \beta_T \cdot T_{FF} + \beta_N \cdot \ln N_d + \beta_\xi \cdot \ln \xi$	0.806	-0.078	0.409	0.497	0.8501
$r = \beta_0 + \beta_T \cdot T_{FF} + N_d + \beta_\xi \cdot \ln \xi$	0.780	-0.078	0.131	0.497	0.8584
$r = \beta_0 + \beta_T \cdot \ln T_{FF} + \beta_N \cdot N_d + \beta_\xi \cdot \ln \xi$	1.114	-0.452	0.131	0.497	0.8589†
$r = \beta_0 + \beta_T \cdot \ln T_{FF} + \beta_N \cdot N_d + \beta_\xi \cdot \xi$	0.206	-0.452	0.131	1.016	0.8387

† The biggest value of the determination coefficient

Within the specified ranges of the average request arrival interval (0.2 to 0.9 hours) and the freight forwarder's tariff (4 to 8 EUR/request), the model reveals a monotonic relationship between these variables and the risk of financial loss. Specifically, increasing the average request arrival interval leads to a higher risk, while increasing the tariff reduces the risk. This implies that to minimize the risk of entering the market, the company should strive to set a higher tariff for its services.

It is important to note that the applicability of this model is limited to the specified parameter ranges. For values outside these ranges, it may be necessary to employ more complex modeling techniques or conduct additional simulations to accurately assess the risk profile.

6 Conclusions

The dynamic and complex nature of the transportation market, characterized by uncertainty, volatility, and competition, poses significant risks to various stakeholders, including freight forwarders, carriers, third-party logistics providers, and shippers. The ability to effectively assess and mitigate these risks is crucial for ensuring the sustainability and profitability of businesses operating within this sector.

The research presented in this paper offers insights into the factors influencing the risk profile of freight forwarders. By employing simulation modeling techniques, we have demonstrated that the probability of financial loss for a freight forwarder is significantly impacted by the average request arrival interval and the tariff charged for services. Specifically, the risk increases with a longer average request interval and decreases with a higher tariff.

These findings provide a foundation for freight forwarders to make informed and justified decisions regarding pricing strategies, resource allocation, and risk management. By setting appropriate tariffs and optimizing operational efficiency, freight forwarders can mitigate the risk of financial loss and enhance their competitive position in the market.

Longer intervals between service requests increase the risk of financial loss. This suggests that freight forwarders should actively seek to optimize their customer base and service offerings to ensure a consistent and predictable flow of requests for their services. This could involve strategies such as: engaging with a wider range of clients across different industries to reduce reliance on a few major customers; offering complementary services such as warehousing, customs clearance, and supply chain consulting to enhance customer relationships and attract new business; expanding into new geographical markets or specialized service areas to capture new opportunities.

Higher tariffs generally lead to lower financial risk; however, it is crucial to achieve a balance between profitability and competitiveness. Freight forwarders should carefully analyze market trends, competitor pricing, and customer value perceptions to determine optimal pricing strategies. This could involve conducting market research, implementing dynamic pricing models, or negotiating favorable terms with carriers.

While this research has made contributions to the understanding of freight forwarder risk, further investigation is necessary to explore additional factors and refine the modeling approach. Future research could delve into the impact of factors such as:

- the possibilities of definition of the demand patterns using the dedicated machine learning algorithms,
- the influence of economic fluctuations and supply chain disruptions on freight forwarder risk,
- the role of competition intensity, market

concentration, and competitor behavior in shaping risk profiles,
- the potential benefits and challenges associated with emerging technologies, such as digital freight platforms and autonomous vehicles.

By considering these additional factors and refining the simulation models, it is possible to develop more comprehensive and accurate assessments of freight forwarder risk. This knowledge can be used in practice to develop robust risk management strategies and improve decision-making processes within the industry of freight transportation.

Acknowledgment

The authors received no financial support for the research, authorship and/or publication of this article.

Conflicts of interest

The authors declare that they have no known competing financial interests or personal relationships that could have appeared to influence the work reported in this paper.

References

[1] TAVARES, F., ALMEIDA, L. Logistics and the circular economy. In: *Reference module in social sciences* [online]. Elsevier, 2024. ISBN 978-0-443-15785-1. Available from: https://doi.org/10.1016/b978-0-443-13701-3.00019-0
[2] BORSOS, P., KOMAN, G. Smart mobility management supported by modern information and communication technologies. *Transportation Research Procedia* [online]. 2023, **74**, p. 1156-1163. ISSN 2352-1457, eISSN 2352-1465. Available from: https://doi.org/10.1016/j.trpro.2023.11.256
[3] NAUMOV, V., BEKMAGAMBETOVA, L., BITILEUOVA, Z., ZHANBIROV, Z., TARAN, I. 4 Mixed fuzzy-logic and game-theoretical approach to justify vehicle models for servicing the public bus line. *Communications - Scientific Letters of the University of Zilina* [online]. 2022, **24**(1), p. A26-A34. ISSN 1335-4205, eISSN 2585-7878. Available from: https://doi.org/10.26552/com.c.2022.1.a26-a34
[4] YANG, R., LI, Y., ZHAMG, B., YANG, R. Location-allocation problem in the emergency logistics system considering lateral transshipment strategy. *Computers and Industrial Engineering* [online]. 2024, **187**, 109771. ISSN 0360-8352, eISSN 1879-0550. Available from: https://doi.org/10.1016/j.cie.2023.109771
[5] NALGOZHINA, N., USKENBAYEVA, R. Automating hybrid business processes with RPA: optimizing warehouse management. *Procedia Computer Science* [online]. 2024, **231**, p. 391-396. eISSN 1877-0509. Available from: https://doi.org/10.1016/j.procs.2023.12.223
[6] ZHAN, J., DONG, S., HU, W. IoE-supported smart logistics network communication with optimization and security. *Sustainable Energy Technologies and Assessments* [online]. 2022, **52**, 102052. eISSN 2213-1396. Available from: https://doi.org/10.1016/j.seta.2022.102052
[7] KAYVANFAR, V., ELOMRI, A., KERBACHE, L., VANDCHALI, H. R., EL OMRI, A. A review of decision support systems in the internet of things and supply chain and logistics using web content mining. *Supply Chain Analytics* [online]. 2024, **6**, 100063. eISSN 2949-8635. Available from: https://doi.org/10.1016/j.sca.2024.100063
[8] CEDILLO-CAMPOS, M., FLORES-FRANCO, J., COVARRUBIAS, D. A physical internet-based analytic model for reducing the risk of cargo theft in road transportation. *Computers and Industrial Engineering* [online]. 2024, **190**, 110016. ISSN 0360-8352, eISSN 1879-0550. Available from: https://doi.org/10.1016/j.cie.2024.110016
[9] COMI, A., HRIEKOVA, O. Managing last-mile urban freight transport through emerging information and communication technologies: a systemic literature review. *Transportation Research Procedia* [online]. 2024, **79**, p. 162-169. ISSN 2352-1457, eISSN 2352-1465. Available from: https://doi.org/10.1016/j.trpro.2024.03.023
[10] OLISKEVYCH, M., TARAN, I., VOLKOVA, T., KLYMENKO, I. Simulation of cargo delivery by road carrier: case study of the transportation company. *Scientific Bulletin of National Mining University* [online]. 2022, **2**, p. 118-123. ISSN 2071-2227, eISSN 2223-2362. Available from: https://doi.org/10.33271/nvngu/2022-2/118
[11] TARAN, I., KARSYBAYEVA, A., NAUMOV, V., MURZABEKOVA, K., CHAZHABAYEVA, M. Fuzzy-logic approach to estimating the fleet efficiency of a road transport company: a case study of agricultural products deliveries in Kazakhstan. *Sustainability* [online]. 2023, **15**(5), 4179. eISSN 2071-1050. Available from: https://doi.org/10.3390/su15054179
[12] ENRIQUE, D. V., LERMAN, L. V., DE SOUSA, P. R., BENITEZ, G. B., SANTOS, F. M. B. CH., FRANK, A. G. Being digital and flexible to navigate the storm: How digital transformation enhances supply chain flexibility in turbulent environments. *International Journal of Production Economics* [online]. 2022, **250**, 108668. ISSN 0925-5273, eISSN 1873-7579. Available from: https://doi.org/10.1016/j.ijpe.2022.108668
[13] FARUK GORCUN, O., CHATTERJEE, P., STEVIC, Z., KUCUKONDER, H. An integrated model for road freight transport firm selection in third-party logistics using T-spherical Fuzzy sets. *Transportation Research Part E: Logistics and Transportation Review* [online]. 2024, **186**, 103542. ISSN 1366-5545, eISSN 1878-5794. Available from: https://doi.org/10.1016/j.tre.2024.103542

[14] BULUT, E. Modeling seasonality using the fuzzy integrated logical forecasting approach. *Expert Systems with Applications* [online]. 2014, **41**(4), p. 1806-1812. ISSN 0957-4174, eISSN 1873-6793. Available from: https://doi.org/10.1016/j.eswa.2013.08.079

[15] LIN, X., LU, Q., CHEN, L., BRILAKIS, I. Assessing dynamic congestion risks of flood-disrupted transportation network systems through time-variant topological analysis and traffic demand dynamics. *Advanced Engineering Informatics* [online]. 2024, **62**, 102672. ISSN 1474-0346, eISSN 1873-5320. Available from: https://doi.org/10.1016/j.aei.2024.102672

[16] MESJASZ-LECH, A., WLODARCZYK, A. The role of logistics infrastructure in development of sustainable road transport in Poland. *Research in Transportation Business and Management* [online]. 2022, **44**, 100841. ISSN 2210-5395, eISSN 2210-5409. Available from: https://doi.org/10.1016/j.rtbm.2022.100841

[17] KOTZEBUE, J. R. Integrated urban transport infrastructure development: The role of digital social geo-communication in Hamburg's TEN-T improvement. *Journal of Transport Geography* [online]. 2022, **99**, 103280. ISSN 0966-6923, eISSN 1873-1236. Available from: https://doi.org/10.1016/j.jtrangeo.2022.103280

[18] MACARIO, R., REIS, V., ANTUN, J. P. Environmentally friendly vehicles for sustainable logistics [online]. In: *Managing Urban Logistics*. Elsevier, 2024. ISBN 978-0-12-814462-6, p. 101-132. Available from: https://doi.org/10.1016/b978-0-12-814462-6.00004-7

[19] KOCSIS SZURKE, S., SUTHEO, G., APAGYI, A., LAKATOS, I., FISCHER, S. Cell fault identification and localization procedure for lithium-ion battery system of electric vehicles based on real measurement data. *Algorithms* [online]. 2022, **15**(12), 467. eISSN 1999-4893. Available from: https://doi.org/10.3390/a15120467

[20] FISCHER, S., KOCSIS SZURKE, S. Detection process of energy loss in electric railway vehicles. *Facta Universitatis, Series: Mechanical Engineering* [online]. 2023, **21**(1), 081. ISSN 0354-2025, eISSN 2335-0164. Available from: https://doi.org/10.22190/fume221104046f

[21] ESWARANATHAN, K., SIVAKUMAR, T., DE SILVA, M. M., KUMARAGE. A. S. Modelling the factors influencing carbon efficiency of consumer choice to promote energy-efficient vehicles. *Transport Economics and Management* [online]. 2024, **2**, p. 130-142. eISSN 2949-8996. Available from: https://doi.org/10.1016/j.team.2024.05.002

[22] SIKDER, M., WANG, CH., RAHMAN, M. M., YEBOAH, F. K., ANDREW ADEWALE ALOLA, A. A., WOOD, J. Green logistics and circular economy in alleviating CO2 emissions: Does waste generation and GDP growth matter in EU countries? *Journal of Cleaner Production* [online]. 2024, **449**, 141708. ISSN 0959-6526, eISSN 1879-1786. Available from: https://doi.org/10.1016/j.jclepro.2024.141708

[23] ZARBAKHSHNIA, N., KARIMI, A. Enhancing third-party logistics providers partnerships: an approach through the D.L.A.R.C.S supply chain paradigm. *Resources, Conservation and Recycling* [online]. 2024, **202**, 107406. ISSN 0921-3449, eISSN 1879-0658. Available from: https://doi.org/10.1016/j.resconrec.2023.107406

[24] PAVLENKO, O., MUZYLYOV, D., SHRAMENKO, N., CAGANOVA, D., IVANOV, V. Mathematical modeling as a tool for selecting a rational logistical route in multimodal transport systems [online]. In: *Industry 4.0 Challenges in Smart Cities*. CAGANOVA, D., HORNAKOVA, N. (Eds.). Cham: Springer, 2022. ISBN 978-3-030-92967-1, eISBN 978-3-030-92968-8, p. 23-37. Available from: https://doi.org/10.1007/978-3-030-92968-8_2

[25] RAJ, R., SINGH, A., KUMAR, V., DE, T., SINGH, S. Assessing the e-commerce last-mile logistics' hidden risk hurdles. *Cleaner Logistics and Supply Chain* [online]. 2024, **10**, 100131. eISSN 2772-3909. Available from: https://doi.org/10.1016/j.clscn.2023.100131

[26] NAUMOV, V., KHOLEVA, O. Studying demand for freight forwarding services in Ukraine on the base of logistics portals data. *Procedia Engineering* [online]. 2017, **187**, p. 317-323. ISSN 1877-7058. Available from: https://doi.org/10.1016/j.proeng.2017.04.381

[27] NAUMOV, V. Modeling demand for freight forwarding services on the grounds of logistics portals data. *Transportation Research Procedia* [online]. 2018, **30**, p. 324-331. ISSN 2352-1457, eISSN 2352-1465. Available from: https://doi.org/10.1016/j.trpro.2018.09.035

[28] YEN, B., MULLEY, C., YEH, C.-J. Performance evaluation for demand responsive transport services: A two-stage bootstrap-DEA and ordinary least square approach. *Research in Transportation Business and Management* [online]. 2023, **46**, 100869. ISSN 2210-5395, eISSN 2210-5409. Available from: https://doi.org/10.1016/j.rtbm.2022.100869

[29] NUGROHO, B., NAZARUDDIN, L. O., SYAMIL, A., NURHASAN, H. M., FATMA, E., NOOR, M. M., SOEHARSONO, I. P. F. M., SARASI, V., FEKETE-FARKAS, M., BALAZS, G. A pattern of collaborative logistics during multiple crises. *International Journal of Disaster Risk Reduction* [online]. 2024, **108**, 104499. eISSN 2212-4209. Available from: https://doi.org/10.1016/j.ijdrr.2024.104499

[30] ALI, I., GLIGOR, D., BALTA, M., BOZKURT, S., PAPADOPOULOS, T. From disruption to innovation: The importance of the supply chain leadership style for driving logistics innovation in the face of geopolitical disruptions. *Transportation Research Part E: Logistics and Transportation Review* [online]. 2024, **187**, 103583. ISSN 1366-5545, eISSN 1878-5794. Available from: https://doi.org/10.1016/j.tre.2024.103583

[31] CHAND, S., LI, Z., DIXIT, V. V., WALLER, S. T. Examining the macro-level factors affecting vehicle breakdown duration. *International Journal of Transportation Science and Technology* [online]. 2022, **11**(1), p. 118-131. ISSN 2046-0430, eISSN 2046-0449. Available from: https://doi.org/10.1016/j.ijtst.2021.03.003

[32] AYBALIKH, A. Investigating effective competition in the Swedish freight market in the presence of network effects, using the case of road transport. *Case Studies on Transport Policy* [online]. 2024, **16**, 101188. ISSN 2213-624X, eISSN 2213-6258. Available from: https://doi.org/10.1016/j.cstp.2024.101188

[33] HUANG, G., LIANG, Y., ZHAO, Z. Understanding market competition between transportation network companies using big data. *Transportation Research Part A: Policy and Practice* [online]. 2023, **178**, 103861. ISSN 0965-8564, eISSN 1879-2375. Available from: https://doi.org/10.1016/j.tra.2023.103861

[34] TSAIRI, Y., TAL, A., KATZ, D. Policy dissonance when wearing the "employer hat": The practice of governmental vehicle reimbursement among public sector employees. *Case Studies on Transport Policy* [online]. 2023, **12**, 100997. ISSN 2213-624X, eISSN 2213-6258. Available from: https://doi.org/10.1016/j.cstp.2023.100997

[35] NAUMOV, V. Evaluation of freight forwarder risk to transportation market entry. *Eastern-European Journal of Enterprise Technologies* [online]. 2015, **4**(3), p. 28-31. ISSN 1729-3774, eISSN 1729-4061. Available from: https://doi.org/10.15587/1729-4061.2015.47699

[36] ANDREJIC, M., KILIBARDA, M. Risk analysis of freight forwarders' activities in organization of international commodity flows. *International Journal for Traffic and Transport Engineering* [online]. 2018, **8**(1), p. 45-57. ISSN 2325-0062 eISSN 2325-0070. Available from: http://dx.doi.org/10.7708/ijtte.2018.8(1).04

[37] ZHOU, S.-P., ZHOU, Y.-W., PENG, B.-T., WANG, H.-J. The risk analysis of international freight forwarding in logistics service supply chain based on risk-MAP. In: 2012 24th Chinese Control and Decision Conference CCDC: proceedings [online]. IEEE. 2012. ISSN 1948-9439, eISSN 1948-9447, p. 3104-3109 Available from: https://doi.org/10.1109/CCDC.2012.6244489

[38] ELBERT, R., BOGUSCH, C., OZSUCU, O. Risk management for air freight forwarders: analysis of flexible price agreements and financial hedging. *Supply Chain Forum: An International Journal* [online]. 2012, **13**(4), p. 40-50. ISSN 1625-8312, eISSN 1624-6039. Available from: https://doi.org/10.1080/16258312.2012.11517305

[39] LIN, X., LIN, H., OU, S. Operation risk and control strategy of international freight forwarder. In: 2nd International Conference on Economic and Business Management: proceedings [online]. Atlantis Press. 2017. ISBN 978-94-6252-423-1, ISSN 2352-5428, p. 58-65. Available from: https://doi.org/10.2991/febm-17.2017.8

[40] Simulation model to mimic the processes of servicing the requests flow by a forwarding company [online] [accessed 2024-11-20]. Available from: https://github.com/naumovvs/forwarder-requests-servicing

DYNAMIC ROUTING IN URBAN TRANSPORT LOGISTICS UNDER LIMITED TRAFFIC INFORMATION

Viktor Danchuk[1], Oleksandr Hutarevych[1,*], Serhii Taraban[2]

[1]Department of Information Analysis and Information Security, Faculty of Transport and Information Technologies, National Transport University, Kyiv, Ukraine
[2]Department of Transport Safety Research, Issues of Normalization, Standardization and Metrology, State Enterprise "State Road Transport Research Institute", Kyiv, Ukraine

*E-mail of corresponding author: oleksandr.hutarevych@gmail.com

Viktor Danchuk 0000-0003-4282-2400, Oleksandr Hutarevych 0009-0003-7355-8160, Serhii Taraban 0000-0002-3886-7369

Resume
A method for online dynamic routing of freight delivery under limited traffic information using an ant colony algorithm, has been proposed. This method leverages real-time IoT data on traffic flow (TF) intensity from traffic sensors on urban road network (URN) sections, combined with averaged historical data on TF parameters (speed, density, intensity) obtained from traffic sensors on representative sections of homogeneous clusters within the URN. The procedure for forming homogeneous clusters within the URN and identifying representative sections is described. The results of simulation studies using the URN of Kyiv as an example indicate the potential of this method for urban transport logistics in conditions of complex traffic.

Article info
Received 5 September 2024
Accepted 29 January 2025
Online 19 February 2025

Keywords:
adaptive information system
AI methods of discrete optimization
dynamic routing, transport logistics
urban road network
IoT technologies
dynamic traveling salesman problem

Available online: https://doi.org/10.26552/com.C.2025.021

ISSN 1335-4205 (print version)
ISSN 2585-7878 (online version)

1 Introduction

Dynamic routing plays a key role in modern urban transportation logistics, enabling real-time management of traffic flows, ensuring consistent service quality for customers, improving road safety, and reducing negative environmental impacts. This requires the use of systems for timely collection and processing data of current dynamic characteristics of traffic flow on sections of the urban road network (URN), as well as efficient intelligent methods for discrete route optimization based on the analysis of this data.

Today, there are numerous advanced innovative technologies available for obtaining the relevant data, such as GPS technologies combined with modern geographic information systems (GIS), the Internet of Things (IoT) with traffic sensors, VANET systems, and others, which allow for automated dynamic routing through the integration of real-time data. Each of these technologies has its own advantages and disadvantages, necessitating further comprehensive research for their improvement.

One of the most promising approaches to monitoring the current state of the URN remains the use of traffic sensors combined with IoT technologies. Unlike many other approaches, this one provides the high accuracy in measuring the dynamics of traffic flow characteristics and allows for real-time data collection and analysis. However, it also has its drawbacks, including the high cost of modern sensors, such as digital video cameras with computer vision, and the limited coverage area, which requires the installation of a large number of sensors to obtain a complete picture. Moreover, there are currently no perfect methods for the real-time discrete route optimization that simultaneously consider the actual configuration of the URN and the dynamics of traffic flows on its sections.

In this context, developing and improving dynamic routing methods in urban transportation

logistics to overcome existing shortcomings remains a relevant problem.

2 Literature review

The problem of dynamic vehicle routing (DVRP) involves finding optimal routes for vehicles in real-time when some or all types of input data change over time [1]. Addressing the challenges of dynamic vehicle routing is crucial for enhancing the efficiency, cost-effectiveness, environmental sustainability, and safety of urban transportation logistics, especially in the context of rapid urbanization and increasing motorization of society. In a fast-changing environment, transport logistics companies, operating within limited time frames, must continuously adapt to these changes and ensure consistent service quality.

Recently, solving of DVRP tasks for e-commerce or last-mile commerce, which is rapidly growing, has become particularly relevant. Therefore, the development of effective and sustainable technologies is imperative to meet this demand and maintain high service levels. Multimodal deliveries, crowdshipping, and parcel lockers offer flexible options for e-commerce, contributing to hyper-connected urban logistics (HCL) for courier services [2-3]. Despite their potential, the effective use of these technologies is hindered by the absence of a comprehensive mathematical apparatus capable of tackling the complex modelling challenges for delivery processes. Here it is necessary to take into account numerous dynamic parameters and real-world constraints, including delivery times, freight volumes, travel distances, fleet characteristics, demand uncertainties, and stochastic customer requirements [2-3]. In this regard, DVRP problems are currently mainly solved taking into account individual constraints. At the same time, a large number of such DVRP are related to the problems of optimizing the route of delivery of goods with changing time windows, the nature and number of customer requests, the influence of weather conditions, etc. [2-7]. However, one of the main factors, affecting the dynamic impact of the environment on the effectiveness of transport logistics companies, remains the unpredictable and sudden changes in traffic on urban road network (URN) sections.

This necessitates the use of systems for timely collection and processing of data on the current dynamic characteristics of traffic flow on URN sections, data processing, and fast intelligent methods for discrete route optimization based on the analysis of this data.

Today, numerous advanced innovative technologies exist for collection and processing relevant data, such as GPS/Galileo technologies combined with modern GIS systems; VANET systems; Internet of Things (IoT) with traffic sensors; big data (BD) processing; blockchain (BC), among others (see, for example, [8-20]). These technologies allow for automated dynamic routing in real-time through the integration of data with modern artificial intelligence (AI) methods for discrete route optimization. The most suitable methods include swarm intelligence (SI) techniques, particularly ant colony optimization (ACO), particle swarm optimization (PSO), artificial bee colony (ABC) algorithms; genetic algorithms (GA); simulated annealing (SA); tabu search (TS); artificial neural networks for machine learning and deep learning; their modifications and hybridizations [21-26].

As the analysis shows, until now, practical aspects of DVRP have largely focused on the use of GIS data, which are derived from global navigation satellite systems (GNSS) technologies, primarily GPS. (see, for example, [8-12]). Typically, the main advantages of GPS technologies, such as wide coverage, integration with other systems, obtaining data on the actual configuration of URN sections, and relevant attributes of these sections (speed limits, congestion, waiting times at intersections, real-time traffic data, etc.) have been utilized. However, most studies have primarily explored the problems of dynamic planning for optimal delivery routes in transport logistics [8-12]. Moreover, route optimization has generally been carried out using classical methods of discrete optimization for small-scale transport logistics problems using historical GIS data. It is also worth noting that one of the most promising directions involves utilizing Galileo GNSS data. Indeed, Galileo PPP and/or Galileo RTK/RTN technologies offer several advantages over GPS technologies. These include higher positioning accuracy, improved signal penetration, and greater compatibility and integration with other GNSS systems, including GPS [13-14]. However, under current conditions, GNSS technologies present several limitations for solving DVRP. For instance, GNSS remains less effective compared to road IoT sensors in urban canyons with complex configurations or tunnels due to multipath signal propagation caused by reflections from structures. Additionally, GNSS PPP requires a relatively long data initialization time (up to 20 minutes [13]), which currently prevents its application for real-time dynamic routing tasks in scenarios involving complex traffic conditions.

In recent years, the use of VANET network systems has played an important role in improving the road safety, enhancing the efficiency of transport logistics systems, and providing convenient services for participants in the transport process (see, for example, [15-17]). Vehicular Ad-Hoc Network (VANET) is a self-organizing network used in the transport environment for communication between vehicles

(V2V technology), between a vehicle and roadside infrastructure (V2I technology), and with personal mobile devices [15]. It is assumed that to solve transport logistics problems, travelers have access to real-time traffic information through V2V/V2I infrastructures and make route decisions accordingly [16-17]. However, VANET presents unique challenges due to its dynamic nature, requiring significant efforts to address. These challenges are related both to data transmission routing in a highly dynamic V2V/V2I information environment and to dynamic routing of logistics paths in a non-stationary URN environment while ensuring stable VANET communication [15-17].

One of the most promising approaches to monitoring the current state of the URN remains the use of traffic sensors combined with IoT and AI technologies. Unlike many other approaches, this one ensures high accuracy in measuring traffic flow dynamics and allows for the real-time data collection and analysis. However, in recent years, the use of traffic data on URN sections obtained through various types of traffic sensors has been relatively less represented in the literature compared to, for example, GIS-derived data (see [18-20]). For instance, authors of [18] presented an intelligent dynamic routing system using machine learning technology to predict speed profiles based on historical traffic data from road sensors. The system includes neural networks for short-term speed prediction depending on the day of travel, congestion levels, and distances between individual sensor locations along the route. In [19], an effective dynamic routing strategy is proposed, which includes the possibility of continuously updating travelers' knowledge of travel times considering adaptive traffic signal control in real transport networks. In [20], a calibration model of an urban network consisting of two mini-roundabouts and one uncontrolled intersection is presented. The simulation process is carried out in the SUMO environment, and traffic data and speeds are collected from recorded video for the selected URN.

Thus, as the analysis shows (see, for example, [18-20]), dynamic routing of logistics flows, considering the non-stationary dynamics of traffic flows on URN sections, has mainly been performed using historical IoT data. The possibility of dynamic route optimization for freight delivery based on real-time IoT and BD data processing about non-stationary traffic dynamics on URN sections was first demonstrated in [21-22]. However, in [21], the computational operations during route optimization using the API from Bing and VRP_Spreadsheet_Solver are too slow, preventing the full real-time implementation. In [22], the input data block for dynamic traffic characteristics on URN sections is limited to manual entry. Moreover, simulation studies on route optimization are conducted within the framework of solving the symmetric dynamic traveling salesman problem (DTSP), which does not fully account for the real configuration and traffic conditions on URN sections [22].

Based on the conducted analysis, the current understanding of dynamic routing of logistics flows under the rapidly changing and non-stationary dynamics of traffic flows on URN sections using IoT data from traffic sensors is incomplete and imperfect. This is primarily due to the limited availability of traffic information from a larger number of different types of sensors and the limited coverage areas of these sensors, which requires the installation of a large number of sensors to obtain a complete picture. However, the installation of modern sensors, such as digital video cameras with computer vision, is not always possible due to their high cost. These reasons also partly explain the lack of adequate adaptive methods for the discrete route optimization for freight delivery (see, for example, [23-26]), which would simultaneously consider the actual configuration of the URN and the real dynamics of traffic flows on its sections during transportation in real-time.

In this context, the objective of this work was to develop an online dynamic routing method for urban transport logistics under limited traffic information. This method is based on the use of current IoT traffic data from sensors on URN sections and averaged historical data on traffic flow parameters obtained from sensors on representative sections of homogeneous clusters that make up the URN.

3 Research methodology

3.1 Description of the method

When modern means of measuring dynamic parameters (intensity q, and density ρ, average speed $\langle v \rangle$) of traffic flow (TF) are available on URN sections, optimizing routes in real-time does not present fundamental difficulties [20]. However, in the real-world operation of URNs, particularly in Ukrainian cities, relatively inexpensive traffic sensors are typically used, which measure only some TF parameters, such as TF intensity q values on specific sections over certain time intervals. This limitation prevents obtaining fully accurate information about the dynamic state of the URN and, consequently, restricts the ability to perform adequate real-time routing under complex traffic conditions. It is important to note that for most AI methods used in routing problems, the optimization parameters are time and/or distance of the route, which often requires knowledge of the average speed $\langle v \rangle$ on URN sections. Therefore, solving the problem of adequate simulation of the dynamic routing processes under limited information about TF dynamic parameters on

network sections at specific times is relevant.

A method for online dynamic routing in urban transport logistics under limited traffic information is proposed. This method is based on the use of current IoT data on TF intensity (q) from traffic sensors on URN sections and averaged historical data on TF parameters (q, ρ, $\langle v \rangle$) obtained from traffic sensors on representative sections of homogeneous clusters that form the URN.

In the first stage, it is proposed to establish a rational TF monitoring network on the URN (see section 3.2) by implementing a step-by-step iterative procedure to identify representative elementary sections within specific homogeneous URN clusters [27-28]. It is recommended to place the traffic sensors that measure dynamic TF parameters (q, ρ, $\langle v \rangle$) on these sections. Accordingly, traffic sensors that measure TF intensity q in real-time are placed on other URN sections.

The formation of a rational TF monitoring network on the URN is based on the assumption that within the studied URN, there is always a certain number of homogeneous URN clusters, where the static and dynamic properties of TF formation on these sections are similar. This means that the TF dynamics across all the modes of its formation, and consequently the shape of the curves representing the relationship $q = q(\langle v \rangle)$ have qualitatively identical characteristics for all sections within a homogeneous URN cluster, differing only in their quantitative values of q and $\langle v \rangle$. Additionally, this means that the normalization coefficients for formation $q = q(\langle v \rangle)$ or a set of sections within a specific URN cluster remain constant. Thus, knowing these normalization coefficients, one can construct the relationship curves $q = q(\langle v \rangle)$ for each section of a homogeneous cluster. Then, using experimentally measured data (q, ρ, $\langle v \rangle$) obtained from sensors on a representative section of the cluster and experimental data q obtained from sensors on other sections of this cluster, it is possible to construct a family of calibration curves $q = q(\langle v \rangle)$ for all the sections of each homogeneous URN cluster. Subsequently, for each calibration curve, the values of $\langle v \rangle$ can be determined based on the known experimental data q. The procedure for constructing such a family of calibration curves is described in section 3.3.

Section 3.4 presents the results of developing an adaptive dynamic routing system for urban transport logistics tasks under limited traffic information. This system implements the procedure for simulating online optimization with dynamic route updates for freight delivery to destinations using a selected AI method of discrete optimization. The system allows simultaneous consideration of the actual URN configuration and the real TF dynamics on its sections during transportation. The optimization problem is solved using an example of the asymmetric dynamic traveling salesman problem (DTSP), where the URN is represented as a weighted bidirectional graph [1]. The graph nodes correspond to delivery points, and the weights of the graph edges are assigned relative discrete values according to the optimization criterion. For instance, this could be the distance between graph nodes, the average travel time or speed, fuel consumption, transportation cost, ecological characteristics, etc. The cost matrix for such a graph contains indirect elements, such as the set of weights corresponding to a specific set of URN section characteristics that the vehicle sequentially overcomes between delivery points. The system enables the construction and dynamic updating of the graph based on real-time TF dynamic parameters obtained from traffic sensors.

For online discrete route optimization with dynamic updates within the DTSP task, a modified version of the classic ant colony optimization (ACO) algorithm was used [29]. Here, it is possible to fix the optimal configuration of a partially traversed route before automatically updating the graph weights based on changes in the dynamic characteristics of URN sections. To achieve this, the algorithm introduces Pre_k - list of graph edges that ant k is required to traverse, disregarding the probabilistic rule of the classical ant colony algorithm. Specifically, while at vertex i of the graph, ant k moves to vertex j if $(i,j) \in Pre_k$; otherwise, the next vertex is determined by the probabilistic rule.

The choice of the ACO modification (ACO_{mod}) for solving urban transport logistics tasks in this work is due to several reasons. First, ACO and its modifications are more versatile compared to most other AI optimization methods (see, for example, [22-23, 25]). This allows for solving routing problems on URNs of the required scale [22]. Moreover, ACO and its modifications generally have higher performance [22-23]. Additionally, the optimization mechanisms in ACO and its modifications are similar to the dynamics of TF, especially in high-density modes. Indeed, according to Boris Kerner's theory [30], the observed phase transition effects between different TF states are due to the manifestation of synergistic self-organization effects resulting from non-equilibrium non-stationary TF dynamics. Similarly, the path optimization process in ACO occurs due to the self-organization effects of ant colony agents during food search and delivery [29]. It is worth noting that such synergistic effects are observed in nonlinear non-equilibrium dissipative systems of various physical natures (see, for example, [31-33]). Thus, the use of ACO_{mod} allows for the simulation of the route optimization processes with dynamic updates in real-time, considering the actual TF dynamics on the transport network sections.

3.2 Formation of a rational traffic flow monitoring network

The primary goal of forming a rational traffic monitoring network is to ensure, on the one hand, the acquisition of reliable information about the current state of the URN and, on the other hand, to reduce the volume of observations required to monitor the dynamics of TF on URN sections.

In this work, the formation of such a monitoring network is based on the assumption outlined in section 3.1. It is proposed to form a rational TF monitoring network on URN sections for the Kyiv city by implementing a step-by-step iterative procedure to identify the representative elementary sections within specific homogeneous URN clusters using the k-means clustering method [27-28]. On these sections, it is recommended to place expensive traffic sensors that can fully measure the main dynamic characteristics of TF (average speed $\langle v \rangle$, intensity q, density ρ). On other sections, it is sufficient to place inexpensive sensors that measure TF intensity q.

The formation of homogeneous clusters that comprise the URN is carried out according to certain individual and group structural characteristics of streets and roads, in stages, with different numbers of steps in the partitioning of the URN, separately for each category of streets and roads (according to DBN B.2.3-5:2018) [34], until the minimum discrepancies between the values of the analyzed structural characteristics of URN elements in each formed cluster are achieved. Group and individual structural characteristics for each URN element are determined based on the magnitude of their impact on traffic parameters. The following are considered as group structural characteristics:

- The implemented traffic scheme concerning permitted directions of movement (one-way or two-way traffic);
- Parameters of the transverse profile of the roadway (number of lanes, lane width, etc.);
- The density of traffic signal regulation (the ratio of the number of traffic lights on each street to its total length).

This division is due to the fact that the impact of road conditions on the main TF parameters is often decisive, as the more frequently road conditions change along a street, the more complex the interaction between vehicles in the TF becomes.

At the same time, it should be noted that in this work, URN elements with a traffic signal regulation density not exceeding 0.5 were classified into separate clusters. This allowed for consideration of the impact of such traffic control devices as traffic lights on the dynamics (character) of TF.

The individual structural characteristics chosen is the parameters of the longitudinal profile of the roadway (length, area, slope, etc.).

The iterative procedure for determining representative sections involves the following sequential steps:

- dividing URN into elements (streets and roads) by categories according to the current classification of streets and roads;
- dividing the elements (streets and roads) into elementary sections with fixed structural features that define the nature and parameters of traffic flow distribution within URN;
- forming homogeneous groups of elementary street and road sections with similar group structural features;
- establishing the nature and parameters of the distribution of individual structural features within the formed homogeneous groups of elementary street and road sections;
- identifying representative elementary sections of streets and roads based on the distribution parameters of the individual structural features within the formed homogeneous groups.

In the first step of implementation of the step-by-step iterative procedure for finding the representative sections, the URN is divided into groups of elements - streets and roads that belong, in accordance with the current classification of roads, to the following categories: city-wide main streets, district main streets, and local streets and roads. Then, within each of the formed groups of streets and roads, the URN elements are divided into sections characterized by specific group and individual structural features. A section is defined as a part of a street or road of a particular category between the two closest intersections, within which the structural configuration of the section remains consistent.

In this context, it should be noted that the functioning of traffic flows on the streets and roads of a city is influenced by various factors, with road conditions often playing a decisive role in the main parameters of traffic flow. The more frequently road conditions change along a street, the more complex the interaction of vehicles in the traffic flow becomes. Therefore, in light of these circumstances, the decision was made to consider the city's streets and roads as a set of elementary sections.

The structural features of the elementary sections of URN were determined using the cartographic web service Google Maps [35], specifically through the combined use of this web service, its Measure Distance tool, and the regulatory document DBN B.2.3-5:2018, which specifies the parameters of various types of cross-sectional profiles of roadways for streets and roads in settlements according to their category.

After this, homogeneous groups (clusters) containing elementary sections with common group structural features are formed. As a result of the step-by-step clustering, city-wide main streets were

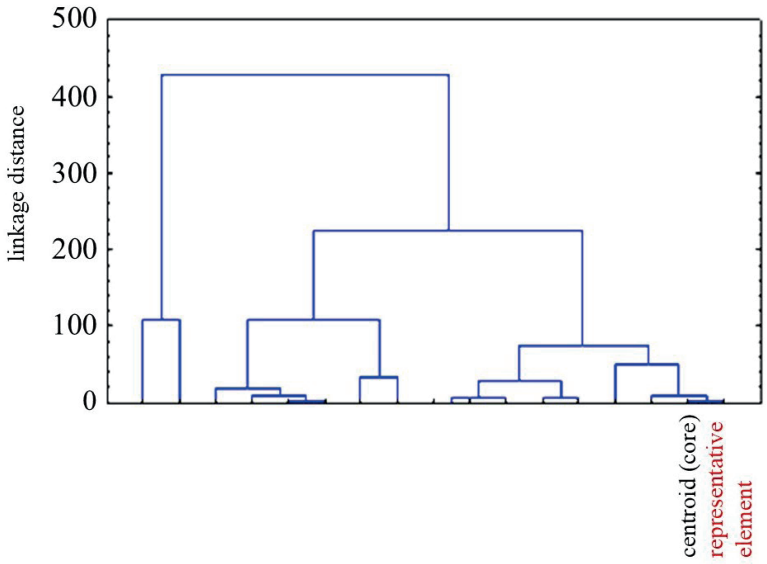

Figure 1 *Dendrogram for Identifying a Representative URN Element (Example of a Homogeneous Cluster)*

divided into three clusters, district main streets into eight clusters, and local streets and roads into 32 clusters.

In the next step, within each cluster, the average statistical values of each individual structural characteristic are established, which serve as the centers of gravity (centroids) of the formed homogeneous groups. These centroids are used to identify representative URN elements through hierarchical cluster analysis (see Figure 1).

In this case, within each cluster, as the representative section is selected the one where TF dynamics are observed in all its modes (free flow, synchronized flow, moving wide cluster, congestion) with the maximum distribution of TF intensity throughout the day.

As a result of the research, conducted within the framework of the method for forming a rational traffic flow monitoring network, representative sections were identified for the studied URN, which allowed for the creation of a rational monitoring network of TF. The dimensionality of this network is approximately 15 times smaller than the dimensionality of the studied set of URN elements. The reduction in dimensionality of URN is achieved by representing the structure of URN as separate clusters, the elements of which are characterized by a high degree of similarity in terms of relevant structural features and the subsequent identification of typical elements (within each formed cluster), whose structural features, in general, provide a comprehensive understanding of both the structural state of the elements within each cluster and URN of the city as a whole. This is justified by, among other things, the main assertion of cluster analysis, which states that each cluster, as a result of such a multidimensional statistical procedure, consists of similar objects, while objects from different clusters are significantly different from each other.

As a result of the clustering, the identified elements of the studied urban road network (URN) of Kyiv reflect (in terms of structural features) 85% of the city-wide main street network, 90% of the district main street network, and approximately 80% of the local street and road network.

3.3 Evaluation of dynamic characteristics of traffic flow on urban road network sections

The relationships between the intensity q and density ρ is considered as a function of the average speed $\langle v \rangle$ of a vehicle in the domain of dense traffic flow, where, according to [26], the regimes of synchronized movement and wide moving vehicle clusters are realized. Here, the average speed $\langle v \rangle$ of the traffic flow (TF) becomes variable. The evaluation of TF dynamic characteristics on URN sections using data from the rational monitoring network was carried out under the assumption described in section 3.1. In this case, the values of the dynamic characteristics $\langle v \rangle$ are determined using the data obtained from the calibration curve of the q versus $\langle v \rangle$ relationship (see 3.1). The procedure for constructing a family of calibration curves for the set of sections within each homogeneous cluster of the studied URN is described below. To do this, the functional relationship $q = q(\langle v \rangle)$ is considered in the form of a polynomial:

$$q(\langle v \rangle) = a_0 + a_1\langle v \rangle + \cdots + a_n\langle v \rangle^n \qquad (1)$$

and limit it to the cubic term.

Strictly speaking, Equation (1) should be

considered at specific values of $\rho(\rho = const)$. However, in general, especially in the domain of dense TF, $\rho \neq const$, so there is a more complex dependence $q = q(\langle v \rangle)$ [30]. Nonetheless, for simulation process, it is sufficient to consider the dependence in this approximation, as it qualitatively captures the main features of TF behavior in the high-density region (synchronized flow, wide moving cluster, congestion) [30].

The following TF characteristics are introduced for a representative section r belonging to homogeneous cluster j : $\langle v \rangle_{rj}$ is the average speed of vehicles in the TF on section r of cluster j of the URN; $q_{rj} = \frac{N_{rj}}{\Delta t_{rj}}$ (vehicles/hour) is the TF intensity (the number of vehicles passing through a specific cross-section of section r during the measurement time Δt_{rj}, normalized to 1 hour); $\rho_{rj} = \frac{N_{rj}}{l_{rj}}$ (vehicles/km) is the TF density (the number of vehicles moving on section r of length l_{rj}, normalized to 1 km).

In the first stage, experimental measurements of q_{rj}, ρ_{rj}, $\langle v \rangle_{rj}$ are carried out on a specific URN section that is representative (r) for a specific j homogeneous cluster of sections of the studied URN. The experimental average values $\langle q \rangle_{rj} \pm \Delta q_{rj}$, $\langle v \rangle_{rj} \pm \Delta v_{rj}, \langle \rho \rangle_{rj} \pm \Delta \rho_{rj}$ are determined. Here, $\Delta q_{rj}, \Delta v_{rj}, \Delta \rho_{rj}$ are the corresponding confidence intervals of the standard deviation. Based on the obtained experimental data, the relationships $q_{rj} = q_{rj}(\langle v \rangle)$ are constructed. These relationships are approximated using polynomials in Equation (1) within the framework of regression analysis, determining the corresponding sets of coefficients $a_0, a_1, \ldots a_n$ for the representative sections. Additionally, from the obtained polynomial relationships $q_{rj} = q_{rj}(\langle v \rangle)$, as well as from empirical data, the values $\langle v_{\min} \rangle_{rj}, q_{rj}(\langle v_{\max} \rangle)$, $\langle v_{rj}(q_{\max}) \rangle, q_{rj}(\langle v_{\min} \rangle)$, $(q_{\max})_{rj}$, $q_{rj}(\langle v \rangle = 0)$ are determined. The latter value corresponds to a traffic jam. Based on this data, normalization coefficients are formed, which characterize the shape of the curves of the $q = q(\langle v \rangle)$ relationship on the corresponding i sections of homogeneous cluster j of the URN. Namely:

$$k_{qj} = \frac{(q_{\max})_{rj}}{q_{rj}(\langle v_{\min} \rangle)}, l_{qj} = \frac{(q_{\max})_{rj}}{q_{rj}(\langle v_{\max} \rangle)}, \quad m_{qj} = \frac{(q_{\max})_{rj}}{q_{rj}(\langle v \rangle = 0)}. \tag{2}$$

Here, the normalization coefficients are determined based on the corresponding TF intensity values in the representative area r of cluster j: $(q_{\max})_{rj}$ is the maximum value of TF intensity; $q_{rj}(\langle v_{\max} \rangle)$ is the TF intensity when the vehicle is moving at the maximum speed $\langle v_{\max} \rangle$; $q_{rj}(\langle v_{\min} \rangle)$ is TF intensity when the vehicle is moving at the minimum speed $\langle v_{\min} \rangle$; $q_{rj}(\langle v \rangle = 0)$ is TF intensity when the vehicle is stationary $(\langle v \rangle = 0)$.

According to the assumption introduced, within a certain URN cluster, the shapes of the $q = q(\langle v \rangle)$ and $\rho(\langle v \rangle) = \rho(\langle v \rangle)$ curves for all sections of this URN cluster are similar and may differ only in their numerical values of the TF dynamic characteristics corresponding to these curves. This means that the normalization coefficients for a set of sections within a specific URN cluster j are identical.

Then, for any section i of a specific URN cluster j, the numerical values of the polynomial coefficients in cubic approximations $a_0^*, a_1^*, a_2^*, a_3^*$ for $q^*_{ij} = q^*_{ij}(\langle v \rangle)$ of section i can be determined by solving a linear system of three equations (3).

Here, $(q_{\max})_{ij}$ is the maximum TF intensity on section i of cluster j of the URN; $q_{ij}^*(\langle v_{\min} \rangle) = \frac{(q_{\max})_{ij}}{k_{qj}}$ is the TF intensity corresponding to $\langle v_{\min} \rangle$ on section i of cluster j; $q_{ij}^*(\langle v_{\max} \rangle) = \frac{(q_{\max})_{ij}}{l_{qj}}$ is the TF intensity corresponding to $\langle v_{\max} \rangle$ on section i of cluster j. The values $(q_{\max}{}^*)_{ij}, q_{ij}^*(\langle v_{\min} \rangle), q_{ij}^*(\langle v_{\max} \rangle)$ are determined from the results of averaging the corresponding historical data over specific time intervals. In this case, the zero-order polynomial coefficient $a_0 = \frac{(q_{\max}{}^*)_{ij}}{m_{qj}}$ (the constant term in each equation of system - Equation (3)). After determining the polynomial coefficients $a_0^*, a_1^*, a_2^*, a_3^*$ according to Equation (3), the functional relationship $q^*_{ij} = q^*_{ij}(\langle v \rangle)$ is constructed for each section i of the corresponding cluster j.

Thus, as a result of this procedure, a family of calibration curves of the approximated relationship $q = q(\langle v \rangle)$ is formed on the URN sections for the entire set of homogeneous clusters that make up the studied URN.

Then, the procedure for simulation online discrete optimization with dynamic route updating is carried out using the selected AI method based on IoT data regarding q, obtained in real-time from each section of the studied URN. Here, during the optimization based on the time criterion, the calibration curves of the approximated relationship $q = q(\langle v \rangle)$ are used

$$\begin{cases} \frac{(q_{\max}{}^*)_{ij}}{k_{qj}} = a_3^* \langle v_{\min} \rangle_{rj}^3 + a_2^* \langle v_{\min} \rangle_{rj}^2 + a_1^* \langle v_{\min} \rangle_{rj} + \frac{(q_{\max}{}^*)_{ij}}{m_{qj}} \\ (q_{\max}{}^*)_{ij} = a_3^* \langle v_{rj}(q_{\max}) \rangle^3 + a_2^* \langle v_{rj}(q_{\max}) \rangle^2 + a_1^* \langle v_{rj}(q_{\max}) \rangle + \frac{(q_{\max}{}^*)_{ij}}{m_{qj}} \\ \frac{(q_{\max}{}^*)_{ij}}{l_{qj}} = a_3^* \langle v_{\max} \rangle_{rj}^3 + a_2^* \langle v_{\max} \rangle_{rj}^2 + a_1^* \langle v_{\max} \rangle_{rj} + \frac{(q_{\max}{}^*)_{ij}}{m_{qj}} \end{cases} \tag{3}$$

to determine the average TF speed $\langle v \rangle$ on the URN sections at specific moments in time. Then, the time to traverse each section i of cluster j is determined as $t_{ij} = \frac{l_{ij}}{\langle v \rangle_{ij}}$, where $l_{ij}, \langle v \rangle_{ij}$ are the length and average TF speed on section i of cluster j, respectively.

It is also worth noting that certain difficulties arise in determining $\langle v \rangle_{ij}$ from the calibration curve, as the same intensity value may correspond to two different $\langle v \rangle_{ij}$ values. To avoid this ambiguity, it is necessary to use the results of historical data on density ρ versus average speed $\langle v \rangle$ obtained on representative sections, or the results of real-time traffic observation analysis on the corresponding URN sections at specific times of the day.

3.4 Adaptive system for dynamic routing under limited traffic information

An adaptive system for dynamic routing of freight delivery is understood as an information system designed to re-optimize the delivery route in real-time as the state of the URN changes due to changes in TF characteristics on URN sections during the freight delivery process [11].

The system considers the freight delivery route optimization problem as an asymmetric dynamic traveling salesman problem (DTSP) represented as a weighted bidirectional graph in the context of the URN (see section 3.1). The general scheme of the system operation is shown in Figure 2.

In this case, the route optimization process is performed based on either distance or time criteria. For distance optimization, it is sufficient to use the structural data of URN sections. For time optimization, the system uses input data from the structural parameters of URN sections and the $\langle v \rangle$ values obtained directly from traffic sensors on representative sections, as well as from the family of calibration curves $q = q(\langle v \rangle)$ for other sections within each homogeneous URN cluster (see sections 3.1-3.3).

As shown in Figure 2, the system allows the user to input a set of delivery points and depot. The system then constructs a weighted bidirectional graph, where the nodes correspond to the delivery points and the depot. Each edge of the graph consists of a sequence of URN sections; whose traversal determines the optimal route between the corresponding pair of delivery points at a specific time of day. Each such URN section in the sequence is characterized by a

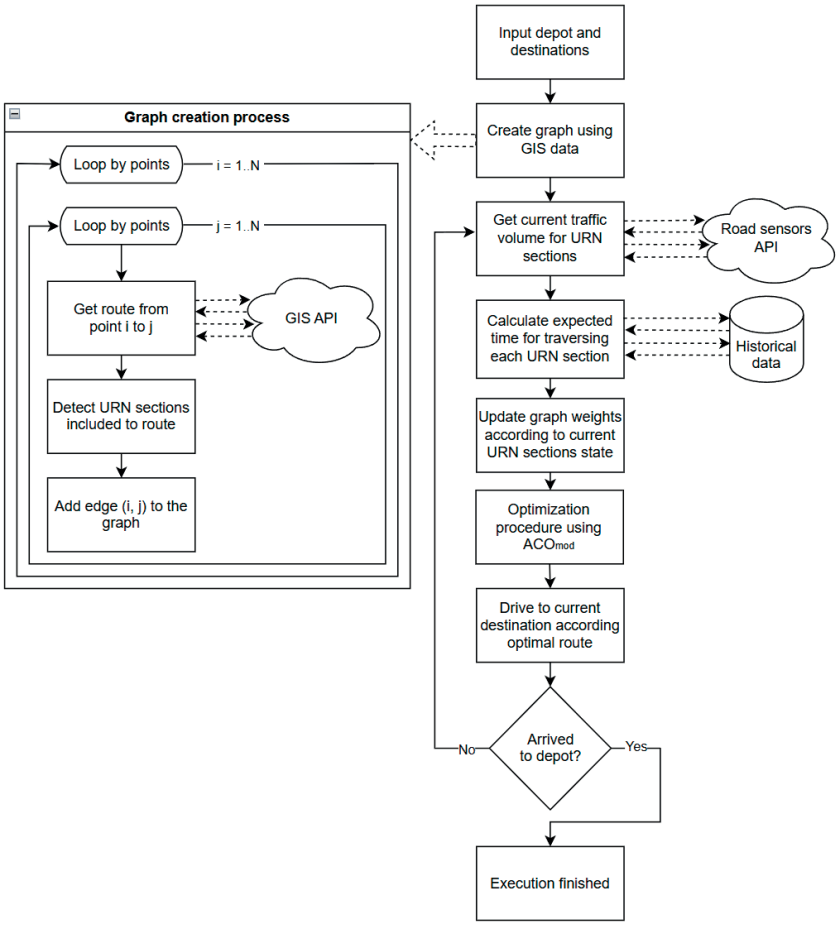

Figure 2 *Flowchart of the adaptive system for dynamic routing of freight delivery within the DTSP problem using the data on changing TF characteristics on URN sections*

certain identifier (road name), length, number of lanes, and traffic direction. In the proposed system, the creation of such a graph is based on GIS data. As shown in Figure 2, for each pair of points (*i, j*) system queries GIS to retrieve the route from point *i* to *j* including a sequence of URN sections in the route and preprocesses this information for subsequent use in graph updates. This data can be obtained using the Routes API service of Bing Maps [36].

After the graph is formed, a procedure is performed to update the graph according to the current state of the URN at a specific time of day. The update procedure involves obtaining the real-time data on the current TF intensity from traffic sensors located on the corresponding URN sections for each section that characterizes each edge of the graph. Using this data and the family of calibration curves $q = q(\langle v \rangle)$ constructed based on historical data on URN characteristics for representative sections of homogeneous clusters, the current average speed of TF on each URN section is determined in the corresponding traffic direction. Using the current speed values on the URN sections and the structural parameters of each section, the expected time to travel the corresponding section is calculated. Ultimately, this allows determining the expected time to traverse each graph edge as the sum of the expected times to traverse the sequence of URN sections that characterize the corresponding graph edge (see Figure 2). Thus, the weights of the edges of the updated graph are characterized by the expected traversal time of each edge, taking into account both the current TF dynamics and the actual URN configuration.

After updating the graph, the freight delivery route optimization procedure is carried out using the modified ant colony algorithm ACO_{mod} (see section 3.1, Figure 2). According to the determined optimal route, the user is directed to the next delivery point.

Upon the user's arrival at this point, the next graph update is performed according to the current URN state. After that, the route re-optimization procedure is carried out using ACO_{mod} on the updated graph. The proposed ACO_{mod} implementation allows fixing the optimal configuration of the partially traversed route before updating the graph, as well. Thus, within the proposed adaptive dynamic routing system, the route re-optimization procedure is carried out until the user is directed back to the depot after completing deliveries to all the specified points.

4 Results and discussion

For the simulation studies, 19 points on the URN of Kyiv were selected (numbered from 0 to 18), corresponding to the addresses of branches of the Ukrainian postal operator "Nova Poshta" [37]. Figure 3 shows the location of delivery points on the Kyiv map. The task was to find the optimal time-based route for a vehicle departing from the depot (point 0) on September 25, 2023, at 07:30:00, delivering goods to points 1-18, and returning to the depot.

The simulation studies were conducted with the following assumptions:

- The type of delivery route is a circular route with sequential delivery of goods;
- The date and time of day are taken into account, but the unloading time at delivery points, the nomenclature, weight, and volume of the cargo are not considered;
- Each edge of the graph corresponds to a fixed sequence of URN sections, describing the optimal path between each pair of delivery points;
- Changes in the expected travel time between nodes depend on current changes in TF characteristics on URN sections;
- Graph updates and route re-optimization are performed while the vehicle is at a delivery point.

To perform the dynamic routing of the delivery process, a basic implementation of the proposed adaptive system was developed on the .NET 6 platform using the C# programming language. The studies were conducted on equipment with an Intel(R) Core(TM) i5-8400 CPU @ 2.80GHz processor, 16 GB of DDR4 RAM, and running Windows 10. The studies showed that the initial construction of the graph with 19 nodes using GIS data took an average of 18.11 seconds, updating the graph based on current information from the traffic sensors took 594 ms (excluding the time to receive information from the traffic sensors), and finding the optimal solution for the graph with 19 nodes by performing 1000 iterations of ACO_{mod} took an average of 2.67 seconds.

The input data array for the dynamic TF characteristics was formed using the q, ρ and $\langle v \rangle$ data obtained from field experiments conducted on representative sections, and the q data obtained in real-time from traffic sensors located on the sections of the studied URN. This is due to the fact that Flir Traficam 2 sensors [38], which are currently used on the URN sections of Kyiv, measure only TF intensity ρ in real-time with a discretization of 2 minutes. Therefore, to construct a family of calibration curves of the approximated $q = q(\langle v \rangle)$ relationship on URN sections for the entire set of homogeneous clusters, field experiments were conducted to determine q, ρ and $\langle v \rangle$ on the representative sections of each URN cluster. During the working days from September 11, 2023, to September 15, 2023, the corresponding values of q, ρ and $\langle v \rangle$ were measured. Averaging was carried out over five measurements. As an example, Figure 4 shows graphs of the dependence of average intensity and average density on the average speed of TF for a representative URN section - Brovary Avenue, exit (Chernihiv direction), which

belongs to a homogeneous cluster of the city-wide main streets.

As can be seen from Figure 4(a), a single intensity value can correspond to two different speed values: the left-hand wing of the curve corresponds to dense traffic, and the right-hand wing to free flow. The current traffic mode is determined based on historical data on traffic flow density in similar time periods relative to the current one for the representative sections of homogeneous clusters.

Table 1 presents the traffic flow characteristics of some URN sections used in the simulation studies. The column "Time" specifies the time at which the traffic data was recorded. For each URN section,

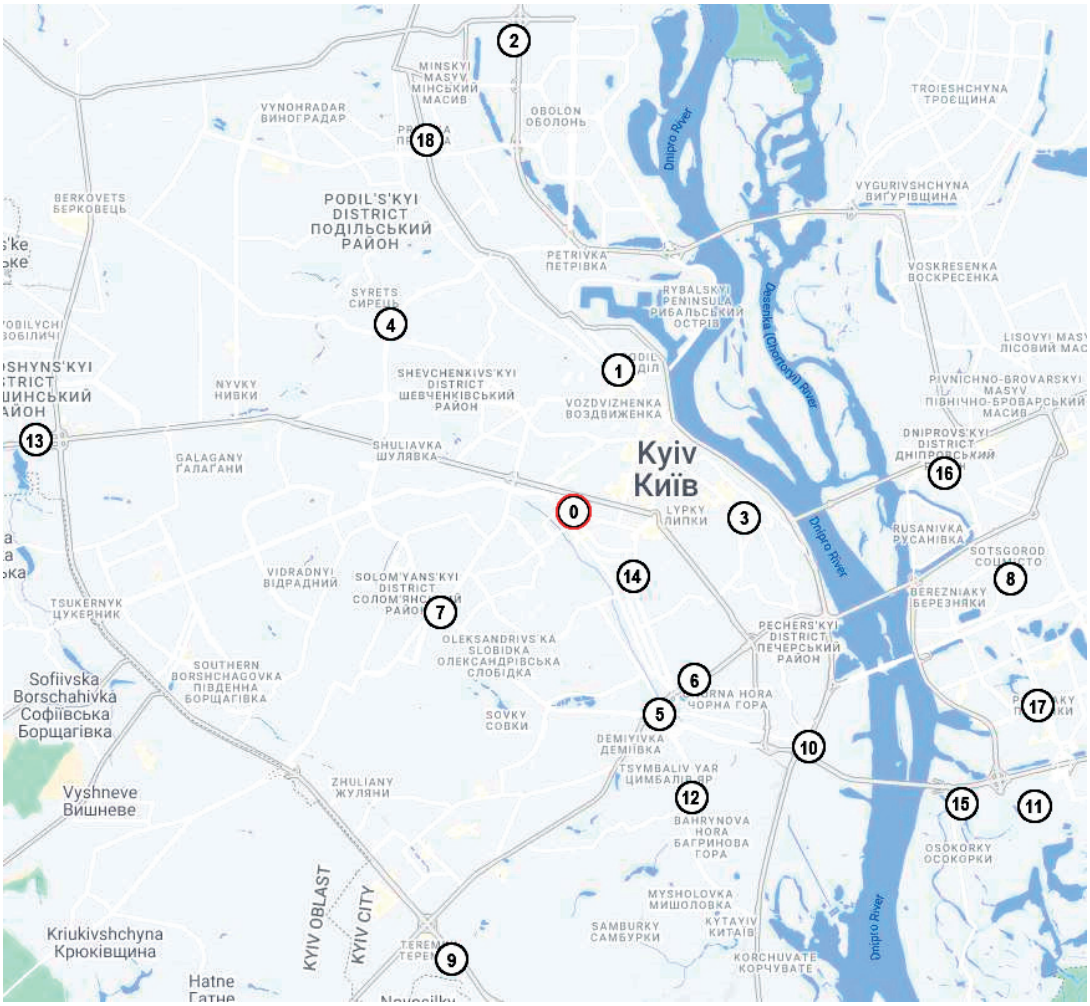

Figure 3 *Locations of the depot (0) and delivery points (1, …, 18) on the map of Kyiv*

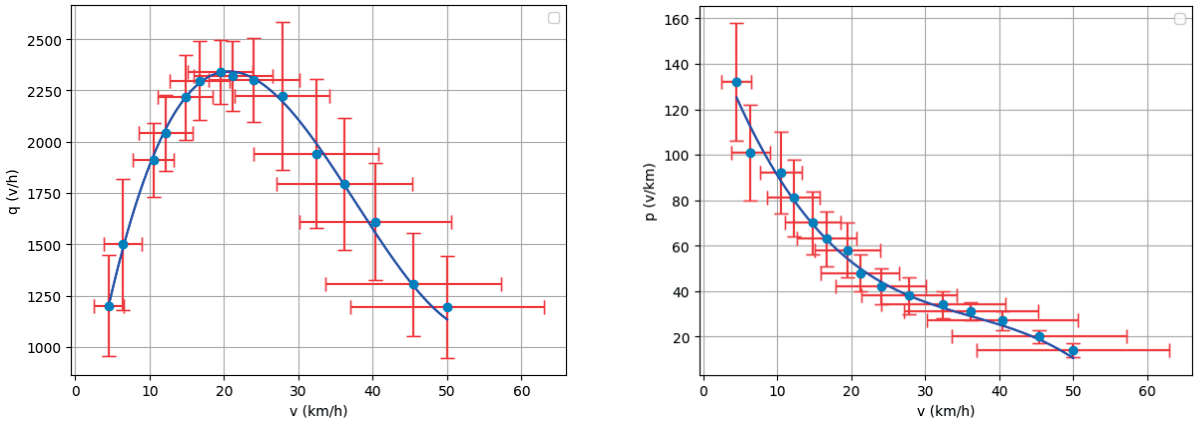

(a) *(b)*

Figure 4 *Graphs of the dependence of average intensity (a) and average density (b) on the average speed of traffic flow based on field experiments: points represent the average values of the TF dynamic parameters; line segments indicate confidence intervals*

two sub-columns are provided: q is experimental traffic flow intensity (vehicles per hour, v/h); $\langle v \rangle$ is average traffic flow speed (kilometers per hour, km/h) calculated based on the intensity. The included URN sections, with the moving direction specified in brackets, are as follows: Section 1 is Beresteiskyi Avenue (SE), Section 2 is Avtozavodska Street (SE), Section 3 is Akademika Zabolotnoho Street (SE), Section 4 is Akademika Zabolotnoho Street (NW), Section 5 is Petra Hryhorenka Avenue (SE), Section 6 is Nauky Avenue (SE).

Table 2 presents the results of the simulation study of dynamic freight delivery routing to the specified points of the "Nova Poshta" postal operator (some re-optimization steps that did not result in route reconstruction are not shown). The column "Current time" contains the current time of day; the column "Proposed route" contains the current optimal delivery route, with the current delivery point where re-optimization is performed marked with an asterisk (*); the column "Optimal route expected time" contains the expected time to complete the optimal route in seconds within the DTSP, obtained from the corresponding optimization results; the column "Current" contains the expected time of the current optimal route at the time of re-optimization; the column "Previous" contains the expected time of the optimal route obtained from the previous re-optimization, but for the current dynamic state of the URN; the column "Initial" contains the expected time of the optimal route obtained from the optimization at the time of departure from the depot, but for the current dynamic state of the URN. In parentheses is the part of the route that is rebuilt as a result of re-optimization.

As seen in Table 2, during the simulation studies using the proposed method of online dynamic freight delivery routing, several effects related to the rebuilding of the optimal route were observed. For example, significant route rebuilding occurs at the times 07:55:20, 08:04:05, and 09:01:28. Additionally, in all the cases, a significant increase in delivery time for the initial configuration of the optimal route is observed at the current times of day compared to

Table 1 *Traffic flow characteristics of some URN sections used in simulation studies*

Time	Section 1		Section 2		Section 3		Section 4		Section 5		Section 6	
	q	$\langle v \rangle$	q	$\langle v \rangle$	q	$\langle v \rangle$	q	$\langle v \rangle$	q	$\langle v \rangle$	q	$\langle v \rangle$
07:30:00	3246	32	1465	36	2190	23	1752	37	673	50	500	50
07:55:20	2488	41.5	2237	19.5	2340	23	1758	37	659	50	675	50
08:13:20	1895	47	2366	19	2322	23	1650	9.5	840	5	683	50
08:37:27	2164	44.5	2777	19	2328	23	1968	14	779	4	930	39
09:01:28	2336	43	1735	30.5	1896	34	1992	14.5	866	47	810	43.5
09:18:01	2222	44	1915	26	1968	32	2022	15	953	44.5	765	46
09:34:39	1667	49	1388	37.5	2286	23	1842	12	913	45.5	908	39.5
09:48:22	3132	34	1414	37	2238	23	1854	12	973	44	818	43.5
10:07:39	3094	34.5	1067	48	1975	32	1598	40	773	50	882	40.5
10:21:01	2993	36	1272	40	1873	34.5	1707	38	986	43.5	720	50

Table 2 *Results of dynamic freight delivery routing in the URN of Kyiv*

Current time	Proposed route	Optimal route expected time, s		
		Current	Previous	Initial
07:30:00	0*1-18-2-4-7-13-9-5-12-10-15-11-8-17-16-3-6-14-0	10390	-	-
07:40:14	0-1*18-2-4-13-9-5-7-12-10-15-11-(17-8)-16-3-6-14-0	10486	10525	10525
07:55:20	0-1-18*2-4-13-(9-12-10-15-17-11-8-16-3-6-5-7-14)-0	10438	10486	10525
08:04:05	0-1-18-2*4-13-(9-14-3-16-15-11-17-8-10-6-12-5-7)-0	12632	17696	15663
08:13:20	0-1-18-2-4*13-9-14-3-16-15-11-17-8-10-6-12-5-7-0	11845	11845	13477
08:23:13	0-1-18-2-4-13*9-14-3-16-15-11-17-8-10-6-12-5-7-0	11887	11887	14136
08:37:27	0-1-18-2-4-13-9*14-3-16-15-11-17-8-10-6-12-5-7-0	12220	12220	15015
08:52:17	0-1-18-2-4-13-9-14*3-16-15-11-17-8-10-6-12-5-7-0	11800	11800	14727
09:01:28	0-1-18-2-4-13-9-14-3*(10-15-11-17-8-16-6)-12-5-7-0	10732	10832	12590
09:13:05	0-1-18-2-4-13-9-14-3-10*15-11-17-8-16-6-12-5-7-0	10704	10704	13252
10:21:01	0-1-18-2-4-13-9-14-3-10-15-11-17-8-16-6-12-5-7*0	10746	10746	16742
10:29:06	0-1-18-2-4-13-9-14-3-10-15-11-17-8-16-6-12-5-7-0*	-	10746	16742

the time of the initial optimal route built at 07:30:00 (see Table 2). These effects are due to a significant increase and redistribution of the number of vehicles on the URN sections at the corresponding times of day. Re-optimization allows for finding such optimal routes in real-time, leading to a significant reduction in delivery time to the correspondent points. For example, at 08:04:05, the initial optimal route expected time is 15663 seconds, while the current optimal route expected time is 12632 seconds. This means that after re-optimizing the route at delivery point 2 (see Table 2), the delivery time is reduced by Δt =15663 s - 12632 s = 3031 s, representing an economic effect of 19.4%.

Thus, the results of the studies conducted within the framework of the online dynamic routing method under the limited traffic information indicate the potential of using the proposed method for urban transport logistics in conditions of complex traffic.

5 Conclusions and recommendations

A method for online adaptive dynamic routing of freight delivery in cities under limited traffic information has been proposed. This method is based on the use of real-time IoT data on traffic flow intensity from the traffic sensors on URN sections and averaged historical data on TF parameters (speed, density, intensity) obtained from traffic sensors on representative sections of homogeneous clusters that make up the URN. An algorithm for forming a rational TF monitoring network in the URN has been developed based on the k-means clustering method to identify homogeneous clusters that constitute the URN and the representative sections within them.

An automated adaptive information system for dynamic routing in urban transport logistics under limited traffic information has been developed. This system includes a procedure for online optimization with dynamic route updating using a modified AI ant colony algorithm. The system allows for simultaneous consideration of the actual URN configuration and the real TF dynamics on its sections during transportation. The optimization problem is solved using an asymmetric DTSP, where the URN is represented as a weighted bidirectional graph.

The results of simulation studies, conducted on the example of Kyiv's URN, indicate the potential of the proposed method for use by transport companies and authorities in urban transport logistics under complex traffic conditions.

In the future, the results of the research could contribute to a promising approach to reducing the carbon footprint. The method facilitates the integration of environmental considerations, particularly through the route optimization based on criteria such as fuel consumption and CO_2 emissions. Aligned with corporate sustainability goals, this creates opportunities to integrate reporting and decarbonization mechanisms into the transport logistics. Furthermore, the proposed method could serve as a foundation for developing a dynamic routing system that considers not only transportation costs and pollutant emissions but the economic incentives for minimizing emissions, such as carbon credits, as well. This would provide a comprehensive approach to enhancing the efficiency of transport logistics and reducing its environmental impact.

Acknowledgment

The authors received no financial support for the research, authorship and/or publication of this article.

Conflicts of interest

The authors declare that they have no known competing financial interests or personal relationships that could have appeared to influence the work reported in this paper.

References

[1] POP, P. C., COSMA, O., SABO, C., SITAR, C. P. A comprehensive survey on the generalized traveling salesman problem. *European Journal of Operational Research* [online]. 2024, **314**(3), p. 819-835 [accessed 2024-08-10]. ISSN 0377-2217. Available from: https://doi.org/10.1016/j.ejor.2023.07.022

[2] SAWIK, B. Optimizing last-mile delivery: a multi-criteria approach with automated smart lockers, capillary distribution and crowdshipping. *Logistics* [online]. 2024, **8**(2), 52 [accessed 2024-08-10]. ISSN 2305-6290. Available from: https://doi.org/10.3390/logistics8020052

[3] GIUFFRIDA, N., FAJARDO-CALDERIN, J., MASEGOSA, A. D., WERNER, F., STEUDTER, M., PILLA, F. Optimization and machine learning applied to last-mile logistics: a review. *Sustainability* [online]. 2022, **14**(9), 5329 [accessed 2024-08-10]. ISSN 2071-1050. Available from: https://doi.org/10.3390/su14095329

[4] ZHANG, H., ZHANG, Q., MA, L., LIU, Y. A hybrid ant colony optimization algorithm for a multi-objective vehicle routing problem with flexible time windows. *Information Sciences* [online]. 2019, **490**, p. 166-190 [accessed 2024-08-10]. ISSN 0020-0255. Available from: https://doi.org/10.1016/j.ins.2019.03.070

[5] BELHAIZA, S., M'HALLAH, R., BRAHIM, G. B., LAPORTE, G. Three multi-start data-driven evolutionary heuristics for the vehicle routing problem with multiple time windows. *Journal of Heuristics* [online]. 2019, **25**(3), p. 485-515 [accessed 2024-08-10]. ISSN 1572-9397. Available from: https://doi.org/10.1007/s10732-019-09412-1

[6] HOOGEBOOM, M., DULLAERT, W. Vehicle routing with arrival time diversification. *European Journal of Operational Research* [online]. 2019, **275**(1), p. 93-107 [accessed 2024-08-10]. ISSN 0377-2217. Available from: https://doi.org/10.1016/j.ejor.2018.11.020

[7] XU, Y. Logistics distribution for path optimization using artificial neural network and decision support system. *Research Square* [online]. 2022, p. 1-17 [accessed 2024-08-10]. Available from: https://doi.org/10.21203/rs.3.rs-1249887/v1

[8] YUAN, J., SONG, J., ZHANG, Y., JIANG, C., XU, F. Planning of dynamic routing of logistics in urban public sports facilities based on MAS. In: 4th International Conference on Transportation Engineering: proceedings. 2013. ISBN 9780784413159. p. 1156-1162.

[9] ABOUSAEIDI, M., FAUZI, R., MUHAMAD, R. Geographic Information System (GIS) modeling approach to determine the fastest delivery routes. *Saudi Journal of Biological Sciences* [online]. 2015, **23**(5), p. 1-27 [accessed 2024-08-13]. ISSN 1319-562X. Available from: https://doi.org/10.1016/j.sjbs.2015.06.004

[10] ROTHKRANTZ, L. Hybrid dynamic route planners. In: 19th International Conference on Computer Systems and Technologies: proceedings. ACM, 2018. ISBN 9781450364256. p. 12-19.

[11] TSOUKAS, V., BOUMPA, E., CHIOKTOUR, V., KALAFATI, M., SPATHOULAS, G., KAKAROUNTAS, A. Development of a dynamically adaptable routing system for data analytics insights in logistic services. *Analytics* [online]. 2023, **2**(2), p. 328-345 [accessed 2024-08-13]. ISSN 2813-2203. Available from: https://doi.org/10.3390/analytics2020018

[12] LYU, Z., PONS, D., ZHANG, Y, JI, Z. Freight operations modelling for urban delivery and pickup with flexible routing: cluster transport modelling incorporating discrete-event simulation and GIS. *Infrastructures* [online]. 2021, **6**(12), 18. ISSN 2412-3811 [accessed 2024-08-13]. Available from: https://doi.org/10.3390/infrastructures6120180

[13] RAZA, S., AL-KAISY, A., TEIXEIRA, R., MEYER, B. The role of GNSS-RTN in transportation applications. *Encyclopedia* [online]. 2022, **2**(3), p. 1237-1249 [accessed 2024-08-13]. ISSN 2673-8392. Available from: https://doi.org/10.3390/encyclopedia2030083

[14] BASTOS, L., BUIST, P., CEFALO, R., GONCALVES, J. A. Kinematic Galileo and GPS performances in aerial, terrestrial, and maritime environments. *Remote Sensing* [online]. 2022, **14**(14), 3414 [accessed 2024-08-14]. ISSN 2074-4292. Available from: https://doi.org/10.3390/rs14143414

[15] BADOLE, M. H., THAKARE, A. D. An optimized framework for VANET routing: a multi-objective hybrid model for data synchronization with digital twin. *International Journal of Intelligent Networks* [online]. 2023, **4**, p. 272-282 [accessed 2024-08-14]. ISSN 2666-6030. Available from: https://doi.org/10.1016/j.ijin.2023.10.001

[16] SAOUD, B., SHAYEA, I., YAHYA, A. E., SHAMSAN, Z. A., ALHAMMADI, A., ALAWAD, M. A., ALKHRIJAH, Y. Artificial Intelligence, Internet of things and 6G methodologies in the context of Vehicular Ad-hoc Networks (VANETs): survey. *ICT Express* [online]. 2024, **10**(4), p. 959-980 [accessed 2024-08-14]. ISSN 2405-9595. Available from: https://doi.org/10.1016/j.icte.2024.05.008

[17] MOUHCINE, E., MANSOURI, K., MOHAMED, Y. Solving traffic routing system using VANet strategy combined with a distributed swarm intelligence optimization. *Journal of Computer Science* [online]. 2019, **14**(11), p. 1499-1511 [accessed 2024-08-15]. ISSN 1549-3636. Available from: https://doi.org/10.3844/jcssp.2018.1499.1511

[18] PARK, J., MURPHEY, Y. L., MCGEE, R., KRISTINSSON, J. G., KUANG M. L., PHILLIPS, A. M. Intelligent trip modeling for the prediction of an origin-destination traveling speed profile. *IEEE Transactions on Intelligent Transportation Systems* [online]. 2014, **15**(3), p. 1039-1053 [accessed 2024-08-15]. ISSN 1558-0016. Available from: https://doi.org/10.1109/tits.2013.2294934

[19] CHAI, H., ZHANG, H. M., GHOSAL, D., CHUAH C.-N. Dynamic traffic routing in a network with adaptive signal control. *Transportation Research Part C: Emerging Technologies* [online]. 2017, **85**, p. 64-85 [accessed 2024-08-16]. ISSN 0968-090X. Available from: https://doi.org/10.1016/j.trc.2017.08.017

[20] YAVUZ, M. N., OZEN, H. Calibration of microscopic traffic simulation of urban road network including mini-roundabouts and unsignalized intersection using open-source simulation tool. *Scientific Journal of Silesian University of Technology. Series Transport* [online]. 2024, **122**, p. 305-318 [accessed 2024-08-16]. ISSN 2450-1549. Available from: https://doi.org/10.20858/sjsutst.2024.122.17

[21] RUSSO, F., COMI, A. Sustainable urban delivery: the learning process of path costs enhanced by information and communication technologies. *Sustainability* [online]. 2021, **13**(23), 13103 [accessed 2024-08-18]. ISSN 2071-1050. Available from: https://doi.org/10.3390/su132313103

[22] DANCHUK, V., COMI, A., WEISS, C., SVATKO, V. The optimization of cargo delivery processes with dynamic route updates in smart logistics. *Eastern-European Journal of Enterprise Technologies* [online]. 2023, **2**(3), p. 64-73 [accessed 2024-08-18]. ISSN 1729-4061. Available from: https://doi.org/10.15587/1729-4061.2023.277583

[23] ZHANG, N. Smart logistics path for cyber-physical systems with internet of things. *IEEE Access* [online]. 2018, **6**, p. 70808-70819 [accessed 2024-08-18]. ISSN 2169-3536. Available from: https://doi.org/10.1109/access.2018.2879966

[24] NG, K. K. H., LEE, C. K. M., ZHANG, S. Z., WU, K., HO, W. A multiple colonies artificial bee colony algorithm for a capacitated vehicle routing problem and re-routing strategies under time-dependent traffic congestion. *Computers and Industrial Engineering* [online]. 2017, **109**, p. 151-168 [accessed 2024-08-18]. ISSN 0360-8352. Available from: https://doi.org/10.1016/j.cie.2017.05.004

[25] ZAJKANI, M. A., BAGHDORANI, R. R., HAERI, M. Model predictive based approach to solve DVRP with traffic congestion. *IFAC-PapersOnLine* [online]. 2021, **54**(21), p. 163-167 [accessed 2024-08-19]. ISSN 2405-8963. Available from: https://doi.org/10.1016/j.ifacol.2021.12.028

[26] LIU, H., LEE, A., LEE, W., GUO. P. DAACO: adaptive dynamic quantity of ant ACO algorithm to solve the traveling salesman problem. *Complex and Intelligent Systems* [online]. 2023, **9**, p. 4317-4330 [accessed 2024-08-19]. ISSN 2198-6053. Available from: https://doi.org/10.1007/s40747-022-00949-6

[27] ARTHUR, D., VASSILVITSKII, S. K-means++: the advantages of careful seeding. In: 18th Annual ACM-SIAM Symposium on Discrete Algorithms: proceedings. 2007. p. 1027-1035.

[28] LIKAS, A., VLASSIS, N., VERBEEK., J. J. The global k-means clustering algorithm. *Pattern Recognition* [online]. 2003, **36**(2), p. 451-461 [accessed 2024-08-17]. ISSN 0031-3203. Available from: https://doi.org/10.1016/s0031-3203(02)00060-2

[29] DORIGO, M., DI CARO, G. The ant colony optimization meta-heuristic. In: *New idea in optimization*. CORNE, D., DORIGO, M., GLOVER, F. (Eds.). London: McGrow-Hill, 1999. ISBN 9780077095062, p. 11-32.

[30] KERNER, B. S. *Introduction to Modern Traffic Flow Theory and Control*. Berlin, Heidelberg: Springer Berlin Heidelberg, 2009. ISBN 9783642026041.

[31] PUCHKOVSKA, G. O., MAKARENKO, S. P., DANCHUK, V. D., KRAVCHUK, A. P., BARAN, J., KOTELNIKOVA, E. N., FILATOV, S. K. Dynamics of molecules and phase transitions in the crystals of pure and binary mixtures of n-paraffins. *Journal of Molecular Structure* [online]. 2002, **614**(1-3), p. 159-166 [accessed 2024-08-25]. ISSN 0022-2860. Available from: https://doi.org/10.1016/s0022-2860(02)00237-5

[32] PUCHKOVSKA, G. O., DANCHUK, V. D., MAKARENKO, S. P., KRAVCHUK, A. P., KOTELNIKOVA, E. N., FILATOV, S. K. Resonance dynamical intermolecular interaction in the crystals of pure and binary mixture n-paraffins. *Journal of Molecular Structure* [online]. 2004, **708**(1-3), p. 39-45 [accessed 2024-08-25]. ISSN 0022-2860. Available from: https://doi.org/10.1016/j.molstruc.2004.02.010

[33] DANCHUK, V. D., KOZAK, L. S., DANCHUK, M. V. Stress testing of business activity using the synergetic method of risk assessment. *Actual Problems of Economics*. 2015, **171**(9), p. 189-198. ISSN 1993-6788.

[34] DBN B.2.3-5: 2018 DBN V.2.3-5:2018. Streets and roads of settlements / Vulytsi ta dorohy naselenykh punktiv. Minrehionbud (in Ukrainien) [online] [accessed 2024-08-25]. Available from: https://e-construction.gov.ua/laws_detail/3199686959802877315?doc_type=2

[35] Google maps [online] [accessed 2024-08-29]. Available from: https://www.google.com/maps

[36] Bing Maps Routes API - Microsoft Learn [online] [accessed 2024-08-29]. Available from: https://learn.microsoft.com/en-us/bingmaps/rest-services/routes/

[37] Nova Poshta branches map - Nova Poshta website [online] [accessed 2024-08-29]. Available from: https://novapost.com/en-ua/departments

[38] Flir official website [online] [accessed 2024-08-29]. Available from: https://www.flir.com/

IMPACT OF FOG LEVELS ON FREE-FLOW SPEEDS IN MIXED TRAFFIC CONDITIONS

Angshuman Pandit*, Anuj Kishor Budhkar

Department of Civil Engineering, Indian Institute of Engineering Science and Technology, Shibpur, Howrah, India

*E-mail of corresponding author: pandit.angshuman333@gmail.com

Angshuman Pandit 0000-0002-1074-0067, Anuj Kishor Budhkar 0000-0002-5931-806X

Resume

The effect of fog levels on drivers' free-flow speeds for various vehicles in mixed traffic conditions is examined in this research. Visibility and free-flow speeds from eight highways are simultaneously collected and analyzed. The findings show distinct driver behavior patterns under different fog conditions. In dense fog, small visibility improvements lead to linear speed increases, while in light fog, speeds are mostly unchanged, though drivers maintain higher speeds than in clear conditions. Regardless of a vehicle type, driving patterns in fog are similar, though specific speeds differ. Cars tend to drive dangerously fast, while trucks remain slower due to limited manoeuvrability. This study offers insights for operational strategies in dense fog, supporting the use of dynamic warning systems and variable speed limits to reduce unsafe speed variations and potential crashes in low visibility.

Article info

Received 30 September 2024
Accepted 16 January 2025
Online 14 February 2025

Keywords:

visibility
free-flow speed
drivers' behaviour
mixed traffic

Available online: https://doi.org/10.26552/com.C.2025.019

ISSN 1335-4205 (print version)
ISSN 2585-7878 (online version)

1 Introduction

Fog is a phenomenon that occurs when tiny water droplets, along with dust and other air particles, are suspended near the ground, scattering light in all directions. While driving in foggy weather, a driver's view is obstructed by fog particles, substantially affecting traffic operation and safety. Globally, millions of road crashes occur annually due to adverse weather conditions like fog [1].

Drivers in foggy conditions have a limited interaction range, as they cannot observe other vehicles' movements, road signs, or obstacles at longer distances. They may adapt to this low visibility by slowing down [2-5] or by following the taillights of a preceding vehicle [6]. However, some drivers may inadvertently increase their speed [7-8]. Studies show that as visibility decreases, drivers exhibit more erratic behavior in terms of acceleration, deceleration, and maintaining a consistent speed [5, 9-11].

Despite the drivers' efforts to anticipate and drive cautiously in reduced visibility, they may struggle to accurately judge safe stopping distances, leading to unsafe driving conditions. The impact of inadequate stopping sight distance is low on clear road segments [12], but it increases with denser fog levels. It is essential to understand how drivers adjust their speed according to varying visibility levels on long road stretches, as stated by McCann and Fontaine (2016) [13]. Therefore, the objective of this paper was to evaluate drivers' choice of free-flow speed under varying fog conditions on straight, unidirectional carriageways, urban and inter-urban highways, and mid-block sections with mixed traffic conditions.

2 Literature review

The literature in the context of present study is classified into effect of fog on traffic parameters, driver behaviour, and the psychological and physiological effects of fog.

2.1 Impact of fog on traffic parameters

Several researchers have studied the effect of fog on traffic parameters, including flow, speed, and headway.

NCHRP 95 [14] reported that the probability of speeding is most prominent in isolated vehicles, increasing from 55% to 69% in dense fog scenarios. Edwards (2002) [15] found that fog decreases the average peak-hour traffic volume by 9.2%. Trick et al. (2010) [16] suggested that the high-density traffic, combined with navigational challenges, adversely impacts older drivers more in clear conditions than in fog.

2.2 Driver behavior in fog

Studies have focused on driver behavior, examining speed, distance headway, and time headway [2, 5, 17]. Research indicates that foggy conditions lead to significantly lower average speeds, with passenger cars being more affected than trucks [4]. Additionally, the distance and time headways between vehicles decrease with reduced visibility [2, 18-22]. Drivers tend to overestimate vehicle spacing in fog, leading to closer following distances [2, 21].

Research shows that drivers' speed, reaction time, and steering vary depending on their experience, visibility, road type, and driving conditions [23-25]. Gao et al. (2020) [26] indicate that drivers in foggy conditions may accelerate earlier to follow leading vehicles closely, while Deng et al. (2019) [27] found that braking reaction time increases by 30% in fog. Furthermore, in mixed traffic scenarios, different categories of vehicles share the same roadway, frequently disregarding the assigned lanes. This situation complicates driving in foggy conditions. Consequently, it is essential to examine driving behavior in such mixed traffic environments.

2.3 Psychological and physiological effects

Fog can lead to risky manoeuvres, physiological fluctuations, and psychological distress, impacting traffic safety [28]. It increases the risk [29] and severity [30] of crashes. Wu et al. (2018) [31] found that fog raised crash risk by 40% in Florida. Additionally, fog can greatly hinder drivers' capacity to identify and react to hazards on the road, thereby increasing the dangers associated with shorter following distances [32]. Incidents occurring in foggy conditions often involve several vehicles and can lead to collisions and pile-ups [33]. Lynn et al. (2002) [34] investigated multivehicle crashes in Virginia attributed to fog and recommended using variable speed limits (VSL) to alert drivers to potential hazards [35-37].

2.4 Insights from literature and objectives of the study

The literature reveals a significant influence of fog on traffic parameters like speed, flow, and headway. However, studies often involve multiple factors, obscuring the pure impact of fog. Investigations should consider solely the impact of fog, keeping other variables consistent. The need for further research is highlighted by inconsistent findings and incomplete mitigation strategies like VSLs. In this study, an attempt is made to provide a clearer understanding of how fog impacts driving behavior, helping to develop better traffic management and safety strategies for foggy conditions. This study addresses the gap in the literature by using the real-world data from various visibility levels to model how drivers choose their speeds under different fog conditions.

The objective of this study was to model drivers' choice of free-flow speed across a broad range of fog conditions on highways with mixed traffic, maintaining consistency in other influencing parameters. The scope of the study involves simultaneous data collection of fog and traffic on mid-block sections on highways during the daytime. In this study, we selected mid-block sections in plain terrain to collect data. This ensured consistency by minimizing external factors such as curves or gradients that could influence drivers' speeds. According to the Indian Highway Capacity Manual [38], vehicles traveling at free-flow speed are those maintaining a time headway of more than 8 seconds with any leading vehicle that shares a lateral overlap with them. We applied this definition to identify vehicles traveling at free-flow speed among all vehicles on the study sections.

3 Data collection

To address the research gap mentioned in the previous section, it was necessary to collect a large amount of traffic data for several traffic and fog conditions. Traffic was recorded using a camcorder with 90x zoom, 10 MP size and high-definition recording capability mounted by the authors at a suitable vantage point (tall tripod or foot over bridge). Data collection was conducted in several urban and inter-urban locations characterized by significant foggy weather. The overall methodology of this study is provided in Figure 1.

Mid-block road sections are meticulously chosen to eliminate external factors such as road geometry, curves, parked vehicles, or other land use that may obstruct vehicle movement, leaving only prevailing fog levels as the variable. The traffic video data was collected during winter mornings, repeatedly at the same locations, to capture a comprehensive range of fog conditions across most sites. Table 1 highlights the traffic data collection locations and their details. NH and SH indicate national highways and state highways in Table 1.

Non-car vehicles, including two-wheelers, three-wheelers, buses, trucks, and light commercial vehicles (LCVs), constituted between 11% and 88% of the total observed traffic across the studied sections, indicating a high level of vehicle heterogeneity.

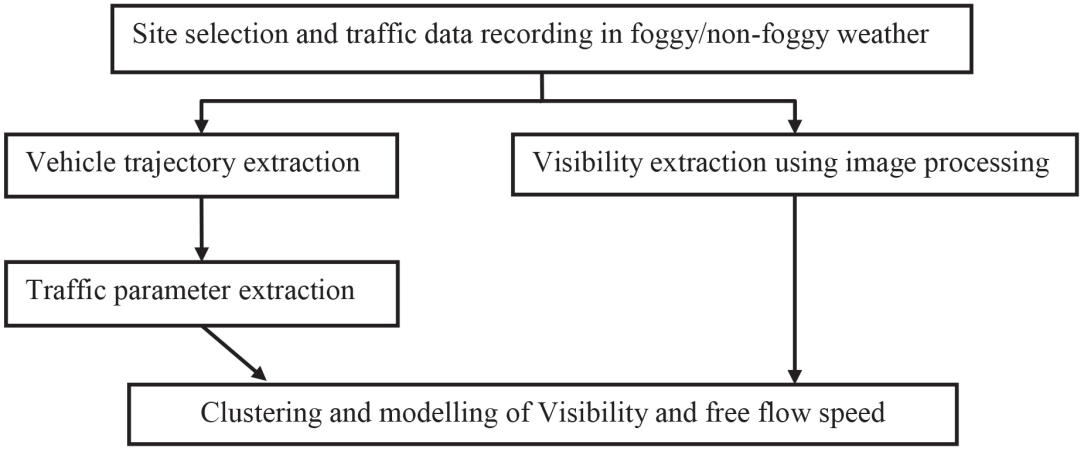

Figure 1 *Flowchart of the overall methodology*

Table 1 *Traffic and fog data collection locations*

S. No	Name of the road	Location of the road	Lanes per carriageway	Type of road
1	NH 16, (Chennai Kolkata Highway)	Salkia, dist Howrah West Bengal	3	Urban
2	West Bengal SH-13	Chandannagar, Dist. Hoogly, West Bengal	2	Inter-urban
3	NH-5	Knowledge City, Dist. SAS Nagar, Punjab	3	Urban
4	NH-7(Chandigarh Patiala Road)	Ramgarh, Dist. SAS Nagar, Punjab	2	Urban
5	NH-7 (Rajpura bypass)	Patiala Road, Dist. Patiala Punjab	2	Inter-urban
6	NH-8	Zirakpur, Dist, SAS Nagar, Punjab	2	Inter-urban
7	NH-44 (Grand Trunk Road)	Rajpura, dist. Patiala, Punjab	3	Inter-urban
8	NH 44, Jammu Delhi Road	Madhopur, Dist Fatehgarh Sahib, Punjab	3	Inter-urban

4 Data extraction

Two-fold data extraction of traffic and fog are conducted simultaneously from the selected traffic locations in Table 1 is presented below.

4.1 Traffic data extraction

The present study uses the YOLOv8 detection algorithm [39] with the DeepSort tracking algorithm for vehicle detection [40]. Pre-training is conducted by manually drawing rectangular boundaries over vehicle images retrieved from the traffic videos, and classifying them into seven different vehicle classes (Figure 2). The algorithm is trained using vehicle image datasets from both foggy and non-foggy weather conditions. Accuracy of new vehicle detection by the trained YOLO model ranges from 50% to 97% with the vehicle types. Then, all the collected videos, totalling over 1900 minutes, underwent automatic vehicle detection by the YOLO (Figure 2). Image coordinates of the bounding box edges for each detected vehicle over every time frame are saved.

The image coordinates of the detected vehicles are then transformed into field coordinates using a camera calibration technique adopted from [41]. The converted field coordinate file contains the columns i, $X_{i,t}$, $Y_{i,t}$, t where i denotes the vehicle number, $X_{i,t}$ and $Y_{i,t}$ denote the longitudinal and lateral coordinates of the vehicle at time t, respectively. By knowing the time of travel of the vehicle over a large trap length (>100 m) for every section, individual vehicle speeds were calculated.

To conduct the analysis on free-flow speed, the IDs (identification numbers) of vehicles travelling at free-flow speed are separated from the overall individual speed dataset, based on the criteria outlined in the Indian Highway Capacity Manual [38]. The term "free-flow condition" means that vehicles can move without being slowed down by prevailing traffic.

4.2 Measurement of visibility

In foggy weather conditions, road visibility can be quantified through the use of various devices such as a Visiometer, Photovoltaic cell [42], Optical sensor [43] etc. Hautiere et al. (2007) [44] have established a novel image-based method to estimate visibility, defining it as the distance at which the contrast threshold of a dark object decreases to 5% of its original value in fog. Say, $BV_{f,w}$ = Brightness of white portion in foggy weather,

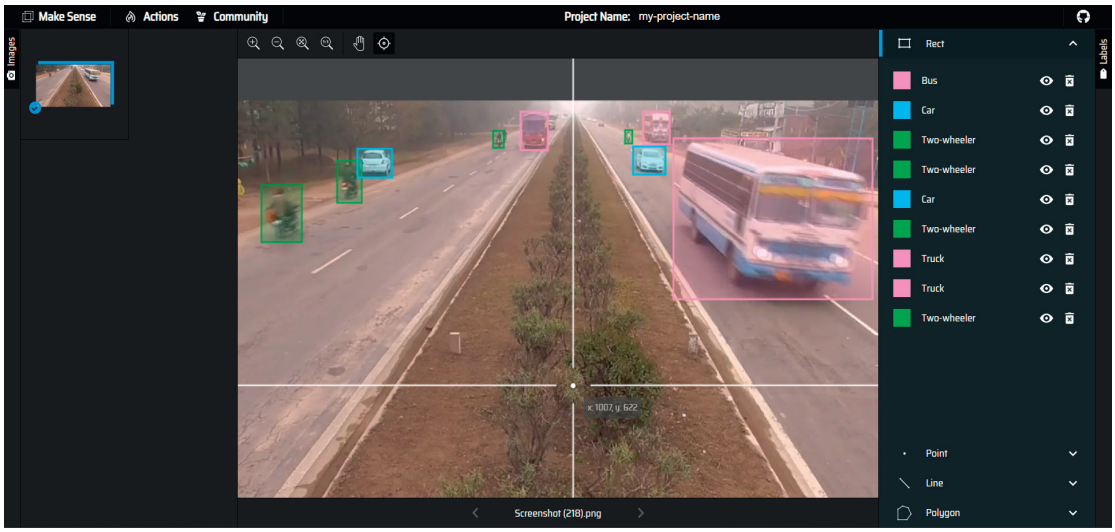

2(a) Manual detection for training

2(b) Automatic vehicle detection

Figure 2 *Vehicle trajectory extraction using YOLOv8*

$BV_{f,b}$ = Brightness of black portion in foggy weather,
$BV_{c,w}$ = Brightness of white portion in clear weather,
$BV_{c,b}$ = Brightness of black portion in clear weather.

The distance in a foggy weather when C_r (Contrast ratio) equals 0.05 is termed as visibility by Hautiere et al. (2007). So, at visibility,

$$C_r = \frac{BV_{f,w} - BV_{f,b}}{BV_{c,w} - BV_{c,b}}. \quad (1)$$

In the present paper, an umbrella was painted black and white and it was moved along the road at every site and every 10-15 min or whenever visibility has drastically changed. $BV_{f,w}$ and $BV_{f,b}$ are recorded using the brightness values of pixels (mouse clicked manually in the video frame), corresponding to the black and white portions of the umbrella at various distances from the camera. $BV_{c,w}$ and $BV_{c,b}$ are recorded earlier in clear weather conditions. The distance of the object from the camera is calculated using the camera calibration [41]. Figure 3 demonstrates the process.

A sample plot for one of the sites of C_r against various distances is shown in Figure 4. Negative exponential curve has the best fit (Equation (2)) $(R^2 = 0.79)$ for these plots. Based on the equation, the distance corresponding to C_r = 1 was calculated.

$$y = 2.68e^{-0.019x}, \quad (2)$$

where, $y = C_r$ and x = distance in m.x = distance.

This analysis of visibility calculation is conducted for visibility up to 800 m and verified with the meteorological data of the nearest weather station at the time of recording. For visibility more than 800 m, only meteorological visibility values are considered.

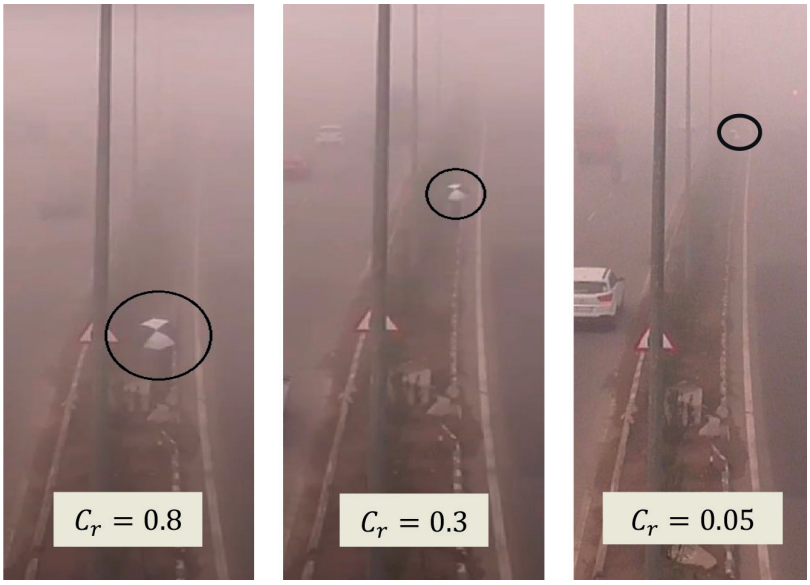

Figure 3 *Estimation of visibility using black and white object*

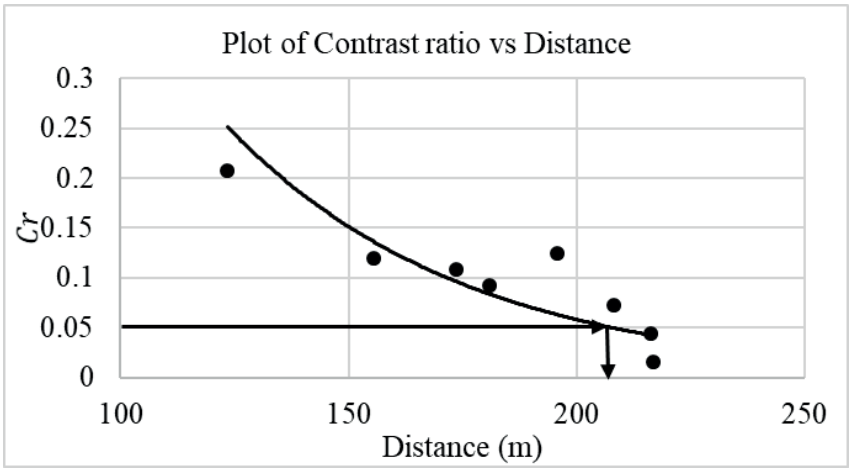

Figure 4 *Contrast ratio vs distance plot for visibility estimation*

5 Data analysis

Out of the entire vehicle dataset, 3,945 vehicles operated in free-flow conditions. The composition included 2,258 cars (57.2%), 627 two-wheelers (15.9%), 276 LCVs (7.0%), 633 trucks (16.0%), 49 buses (1.2%), and 102 three-wheelers (2.6%). Further analysis focused on cars, trucks, LCVs, and two-wheelers, and excluded buses and three-wheelers due to their limited sample sizes. Visibility values during the travel were recorded for these vehicles, as well and plotted against free-flow speed on a logarithmic graph (Figure 5).

Figure 5 shows an initial increase in the free-flow speed with visibility up to a certain limit, then a reduction with further visibility improvement. Further, contour maps were generated to display the distribution of the dataset, including percentage frequency and cumulative frequency (Figure 6). These maps reveal three distinct sections, prompting further investigation into potential differences in driver behavior across these regions.

5.1 Clustering of visibility

A box-and-whisker plot is shown in Figure 7 for separate vehicle types for the same visibility grouping of 100 m intervals each. From the box-and-whisker plot, one can make the following observations:

- At lower visibility levels, free-flow speed increases with visibility.
- Median value of the free-flow speed has increased for visibility 0 to 300 m after which there has been a decrease in the free-flow speed for visibility 300 m to 500 m. Thereafter free-flow speed has remained consistent.
- Contrary to the larger spread of the dataset in Figure 5, vehicle type-wise free-flow speed is not observed to have a large variation (Figure 7).
- All the vehicle types have similar speed-visibility plot patterns. Cars have a higher mean free-flow speed in every visibility range as compared to other vehicle types.

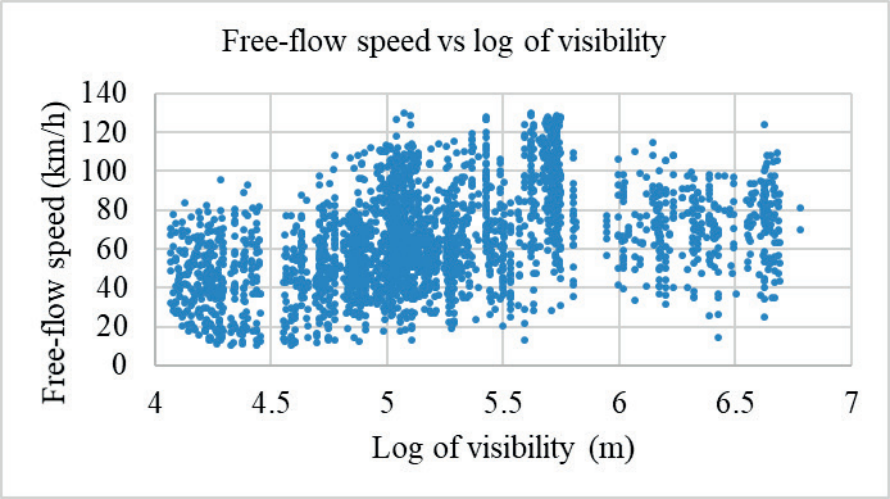

Figure 5 *Free-flow speed vs log of visibility*

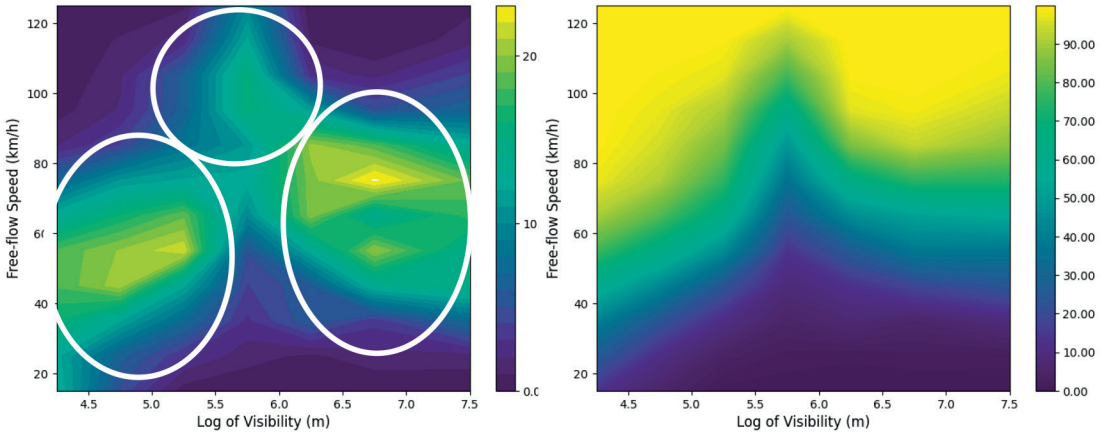

a) Contour map of percentage frequency *b) Contour map of cumulative percentage frequency*

Figure 6 *Contour plot of percentage frequency and cumulative percentage frequency of free-flow speed vs visibility*

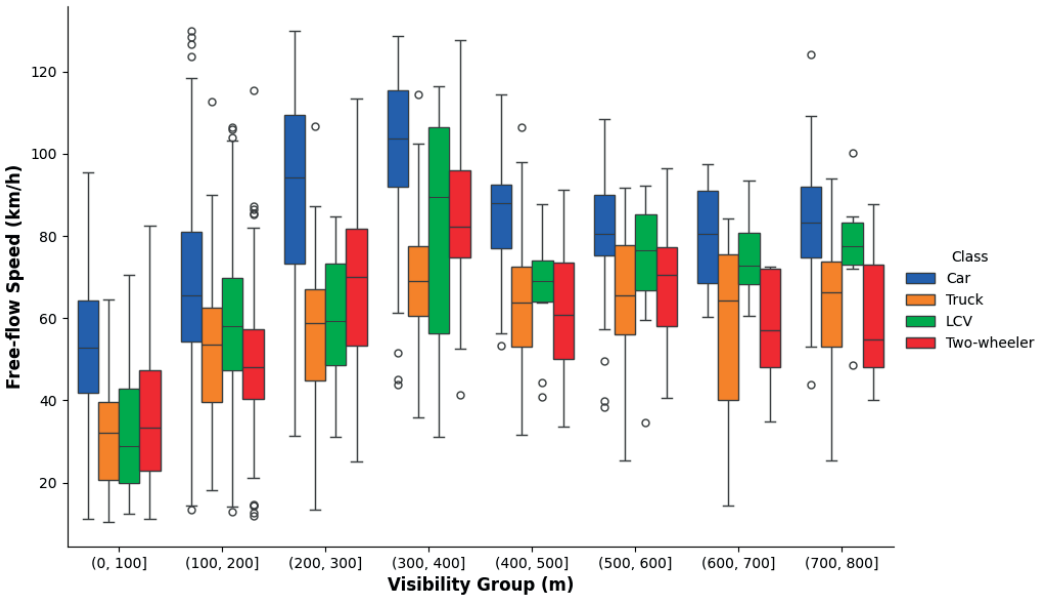

Figure 7 *Box and whisker plot of Free-flow speed vs Visibility groups*

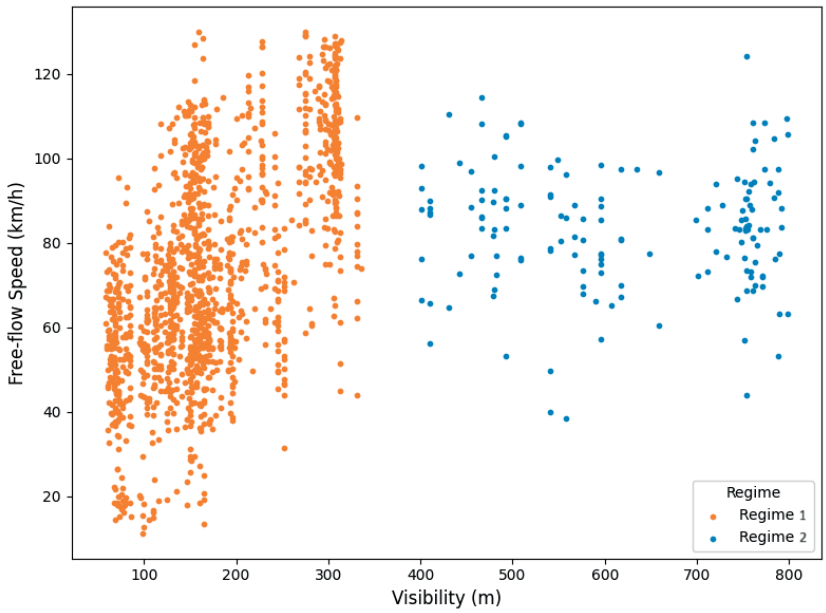

Figure 8 *Clustering of visibility with free flow speed for cars showing two distinct clusters*

The one-way ANOVA indicates a significant overall difference in means across the visibility groups 1-8 ($p < 0.05$). Pairwise ANOVA reveals statistically different free-flow speeds at most group levels ($p < 0.05$), except for groups 2 and 6 ($p = 0.07$), groups 3 and 7 ($p = 0.59$), and groups 5, 6, and 7. From the ANOVA test and box-and-whisker plot, it is evident that drivers reduce speed in visibility up to 200 m, then increase speeds between 200 m and 400 m, albeit higher than in clearer conditions (> 400 m visibility). Authors of [7-8] also observed this counterintuitive result, suggesting that drivers may increase speed at medium or shallow visibility levels due to a perceived decrease in visible information in the peripheral field of view.

It is essential to determine if the speed changes continuously with visibility or if there are specific fog levels where it changes abruptly, which can be confirmed by identifying distinct clusters. To advance in this direction, K-means clustering has been opted for the foggy dataset (up to 800 m) only. By performing a hard clustering analysis, one can distinctively identify the fog level where the driver behaviour changes. The optimum number of clusters is identified by the Silhouette score [45]. The Silhouette score values for 2, 3, 4, and 5 numbers of clusters are 0.75, 0.59, 0.59, and 0.50 respectively. Thus, the optimum number of clusters in foggy weather is two. The clustering of free-flow speed data of cars in foggy weather is shown in Figure 8, other vehicle type datasets can be clustered similarly. Considering a separate regime for clear weather conditions, the entire dataset is now clustered into three regimes as mentioned below. The regimes are shown for cars and similar regime boundaries are observed for other vehicle types.

(1) Regime 1: Visibility values less than 382 m. (speed increases with visibility)
(2) Regime 2: Visibility values 382 m to 800 m. (higher speeds and shallow fog)
(3) Regime 3: Non-foggy data (clear weather conditions).

The clustering analysis reveals three distinct ways in which the drivers perceive fog. We checked the regime 1-regime 2 boundary for different vehicle types and found it lying at almost the same range (< 382 m for cars, < 382 m for trucks, < 390 m for LCVs, and < 400 m for two-wheelers). This suggests that driver behavior patterns with fog remain consistent across vehicle types. Thus, drivers assess fog levels independent of their vehicle type.

5.2 Modelling of free-flow speed vs visibility

Distinct regime-wise models are necessary to illustrate how visibility affects the free-flow speed across different fog levels. In this regard, regression curves are plotted for all the vehicle classes in regime 1. In regime 2, there is no significant relationship between visibility and free-flow speed, but mean speed is notably higher than in regime 3. A linear relationship between free-flow speed and visibility levels can accurately represent the trend of visibility versus speed across all the vehicle types for regime 1. Increasing the degree of the equation does not significantly enhance the goodness of fit of the regression curve. Consequently, the entire dataset is modelled as regression lines, (Equation (3)) differently for different vehicle types.

$$u = av + b + R \tag{3}$$

where u = free-flow speed in km/h, v = visibility in m, a = slope and b = intercept of the regression line, R = Residual of the corresponding regime. Table 2 shows the

regression parameters for all vehicle types. The mean and standard deviation values against the corresponding regime and vehicle type are also expressed in Table 2. Overall, the residuals (R) are observed to statistically best follow Gamma (3P) distribution as ascertained by the Kolmogorov-Smirnov test, but they do closely follow normal distribution as well. We assess the consistency of residual spread about the regression curve with changes in visibility. Initially, the Goldfeld-Quandt (G-Q) test is conducted on regime 1 dataset for each vehicle type. The resulting p-values for cars, trucks, LCVs, and two-wheelers are 0.01, 0.85, 0.71, and 0.80, respectively, indicating heteroscedastic residuals in the cars' dataset. To address this, residuals are modified (R_m) linearly with visibility. Subsequent G-Q tests on the modified residuals confirm homoscedasticity, allowing them to be modelled as a single distribution. The equation of Gamma (3P) distribution is given as,

$$f(x) = \frac{\alpha}{\beta}\left(\frac{\beta}{x-\gamma}\right)^{(\alpha-1)} \exp\left(-\left(\frac{\beta}{x-\gamma}\right)^{\alpha}\right), \quad \gamma \le x < \infty, \tag{4}$$

where, α = shape parameter, β = scale parameter and γ = location parameter.

All distribution parameters and p-values are shown in Table 2.

Table 2 shows that the standard deviation of free-flow speed is higher in regime 1 (dense fog) than in regime 2 (shallow fog) for all vehicle types, indicating greater speed variability and potentially higher crash risk [46]. An F-test reveals f-values of 25.47, 35.19, 27.89, and 9.12 for cars, trucks, LCVs, and two-wheelers, respectively, indicating significant variance differences in free-flow speeds between the two regimes for each vehicle type. We use the linear regression values from Table 2 in Equation (3) and plot them in Figure 9, along with the corresponding safe stopping sight distance (SSD) curves for comparison. The SSD calculations consider deceleration, road friction (0.35), and reaction time (2.5 sec) as per AASHTO (2018) [47]. Vehicles travelling below the safe SSD curve are considered safe, whereas those with free-flow speeds above the curve may pose a risk during the emergency braking.

Cars generally maintain higher free-flow speeds in foggy conditions compared to other vehicle types, with trucks having the lowest speeds, perhaps due to their limited manoeuvrability. Regression curves show that at visibilities below 60 m, the safe speed for cars determined by SSD criteria is higher than the modelled speed. In regime 1, 14.85% of cars exceed the safe SSD speed, while less than 1% of other vehicles do. This indicates a higher risk of collisions for cars in dense fog if they do not adhere to safe SSD. This result can help

Table 2 *Linear regression parameters of free flow speed-visibility models*

Vehicle type	a	b	Mean free-flow speed		Standard deviation of free-flow speed		Parameters of Gamma (3P) distribution			
			Regime 1	Regime 2	Regime 1	Regime 2	α	β	γ	p-value of residuals with observed distribution
Car	0.21	37.12	72.82	83.22	25.43	14.48	220.48	0.03	-5.7	0.24
Truck	0.13	29.79	52.31	63.41	18.54	17.37	117.48	1.49	-175.6	0.62
LCV	0.18	25.7	47.49	70.72	22.32	13.95	41.8	2.96	-124.2	0.99
Two-wheeler	0.2	20.41	52.62	62.01	20.65	15.84	108.52	1.5	-163.4	0.71

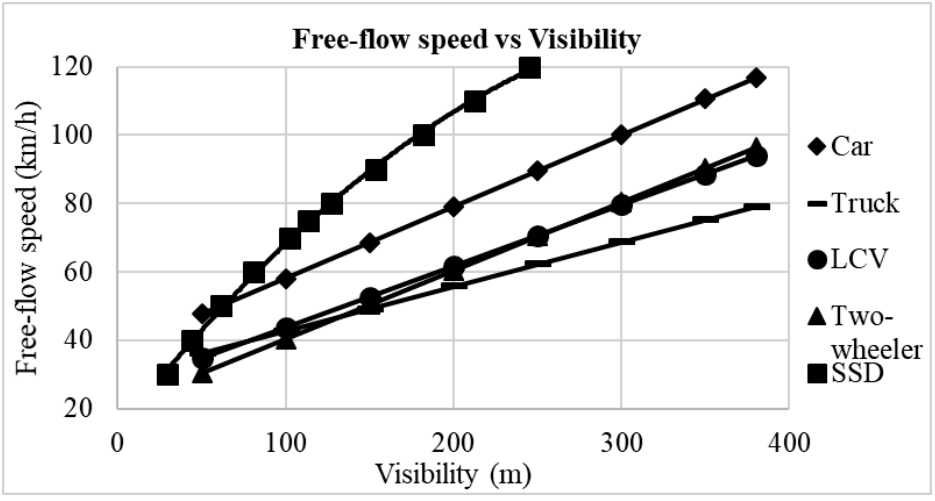

Figure 9 *Linear regression plots of Free flow speed vs Visibility for Regime 1 and safe stopping sight distances for different visibilities*

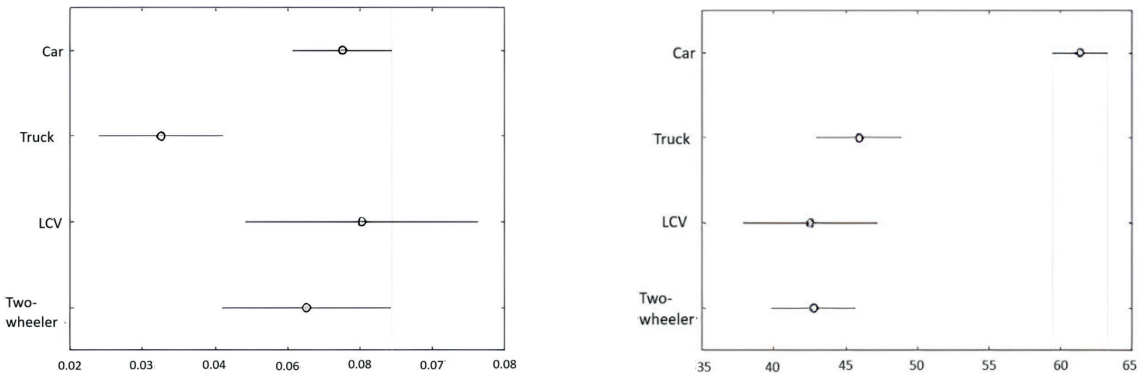

Figure 10 *Slope (left) and intercept (right) comparison of the regression models for different vehicle types*

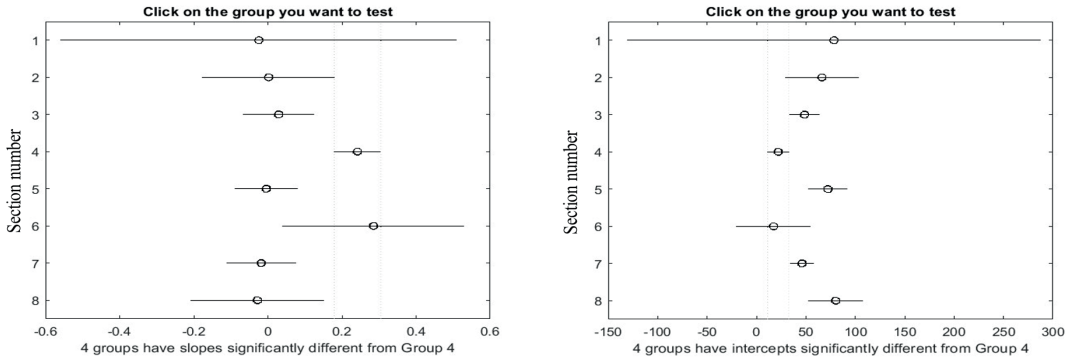

Figure 11 *Slope (left) and intercept (right) comparison of the regression models for different sections*

to improve the road safety by informing the development of targeted safety campaigns for car drivers, adaptive traffic control measures for over-speeding vehicles, and effective traffic regulations during dense fog.

5.3 Comparison of obtained model for different types of vehicles

Figure 10 shows the analysis of covariance and the variation in slopes and intercepts among vehicle types. Trucks have a statistically lower slope, indicating consistent driving despite a decline in visibility, as their speeds are already limited in clear conditions and do not significantly decrease further. Cars have a higher intercept, showing higher free-flow speeds at zero-visibility. The intercepts for trucks, LCVs, and two-wheelers are similar, but cars' intercepts are significantly higher. This indicates that cars are driven faster than other vehicles, and car drivers do not exercise sufficient caution at very low visibility levels.

5.4 Location-wise validation of the model

The site-wise variation of slope and intercept for the regime 1 dataset is examined through analysis of covariance (Figure 11) to determine if the relationship between the free-flow speed and visibility holds true across different locations. While there is a slight variation in slopes between sites, the intercept remains statistically consistent for each section, suggesting uniform driver behavior across these locations.

6 Summary of findings and future scope

In this study it was examined how fog affects vehicle free-flow speeds on inter-urban and urban highways in mixed traffic. Results show a rising trend between the fog levels and vehicle speeds at low visibility (below 382 m). In contrast, at higher visibility levels (382-800 m), drivers tend to drive faster than in clear conditions and do not significantly adjust their speed for fog. This behavior is consistent across all vehicle types, although trucks show less variation due to their lower maximum speeds. To summarise, the research conducted in this paper can provide the following insights:

1. Free-flow speeds in foggy weather increase initially with visibility up to 382 m, then remain consistent but higher than in clear weather conditions.
2. Drivers perceive fog levels differently, with consistent variations across vehicle types, as observed through clustering analysis. The fog perception for each regime (dense, shallow or no-fog) needs separate modelling.
3. Linear plots for driving in denser fog demonstrate that the free-flow speeds increase with visibility, with varying rates for different vehicle types. For cars, trucks, LCVs and two-wheelers moving in

foggy weather, the free flow speeds increase by 2.1, 1.3, 1.8 and 2 km/h, respectively, with every 10 m improvement in visibility levels.
4. In dense fog (< 382 m), 14.85% of cars exceed the safe speed, posing potential safety risks.
5. Speeds remain consistent in shallow fogs (382-800 m visibility) but are approximately 10% higher than in clear weather conditions for all the vehicle types.
6. Cars consistently have the highest speeds across all visibility conditions, while trucks are the least affected by visibility as their speeds are already limited in clear conditions.

The findings from this study can be useful input tools for traffic planners, road designers and for a work zone safety in fog. The authors propose the following suggestions for safe and efficient operations in foggy weather, as an immediate application of this paper.

- Practitioners can highlight this inadvertent speed increase in road safety programs using visual aids (e.g., photographs), implement it in driver training modules, enforce it through adaptive speed limit signs, and integrate it into advanced driver assistance systems to mitigate risky driving behaviors.
- As cars drive faster than safe stopping sight distances in low visibility (0-382 m), drivers need to stay alert to avoid speed variations. Practitioners can install dynamic warning systems, implement variable speed limits, especially on roads with changing geometries and at work zones.
- Variable speed limits can be implemented to mitigate the speed variation between changing fog levels, to prevent a sudden backward shockwave propagation. The speed limits can be ascertained by calculating safer accelerations or decelerations, along with the findings in this paper, as the fog levels vary on a longer stretch of road.

This study focused solely on free-flow speed for analysis, but a comprehensive understanding of driving in foggy weather should examine car-following characteristics like headway, acceleration, and deceleration in foggy conditions. Researchers can use the outcomes from this study to simulate how varying fog levels on a road affect vehicle speed and generate the simulated shockwaves resulting from abrupt visibility changes. Implementing these findings in live speed display devices can help to adjust speeds gradually, reducing the backward shockwave caused by sudden visibility drops. Future studies on shockwave propagation in fog can further reduce fog-related accidents. This paper provides foundational insights for such research and practical applications.

Acknowledgment

The authors received no financial support for the research, authorship and/or publication of this article.

Conflicts of interest

The authors declare that they have no known competing financial interests or personal relationships that could have appeared to influence the work reported in this paper.

References

[1] Federal Highway Administration. Highway statistics 2004. USA: Federal Highway Administration, 2006.
[2] CAVALLO, V. Perceptual distortions when driving in fog. In: Conference on Traffic and Transportation Studies ICTTS: proceedings [online]. 2002. Available from: https://doi.org/10.1061/40630(255)135
[3] EDWARDS, J. B. Speed adjustment of motorway commuter traffic to inclement weather. *Transportation Research Part F: Traffic Psychology and Behaviour* [online]. 1999, **2**(1), p. 1-14. ISSN 1369-8478, eISSN 1873-5517. Available from: https://doi.org/10.1016/S1369-8478(99)00003-0
[4] PENG, Y., ABDEL-ATY, M., LEE, J., ZOU, Y. Analysis of the impact of fog-related reduced visibility on traffic parameters. *Journal of Transportation Engineering, Part A: Systems* [online]. 2018, **144**(2), 04017077. ISSN 2473-2907, eISSN 2473-2893. Available from: https://doi.org/10.1061/jtepbs.0000094
[5] TU, H., LI, Z., LI, H., ZHANG, K., SUN, L. Driving simulator fidelity and emergency driving behavior. *Transportation Research Record: Journal of the Transportation Research Board* [online]. 2015, **2518**(1), p. 113-121. ISSN 0361-1981, eISSN 2169-4052. Available from: https://doi.org/10.3141/2518-15
[6] AL-GHAMDI, A. S. Experimental evaluation of fog warning system. *Accident Analysis and Prevention* [online]. 2007, **39**(6), p. 1065-1072. ISSN 0001-4575, eISSN 1879-2057. Available from: https://doi.org/10.1016/j.aap.2005.05.007
[7] PRETTO, P., VIDAL, M., CHATZIASTROS, A. Why fog increases the perceived speed. In: Driving Simulation Conference DSC 2008: proceedings. 2008.
[8] SNOWDEN, R. J., STIMPSON, N., RUDDLE, R. A. Speed perception fogs up as visibility drops. *Nature* [online]. 1998, **392**, 450. ISSN 0028-0836, eISSN 1476-4687. Available from: https://doi.org/10.1038/33049
[9] HOOGENDOORN, R. G., HOOGENDOORN, S. P., BROOKHUIS, K. A., DAAMEN, W. Adaptation longitudinal driving behavior, mental workload, and psycho-spacing models in fog. *Transportation Research Record: Journal*

of the Transportation Research Board [online]. 2011, **2249**(1), p. 20-28. ISSN 0361-1981, eISSN 2169-4052. Available from: https://doi.org/10.3141/2249-04

[10] HOOGENDOORN, R. G. Empirical research and modelling of longitudinal driving behavior under adverse conditions [online]. Doctoral thesis. Delft, Netherlands: TRAIL Research School, 2012. Available from: http://resolver.tudelft.nl/uuid:1e0117ef-d0db-4d00-bce6-203d75a30ddc

[11] PEI, Y., CHENG, G. Research on the relationship between discrete character of speed and traffic accident and speed management of freeway. *China Journal of Highway and Transport*. 2004, 17(1), p. 74-78. ISSN 1001-7372.

[12] Stopping Sight Distance - Federal Highway Administration FHWA [online]. 2022. Available from: https://safety.fhwa.dot.gov/geometric/pubs/mitigationstrategies/chapter3/3_stopdistance.cfm

[13] MCCANN, K., FONTAINE, M. D. Assessing driver speed choice in fog with the use of visibility data from road weather information systems. *Transportation Research Record: Journal of the Transportation Research Board* [online]. 2016, **2551**(1), p. 90-99. ISSN 0361-1981, eISSN 2169-4052. Available from: https://doi.org/10.3141/2551-11

[14] KOCMOND, W. C., PERCHONOK, K. Highway fog. NCHRP Report 95. Washington, D. C.: Transportation Research Board, 1970.

[15] EDWARDS, J. B. Motorway speeds in wet weather: the comparative influence of porous and conventional asphalt surfacings. *Journal of Transport Geography* [online]. 2002, 10(4), p. 303-311. ISSN 0966-6923, eISSN 1873-1236. Available from: https://doi.org/10.1016/S0966-6923(02)00044-3

[16] TRICK, L. M., TOXOPEUS, R., WILSON, D. The effects of visibility conditions, traffic density, and navigational challenge on speed compensation and driving performance in older adults. *Accident Analysis and Prevention* [online]. 2010, **42**(6), p. 1661-1671. ISSN 0001-4575, eISSN 1879-2057. Available from: https://doi.org/10.1016/j.aap.2010.04.005

[17] YAN, X., LI, X., LIU, Y., ZHAO, J. Effects of foggy conditions on drivers' speed control behaviors at different risk levels. *Safety Science* [online]. 2014, **68**, p. 275-287. ISSN 0925-7535, eISSN 1879-1042. Available from: https://doi.org/10.1016/j.ssci.2014.04.013

[18] BOER, E. R., CARO, S., CAVALLO, V. A Cybernetic perspective on car following in fog. In: Driving Assessment Conference 4 2007: proceedings [online]. 2007. p. 452-458. Available from: https://doi.org/10.17077/drivingassessment.1275

[19] BROUGHTON, K. L. M., SWITZER, F., SCOTT, D. Car following decisions under three visibility conditions and two speeds tested with a driving simulator. *Accident Analysis and Prevention* [online]. 2007, **39**(1), p. 106-116. ISSN 0001-4575, eISSN 1879-2057. Available from: https://doi.org/10.1016/j.aap.2006.06.009

[20] CARO, S., CAVALLO, V., MARENDAZ, C., BOER, E. R., VIENNE, F. Can headway reduction in fog be explained by impaired perception of relative motion? *Human Factors: The Journal of the Human Factors and Ergonomics Society* [online]. 2009, **51**(3), p. 378-392. ISSN 0018-7208, eISSN 1547-8181. Available from: https://doi.org/10.1177/0018720809339621

[21] SAFFARIAN, M., HAPPEE, R., DE WINTER, J. C. F. Why do drivers maintain short headways in fog? A driving-simulator study evaluating feeling of risk and lateral control during automated and manual car following. *Ergonomics* [online]. 2012, **55**(9), p. 971-985. ISSN 1366-5847. Available from: https://doi.org/10.1080/00140139.2012.691993

[22] WHITE, M. E., JEFFERY, D. J. *Some aspects of motorway traffic behaviour in fog*. Berkshire: Highway Traffic Division, 1980. ISSN 0305-1293.

[23] LIANG, W. L., KYTE, M., KITCHENER, F., SHANNON, P. Effect of environmental factors on driver speed. *Transportation Research Record: Journal of the Transportation Research Board* [online]. 1998, **1635**(1), p. 155-161. ISSN 0361-1981, eISSN 2169-4052. Available from: https://doi.org/10.3141/1635-21

[24] MUELLER, A. S., TRICK, L. M. Driving in fog: the effects of driving experience and visibility on speed compensation and hazard avoidance. *Accident Analysis and Prevention* [online]. 2012, **48**, p. 472-479. ISSN 0001-4575, eISSN 1879-2057. Available from: https://doi.org/10.1016/j.aap.2012.03.003

[25] ROSEY, F., AILLERIE, I., ESPIE, S., VIENNE, F. Driver behaviour in fog is not only a question of degraded visibility - a simulator study. *Safety Science* [online]. 2017, **95**, p. 50-61. ISSN 0925-7535, eISSN 1879-1042. Available from: https://doi.org/10.1016/j.ssci.2017.02.004

[26] GAO, K., TU, H., SUN, L., SZE, N. N., SONG, Z., SHI, H. Impacts of reduced visibility under hazy weather condition on collision risk and car-following behavior: implications for traffic control and management. *International Journal of Sustainable Transportation* [online]. 2020, **14**(8), p. 635-642. ISSN 1556-8318. Available from: https://doi.org/10.1080/15568318.2019.1597226

[27] DENG, C., WU, CH., CAO, S., LYU, N. Modeling the effect of limited sight distance through fog on car-following performance using QN-ACTR cognitive architecture. *Transportation Research Part F: Traffic Psychology and Behaviour* [online]. 2019, **65**, p. 643-654. ISSN 1369-8478, eISSN 1873-5517. Available from: https://doi.org/10.1016/j.trf.2017.12.017

[28] PENG, Y., ABDEL-ATY, M., SHI, Q., YU, R. Assessing the impact of reduced visibility on traffic crash risk using microscopic data and surrogate safety measures. *Transportation Research Part C: Emerging Technologies* [online]. 2017, **74**, p. 295-305. ISSN 0968-090X, eISSN 1879-2359. Available from: https://doi.org/10.1016/j.trc.2016.11.022

[29] HAMILTON, B., TEFFT, B., ARNOLD, L., GRABOWSKI, J. Hidden highways: fog and traffic crashes on America's roads (technical report). Washington, D. C.: AAA Foundation for Traffic Safety, 2014.

[30] YANNIS, G., KONDYLI, A., MITZALIS, N. Effect of lighting on frequency and severity of road accidents. *Proceedings of the Institution of Civil Engineers: Transport* [online]. 2013, **166**(5), p. 271-281. ISSN 0965-092X, eISSN 1751-7710. Available from: https://doi.org/10.1680/tran.11.00047

[31] WU, Y., ABDEL-ATY, M., LEE, J. Crash risk analysis during fog conditions using real-time traffic data. *Accident Analysis and Prevention* [online]. 2018, **114**, p. 4-11. ISSN 0001-4575, eISSN 1879-2057. Available from: https://doi.org/10.1016/j.aap.2017.05.004

[32] D'ADDARIO, P. M. Perception-response time to emergency roadway hazards and the effect of cognitive distraction. Thesis. Toronto: University of Toronto, 2014

[33] KIM, Y.-K., KIM, H., SEO, J.-W., AN, H.-Y., CHOI, Y.-H. Meteorological analysis of the sea fog in winter season on Gyeonggi Bay, Yellow Sea: a case study for the 106-vehicle pileup on February 11, 2015. *Journal of Coastal Research* [online]. 2017, **79**(sp1), p. 124-128. ISSN 0749-0208. Available from: https://doi.org/10.2112/SI79-026.1

[34] LYNN, C., SCHREINER, CH., CAMPBELL, R. Reducing fog-related crashes on the Afton and Fancy Gap Mountain Sections of I-64 and I-77 in Virginia. Final contract report. Charlottesville, Virginia: Virginia Transportation Research Council, 2002.

[35] CHENG, G. Research on the method of setting speed limits on freeway and urban expressway. China: Harbin Institute of Technology, 2007.

[36] CHOI, S., OH, C. Proactive strategy for variable speed limit operations on freeways under foggy weather conditions. *Transportation Research Record: Journal of the Transportation Research Board* [online]. 2016, **2551**(1), p. 29-36. ISSN 0361-1981, eISSN 2169-4052. Available from: https://doi.org/10.3141/2551-04

[37] LI, X., YAN, X., WONG, S. C. Effects of fog, driver experience and gender on driving behavior on S-curved road segments. *Accident Analysis and Prevention* [online]. 2015, **77**, p. 91-104. ISSN 0001-4575, eISSN 1879-2057. Available from: https://doi.org/10.1016/j.aap.2015.01.022

[38] Indian highway capacity manual Indo-HCM. New Delhi: Central Road Research Institute, 2017.

[39] JOCHER, G., CHAURASIA, A., QIU, J. YOLO by Ultralytics Version 8.0.0. Computer software [online]. 2023. Available from: https://github.com/ultralytics/ultralytics

[40] TAO, J., WANG, H., ZHANG, X., LI, X., YANG, H. An object detection system based on YOLO in traffic scene. In: 2017 6th International Conference on Computer Science and Network Technology ICCSNT: proceedings [online]. IEEE. 2017. eISBN 978-1-5386-0493-9. Available from: https://doi.org/10.1109/ICCSNT.2017.8343709

[41] FUNG, G. S. K., YUNG, N. H. CH., PANG, G. K. H. Camera calibration from road lane markings. *Optical Engineering* [online]. 2003, **42**(10). eISSN 1560-2303. Available from: https://doi.org/10.1117/1.1606458

[42] DUMONT, E., CAVALLO, V. Extended photometric model of fog effects on road vision. *Transportation Research Record: Journal of the Transportation Research Board* [online]. 2004, **1862**(1), p. 77-81. ISSN 0361-1981, eISSN 2169-4052. Available from: https://doi.org/10.3141/1862

[43] OVSENIK, L., TURAN, J., MISENCIK, P., BITO, J., CSURGAI-HORVATH, L. Fog density measuring system. *Acta Electrotechnica et Informatica* [online]. 2013, **12**(2), p. 67-71. ISSN 1335-8243, eISSN 1338-3957. Available from: https://doi.org/10.2478/v10198-012-0021-7

[44] HAUTIERE, N., AUBERT, D., DUMONT, E. Mobilized and mobilizable visibility distances for road visibility in fog. In: 26th Session of the CIE: proceedings. 2007.

[45] ROUSSEEUW, P. J. Silhouettes: a graphical aid to the interpretation and validation of cluster analysis. *Journal of Computational and Applied Mathematics* [online]. 1987, **20**, p. 53-65. ISSN 0377-0427, eISSN 1879-1778. Available from: https://doi.org/10.1016/0377-0427(87)90125-7

[46] GAO, K., TU, H., SHI, H. Stage-specific impacts of hazy weather on car following. *Proceedings of the Institution of Civil Engineers: Transport* [online]. 2019, **172**(6), p. 347-359. ISSN 0965-092X, eISSN 1751-7710. Available from: https://doi.org/10.1680/jtran.16.00182

[47] American Association of State Highway and Transportation Officials. A policy on geometric design of highways and streets: the green book. 7. ed. Washington, D. C.: American Association of State Highway and Transportation Officials, 2018. ISBN 978-1-56051-676-7.

KOMUNIKÁCIE
COMMUNICATIONS

VEDECKÉ LISTY ŽILINSKEJ UNIVERZITY
SCIENTIFIC LETTERS OF THE UNIVERSITY OF ZILINA
journal for sciences in transport

VOLUME 27 Number 2

April 2025

Each paper was reviewed by at least two reviewers.
Individual issues of the journal can be found on: http://komunikacie.uniza.sk
The full author quidelines are available at: https://komunikacie.uniza.sk/artkey/inf-990000-0400_Author-guidelines.php
Published quarterly by University of Žilina in EDIS - Publishing House of the University of Žilina.
Transport journal Komunikácie / Communications is currently indexed, abstracted and accepted by CEEOL, CLOCKSS, Crossref (DOI), digitálne pramene, DOAJ, EBSCO Host, Electronic Journals Library (EZB), ERIH Plus, Google Scholar, Index Copernicus International Journals Master list, iThenticate, JournalGuide, Jouroscope, Norwegian Register for Scientific Journals Series and Publishers, Portico, ROAD, ScienceGate, SCImago Journal & Country Rank, SciRev, SCOPUS, Web of Science database, WorldCat (OCLC).

Journal for sciences in transport Komunikácie - vedecké listy Žilinskej univerzity v Žiline / Communications - Scientific Letters of the University of Žilina has been selected for inclusion in the Web of Science™.

Contact:
Komunikácie - vedecké listy Žilinskej univerzity v Žiline
Communications - Scientific Letters of the University of Žilina
University of Žilina
Univerzitná 8215/1
010 26 Žilina
Slovakia

E-mail: komunikacie@uniza.sk
Web: https://komunikacie.uniza.sk

ISSN (print version): 1335-4205
ISSN (online version): 2585-7878

Registered No. (print version): EV 3672/09
Registered No. (online version): EV 3/22/EPP
Publisher, owner and distribution:
University of Žilina, Univerzitná 8215/1,
010 26 Žilina, Slovakia

Company identification number IČO: 00 397 563
Frequency of publishing: four times a year
Circulation: 30 printed copies per issue
Print edition price: 100 Euro (price without VAT)
Article Processing Charge (APC): 400 Euro
(price without VAT)

Publishing has been approved by:
Ministry of Culture, Slovak Republic

TRANSCOM, International Scientific Conference on Sustainable, Modern, and Safe Transport, aims to establish and expand international contacts and cooperation. The main purpose of the conference is to provide young scientists with an encouraging and stimulating environment in which they present the results of their research to the scientific community. TRANSCOM has been organised regularly every other year since 1995. Between 160 and 400 young researchers and scientists regularly participate in the event. The conference is organised for PhD students and young scientists up to the age of 35 and their tutors. Young workers are expected to present the results they had achieved.

IMPORTANT DATES

- January 31, 2025
  FULL PAPERS SUBMISSION
- March 21, 2025
  NOTIFICATION OF ACCEPTANCE
- April 17, 2025
  CONFERENCE FEE PAYMENT
- May 10, 2025
  CONFERENCE PROGRAMME
- May 21 - 23, 2025
  CONFERENCE

TOPICS

- Operation and Economics in Transport
- Mechanical Engineering in Transport
- Electrical Engineering in Transport
- Civil Engineering in Transport
- Management Science and Informatics in Transport
- Safety and Security Engineering in Transport
- Education in Transport

CONTACT

University of Zilina, Department for Science & Research
Univerzitna 8215/1, 010 26 Zilina, Slovakia
e-mail: transcom@uniza.sk
www.transcom-conference.com

UNIVERSITY
OF ŽILINA